Evaluation of the role of autophagy in ovarian cancer chemoresistance

A thesis submitted to the National University of Ireland, Cork

Fulfilling the requirements for the degree of

Doctor of Philosophy

By

Jennifer Quinn, BSc, MSc

Student No: 116222951

University College Cork

Cancer Research @ UCC,

Head of department: Prof. Roisin Connolly

Under the supervision of:

Dr. Sharon McKenna, BSc. PhD.

Dr. Tracey O'Donovan, BSc. PhD.

2019/2020

Table of Contents

Acknowledgements xii

Thesis abstract xiv

Abbreviations xvii

Chapter 1: General Introduction 1

1.1 Ovarian Carcinoma 2

1.1.1 Incidence of ovarian carcinoma 2

1.1.2 Screening and diagnosis 2

1.1.3 Histological subtypes of Ovarian Cancer 5

1.1.3.1 Epithelial Tumours 6

1.1.3.2 Germ Cell tumours 7

1.1.3.3 Sex Cord Stromal Tumours 8

1.1.4 Ovarian cancer risk factors 9

1.1.4.2 Family History 9

1.1.4.3 Environmental risk factors 11

1.1.5 Staging of ovarian cancer 12

1.1.6 Management of ovarian cancer 15

1.1.6.1 Surgical management 15

1.1.6.2 Chemotherapeutics and targeted therapies 15

1.1.6.2.1 Chemotherapy 15

1.1.6.2.2 PARP inhibitors 18

1.1.6.2.3 Anti-angiogenic agents.....20

1.1.6.2.4 Immunotherapies in ovarian cancer.....22

1.1.7 Molecular pathogenesis of ovarian carcinoma.....26

1.1.7.1 Genomic landscape of ovarian cancer.....26

1.1.7.1.2 Sporadic ovarian cancer.....26

1.1.7.2 Epigenetic drivers.....30

1.1.7.2.1 MicroRNA.....30

1.1.7.2.2 Long non-coding RNAS.....32

1.1.7.3 Tumour microenvironment in ovarian cancer pathogenesis.....33

1.1.7.3.1 Adipocytes.....34

1.1.7.3.2 T cells.....34

1.1.7.3.3 Macrophages.....35

1.1.7.3.4 The role of ascites in metastasis and chemoresistance.....36

1.1.8 Mutation signatures and biomarkers for ovarian cancer.....38

1.1.8.1 Utilisation of mutation signatures in the clinic.....38

1.1.8.2 Prognostic implications of the C1-C5 classification of high-grade serous tumours.....39

1.1.8.3 Diagnostic and prognostic biomarkers for ovarian cancer.....41

1.1.9 Molecular mechanisms of chemoresistance in ovarian cancer.....42

1.1.9.1 Alterations in drug transport and metabolism.....42

1.1.9.2 DNA repair pathways in resistance.....43

1.1.9.3 Survival Pathways and resistance.....44

1.1.9.3.1 PIK3/AKT and STAT3 44

1.1.9.3.2 Autophagy and chemo-resistance 46

1.2 Cell death mechanisms in cancer 47

1.2.1 Apoptosis 47

1.2.2 Necrosis and Necroptosis 49

1.2.3 Mitotic Catastrophe 50

1.2.4 Immunogenic Cell Death 51

1.3 Molecular regulation of Autophagy 52

1.3.1 What is autophagy? 52

1.3.2 Types of autophagy 52

1.3.3 Autophagic vesicle formation and trafficking 53

1.3.3.1 Formation of the autophagosome 53

1.3.3.2 Autophagosome elongation 54

1.3.3.3 Autophagosome/Lysosome tethering and fusion 56

1.3.4 Signalling pathways regulating autophagy 57

1.3.4.1 PI3K/AKT/mTOR signalling 57

1.3.4.2 AMPK 58

1.3.4.3 TFEB (transcription factor EB) 59

1.3.4.4 P53 59

1.4 Selective Autophagy 60

1.4.1 Mitophagy 60

1.4.2 Nucleophagy 61

1.4.3 Aggrephagy 62

1.5 Other forms of autophagy 63

1.5.1 Non-canonical autophagy 63

1.5.2 LC3-associated phagocytosis 66

1.6 Unconventional protein secretion 67

1.6.1 Secretory autophagy 67

1.6.2 Exosome secretion 68

1.7 Autophagy and Cancer 70

1.7.1 Autophagy as a tumour suppressor 70

1.7.2 Autophagy in tumour progression 71

1.7.3 Modulating autophagy for cancer treatment 72

1.7.4 Autophagy in ovarian cancer 75

1.8 Thesis hypothesis and aims 78

1.9 References 79

Chapter Two: Evaluation of the response of a panel of ovarian cancer cell lines to paclitaxel and carboplatin 99

2.1 Abstract 100

2.2 Introduction 102

2.3 Materials and Methods 104

2.3.1 Cell culture and Reagents 104

2.3.2 Drug treatments 105

2.3.3 Colony formation assay....108

2.3.4 Evaluation of morphology....108

2.3.5 Evaluation of caspase-3 activity by flow cytometry....109

2.3.6 Western Blotting....109

2.3.7 Cyto-ID Autophagy Detection kit....110

2.3.8 Immunofluorescence....110

2.3.9 Statistical Analysis....111

2.4 Results....112

2.4.1 Working concentrations of paclitaxel and carboplatin were established for a panel of human and one murine ovarian cancer cell line....112

2.4.2 Assessment of apoptosis induction in ovarian cancer cell lines following treatment with paclitaxel and carboplatin....118

2.4.3 Apoptosis is decreased, and recovery is increased, in ovarian cancer cells following a single round of paclitaxel treatment....126

2.4.4 Ovarian cancer cells express key autophagy proteins....130

2.4.5 Basal autophagy is present in human ovarian cancer cell lines....132

2.4.6 Assessment of induction of autophagic flux following drug treatment....135

2.5 Discussion....145

2.6 References....150

Chapter Three: Evaluation of pharmacological modulators of autophagy: chloroquine, lithium and brefeldin A, on a panel of ovarian cancer cell lines. 153

3.1 Abstract....154

3.2 Introduction 155

3.3 Materials and Methods 157

3.3.1 Cell culture and Reagents 157

3.3.2 Drug treatments 158

3.3.3 Colony formation assay 160

3.3.4 Cyto-ID autophagy detection kit 160

3.3.5 Western Blotting 161

3.3.6 Evaluation of morphology 161

3.3.7 Statistical Analysis 162

3.4 Results 163

3.4.1 Inhibition of autophagy with CQ sensitises ID8-luc2 cells to paclitaxel and carboplatin 163

3.4.2 Assessment of the effect of CQ on recovery of OVCAR-3 and OVCAR-4 cells following treatment 165

3.4.3 Inhibition of autophagy with chloroquine sensitises OVCAR-5 and OVCAR-8 cells to paclitaxel and carboplatin 167

3.4.4 Lithium significantly enhances chemosensitivity in a panel of OC cell lines 169

3.4.5 Evaluation of the effects of lithium on autophagy 173

3.4.5.1 Evaluation of the effects of lithium on autophagy in ID8-luc2 cells ... 173

3.4.5.2 Evaluation of the effects of lithium on autophagy in OVCAR-5 and -8 cells 176

3.4.6 Non-canonical autophagy may contribute to basal autophagy in OVCAR-5 and OVCAR-8 cells 179

3.4.7 Non-canonical autophagy may contribute to the response to paclitaxel in OVCAR-5 and OVCAR-8 cells 181

3.5 Discussion 183

3.6 References 189

3.7 Supplementary figures 192

Chapter Four: Inhibition of autophagy reduces recovery and enhances chemo-sensitivity in ovarian cancer cells following treatment with paclitaxel 194

4.1 Abstract 195

4.2 Introduction 196

4.3 Materials and Methods 198

4.3.1 Cell culture and Reagents 198

4.3.2 siRNA transfection 198

4.3.3 Drug treatments 199

4.3.4 Colony formation assay 199

4.3.5 Western Blotting 200

4.3.6 Statistical Analysis 200

4.4 Results 202

4.4.1 Inhibition of autophagy demonstrates its role in chemoresistance in ID8-luc2 cells 202

4.4.2 Knockdown of key autophagy genes BECN1 and ATG5 sensitises OVCAR-5 and OVCAR-8 cells to paclitaxel 204

4.4.3 Knockdown of Rab9 and BECN1 sensitises OVCAR-5 and OVCAR-8 cells to paclitaxel 208

4.5 Discussion 212

4.6 References 215

Appendix 1: 216

Uncropped western blots 216

1. Uncropped western blots 217

Chapter Five: Autophagy is involved in the recovery of DNA content following paclitaxel treatment 219

5.1 Abstract 220

5.2 Introduction 221

5.3 Materials and Methods 223

5.3.1 Cell culture and Reagents 223

5.3.2 Drug treatments 223

5.3.3 Immunofluorescence 224

5.3.4 siRNA transfection 224

5.3.5 Cell Cycle Analysis 225

5.4 Results 226

5.4.1 ID8-luc2 cells recover a typical DNA profile following paclitaxel and carboplatin treatment, and this is impeded by chloroquine 226

5.4.2 Nuclear material colocalises with LC3 and LAMP1 after paclitaxel treatment in ID8-luc2 cells....229

5.4.3 OVCAR-8 cells can recover a typical DNA profile following paclitaxel treatment, which is not impeded by CQ....231

5.4.4 Nuclear material colocalises with LC3 and LAMP1 after paclitaxel treatment in OVCAR-8 cells....233

5.4.5 Knockdown of key autophagy genes in OVCAR-8 cells impedes the recovery of the parental cell cycle profile....236

5.5 Discussion....239

5.6 References....242

Chapter Six: General Discussion....244

6.1 Key findings from thesis work....245

6.2 General Discussion....247

6.3 References....260

Appendix 2: National Cancer Control Programme GP Ovarian Cancer Referral Guidelines....262

2. National Cancer Control Programme (NCCP) Ovarian cancer referral guidelines 263

Appendix 3: Cell line information....266

3. Cell Line Information....267

3.1 ID8-luc2 cell line....268

3.2 OVCAR-3 cell line....269

3.3 OVCAR-4 cell line.....270

3.4 OVCAR-5 cell line.....272

3.5 OVCAR-8 cell line.....273

Appendix Four: Project Outputs.....275

4.1 Manuscripts currently in preparation for submission: 276

4.2 Poster and Oral presentations.....276

Declaration

This is to certify that the work I am submitting is my own and has not been submitted for another degree, either at University College Cork or elsewhere. All external references and sources are clearly acknowledged and identified within the contents. I have read and understood the regulations of University College Cork concerning plagiarism.

Signed: _____

Jennifer Quinn

Acknowledgements

My PhD has been a challenging, rewarding and fulfilling experience. I feel extremely privileged to have been given this opportunity, and I would like to express my gratitude to those who helped me on this journey.

Firstly, I must thank my PhD supervisors Dr. Sharon McKenna and Dr. Tracey O'Donovan. I could not have wished for better supervisors. They have been there to guide, teach and support me, both personally and professionally. Their dedication and passion for science has inspired me, and the knowledge and skills they have taught me are invaluable. Words cannot thank them both enough.

I would also like to acknowledge Breakthrough Cancer Research, Seamus Carr and all his family, friends and fundraisers, whose joint funding of the Brid Carr ovarian cancer research scholarship, made this project possible. I am extremely grateful for their support.

Thank you to my colleagues at Cancer research @ UCC who have supported me along the way. I would like to thank Suzanne Crotty for her time and expertise in assisting me with confocal imaging. I would particularly like to thank Juliet, whose friendship, kindness, and love carried me through. To Yensi, who shared in the up and downs with me, encouraged me and always believed in me.

I would not be where I am today without the unconditional love and support of my family. To my mother, Amanda, and my father, Laurence, words cannot express how grateful I am to you both for making me the woman I am, and for helping me to achieve my dreams. To my brother Laurence, for always making me laugh. I would like to thank my grandad Leo, for always believing in me, and keeping me company on the train journeys back to Dublin. I know he would be so proud of this thesis.

Lastly, and most importantly, to my twin sister Leah. My biggest supporter, she has always been by my side to encourage me and pick me up when I was down. I cannot express my gratitude enough for her love and support.

Thesis abstract

Ovarian cancer (OC) is the leading cause of death in women from gynaecological malignancies. Late stage diagnosis occurs in most women due to the benign nature of disease symptoms. Cytoreductive surgery and chemotherapy remains the standard of care for patients. Chemotherapy resistance is the biggest challenge faced in the clinic, with over 80% of women experiencing disease recurrence. As such, it is vital to identify and target the mechanisms which drive resistance in order to improve patient outcomes.

We have evaluated a panel of ovarian cancer cell lines for their response to two clinically relevant chemotherapies, paclitaxel and carboplatin. From our analysis, two subgroups of cells with differential drug responses emerged. The cell lines which were most sensitive to both drugs (OVCAR-3 and -4) displayed the highest levels of active caspase-3, a marker of apoptosis, while the most resistant cells (ID8-luc2, OVCAR-5 and -8) displayed the lowest levels of active caspase-3. OC patients receive their treatment in cycles, with treatment free intervals between doses. To mimic this, the cell lines with the highest drug-induced apoptosis levels were recovered for 7 days after treatment and were then re-challenged with paclitaxel. Following this re-challenge, apoptosis levels were found to be significantly decreased compared to the initial toxicity, while clonogenic recovery was significantly increased, providing a novel insight into one of the ways OC cells may become resistant to treatment.

We then evaluated the autophagy competency of the OC cell line panel. All of the cell lines were found to express the key autophagy proteins Beclin 1, LC3 and the Atg5/12 conjugate, although to different levels. To assess basal autophagy, chloroquine (CQ) was used to prevent autophagosome turnover. Each of the cell lines demonstrated the ability to undertake basal autophagy, although to varying levels. We then assessed the

effect of paclitaxel and carboplatin on autophagy induction. Interestingly, the cell lines could again be sub-grouped based on their autophagy induction. Reflecting the same groups as the apoptosis data, the OVCAR-3 and -4 cells displayed the lowest levels of autophagy induction, while the ID8-luc2, OVCAR-5 and -8 cells had the highest autophagy induction. It is notable that the OVCAR-8 cells were found to have the highest autophagy levels but expressed the lowest levels of Beclin 1 and Atg5/12. This data has particular relevance in clinical biomarker studies as it suggests that autophagy protein expression levels do not correlate with OC cells ability to undergo autophagy.

Autophagy has been implicated in OC chemoresistance, and it is emerging as an attractive therapeutic target. We therefore examined the effect of two autophagy modulators, CQ and lithium, on the chemosensitivity of the OC cell lines. Interestingly, both CQ and lithium exerted significant chemosensitising effects, but only in the cell lines which displayed high levels of autophagy (ID8-luc2, OVCAR-5 and -8). In the OVCAR-3 and -4 cells, the addition of CQ provided either no effect or a protective effect following treatment. These data suggest that the use of such modulators will only benefit a subset of patients, but in these patients, they could have significant therapeutic benefit. Brefeldin A, which inhibits transport from the Golgi, has been reported to inhibit the non-canonical Atg5/Atg7-independent autophagy pathway. Following treatment with CQ, the addition of brefeldin A significantly reduced autophagosome accumulation. Similarly, the addition of brefeldin A following paclitaxel treatment significantly reduced autophagosome accumulation. These data suggest that Atg5/Atg7-independent autophagy may be present in OC cells both basally and in response to treatment.

The contribution of autophagy to chemoresistance in OC cells was then assessed in the cell lines that displayed high levels of autophagy. We have shown that knockdown

of BECN1 and ATG5 by siRNA significantly reduces the recovery of ID8-luc2 and OVCAR-8 cells following paclitaxel treatment. To assess a role for Atg5/Atg7-independent autophagy in paclitaxel response, the non-canonical gene Rab9 was knocked down using siRNA along with BECN1. Knockdown of these genes significantly reduced clonogenic recovery in OVCAR-8 cells following paclitaxel treatment. These data suggest that both the canonical and non-canonical autophagy pathways may contribute to chemoresistance in OC cells.

We have also shown that OC cells can recover their DNA profile following recovery from paclitaxel treatment. Importantly, inhibition of autophagy with CQ could impede this recovery in ID8-luc2 cells. Furthermore, siRNA knockdown of BECN1 and ATG5 in OVCAR-8 cells could also impede the recovery of the DNA profile. Additionally, we observed the localisation of the autophagy markers LC3 and LAMP1 with fragmented nuclear material after paclitaxel treatment. Taken together, these data support the possibility that a selective type of autophagy, termed nucleophagy, may be active in OC cells and contribute to recovery following paclitaxel treatment.

Here, we have made potentially clinically relevant observations. We have highlighted reduced apoptosis competency following drug re-challenge and shown that autophagy modulators are effective only in a subgroup of cell lines with high autophagy levels. We have provided a novel insight into a role for canonical and non-canonical autophagy in OC chemoresistance, and demonstrated for the first time a potential role for nucleophagy in OC cell recovery. It is hoped that autophagy inhibitors, along with appropriate biomarkers, may be incorporated into treatment strategies to overcome treatment resistance and improve OC patient outcomes.

Abbreviations

℃	Degrees Celsius
AA	Arachidonic acid
AJCC	American Joint Committee on Cancer
AMPK	Adenosine monophosphate protein kinase
APAF-1	Apoptotic protease-activating factor-1
ATG	Autophagy related
ATM	Ataxia-telangiectasia mutated
ATP	Adenosine triphosphate
ATR	ATM and Rad-3 related
BEP	Bleomycin, etoposide, cisplatin
BMI	Body mass index
BNIP3	BCL2 and adenovirus E1B 19 kDa-interacting protein 3
BRIP1	BRCA1 interacting protein C-terminal helicase 1
BNIP3L	BNIP3-like
CIMD	Caspase-independent mitotic death
CIPN	Chemotherapy-induced peripheral neuropathy
CMA	Chaperone mediated autophagy
CML	Chronic myeloid leukaemia
COSMIC	Catalogue of somatic mutations in cancer
CQ	Chloroquine
CRT	Calreticulin

CSC	Cancer stem cell
CTL	Cytotoxic T cell
DAI	DNA activator of interferon
DAMP	Danger associated molecular pattern
DC	Dendritic cell
DISC	Death-inducing signalling complex
DMEM	Dulbecco’s modified eagles medium
DMSO	Dimethyl sulfoxide
DRAM	Death-inducing signalling complex
DR	Death receptor
ECM	Extra cellular matrix
ELCS	Envelope limited chromatin sheets
EMA	European Medicine’s Association
EMT	Epithelial mesenchymal transition
EOC	Epithelial ovarian cancer
FADD	Fas-associated death domain
FasL	Fas ligand
FCS	Fetal calf serum
FDA	Food and drug administration
FIGO	Federation of Gynecology and Obstetrics
FFPE	Formalin-fixed paraffin-embedded
GP	General practitioner

GTPase	Guanosine triphosphatase
HBOC	Hereditary breast and ovarian cancer syndrome
HCC	Hepatocellular carcinoma
HDAC	Histone deacetylase
HCQ	Hydroxychloroquine
HGSOC	High grade serous ovarian carcinoma
HK2	Hexokinase 2
HLA	Human leukocyte antigen
HNPCC	Hereditary non-polyposis colorectal cancer
HOST2	Human OC-specific transcript 2
HOTAIR	Hox transcript antisense intergenic RNA
HPNC	Human peritoneal mesothelial cell
HSP	Heat shock protein
IAP	Inhibitor of apoptosis
ICD	Immunogenic cell death
IgG	Immunoglobulin
ILV	Intraluminal vesicle
IMPase	Inositol monophosphatase
IP	Intraperitoneal
KEGG	Kyoto Encyclopedia of Genes and Genomes
LAP	LC3-associated phagocytosis
LGSOC	Low grade serous ovarian cancer

LCD	Lysosomal cell death
LIR	LC3 interacting region
LMP	Lysosomal membrane permeabilisation
lncRNA	Long non-coding RNA
LPS	Lipopolysaccharide
MLKL	Mixed lineage kinase-domain like
MMC	Mouse mammary carcinoma
MMP-9	Matrix-metalloprotease-9
MMR	Mismatch repair
MN	Micronuclei
MOMP	Mitochondria outer membrane permeabilisation
MVB	Multivesicular body
NCCD	Nomenclature Committee on Cell Death
NCCP	National cancer control programme
NCS1	Neuronal calcium sensor 1
NER	Nucleotide excision repair
NK	Natural killer
NSCLC	Non-small cell lung cancer
OC	Ovarian cancer
OSE	Ovarian surface epithelium
PBMC	Peripheral blood mononuclear cell
PDS	Primary debulking surgery

PE	Phosphatidylethanolamine
PFA	Paraformaldehyde
PFS	Progression-free survival
PIKK	PI3K-related kinase family
PKM2	Pyruvate kinase M2
PRR	Pattern recognition receptor
PtdIns 3-kinase	Phosphatidylinositol 3-kinase
RCD	Regulated cell death
RFS	Recurrence-free survival
RHEB	Ras homolog enriched in brain
RICTOR	Rapamycin-insensitive companion of mTOR
ROS	Reactive oxygen species
RPMI	Roswell park memorial institute
SCNA	Somatic copy number alteration
shRNA	Short hairpin RNA
SITC	Serous tubal intraepithelial carcinoma
SMAC	Second mitochondria-derived activator of caspase
STAT3	Signal transducer and activator of transcription-3
STUB1	STIP1 homology and U-Box containing protein 1
TCGA	The Cancer Genome Atlas
TFEB	Transcription factor EB

TGFBIp	Transforming growth factor-β-induced protein
TLR	Toll-like receptor
TNF	Tumour necrosis factor
TNFR1	TNF-receptor 1
TNM	Tumour node metastasis
TRADD	TNF receptor-associated death domain
TRPML1	Transient receptor potential calcium channel mucolipin subfamily member 1
TSC1/2	Tuberous sclerosis 1 and 2
TVUS	Trans-vaginal ultrasound
TXNDC17	Thioredoxin domain containing 17
UCA1	Urothelial carcinoma associated 1
UPR	Unfolded protein response
VPS	Vacuolar sorting protein
ZBP1	Z-DNA binding protein-1

Chapter 1: General Introduction

1.1 Ovarian Carcinoma

1.1.1 Incidence of ovarian carcinoma

Ovarian cancer (OC) is the seventh most common gynaecological malignancy among women worldwide, with epidemiological data indicating that the highest age adjusted occurrences are found in developed regions of the world, namely north America and Europe (C. Wang *et al.*, 2017)(Reid, Permuth and Sellers, 2017). In Ireland, ovarian cancer was the fourth most commonly diagnosed cancer among women between 2015 and 2017 (National Cancer Registry Ireland). Ovarian cancer is prevalent among older women, with over one third of all invasive cancers diagnosed in women aged between 60 and 74 years. The mortality rate has remained largely unchanged, with 5-year survival remaining less than 40% (National Cancer Registry Ireland). A better understanding of the molecular mechanisms underlying the various subtypes of OC is imperative in order to aid the discovery and development of new treatments to improve patient outcomes.

1.1.2 Screening and diagnosis

The introduction of prophylactic screening in ‘at risk’ populations has contributed to the early detection and increased survival rates among people with cervical cancer. Prophylactic screening has also proven to be a critical factor in the improved survival rates observed in other solid malignancies such as breast cancer, while Bowel Screen has recently been implemented for the early detection of colorectal cancer in Ireland. However, there are currently no reliable markers for the early detection of OC.

Ovarian cancer is often dubbed the ‘silent killer’ due to the vague and non-specific symptomatic nature of the disease. Despite this, symptoms of ovarian cancer are

present during the early stages of disease, on average 3 to 6 months prior to consulting a physician (Goff, 2012). The most common symptoms reported include abdominal discomfort, such as bloating and nausea, which can often be mistaken for gastrointestinal ailments. Due to the benign nature of the symptoms, the majority of ovarian cancers are diagnosed at an advanced stage (III or IV), resulting in poor survival rates.

Women who experience symptoms typically consult with their physician for an initial examination. This includes a physical examination, to determine the presence of a pelvic mass or ascites, or signs of shallowed breathing, an indicator of pleural effusion which is a common symptom of OC. A referral to a specialised gynaecologist is the next step, where trans-vaginal ultrasound (TVUS) and blood CA125 levels may be assessed. Serum CA125 levels above 35 UI/ml are considered abnormal. The risk malignancy index (RMI) is utilised in order to distinguish benign from malignant masses, which incorporates CA125 levels, menopausal status and ultrasound features. Premenopausal women are assigned a score of 1, while post-menopausal women receive a score of 3 (Karimi-Zarchi *et al.*, 2015). The study by Karimi-Zarchi *et al.* (2015) highlighted the relatively high specificity of using RMI to distinguish patients with malignant masses at an initial stage for further interventions.

A number of studies have also been undertaken to assess the potential utility of TVUS as an early detection method. The University of Kentucky Markey Cancer Centre's ovarian cancer screening program conducted TVUS on over 45,000 women. The study found that regular TVUS examinations were proficient at detecting early stage cancers. In addition, women whose cancer was detected at an early stage and underwent treatment were found to have a better outcome (van Nagell *et al.*, 2011).

However, due to economic reasons it is unlikely that TVUS would be utilised as a screening tool in the general 'low risk' population.

The prostate lung colorectal and ovarian screening trial (PLCO) assessed the impact of annual CA125 and TVUS screening on OC mortality. When compared to a control cohort of women, who received standard care and were not offered screening, no reduction in OC mortality was found (Buys *et al.*, 2011). In 2017, extended patient follow-up by a further 6 years, corroborated the initial study findings, reporting no benefit of CA125 and TVUS screening on mortality rates (Pinsky *et al.*, 2016).

Another large study was conducted to assess the impact of screening on OC related deaths. The United Kingdom Collaborative Trial of Ovarian Cancer Screening (UKCTOCS) study recruited over 200,000 postmenopausal women from England, Northern Ireland, and Wales (Jacobs *et al.*, 2016). Prevalent cases, classed as women diagnosed with OC before screening commenced, were excluded. Women were randomised into one of three groups – multimodal screening (MMS), whereby CA125 screening in combination with the risk of OC calculation was used, annual transvaginal ultrasound screening (USS), or no screening. Ovarian cancer death was the primary outcome, while death by OC and primary peritoneal cancer was the secondary outcome. The primary results from the study revealed no significant reduction in mortality in the screened groups. However, following the exclusion of prevalent cases a significant reduction in mortality was found in the MMS group, revealing a 28% reduction in mortality following 7 years of screening. While this result was encouraging, the authors concluded that further follow up of patients would be required to accurately assess both the cost and efficacy of screening for OC patients.

In Ireland, in 2016 new referral guidelines were introduced by the National Cancer Control Program to help GP's identify and prioritise women with suspected ovarian cancer. These are included in Appendix 1. The aim is to facilitate earlier detection by highlighting symptoms that may be suggestive of ovarian cancer. It provides GPs with a step-wise algorithm for assessing worrisome symptoms.

1.1.3 Histological subtypes of Ovarian Cancer

Ovarian cancer is a broad term, which describes a range of distinct histological subtypes. Identifying the subtype is important in terms of both treatment and patient outcome. Ovarian cancer can be broadly separated into four subtypes: epithelial, germ cell, sex cord stromal, and metastatic tumours, as illustrated in Figure 1.1. While some OC tumours originate from cells within the ovary itself, such as germ cell tumours, other tumours, such as epithelial tumours, including high grade serous cancers (HGSOC), are proposed to originate from the fallopian tubes (Venkatesan, 2017)(Xiang, L, *et al*., 2018). Elucidating the cellular origin and subsequent pathogenesis of the OC subtypes is imperative in aiding the development of new treatments.

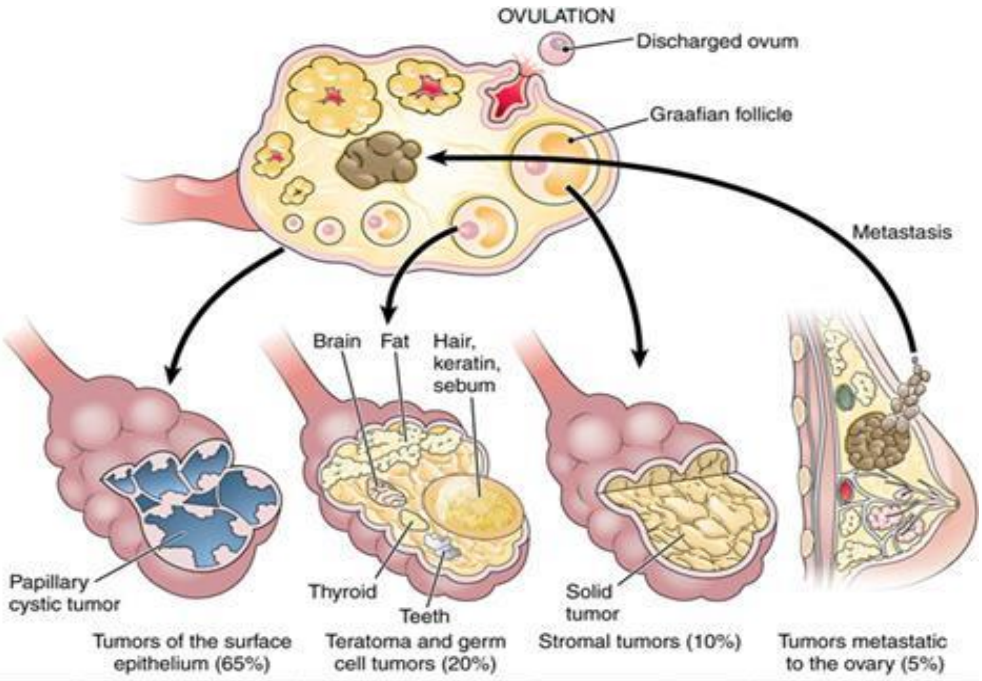

Cell of origin:	Surface epithelial cells	Germ cells	Sex cord, stromal cells	Metastasis to ovaries (Krukenberg)
Proportion (%) of ovarian tumors:	65-70%	15-20%	5-10%	5%
Proportion (%) of malignant ovarian tumors:	90%	3-5%	2-3%	5%
Age group affected:	>20 years	>25 years	All ages	Adults
Types:	• Serous tumor • Mucinous tumor • Endometrioid tumor • Uncommon types • Cystadenocarcinoma	• Teratoma • Dysgerminoma • Uncommon types	• Fibroma • Granulosa-theca cell tumor • Sertoli-Leydig cell tumor	Metastases from: • Breast • Lung • Colon • Other sites

Figure 1.1: The above image describes the four histological subtypes of ovarian cancer, along with their incidence. From: Soslow, R. A. (2008) 'Histologic Subtypes of Ovarian Carcinoma', International Journal of Gynaecological Pathology.

1.1.3.1 Epithelial Tumours

Epithelial tumours comprise the vast majority of ovarian cancers diagnosed, of which serous tumours are most prevalent. Ovarian carcinomas of epithelial origin include serous, intestinal mucinous, endometrioid and clear cell (Soslow, 2008). Serous cancers can be defined as low or high grade, with high grade serous ovarian

carcinomas most commonly diagnosed. Both low and high grade serous tumours tend to present at a late stage (III or IV) and can be distinguished from one another by their varied genetic alterations and route of pathogenesis (McCluggage, 2011). HGSOC often originate as serous tubal intraepithelial carcinomas (SITC) in the fimbria of the fallopian tube (Karnezis *et al.*, 2016). Supporting the theory of a fallopian tube origin for HGSOC, precursor lesions were identified in high risk patients undergoing prophylactic salpingo-oophorectomies (Medeiros *et al.*, 2006; Callahan *et al.*, 2007). Endometrioid tumours remain the second most commonly diagnosed tumours, with many arising due to a state of chronic inflammation associated with endometriosis. They typically present at an early stage (I) and are usually well differentiated (McCluggage, 2011). Mucinous tumours, often described as intestinal, are very rare, originating from mucinous cystadenomas, progressing in a sequential manner. The vast majority are unilateral, involving only one ovary, and diagnosed at an early stage (I) (McCluggage, 2011). Clear cell carcinomas have a poor prognosis compared to other epithelial subtypes when diagnosed at an advanced stage and are known to be more resistant to first line platinum therapies (Mabuchi, Sugiyama and Kimura, 2016). Interestingly, the incidence of clear cell carcinomas varies according to ethnicity, with approximately 4% in Caucasians, 3.1% in black people and 11.1% among Asian populations, although a reason for this has not been elucidated (Anglesio *et al.*, 2011).

1.1.3.2 Germ Cell tumours

Germ cell tumours are rare tumours which arise from oocytes within the ovaries. Histological subtypes include dysgerminoma, yolk sac tumour, choriocarcinoma and immature teratoma (Low, Ilancheran and Ng, 2012). Dysgerminoma is the most

common germ cell tumour, accounting for 2% of cases. These tumours are prevalent in younger women of reproductive age, typically under the age of 30. Germ cell tumours almost always present unilaterally and are exceptionally chemosensitive. Fertility preserving surgery is recommended, even with the presence of metastatic disease. Unilateral salpingo-oophorectomy and preservation of the contralateral ovary and uterus is recommended (Gershenson, 2007). Adjuvant chemotherapy is administered to women with stage IA disease or later (Low, Ilancheran and Ng, 2012). The BEP (bleomycin, etoposide, cisplatin) regimen is widely used, with overall survival ranging from 87 to 98% (Dimopoulos *et al.*, 2004) (Williams *et al.*, 1994).

1.1.3.3 Sex Cord Stromal Tumours

Sex cord stromal tumours are rare neoplasms, representing 7% of ovarian tumours diagnosed. Such tumours arise from a heterogeneous mix of either sex cord or stromal cells. Sex cord cells include granulosa and sertoli cells, while examples of stromal cells include fibroblasts, theca and leydig cells (Horta and Cunha, 2015). Sex cord stromal tumours are diagnosed across a broad age spectrum but tend to present in younger women. Stage 1 disease is commonly diagnosed and treated with primary surgery, resulting in favourable outcomes for patients. Platinum chemotherapy can be administered to patients with advanced stage or recurrent disease, with response rates of up to 80% (Ray-Coquard *et al.*, 2014).

1.1.4 Ovarian cancer risk factors

1.1.4.1 Age

As with most cancers, the risk of developing OC increases with age. Although OC is diagnosed in younger women, the majority of cases are diagnosed in postmenopausal women over the age of 50. In Ireland, during the period 2005-2015, the median age group at diagnosis was 65-69 years (National Cancer Registry Ireland).

1.1.4.2 Family History

Arguably the most significant risk factor for the development of OC is a family history of the disease. Approximately 10% of all ovarian cancers diagnosed arise due to a hereditary genetic predisposition. While several syndromes are linked to hereditary ovarian cancer - Li-Fraumani, Cowden and Peutz-Jeghers, it is hereditary non-polyposis colorectal carcinoma (HNPCC), also known as Lynch Syndrome, and hereditary breast and ovarian cancer syndrome (HBOC) which are the most tightly linked (Lindor *et al.*, 2008). As would be expected, women with HBOC syndrome have a family history of breast and/or ovarian cancers, passed through successive generations in an autosomal dominant manner. Studies into the genetic causation of hereditary ovarian cancers have predominantly focused on the BRCA1 and BRCA2 genes. BRCA genes are involved in homologous recombination DNA repair, a high-fidelity pathway used to repair double strand breaks. Women who carry mutations in these genes, namely BRCA1, have a significantly increased lifetime risk of developing ovarian cancer; 25-65% when compared to the general populations risk of only 1.5% (Lindor *et al.*, 2008). Germ line mutations in the BRCA1 or BRCA2 genes, which are involved in DNA repair, account for 90% of hereditary cases. The remaining 10% are

attributable to mutations in mismatch repair genes, namely hMLH1 and hMSH2, which are associated with HNPCC (Prat, Ribe and Gallardo, 2005). Cumulative lifetime risks of developing OC are 40% for BRCA1 carriers and 18% for BRCA2 carriers (Chen and Parmigiani, 2007). Ovarian cancers driven by BRCA mutations tend to present earlier, with serous cancers being the predominant subtype. Numerous studies have indicated that the presence of a germline BRCA mutation is associated with better prognosis, including a study by Ben-David *et al.*(2002) reporting BRCA mutation to be an independent prognostic factor (Rubin *et al.*, 1996)(David *et al.*, 2002). However, there are a small proportion of patients with a strong family history of OC who do not carry a BRCA mutation. The advent of next generation sequencing has allowed large scale screening of entire genomes, revealing multiple mutations which may also contribute to OC risk. Among 466 women tested in a recent study, the most significant alterations were found in genes involved in the homologous repair pathway, highlighting its significance in ovarian cancer pathogenesis. BRIP1, a member of the Homologous Recombination repair pathway which interacts with BRCA, was found to be the most prevalent mutation among the cohort (Chen and Parmigiani, 2007). Further studies have uncovered mutations in several other important DNA repair proteins, including RAD51C and RAD51D, with RAD51C mutations detected in 2.9% of highly penetrant ovarian cancer families (Kroeger and Drapkin, 2017) (Lilyquist *et al.*, 2017). Mutations in the lower fidelity mismatch repair pathway, including MLH1, MSH2 and MSH6, are known to underpin Lynch syndrome, which also carries an increased risk of developing OC at 6-8% (Lu and Daniels, 2013). Such mutations in multiple DNA repair pathways provides a rationale for the efficacy of the FDA approved PARP inhibitor Olaparib as a maintenance therapy in women regardless of BRCA status.

1.1.4.3 Environmental risk factors

Reproductive risks have been widely reported to contribute to OC development. In 1971, Fathalla put forward the 'incessant ovulation' hypothesis, that repeated cycles of ovulation from menarche to menopause during a woman's lifetime increases the risk of developing OC. It was suggested that repeated cycles of damage and subsequent repair at the ovarian surface epithelium predisposes to genetic instability and thus malignant transformation. Supporting this idea is the finding that women on the oral contraceptive pill have a reduced risk for OC development (Beral *et al.*, 2008). Similarly, parity has also been shown to reduce the risk of developing OC, reportedly due to the decrease in the number of ovulatory cycles (Fathalla, 2013). Parity describes the number of pregnancies carried to 20 weeks in the United States, and 24 weeks in the United Kingdom (Opara and Zaidi, 2007).

In recent years, the role of obesity in promoting and propagating cancer has come to the forefront and is particularly relevant in hormone driven cancers. Cancer has often been described as a wound that does not heal, in a constant state of systemic inflammation. Adipose cells can themselves be described as hormones and contribute to providing a microenvironment in which cancer cells can thrive. This is particularly pertinent when describing OC, due to the proximity of the omentum, which is a common site of metastasis. While there are conflicting theories in the literature, the consensus appears to be that increased obesity and BMI (body mass index) are associated with an increased risk of OC only in pre-menopausal women (Z. Liu *et al.*, 2015) (Kuper, Cramer and Titus-Ernstoff, 2002).

Talcum powder was first suggested to be a carcinogen, due to its chemically similar structure to asbestos, which is a carcinogen linked to OC development following work place exposure (Acheson *et al.*, 1982). Results are conflicting, and while some studies

have suggested a link between perineal talc exposure and increased risk for OC, no biological basis for this has been shown (Muscat and Huncharek, 2008).

1.1.5 Staging of ovarian cancer

The staging of ovarian cancer is based on the International Federation of Gynecology and Obstetrics (FIGO) surgical system, in conjunction with corresponding Tumour Node Metastasis (TNM) classifications devised by the American Joint Committee on Cancer (AJCC), as outlined in table 1.1. FIGO broadly classifies four stages of disease (I-IV), with further sub classifications based on the extent of disease spread. In 2014 FIGO updated its classifications, eliminating sections believed to be redundant. Stage I describes disease confined to one or both ovaries or fallopian tubes. Stage II classifies disease which has extended to extra-ovarian pelvic organs, such as the bowl or bladder. Cancer cells may also be present in the fluid of the abdomen. Subsequent to FIGO classification revisions in 2014, stage IIB is no longer sub classified, while stage IIC has been removed completely (Prat *et al.*, 2015). Stage III cancers comprise the vast majority of cancers diagnosed, with high grade serous carcinomas being the most prevalent. These tumours are typified by spreading along the abdominal and pelvic peritoneum. Although a rare occurrence, FIGO revisions provide for a new classification, IIIA1, defining disease present in retroperitoneal lymph nodes with the absence of intraperitoneal dissemination (Prat *et al.*, 2015). Stage IV describes distant metastasis, such as the presence of pleural effusion or parenchymal liver metastasis (Prat *et al.*, 2015).

FIGO classification	**Tumour Extension**	**TNM classification**
I	Tumour limited to the ovaries or fallopian tubes	T1
IA	Tumour limited to one ovary; capsule intact, no tumour on ovarian surface; no malignant cells in ascites or peritoneal washings	T1a
IB	Tumour limited to both ovaries; capsule intact, no tumour on ovarian surface; no malignant cells in ascites or peritoneal washings	T1b
IC	Tumour limited to one or both ovaries with any of the following: **IC1:** surgical spill intraoperatively **IC2:** capsule ruptured before surgery or tumour on ovarian surface **IC3**: malignant cells present in ascites or peritoneal washings	T1C
II	Tumour involves one or both ovaries or fallopian tubes with pelvic extension (below pelvic brim)	T2
IIA	Extension and/or implants in the uterus and/or fallopian tubes and/or ovaries	T2a
IIB	Extension and/or implants in other pelvic intraperitoneal tissues	T2b
III	Tumour involves one or both ovaries, or fallopian tubes, with cytologically or histologically confirmed spread to the peritoneum outside the pelvis and/or metastasis to the retroperitoneal lymph nodes	T3
IIIA	Metastasis to the retroperitoneal lymph nodes with or without microscopic peritoneal involvement beyond the pelvis	T1, T2, T3aN1
IIIA1	Positive retroperitoneal lymph nodes only (cytologically or histologically proven)	T3a
IIIA(i)	Metastasis of ≤ 10mm in greatest dimension (tumour dimension, not lymph node dimension)	T3a/T3aN1

IIIA (ii)	Metastasis of > 10mm in greatest dimension	
IIIA2	Microscopic, extra pelvic peritoneal involvement (above the brim) with or without involvement of retroperitoneal lymph nodes	T3a/T3aN1
IIIB	Macroscopic, extra pelvic, peritoneal metastasis ≤ 2cm in greatest dimension with or without involvement of retroperitoneal lymph nodes	T3b/T3bN1
IIIC	Macroscopic, extra pelvic, peritoneal metastasis > 2cm in greatest dimension with or without involvement of retroperitoneal lymph nodes (includes extension to capsule of liver or spleen)	T3c/T3cN1
IV	Distant metastasis excluding peritoneal metastasis	
IVA	Pleural effusion with positive cytology	Any T, Any N
IVB	Metastasis to extra abdominal organs including parenchymal metastasis, inguinal lymph nodes and lymph nodes outside of abdominal cavity	M1

Table 1.1: Details of the TNM (tumour node metastasis) staging system and the International federation of gynaecology and obstetrics (FIGO) classifications are described (Mutch and Prat, 2014).

1.1.6 Management of ovarian cancer

1.1.6.1 Surgical management

Clinical management of ovarian cancer is unique, given that regardless of stage or histological classification, surgery is indicated first. A primary debulking surgery (PDS) is usually performed on women with a suspected ovarian cancer. This surgery is important to not only effectively resect tumour, but also to determine the cancer stage. This can be done by performing peritoneal washings and scrapings, and by visual evidence of cancer spread beyond the ovaries. A number of studies have identified optimal debulking as a primary prognostic factor, thus it is recommended such surgeries are performed by those with specialist training, such as gynaecology oncologists.

1.1.6.2 Chemotherapeutics and targeted therapies

1.1.6.2.1 Chemotherapy

The earliest regimen of chemotherapeutics used in the treatment of advanced ovarian cancer consisted of intravenous administration of doxorubicin (an anthracycline) coupled with cyclophosphamide (a DNA cross linker). In the 1980's, the platinum drug cisplatin was added to this regime. Following subsequent clinical trials, cisplatin and cyclophosphamide became the standard of care for first line treatment of ovarian cancer.

Current recommendations state that surgery alone is indicated for early stage IA or B tumours. Patients with stage III and IV disease receive adjuvant chemotherapy following PDS. The current standard of care involves the administration of a platinum

compound, such as cisplatin or carboplatin, in conjunction with a taxane agent, such as paclitaxel. Carboplatin and paclitaxel are the preferred combination due to their combined lower toxicity profile.

A major challenge in the clinical management of OC is the high rate of disease recurrence. Approximately 80% of women that exhibit an excellent response to first line therapy present with recurrent disease. In this instance, second line treatment depends upon the length of time until recurrence. Recurrent ovarian cancer can be classified as platinum sensitive or platinum resistant. Platinum sensitive patients generally receive a second round of platinum agents. Platinum resistant patients are offered alternative drugs, such as liposomal doxorubicin, gemcitabine or etoposide. However, response to these second line therapies remains poor, highlighting the need for targeted therapies.

While PDS is important in the management of OC, not all women are eligible for PDS, due to the existence of precluding comorbidities, poor performance criteria or old age. The nutrition status of the patient is an important factor to assess pre-surgery. Low prealbumin levels are associated with malnutrition and postoperative complications and morbidity in OC patients (Geisler *et al.*, 2007). Neoadjuvant chemotherapy allows such patients to improve their nutritional status before debulking surgery. A number of clinical indicators may also identify patients where optimal debulking is unlikely, and who should receive neoadjuvant chemotherapy. Such indicators include extraperitoneal disease spread (such as lung metastasis), diaphragmatic or liver disease greater than 2cm, bowel adhesions or thickening and the detection of ascites in a minimum of two-thirds of CT scan slices (Nelson, Rosenfield and Schwartz, 1993) (Wright *et al.*, 2016). In these instances, neoadjuvant chemotherapy is administered to reduce the tumour burden, after which, interval debulking surgery can be performed.

A comprehensive review of guidelines surrounding neoadjuvant chemotherapy and interval debulking for advanced OC patients was conducted by (Wright *et al.*, 2016).

Given that the peritoneal cavity is the primary site of disease spread, intraperitoneal (IP) administration of chemotherapy drugs was developed as a means to deliver targeted and more concentrated doses to tackle disseminated disease. A number of large scale trials were designed to assess any benefits of IP chemotherapy. Results from the GOG-172 study revealed significant improvements in both progression-free survival (PFS) and overall survival (OS) when cisplatin and paclitaxel were administered IP as opposed to IV (Armstrong *et al.*, 2006). IP administration however proved toxic, with less than half of patients completing the planned number of therapy cycles. Further analysis of the GOG-172 study also revealed that in patients with aberrant expression of BRCA1, IP cisplatin increased survival to 84 months, up from 47 months in patients receiving IV cisplatin (Lesnock *et al.*, 2013). Following a meta-analysis of IP chemotherapy trials by the National Cancer Institute (NCI), it recommended the use of IP cisplatin for optimally debulked stage III OC patients. Despite this recommendation, IP administration has yet to be widely adopted. Further trials were conducted which compared IP to IV administered carboplatin, which is more clinically relevant. The GOG-252 study of women with newly diagnosed advanced OC revealed no survival benefit of IP chemotherapy compared to IV carboplatin administration (Walker et al., 2019). It has been hypothesised however, that the concurrent administration of bevacizumab in this trial may have adversely impacted the efficacy of IP chemotherapy. The Intraperitoneal Therapy for Ovarian Cancer with Carboplatin (iPOCC) trial compared the efficacy and safety of IP versus IV carboplatin with weekly IV paclitaxel, without bevacizumab, and thus may give a

more accurate comparison of IV versus IP carboplatin (Fujiwara et al., 2011). Survival analysis is expected to be competed in 2020.

As mentioned at the start of this section, paclitaxel and carboplatin are the preferred chemotherapy doublet used in the clinic. Paclitaxel functions in the cell as a microtubule stabiliser. It binds to the β tubulin subunit of the microtubule and reduces the threshold amount of purified tubulin subunits required for polymerisation into microtubules. It also enhances the number the tubulin subunits which assemble, stabilising the microtubule (Schiff, Fant and Horwitz, 1979). Cancer cells treated with paclitaxel undergo mitotic arrest, due to the activation of the spindle assembly checkpoint. Carboplatin causes the formation of intra and interchain DNA adducts by covalently binding to purine bases. The formation of such adducts impedes DNA replication and transcription (Todd and Lippard, 2009).

1.1.6.2.2 PARP inhibitors

Currently, Olaparib is FDA approved for use in a select cohort of patients with recurrent OC. Only those who carry a BRCA mutation and have received three prior chemotherapeutic options are eligible to receive Olaparib (Bixel and Hays, 2015). However, as will be discussed later in this review, PARP inhibitors have also shown to be beneficial in women without BRCA mutations, but with defects in other DNA repair genes. PARP inhibitors such as Olaparib exploit the synthetic lethality model, whereby a combination of gene mutations results in cell death, as shown in figure 1.2. Women with BRCA mutations have defective DNA repair pathways used to mend double strand breaks, such as homologous recombination and non-homologous end joining. BRCA defect alone is not enough to elicit a lethal phenotype, as single strand

break repair pathways such as nucleotide excision repair (NER), base excision repair (BER) and mismatch repair still function to repair damage. PARP is a key enzyme involved in such single strand repair pathways, whose inhibition via Olaparib renders the cell unable to repair DNA damage, resulting in cell death. The administration of Olaparib was shown to extend the time to recurrence from 4.3 months to 11.2 months compared to the placebo group (Ledermann *et al.*, 2014). The SOLO1 trial evaluated the use of olaparib as a maintenance therapy in newly diagnosed patients with advanced (stage III or IV) HGSOC or endometrioid cancer, with a BRCA1 or 2 mutation, or both (Moore *et al.*, 2018). Women in the trial had either a complete or a partial response to platinum chemotherapy. Compared to patients who received a placebo, a significant improvement in PFS was observed in patients who received Olaparib as a maintenance therapy. The authors reported a 70% reduction in the risk of disease progression or death following Olaparib treatment. While the advent of such treatments has been proven to successfully improve PFS, they have not been shown to improve the patient's OS. Recent studies suggest that patients with mutations in other DNA repair genes will also have a good response to PARP inhibitors. The recent approval of PARP inhibitors including olaparib, rucaparib and niraparib by the FDA and European Medicines Agency (EMA) for use in all platinum sensitive patients regardless of BRCA mutation status supports this. The phase III NOVA trial found that the addition of niraparib as maintenance therapy, in platinum sensitive patients could improve PFS, regardless of BRCA mutation status (NCT01847274). In the absence of PARP, DNA damage is repaired via homologous recombination repair (HRR). Defects in HRR related genes, including ATM, CHEK2 and RAD51C represent a small portion of HGSOC patients, but may have clinical utility in identifying those patients with BRCA mutation who will benefit from PARP inhibition

(Matsumoto *et al.*, 2019). Through research and a deeper understanding of the molecular pathogenesis of OC, it is hoped that treatments will serve not only to extend time to progression, but to achieve meaningful and potentially curative responses in patients.

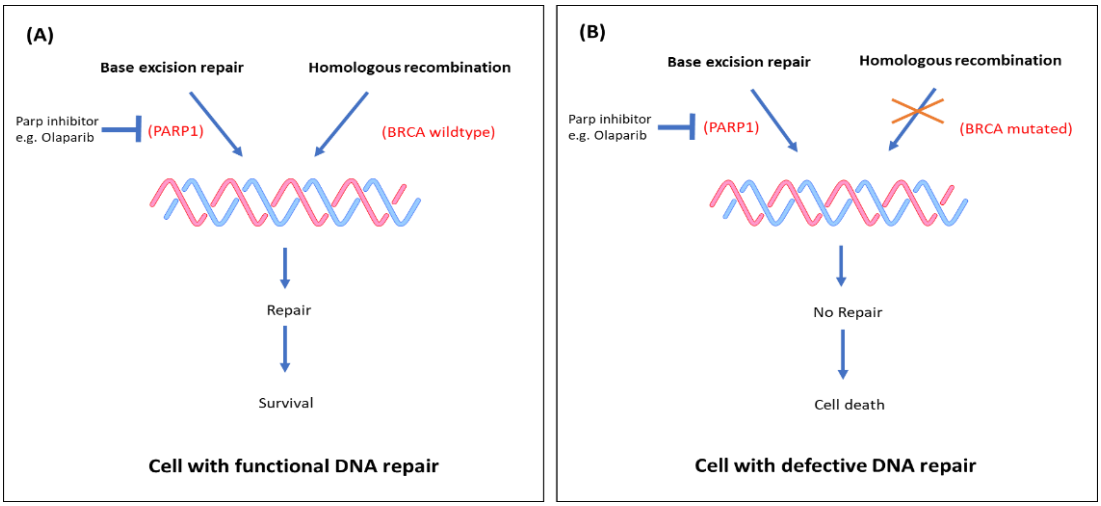

Figure 1.2: The use of PARP inhibitors is predicated on BRCA mutation resulting in defective homologous recombination repair. Cells use various pathways to repair DNA damage. (A) PARP inhibition in cells with functional homologous recombination can still repair damage via this pathway. (B) Inhibiting PARP in BRCA-mutated, homologous recombination-defective cells, means the cell has no pathway to repair DNA damage. *(Adapted with permission from JD Iglehart and DP Silver. (2009) NEJM 361:189–191, copyright Massachusetts Medical Society.)*

1.1.6.2.3 Anti-angiogenic agents

Angiogenesis, the process of forming new blood vessels, plays an integral role in tumour growth and metastasis. In ovarian cancer, it also has a role in the development of malignant ascites (Graybill *et al.*, 2015). The anti-VEGF monoclonal antibody Bevacizumab is the most widely studied anti-angiogenic, which has shown efficacy in other solid malignancies including colorectal and breast cancer. Bevacizumab has

approval for use in women as a first line therapy, and in women with stage III or IV cancer with residual disease following surgery. It is also approved for use in the recurrent setting, for women with either platinum sensitive or platinum resistant disease. Two large phase III trials conducted, GOG-218 and ICON7, demonstrated improved PFS in poor prognosis women following administration of Bevacizumab in conjunction with carboplatin and paclitaxel in the first line setting (Burger *et al.*, 2011; Perren *et al.*, 2011). Despite this, the final OS results revealed that the addition of Bevacizumab to platinum chemotherapy provided no OS benefit in the study population (Oza *et al.*, 2015). Additionally, further trials have evidenced significant improvement in PFS with the addition of Bevacizumab in the recurrent setting. The addition of Bevacizumab to carboplatin or gemcitabine in platinum-sensitive and platinum-resistant relapsed disease significantly improved PFS for these women (Aghajanian *et al.*, 2012; Pujade-Lauraine *et al.*, 2014). However, following publication of the final analysis of OS from the GOG-218 study, no survival benefit was observed in patients receiving bevacizumab with their chemotherapy (Tewari *et al.*, 2019). A meta-analysis assessed the efficacy of anti-angiogenic agents in the recurrent ovarian cancer setting and associated toxicities. The addition of VEGF antagonists was found to provide an OS benefit to platinum sensitive patients, but not to platinum resistant cohorts, and also resulted in enhanced toxicities (Yi *et al.*, 2017). Due to the unwarranted toxicities arising from anti-angiogenic therapies, elucidating clinically relevant markers to identify patients who will respond to treatment is necessary. An ongoing phase IV trial MITO16/MANGO-2 aims to assess clinical factors and biological markers to aid in the identification of patients which will benefit from the addition of Bevacizumab to first line chemotherapy (NCT01462890).

1.1.6.2.4 Immunotherapies in ovarian cancer

Dendritic cells (DCs) are the most potent antigen presenting cells, displaying antigen for the activation of T cells. In the cancer setting, their numbers are usually quite low. DC therapy involves harvesting the patients DCs, growing them and exposing them to tumour antigen before reinfusing high numbers back into the patient. Natural killer (NK) cells are key players in the innate immune response, unique in the fact that they do not require antigens or MHC to elicit their effects. Thus, they can elicit a rapid response to virus-infected cells or importantly, tumour antigens, whilst sparing healthy cells that express MHC class 1 molecules (Pampena and Levy, 2015). The addition of NK cells to DC therapy was introduced following evidence that NK cells can eliminate immature DCs whilst selecting for a highly immunogenic subset of activated DCs (Ferlazzo *et al.*, 2002). A case study reported in 2017 has highlighted the potential of DC/NK cell therapy in enhancing chemotherapeutic efficacy and inducing a durable remission. A 74 year - old woman presented with severe ascites and large masses on the left ovary. A diagnosis of serous carcinoma with metastasis to the omentum and peritoneum was made. During the implementation of a chemotherapy regimen, comprising docetaxel and paclitaxel, the patient also received infusions of monocyte derived DCs, which had been exposed to tumour antigens, CA-125, WT1, NY-EOS1 and telomerase, along with NK cells. These antigens were selected based on the patient's human leukocyte antigen (HLA) type. Three months following initiation of the DC/NK cell therapy, there was no evidence of ascites, while the peritoneal mass had shrunk in size enabling laparoscopic debulking. In this case the patient went into remission and was still cancer free 13 months on (Sasada, Abe and Abe, 2017).

Similar to DCs, NK cells present in ascites have been found to be malfunctioning. As part of their function, NK cells release cytokines such as TNF-α and IFNγ. In a bid to

enhance NK cell activity from ovarian ascites, a study by Geller *et al*. (2017) combined a novel IL-15 super agonist and the PD-L1 antagonist Pembrolizumab. Expression of TNF- α and IFNγ was found to be enhanced following this combination treatment, resulting in a significant decrease in tumour burden in a mouse model of ovarian cancer (Geller *et al.*, 2017). IL-15 stimulates NK cell growth and expansion, as well as aiding their cytolytic capabilities (Rautela and Huntington 2017). While immunotherapies have been trialled and shown to have efficacy, particularly in melanomas, clinical trials of immune therapies for ovarian cancer is a recent occurrence. Tumour-associated macrophages are the most abundant immune cells which infiltrate the ovarian microenvironment, eliciting an anti-inflammatory effect. Colony stimulating factor, also referred to as CSF-1, is essential for proliferation and survival of macrophages. The use of an anti-CSF-1 mAB in mice models effectively depleted tumour associated macrophages, while simultaneously increasing the numbers of $CD4^+$ and $CD8^+$ cytotoxic T cells (Krishnan et al 2017). This paved the way for a clinical trial with a humanised anti-CSF-1 antibody developed by Roche in 2011. Early results from this trial (NCT01494688) indicate the antibody is well tolerated and can deplete tumour associated macrophages. T cells, such as $CD4^+$ and $CD8^+$ cytotoxic T cells, are key effector cells in mounting an immune response. CTLA-4 is a negative regulator of T cell activity, resulting in what is known as T cell anergy. In an immune supressed tumour microenvironment, blocking CTLA-4 results in the activation of $CD4^+$ and $CD8^+$ T cells. The anti-CTLA-4 monoclonal antibody Ipilimumab (Yervoy, Bristol Meyers Squibb) has had efficacy in melanoma patients and was FDA approved in 2011. A phase II study is currently underway assessing the efficacy of Ipilimumab as a monotherapy in platinum sensitive ovarian cancer (NCT01611558). Another trial to study the efficacy of immune checkpoint blockade

was the phase II KEYNOTE-100 study (NCT02674061). KEYNOTE-100 is the largest study to date to assess the safety and efficacy of the monotherapy Pembrolizumab, an anti-PD-1 antibody, in patients with recurrent OC. The objective response rate (ORR), although durable (≥ 6 months), was modest at just 8%. Importantly, higher PD-L1 expression corresponded to a better response, highlighting its potential role as a clinical maker to predict response.

The Javelin solid tumour trial assessed the safety and efficacy of Avelumab, a PD-L1 inhibitor, in advanced OC patients, with recurrent and/or resistant disease who previously received platinum chemotherapy. Monotherapy Avelumab showed anti-tumour efficacy and acceptable safety (Disis *et al.*, 2019). The Javelin Ovarian 100 trial aimed to assess the efficacy of Avelumab in combination with or following carboplatin/paclitaxel in OC patients with advanced disease (stage III or IV), who were treatment naïve (NCT02718417). Interim analysis indicated no benefit to PFS in patients receiving Avelumab over chemotherapy alone, resulting in the termination of the trial. The Javelin Ovarian PARP 100 trial was designed to assess the efficacy of combining Avelumab with chemotherapy, followed by a maintenance therapy of Avelumab with the PARP inhibitor talazoparib in women with stage III or IV disease (Eskander *et al.*, 2019). However, results from the Javelin Ovarian 100 trial prompted investigators to discontinue the trial. Finally, the Javelin 200 trial evaluated the efficacy of Avelumab in combination with pegylated-liposomal doxorubicin (PLD) versus PLD alone in platinum resistant/refractory patients (Pujade-Lauraine *et al.*, 2019). No survival benefit was found when avelumab was administered with PLD compared with PLD alone.

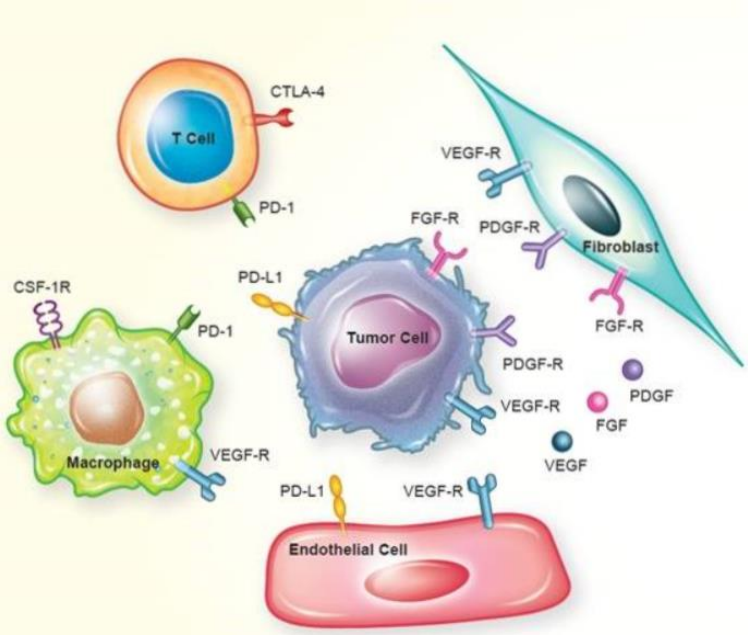

Molecular Target	Therapeutic Agent	Mechanism of Action	Hazard ratio for PFS and OS (95% CI)	Reference (Study)
VEGF	Bevacizumab	Monoclonal antibody to VEGF-A	HR-PFS: 0.72 (0.63–0.82) HR-OS: 0.89 (0.75–1.04)	Burger RA, et al. *NEJM*. 2011;365:2473–2483. [66] (GOG-218)
			HR-PFS: 0.81 (0.70–0.94) HR-OS: 0.99 (0.85–1.14)	Perren TJ, et al. *NEJM*. 2011;365:2484–2496. [67] (ICON7)
			HR-PFS: 0.48 (0.38–0.60) HR-OS: 0.85 (0.66–1.08)	Pujade-Lauraine E, et al. *J Clin Oncol*. 2012;30 (18suppl): LBA5002. (AURELIA)
			HR-PFS: 0.53 (0.41–0.70) HR-OS: 0.96 (0.76–1.21)	Aghajanian C, et al. *J Clin Oncol*. 2012;30:2039–2045. [152] (OCEANS)
			HR-PFS: 0.61 (0.52–0.72) HR-OS: 0.83 (0.68–1.005)	Coleman RL. SGO 2015. (GOG-213)
	Aflibercept	Soluble VEGFR	Not available (ongoing)	Coleman RL, et al. *Lancet Oncol*. 2011;12:1109–1117. [81]
FGFR, VEGFR, PDGFR	Nintedanib	Receptor tyrosine kinase inhibitor for FGFR1–3, VEGFR1–3, PDGFR α,β	HR-PFS: 0.84 (0.72–0.98) HR OS: Not available	Du Bois A, et al. *J Clin Oncol*. 2013;31 (18suppl): LBA5503. (AGO-OVAR12)
VEGFR, PDGFR, c-kit	Cediranib	Receptor tyrosine kinase inhibitor for VEGFR 1–3, PDGFR-α, c-kit	HR-PFS: 0.57 (0.44–0.74) HR-OS: 0.70 (0.51–0.99)	Ledermann JA, et al. *Eur J Cancer*. 2013;49 (suppl): LBA (ICON6)
	Pazopanib	VEGFR 1–3, PDGFR α,β, c-kit	HR-PFS: 0.77 (0.64–0.91) HR-OS: 0.99 (0.75–1.32)	Du Bois A, et al. (AGO-OVAR16)
PD-1	Nivolumab	Anti-PD1 antibody	Not available (ongoing)	Hamanishi J, et al. *J Clin Oncol*. 2014;32 (suppl): 5511.
	Pembrolizumab	Anti-PD1 antibody	Not available (ongoing)	Varga A, et al. *J Clin Oncol*. 2015:33 (suppl): 5510.
PD-L1	Avelumab	Anti-PD-L1 antibody	Not available (ongoing)	Disis ML, et al. *J Clin Oncol*. 2015;33 (suppl): 5509.

VEGF(R): Vascular endothelial growth factor (receptor)
FGFR: Fibroblast growth factor receptor
PDGFR: Platelet-derived growth factor receptor
PD-1: Programmed cell death protein 1
PD-L1: Programmed death-ligand 1
PFS: Progression free survival
OS: Overall survival

Figure 1.3. **Summary of therapies targeting the tumour microenvironment in ovarian cancer**. The agents listed have demonstrated safety/efficacy in phase I/II trials, and/or improved survival in phase III trials. VEGF(R): vascular endothelial growth factor (receptor), FGFR: fibroblast growth factor receptor, PDGFR: platelet-derived growth factor receptor, PD-1: programmed cell death protein 1, PD-L1: programmed death-ligand 1, PFS: progression-free survival, OS: overall survival, CI: confidence interval, HR: hazard ratio. From: Hansen *et al.*, 2016.

1.1.7 Molecular pathogenesis of ovarian carcinoma

1.1.7.1 Genomic landscape of ovarian cancer

1.1.7.1.2 Sporadic ovarian cancer

New classifications have broadly divided OC tumours into two categories, Type I and Type II tumours. Recent large scale genomic studies have validated this subdivision and have further expanded the grouping of ovarian tumours according to their genetic features (see Table 1.2). Type I tumours, including low grade serous OC tumours (LGSOC) and clear cell tumours, are typically described as indolent and follow a less aggressive clinical course, with disease commonly confined to one ovary. Mutations in genes such as KRAS, PIK3CA, ARID1A and PTEN are frequently found (Y. K. Wang *et al.*, 2017). Conversely, Type II tumours, including high grade serous carcinomas (the most common subtype), follow an aggressive course and typically spread beyond the ovaries. Type II tumours almost universally harbour p53 mutations which are rarely found in Type I tumours. Mutations in genes involved in homologous recombination repair are common in Type II tumours, as are mutations in genes such as FOXM1, RB1 and NOTCH 3 (Testa *et al.*, 2018). In addition, type II tumours display chromosomal instability, while Type I are relatively stable. While this broad classification may be suited to Type II tumours, as molecular and cell of origin studies advance, it is becoming clear that Type I tumours are too heterogenous to group together. Going forward, Type I tumours should be classified as distinct diseases and not automatically considered to be indolent. This is evidenced by the fact that mucinous OC (classified as Type I) can be clinically aggressive and have high proliferation rates (Kobel *et al.*, 2008). Of all the histological subtypes, LGSOC and HGSOC best fit the Type I and II dualistic model (Salazar, Campbell and Gorringe, 2018).

Several studies on high grade serous ovarian cancers suggest that they are relatively unique in that they are driven not by repeated point mutations, but rather by copy number alterations. Copy number alterations manifest themselves as structural changes to the genome, including chromosomal deletions or gains, which can vary considerably in size. To elucidate potential therapeutic targets, the cancer genome atlas undertook a comprehensive analysis of 489 high grade serous ovarian cancer patient samples. Matched 'normal' DNA was also obtained and analysed for each patient. Mutation analysis, via the Illumina GAIIx and ABI SOLid 3 platforms, revealed significant mutations in six genes: RB1, NF1, FAT3, CSMD3, GABRA6 and CDK1 (The Cancer Genome Atlas, 2011). High grade serous cancers were found to have strikingly high levels of somatic copy number alterations (SCNAs). One of the most prominent copy number alterations in ovarian cancer occurs at the 19q12 locus, found to be driven by the CCNE1 gene. This regulates the cell cycle and can cause unwarranted DNA replication and centrosome amplification, thus leading to chromosomal instability (Kroeger and Drapkin, 2017). CCNE1 amplification has been heralded as the leading chromosomal aberration associated with disease relapse following first line chemotherapy (Etemadmoghadam *et al.*, 2009; Naomi *et al.*, 2010).

A recent study was able to identify an amplification in the GAB2 gene, involved in MAPK and PI3K signalling, as being responsible for the transformation of immortalised ovarian and fallopian tube epithelial cells (Dunn *et al.*, 2014). Investigating the functional relevance of such SCNAs is important in understanding the genetic drivers of ovarian cancer development.

A study by Sakai *et al*. (2017), utilised next generation sequencing on formalin-fixed paraffin-embedded (FFPE) tissue from 24 patients to detect mutations in several tumour suppressor genes, including TP53 (53% of samples) and FBXW7 (8.3% of

samples). P53 mutations are present in more than 95% of high grade serous tumours and data suggests that early p53 mutation is necessary for tumour initiation; while BRCA1/2 mutations were detected in 40-50% of high grade serous cancers (Sakai *et al.*, 2017). Given that these genes play integral roles in maintaining genomic stability, it provides a rationale for the chaotic chromosomal rearrangements found in high grade serous tumours and correlates with a poor prognosis.

Tumour	Type	Cells of Origin	Precursor lesion	More frequent mutations	Familial risk
Endometrioid cancer	I	Endometrial epithelial cells	Endometrioid borderline tumour	ARID1A, PIK3CA, TERT	Lynch Syndrome
Ovarian Clear Cell carcinoma	I	Endometrial epithelial cells	Endometrioid borderline tumour	ARID1A, PIK3CA, PTEN, CTNNB1, KRAS, TP53, RPL22	Lynch syndrome
Mucinous carcinoma	I	unknown	Cystadenoma, mucine borderline tumours, Brenner tumours	KRAS, TP53, CDKN2A, BRAF, RNF43	Unknown
Brenner tumour	I	Transitional-like cells of fallopian tube	Benign Brenner tumour	Sporadic point mutations, MYC amplification	Unknown
Low-grade serous carcinoma	I	Fallopian tube progenitor cell or secretory epithelial cell	Serous borderline tumours	KRAS, NRAS, BRAF, EIF1AX, USP9X, FFAR1, NF1, HRAS	Unknown
Seromucinous carcinoma	I	Same as for endometrioid, low-grade serous and mucinous	Same as for endometrioid, low-grade serous and mucinous	KRAS, PIK3CA, PTEN, ARID1A	Unknown
High-grade serous ovarian carcinoma	II	Fallopian tube progenitor cell or secretory epithelial cell	SITC, SCOUT, TP53 signature	TP53, BRCA1, BRCA2, CNAs of CCNE1 amplification, PTEN, RB1 and NF1 loss	BRCA1, BRCA2, BRIP1, PALB2, RAD51C, RAD541D
Ovarian carcinosarcoma or malignant Mullerian mixed	II	Unknown	Unknown	TP53, PI3KCA, PPP2R1A, KRAS, PTEN, CHD4, BCOR, histone H2A and H2B	Unknown
Ovarian granulosa cell tumours	Adult juvenile	Sex cord stromal cells (or granlosa cells)	Unknown	FOX2L in 87% of adult-type patients	Unknown
Sertoli-leydig cell tumour	N/A	Granulosa cells or other stromal cells	None	DICER1	DICER1 syndrome
Small cell carcinoma of the ovary, hypercalcaemic type	N/A	Rare resident ovarian cells	None	SMARCA4	RTPS2 (SMARCA4)

Table 1.2: Summary of ovarian tumour subtypes, cells of origin and defining genetic mutations from a review by (Testa *et al.*, 2018) .

1.1.7.2 Epigenetic drivers

1.1.7.2.1 MicroRNA

MicroRNA are small non-coding RNA molecules which function to post-transcriptionally regulate gene expression. miRNA regulate a large and diverse array of cellular processes and have been previously reported to be aberrantly expressed among various cancer types. DROSHA is an RNase II, which recognises primary-microRNAs (Pri-mRNA) and generates a precursor micro-RNA (pre-miRNA). The pre-miRNA is then transported to the cytoplasm where it is processed by DICER, resulting in two mature single-stranded microRNA molecules which can then be loaded onto the RISC complex and suppress gene expression (Shukla, Singh and Barik, 2011). Low expression of DICER was found to be associated with reduced median survival and advanced disease stage in serous tumours (Merritt *et al.*, 2008). Similarly, low levels of DROSHA was associated with reduced median survival along with 'suboptimal cytoreduction'. The combined reduction in both DICER and DROSHA was found to be a predictor of death from OC, while an increase in both was associated with increased median survival (Wang, Ivan and Hawkins, 2017). Given that low levels of expression of the miRNA machinery correlates with poor prognosis, a meta-analysis has suggested that it is the 'global loss of miRNA' which contributes to the poor prognosis in epithelial ovarian cancer (EOC), with the loss of DICER effectively equating to a loss of a tumour-suppressor.

In the cancer setting, miRNAs are known to play either oncogenic or tumour suppressor roles. miR-133a is a prominent tumour suppressor miRNA, found to be markedly downregulated in all 70 EOC tissue samples analysed. This downregulation of miR-133a was associated with 'advanced clinical stages, poor histological differentiation and lymph node metastasis'(LUO *et al.*, 2014). In line with this, an

analysis of 164 ovarian cancer tissue samples revealed that miR-129-5p was significantly decreased when compared to non-cancerous ovarian samples. This correlated with a higher FIGO stage, histological differentiation and pelvic metastasis (Tan *et al.*, 2015). Expression of miR-181a correlated with a reduced progression free and overall survival. This miR was reported to modulate TGF-β signalling and induce epithelial-mesenchymal-transition (EMT) (Parikh *et al.*, 2014). A common aberration found in ovarian cancers is the downregulation of the *Let-7* microRNA. One of its targets, HMGA2, a DNA binding factor important for the regulation of cell growth, differentiation and apoptosis, is consequently over expressed (Testa *et al.*, 2018). HGMA2 overexpression is found in 65% of ovarian cancers, with the highest prevalence in high grade serous cancers (Mayr, Hemann and Bartel, 2007). *Let-7*/HGMA2 dysregulation provides a molecular marker to enable the distinction of Type I and Type II tumours, with *Let-7* downregulated tumours being less differentiated (Shell *et al.*, 2007). Low *Let-7* expression also results in the increased expression of BRCA1 and RAD51, key players in the repair of double strand DNA breaks. High BRCA1 and RAD51 expression coupled with low *Let-7* expression was found in chemoresistant EOC compared to the sensitive group (Xiao *et al.*, 2017). Chemosensitivity could be improved by over expressing *Let-7* with an antagomir, demonstrating a role for this miR in chemoresistance.

Various miRNA's have been found to differentiate clear-cell from serous tumours, including miR-132, miR-9, miR-126, miR-34s and miR-21 (Wang, Ivan and Hawkins, 2017). In CD44+/CD133+ clear cell ovarian tumours, miR 134-3p was found to be downregulated. The down-regulation of this miR is believed to play a pathogenic role, given it directly targets RAB27A, which plays a role in the downregulation of stem cell markers and adhesion proteins (Chang *et al.*, 2017).

A role for miRNA's in explaining the heterogeneity observed in EOC has recently been proposed and it involves the inappropriate activation of the *HoxA* genes, which are involved in regulating body formation during development. The HOX genes responsible for the differentiation of EOC subtype are primarily found in the 3'-region of the *HoxA* genes. HOXA7 is expressed in endometrial and endocervical epithelia but not ovarian surface epithelium cells (OSE) and is targeted by miR-196. This miR controls the degree of EOC differentiation and promotes a low-grade phenotype. Using a model of *in-vitro* transformed OSE cells, induction of stable HOXA7 expression resulted in the formation of low-grade phenotype tumours which also had stable expression of E-cadherin (Mezzanzanica *et al.*, 2010). In a study comparing EOC versus immortalised ovarian surface epithelium cells (IOSE), of the 35 miRNA which were differentially expressed, only 4 were found to be up-regulated. A comparison of late vs early stage and high vs low-grade EOC, found there was a total down-regulation of these miRNAs. It was found that in advanced EOC, genomic copy number losses and epigenetic silencing may account for 15-36 % of this miRNA down-regulation, respectively. It was also found that of these down-regulated miRNA's in late stage EOC, 25% were clustered across chromosomes 14, 19 and X (Mezzanzanica *et al.*, 2010).

1.1.7.2.2 Long non-coding RNAS

Long non-coding RNAs (lncRNAS) are non-coding RNAs which can regulate gene transcription via the recruitment of chromatin modifying enzymes. One of the most widely studied lncRNA's in cancer is H19. This LncRNA plays an oncogenic role in OC, and overexpression of H19 is associated with metastasis in OC cells (Matouk *et al.*, 2014). Overexpressing histone h1.3, which represses H19, in OVCAR-3 cells,

decreased their growth rate and colony formation (Liu *et al.*, 2013). Human OC-specific transcript 2 (HOST2) is highly expressed in the 4 major 'clinico-pathological' subtypes of OC. It is believed that this lncRNA plays a pathogenic role in OC by acting as an oncogene. HOST2 acts a molecular sponge which controls the availability of miR-let-7b, which is a potential tumour suppressor gene, thereby inducing proliferation, invasion and tumour cell migration (Gao *et al.*, 2015). Urothelial carcinoma associated 1 (UCA1) could act as both a biomarker and therapeutic target for OC. Its overexpression was found to be associated with lymph node metastasis, chemoresistance and poor overall survival in OC patients (Zhang *et al.*, 2016). It could also serve as a therapeutic target given that knockdown of UCA1 reduced the cells ability to migrate and invade. Other lncRNA's have been shown to play a role in OC, such as Hox transcript antisense intergenic RNA (HOTAIR) and PVT1. HOTAIR was found to be expressed in OC tissues which were benign and late-stage versus early stage tumours (Wang et al, 2015). The over-expression of PVT1, due to amplification of *8q24*, was recently found to induce cisplatin, or carboplatin + docetaxel resistance through the regulation of apoptotic pathways. The downregulation of PVT1 in OC cell lines inhibited proliferation and induced a strong apoptotic response **(**Ma et al, 2016).

1.1.7.3 Tumour microenvironment in ovarian cancer pathogenesis

In order to fully elucidate and understand cancer biology, it is imperative to study not only the cancer cells themselves, but also the tumour microenvironment. The ovarian tumour microenvironment comprises a milieu of cells, including various immune cells, fibroblasts, and adipocytes. In addition, malignant ascites, a build-up of peritoneal fluid, also contains a host of cytokines, chemokines and growth factors which can aid tumour progression, metastasis, and drug resistance. Understanding the

complex interactions of microenvironment components with cancer cells will enable improved therapeutic targeting.

1.1.7.3.1 Adipocytes

Among the milieu of cells residing in the tumour microenvironment, a role for adipocytes in promoting tumour growth and chemoresistance has emerged. Traditionally adipocytes are cells which synthesize and store fat. However, recent studies have demonstrated their ability to secrete chemokines, hormones and growth factors into the tumour microenvironment to facilitate and support tumour growth and spread. A study by Niemann *et al*. (2011) illustrated that omentum-associated adipocytes could drive preferential migration of ovarian cancer cells to the omentum in a mouse model. This effect was elicited through the secretion of adipokines such as IL-6, IL-8 and CCL2 (Nieman *et al.*, 2011). Visceral adipocytes in the ovarian microenvironment can promote tumour growth and metastasis by supplying fatty acids. Ovarian cancer cells which had been co-cultured with patient adipocytes derived from the omentum had high levels of the fatty acid receptor CD36. The use of an anti-CD36 monoclonal antibody effectively reduced tumour burden in a xenograft model. Moreover, when compared to matched controls, metastatic tissue expressed higher levels of CD36 (Ladanyi *et al.*, 2018). Thus, targeting adipocyte-induced CD36 expression could attenuate tumour metastasis. Intriguingly, a novel role for adipocytes in altering apoptotic protein expression has been identified. Adipocytes in epithelial ovarian cancer could upregulate BCL_{XL} expression and this was correlated with chemoresistance (Cardenas et al, 2017).

1.1.7.3.2 T cells

T cells play a central role in cell-mediated immunity, recognising antigens from virus infected or tumour cells presented to them other immune cells, for example dendritic

cells. T cells function not only to drive an immune response, via cytotoxic T cells, but also to repress it, via suppressor T cells. Accumulation of cytotoxic $CD8^+$ T cells within the tumour microenvironment has consistently been associated with improved outcomes for ovarian cancer patients (Hwang *et al.*, 2012; Hermans *et al.*, 2014). A subset of T cells, known as Tregs, serve as suppressors of immune cells to maintain tolerance to self-antigens and thus prevent autoimmune disease. The ovarian tumour microenvironment favours the induction and maturation of Tregs via upregulating the CCL2/CCL17 axis, which traffics Tregs to tumours. When compared to non-cancerous ovaries, ovarian tumours and ascites were found to have higher CCL2 mRNA levels. A study conducted with 104 ovarian cancer patients revealed that CCL2- mediated accumulation of Tregs in ovarian tumours was associated with reduced survival and increased risk of mortality (Curiel *et al.*, 2004).

1.1.7.3.3 Macrophages

Macrophages are a subset of white blood cells which engulf and digest foreign bodies via phagocytosis. They can be broadly classified into two subgroups, M1 and M2. M1 macrophages are classically activated, usually by IFN-γ and eliminate viruses and bacteria from the body. In contrast, M2 macrophages are activated by cytokines such as IL-10 and IL-4 and function in wound healing and repair. M1 macrophages which infiltrate tumours can be polarised to an M2 phenotype, enhancing tissue restoration and dampening local immune response (Martinez and Gordon, 2014). The ability of ovarian cancer cells to polarise M1 macrophages to the M2 phenotype has been documented (Hagemann *et al.*, 2006). Co-culture experiments have revealed the crosstalk between ovarian cancer cells and macrophages to support tumour progression. Macrophages co-cultured with ovarian cancer cells developed a

phenotype which resembles macrophages isolated from human tumours. A significant increase in the expression of genes such as CCL2, CCL22, TNF-α and VEGF was observed following co-culture with ovarian cancer cells (Hagemann *et al.*, 2006). Importantly, this effect was not recapitulated by co-culturing with healthy ovarian surface epithelial cells. The importance of tumour associated macrophages (TAMs), believed to have a phenotype resembling M2 macrophages, in aiding ovarian cancer metastasis was evidenced by Yin and colleagues (Yin *et al.*, 2016). To enable migration to distant sites, cancer cells need to be able to survive anoikis, a type of cell death elicited when cells no longer have ECM support. Small clusters of free moving cells known as spheroids were detected in the peritoneal fluid of 128 ovarian cancer patients. High numbers of macrophages within spheroids were correlated with poor overall survival. By secreting EGF, TAMs active EGF signalling in the cancer cells, leading to an upregulation of the VEGF-C/VEGFR-3 autocrine signalling axis. As a result, ICAM-1 is upregulated, and provides a means by which spheroids can attach to macrophages via integrins (Yin *et al.*, 2016). In addition to macrophages, ovarian tumours also have infiltration of dendritic cells (Krempski *et al.*, 2011).

1.1.7.3.4 The role of Ascites in metastasis and chemoresistance

Ovarian cancer can be defined as a peritoneal malignancy, meaning transcoelomic spread of cancer cells is the primary route through which cancer cells adhere to the omentum and serous linings of other organs in the peritoneal cavity. The peritoneal environment is formed from effusions which accumulate within the abdominal cavity, commonly known as ascites. This has its own unique molecular profile, which may aid cancer metastasis and chemoresistance. OC accounts for 38% of all malignant ascites diagnosed in women (Parsons, Lang and Steele, 1996).

A study by Matte *et al*. (2012) conducted on 10 ovarian cancer patients identified several cytokines significantly upregulated in the ascites, including adiponectin, angiogenin, ICAM-1, IL-6, PDGF-BB and RANTES (Matte *et al.*, 2012). Cytokines present in ascites such as IL-6 can induce STAT3 signalling, a pathway influential in mediating chemoresistance via inhibiting pro-apoptotic signalling (Pogg Von Strandmann *et al.,* 2017). A recent study by Mikula-Pietrasik *et al*. (2017) has evidenced a pro-angiogenic role for ovarian malignant ascites. This study was conducted with 48 ovarian cancer patients with different subtypes and grades of disease. Half of the cohort studied had tumours without ascites, while ascites was collected for the remaining 24 patients. Control samples were obtained from women undergoing surgery for the removal of non-cancerous lesions. Antigens against CD31 and CD34, markers of endothelial cells, were used on paraffin fixed tumour specimens. Interestingly, tumours which formed in the presence of ascites displayed higher expression of both antigens when compared to tumours formed in the absence of ascites. Furthermore, analysis of the gap junction protein Connexin-43 was found to be exceptionally high in vascular smooth cells of tumours formed in the presence of ascites (Mikula-Pietrasik *et al.,* 2017). Connexins play a role in angiogenesis through branch formation and their loss has been shown to impair the angiogenic process (C. Gartner *et al*., 2012). These studies illustrate that malignant ascites is eliciting a pro-angiogenic effect and may offer novel therapeutic targets.

1.1.8 Mutation signatures and biomarkers for ovarian cancer

1.1.8.1 Utilisation of mutation signatures in the clinic

Advances in next generation sequencing has enabled a wealth of genetic data to be collected from tumours of cancer patients. Large databases exist, including TCGA (The Cancer Genome Atlas), COSMIC (Catalogue of Somatic Mutations in Cancer) and cBioportal to name but a few. However, these databases have yet to be successfully implemented into clinically useful tools. Discovery of the BRCA gene epitomises the potential of translating genetic analysis of tumours to the clinic. As discussed earlier, patients with a BRCA mutation are particularly responsive to PARP inhibitors such as Olaparib.

There is also potential for mutation signatures to be used in diagnosis and prognosis. The HPRT locus is important for mismatch repair (MMR), with defects in this repair pathway leading to chemoresistance. A recent study identified gene expression changes in HGSOC patients pre- and post-neoadjuvant chemotherapy. Significant changes in expression (greater than 2-fold change) were noted for a total of 86 genes. A BRCA1/2 mutational signature identified was found to have prognostic significance in relation to survival and overall survival rates. Patients with the mutational signature had a progression free survival of 55.2 months, and an overall survival of 46.3 months. In stark contrast, patients lacking the mutational signature had a survival of 38 months, with an overall survival of 23.6 months (Arend *et al.*, 2018). The TCGA (The Cancer Genome Atlas) was also utilised to derive a signature prognostic of lymphatic invasion, a factor known to confer disease aggression and patient survival (Paik *et al.*, 2018). Looking forward there is an urgent need to re-evaluate and assess the genetic data already gathered to try and elucidate potential clinical value. It is clear there are fantastic resources of information available which are being severely under-utilised.

1.1.8.2 Prognostic implications of the C1-C5 classification of high-grade serous tumours

Targeted cancer therapy, whereby mutation profiles and immune signatures are used to deliver a highly personalised, effective and less toxic treatment, have revolutionised cancer treatment. As alluded to earlier, ovarian cancer is a highly heterogenous disease, displaying both inter- and intra-patient variability, making it particularly susceptible to targeted therapies. Tothill *et al.* (2008) were able to identify molecular subtypes of high grade serous ovarian carcinoma and use these to infer chemo-response and patient prognosis. Four predominant subtypes emerged from this study to describe high grade serous tumours, named C1, C2, C4 and C5, as described in Table 1.3 below (C. Wang *et al.*, 2017). These subtypes are predictive of prognosis and may be useful in designing combination therapies for OC in the future.

Subtype	Main features	Genes Expressed	Main pathways	Clinical Outcome
C1/Mesenchymal (28%)	Extensive myofibroblast infiltration (desmoplasia) Mesenchymal gene expression signature	↑ COLL11A1, CXCL14, POSTN, SNAIL2, VCAN, ZEB1	Focal adhesion, ECM receptor interaction JAK-STAT signalling TGF-β signalling VEGF signalling Fibroblast signature EMT/Stem cell	Negative prognosis
C2/Immunoreactive (21.5%)	Extensive intratumoural T lymphocyte infiltration	↑ CXCL10, CXCL11, PSMB8, PSMB9, TAP1	T-cell receptor signalling Toll-like receptor. Antigen presentation machinery	Better prognosis
C5/Proliferative (20.5%)	Low expression of differentiation markers, limited inflammatory infiltration, activation of oncogenic pathways and stem cell factors. Lower BRCA1-2 mut. rate	↑ HMGA2, SALL2, SOX11, TCF7L1	Cell cycle NOTCH signalling	Negative prognosis
C4/Differentiated	Gene signature resembling serous borderline tumours	↑ COLEC11, DEFB1, ITGB4, MGLL, MLPH, STAR	Ribosome Metabolism Cytochrome p450	Intermediate prognosis
C4/Anti-mesenchymal (12.5%)	Downregulation of the genes typically upregulated in the mesenchymal subtype Lower BRCA1-2 mutation rate	↓ COLL11A1, DCN, FAP, POSTN, VCAN, ZEB1	Oxidative phosphorylation Peroxisome Butanoate metabolism	Better prognosis

Table 1.3: Summary of C1-C5 classification: immune signatures, corresponding gene profiles and prognostic significance from (Testa *et al.*, 2018).

1.1.8.3 Diagnostic and prognostic biomarkers for ovarian cancer

Cancer antigen 125 (CA125) is a protein expressed by epithelial tissues, currently approved by the FDA for use a surveillance aid in women diagnosed with OC. A CA125 value above 35 UI/ml is considered above normal. While 85% of women with metastatic OC display elevated CA125 levels, there are limitations which reduce both the specificity and sensitivity of this protein. Approximately fifty percent of women with stage I disease display normal levels of CA125 pre-operatively. In addition, a number of benign ovarian conditions have been shown to elevate CA125 levels, including endometriosis, uterine fibroids, and menstruation (Nowak *et al.*, 2015). As such, research has aimed at elucidating other biomarkers. Human epididymis protein 4 (HE4), while absent from ovarian surface epithelium, is found in the epithelium of fallopian tubes and the endometrium. This protein was found to be more sensitive than CA125, with elevated HE4 expression detected in OC patients with normal CA125 levels. Unlike CA125, HE4 expression is unaffected by benign conditions such as endometriosis and during menstruation (Hallamaa *et al.*, 2012). The examination of HE4 alongside CA125, factoring in menopausal status, led to the development of the Risk Of Malignancy Algorithm (ROMA). The FDA approved ROMA as a diagnostic aid in women presenting with a pelvic mass (Moore *et al.*, 2009). In 2009, a 5-protein panel of biomarkers, termed OVA-1 (consisting of β-2 microglobulin, transferrin, apolipoprotein A-1, transthyretin and CA125), was FDA approved to aid in the presurgical evaluation of ovarian masses. Following on from this, in 2016 an OVA-1 panel with higher specificity, called OVERA, was approved. Despite this progress, research is ongoing to elucidate less invasive biomarkers with higher specificity and sensitivity which can detect OC in the early stages of disease.

1.1.9 Molecular mechanisms of chemoresistance in ovarian cancer

The poor survival rates associated with ovarian cancer are attributable to several factors, predominantly the late stage of disease at diagnosis. As discussed earlier, the treatment of ovarian cancer has remained largely unchanged, with surgery and chemotherapy still the mainstays of treatment. While clinical trials with targeted agents are slowly getting underway, bringing a treatment from bench to beside is a costly and slow process. While the vast majority of patients exhibit an excellent response to first line chemotherapy, a substantial number of women will experience recurrent refractory disease. Once the disease has relapsed, subsequent regimens tend to be aimed at prolonging and improving the quality of life for patients. Thus, elucidating the molecular mechanisms which beget chemoresistance is imperative in improving patient outcomes. A complex array of mechanisms have been implicated in OC chemoresistance, including altered expression of drug efflux pumps, survival signalling pathways and DNA damage responses.

1.1.9.1 Alterations in drug transport and metabolism

Multidrug resistance remains the biggest challenge faced in the management of OC. The overexpression of drug efflux transporters is a key resistance mechanism utilised by cancer cells. These pumps function by reducing the amount of chemotherapy drug which accumulates within a cell, reducing or abolishing the drugs activity. Permeability-glycoprotein (P-gp), a member of the ATP cassette binding (ABC) family of transporters, is one of the best studied efflux pumps, encoded by the MDR1 gene. It can effectively expel a wide range of chemotherapy agents, including taxanes and platinum drugs (Leonard, Fojo and Bates, 2003). Increased expression of P-gp has been shown to negatively impact survival in OC patients (Sedlakova *et al.*, 2015).

Copper exporters, such as ATP7A have also been demonstrated to play a role in platinum resistance. ATP7A sequesters platinum drugs into intracellular compartments thus inhibiting its interaction with nuclear DNA (Samimi *et al.*, 2004). ATP7A is overexpressed in cisplatin resistant OC cell lines, and it's overexpression in OC patients is associated with reduced survival (Samimi *et al.*, 2003).

Altered metabolism of chemotherapeutic in drugs in cancer cells can also contribute to resistance. Members of the cytochrome p450 family of haemoproteins, involved in phase one drug metabolism, catalyses the oxidation of xenobiotics, including chemotherapy drugs, leading to their degradation. One such member, CYP1B1 was found to be overexpressed in malignant versus benign tissue obtained from patients (Zhu *et al.*, 2015). The same study also demonstrated that CYP1B1 expression was associated with paclitaxel resistance in OC cell lines, and its inhibition (using α-naphthoflavone) sensitised the cells to paclitaxel (Zhu *et al.*, 2015).

1.1.9.2 DNA repair pathways in resistance

Given that the primary cytotoxic agents used to treat ovarian tumours are DNA damaging agents, it is little surprise that DNA repair pathways play an important role in resistance. Of the low fidelity repair pathways, nucleotide excision repair (NER) and mismatch repair (MMR) have been implicated in platinum resistance. Platinum agents such as carboplatin and cisplatin cause inter- and intra-strand adducts to form on DNA. Typically, this results in a cell cycle arrest where the damage is rectified, or the cell undergoes apoptosis. NER uses a plethora of proteins to identify, remove and replace damaged nucleotides. Enhanced NER has been correlated with platinum resistance, specifically expression of the protein ERCC1, which complexes with XPF

to excise 5' adducts (Dabholkar *et al.*, 1994; Selvakumaran *et al.*, 2003). MMR recognises and replaces mismatched or unmatched bases. As mentioned earlier, ovarian cancers are deficient in several MMR genes, including MLH1, which enables a cell to continue proliferating in the presence of a platinum agent while evading apoptosis (Strathdee *et al.*, 1999)(Zeller *et al.*, 2012).

1.1.9.3 Survival Pathways and resistance

1.1.9.3.1 PIK3/AKT and STAT3

PIK3 is a serine/threonine protein kinase which regulates several cellular processes including proliferation, metabolism and growth. Aberrant activation of this pathway is frequent in Type 1 ovarian tumours (as described earlier) and has been shown to play a role in chemoresistance (Carden, 2012). Amplification of PIK3CA is evident in up to 40% of ovarian cancers (Huang *et al.*, 2011). Interestingly, P53 has emerged as an important player in PIK3C-mediated chemoresistance. In addition to AKT, P53 inhibits PI3K by binding to the promoter of the PIK3CA gene, thus preventing its transcription. In OC, wild-type P53 is found to be involved in chemoresistance through PI3K/AKT and XIAP. In order to combat this resistance through inhibition of components of the PI3K/AKT pathway, the presence of wild-type P53 is necessary (Abraham and O'Neill, 2014). The role of AKTs in OC has been well characterised. Activation of the PI3K/AKT pathway in OC cells stimulates proliferation, migration and invasion, and inhibits both apoptosis and autophagy. Inhibition of AKT sensitizes chemoresistant OC cells to cisplatin by disrupting the cell cycle, causing S and G2/M phase arrest (Zhang *et al.*, 2016). Other studies have also suggested a role for AKT in resistance to platinum agents. Exposure to platinum induced an AKT-dependent, pro-

survival, DNA damage response in platinum-resistant, but not platinum-sensitive cells. AKT translocates to the nucleus in platinum resistant cells where it is phosphorylated by DNA-PK. This activation of AKT inhibits platinum-mediated apoptosis (Stronach *et al.*, 2011).

Signal transducer and activator of transcription-3 (STAT3) is a transcription factor involved in cytokine and growth factor signalling. A study by Gyoung Jung and colleagues identified increased STAT3 signalling in cells resistant to platinum agents compared to their sensitive parental counterparts. Furthermore, a transcriptional regulator of STAT3 activity in ovarian cancer cells, PBX1, was identified. PBX1 is highly expressed in ovarian cancer and is a known effector in the NOTCH3 pathway, which serves to maintain stemness and promote platinum resistance. Importantly, PBX1 was found to be upregulated in tissue obtained from patients with recurrent disease when compared to primary cancerous tissues and predicted a worse outcome for patients following platinum treatment. Targeting the PBX1/STAT3 axis significantly reduced tumour growth *in vivo* (Jung *et al.*, 2016). A study by Chen *et al*. (2017) has found STAT3 to be enriched in ovarian cancer stem cells, where it can activate WNT/β-catenin signalling through targeting of miR-92a. Combining STAT3 inhibition with paclitaxel treatment could effectively abrogate peritoneal seeding and prolong survival in a mouse model of ovarian cancer (Chen *et al.*, 2017). This signifies STAT3 as a potentially valuable therapeutic target, particularly as disease recurrence is the major clinical challenge faced when treating ovarian cancer. Targeting the cancer stem cell population via STAT3 inhibition could prove to be an effective strategy to combat disease recurrence.

1.1.9.3.2 Autophagy and chemo-resistance

Autophagy is an evolutionally conserved process, which is upregulated in response to various types of stressful stimuli. By upregulating this process, cells can adapt to and recover from a multitude of cellular insults including nutrient depletion, accumulation of protein aggregates, endoplasmic reticulum stress and DNA damage. This has important implications when discussing chemoresistance. Previous studies have implicated a role for autophagy in enabling cancer cells to recover from chemotherapeutic insult (Wang and Wu, 2014; Pagotto *et al.*, 2017). In fact, the DNA damage response can directly induce autophagy. Ataxia-telangiectasia mutated (ATM) and ATM and Rad3-related (ATR) have been shown to activate TSC2 via the LKB1/AMPK pathway and inhibit mTOR1 (Tripathi *et al.*, 2013). This inhibition of mTOR leads to the activation of the autophagy pathway. The cisplatin resistant ovarian cancer cell line A2780cp was found to have elevated levels of autophagy compared to its sensitive counterpart, and blockade of autophagy via the chemical inhibitor 3-MA or Beclin-1 knockdown could effectively re-sensitise the cells to cisplatin (Bao *et al*., 2015). Cancer stem cells (CSCs) are at the forefront of studies into treatment resistance across a broad spectrum of cancers. A key hallmark of CSCs is their chemoresistance, which makes them extremely difficult to eliminate. Thus, it has been suggested that this subpopulation of cells are responsible for tumour regrowth and clinical relapse. An interesting study by Pagotto *et al*. (2017) isolated a $CD44^+$ $CD117^+$ positive putative cancer stem cell subpopulation from epithelial ovarian cancer ascites. This subpopulation of CSCs was found to have higher levels of basal autophagy when compared to its non-stem cell counterparts. CSCs have a unique ability to form spheroids *in-vitro*. The spheroid forming capacity of the $CD44^+$ $CD117^+$ positive CSCs was greatly reduced following treatment with carboplatin plus chloroquine, an

autophagy inhibitor (Pagotto *et al.*, 2017). This effect was not recapitulated with either compound alone, implying a role for autophagy in CSC carboplatin resistance.

1.2 Cell death mechanisms in cancer

1.2.1 Apoptosis

The term 'apoptosis' was first coined by Kerr *et al*. (1972) to describe a process by which cells trigger their own destruction in response to certain stimuli (Kerr, Wyllie and Currie, 1972). Since its discovery it has been become one of the most studied biological processes, with functions ranging from embryonic development, immune system maintenance and normal cell homeostasis. Conversely, its deregulation has been implicated in a number of pathological conditions including autoimmune disease and cancer (Singh, Letai and Sarosiek, 2019).

Several morphological features enable the identification of cells undergoing apoptosis. First, cells shrink, and the chromatin condenses. The cell membrane begins to bulge and bleb, before the cell finally breaks into apoptotic bodies, which can then be cleared via phagocytosis.

Apoptosis is elicited via two main pathways, the intrinsic pathway, stimulated by intracellular stimuli including DNA damage and nutrient depravation, and the extrinsic pathway triggered via extracellular stimuli such as signals from cytotoxic T cells. Both pathways converge with the activation of executioner caspases. The intrinsic pathway is mediated via the mitochondria. Apoptotic stimuli result in the activation of BH-3 only proteins, which in turn activate BAX and BAK. BAX and BAK become oligomerised within the mitochondrial outer membrane, leading to

mitochondrial outer membrane permeabilization (MOMP) (Lopez and Tait, 2015). The release of mitochondrial proteins, notably cytochrome c, second mitochondria-derived activator of caspase (SMAC) and Omi, serve to activate caspases. Cytochrome c is an integral component of the apoptosome, formed in conjunction with pro-caspase 9, dATP and APAF-1 (apoptotic protease-activating factor-1). This complex converts pro-caspase-9 to the active caspase-9, which in turn activates the executioner caspases-3 and -7 (Hassan *et al.*, 2014)(Green and Llambi, 2015).

The extrinsic pathway is triggered via the binding of a cell death ligand to the tumour necrosis factor (TNF) family of death receptors. Well characterised ligand-receptor pairs include TNF (Tumour Necrosis Factor) which binds the TNFR1 (TNF-Receptor 1), FasL (Fas Ligand or CD95) which binds the Fas receptor (FasR or Apo1) and TRAIL (TNF-related apoptosis-inducing ligand) which binds DR4 (Death Receptor 4) or DR5 (Death Receptor 5). Following receptor stimulation, an adaptor protein, such as Fas-associated death domain (FADD) or TNF receptor-associated death domain (TRADD) is recruited, followed by pro-caspase-8 and -10 forming the death-inducing signaling complex (DISC). The pro-caspases-8 and -10 are activated by the DISC, leading to the subsequent activation of the effector caspases -3 and -7 (Pfeffer and Singh, 2018). The extrinsic pathway can activate the intrinsic mitochondrial pathway via the BH3-only protein Bid. Bid is cleaved by caspase-8 activated at the DISC to form tBid, which translocates to the mitochondrial membrane leading to its disfunction and apoptosome formation (Li *et al.*, 1998).

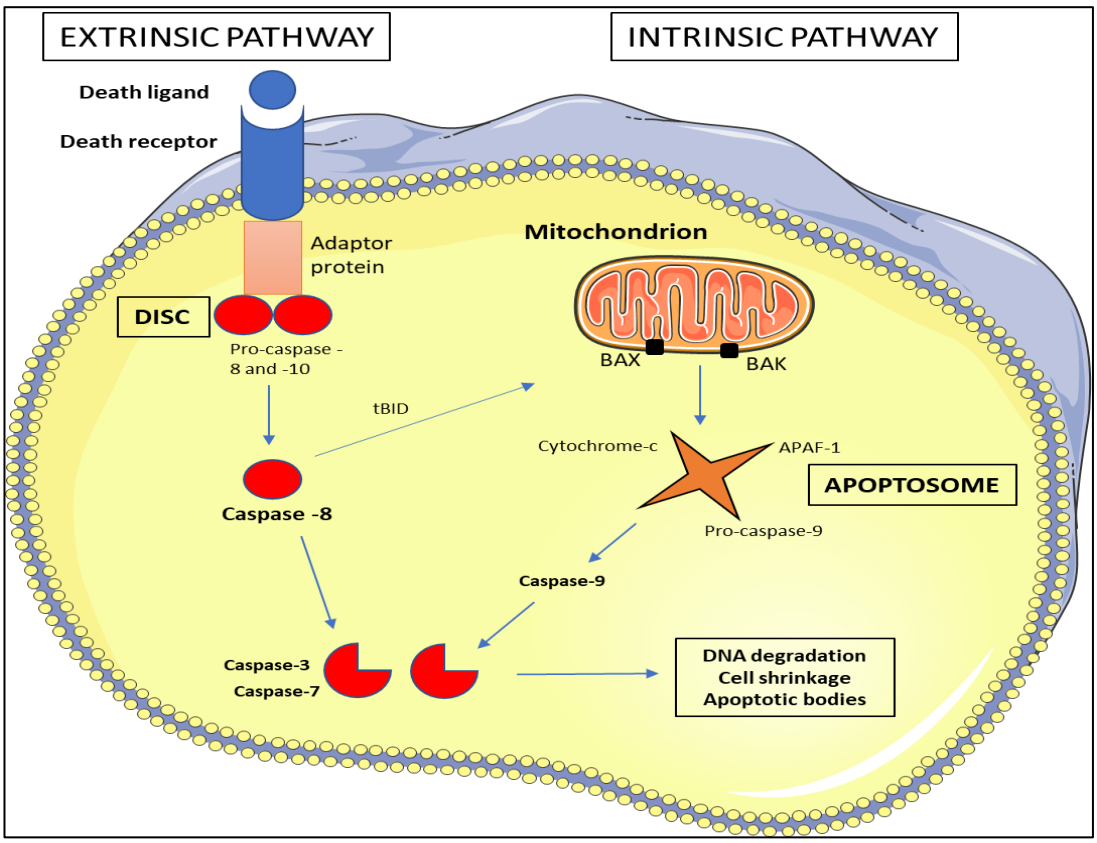

Figure 1.4: Schematic illustration of the apoptosis pathways. Representative image of the intrinsic and extrinsic apoptosis pathways, which converge with the activation of the executioner caspases -3 and -7.

1.2.2 Necrosis and Necroptosis

Necrosis is derived from the Greek expression 'the stage of dying, the act of killing'. Necrotic cells can be distinguished morphologically by early rupturing of the plasma membrane, dilation of cytoplasmic organelles and visible swelling of the cells (Golstein and Kroemer, 2007). Necrosis was thought to be an uncontrolled process; however evidence suggests that its occurrence and progression may be tightly regulated. It has also been shown that inhibition of certain proteins involved in apoptosis and autophagy can induce necrotic cell death (Golstein and Kroemer, 2007).

Necroptosis is a form of regulated cell death (RCD), triggered in response to intra- and extra-cellular stress stimuli, and sensed via death receptors, including FAS and TNFR1, pathogen recognition receptors (PRRs) including TLR3,TLR4 and Z-DNA binding protein 1 (ZBP1) - also known as DNA activator of Interferon (DAI) (Dhuriya and Sharma, 2018) (Galluzzi *et al.*, 2014). In the presence of caspase-8, RIPK1 and RIPK3 are inactivated, leading to apoptosis. In the absence of caspase, RIPK1 and RIPK3 remain active and form a complex called 'the necrosome' (Seifert and Miller, 2017). Following receptor stimulation, RIPK3 is activated by RIPK1, which in turn phosphorylates MLKL (Mixed Lineage Kinase-domain Like), generating MLKL oligomers which translocate to the plasma membrane and trigger its permeabilization (Quarato *et al.*, 2016).

1.2.3 Mitotic Catastrophe

Mitotic catastrophe is a regulated mechanism that functions to attenuate the survival of cells that are unable to complete mitosis. Failure to complete mitosis can be due to a number of factors, including DNA damage, failures in mitotic machinery or defective mitotic checkpoints (Vitale *et al.*, 2011). According to the Nomenclature Committee on Cell Death (NCCD), mitotic catastrophe itself is not a form of regulated cell death per se. The term mitotic death, a specific from of cell death, eliciting an intrinsic apoptotic process driven by mitotic catastrophe, should be used (Galluzzi *et al.*, 2018). Mitotic catastrophe can be identified morphologically by marked nuclear changes, including micronucleation and/or multinucleation, both consequences of aberrant chromosomal segregation (Vitale *et al.*, 2011).

1.2.4 Immunogenic Cell Death

Each day, millions of cells are turned over, primarily via apoptosis, to maintain whole body homeostasis. To avoid detection by the immune system and avoid a catastrophic autoimmune response, this process is confined within membranous bodies which are then rapidly cleared via phagocytosis (Serrano-del Valle *et al.*, 2019). In comparison to necrosis, typically considered to be immunogenic, apoptosis has long been thought to be a poorly immunogenic process. The term immunogenic cell death (ICD) is used to describe a cell death process resulting in the release of DAMPS (damage associated molecular patterns). ICD has the ability to transform dying or dead cells into 'vaccines', enabling an immune response to be mounted in response to cancer-derived neo-epitopes (Galluzzi *et al.*, 2017). To date, a small number of anti-cancer therapies including the chemotherapy oxaliplatin, along with radiotherapy, are bona fide ICD inducers (Garg *et al.*, 2017) (Adkins *et al.*, 2014). Such inducers trigger stress responses, including ER stress, ROS generation, autophagy, and unfolded protein response (UPR), critical for the trafficking and release of DAMPS. During ICD, dying cells expose 'find me signals' such as the heat shock proteins (HSP) 70 and 90, and calreticulin (CRT), recognised by CD91 macrophage receptors facilitating the engulfment of dying cells (Spisek *et al.*, 2007) (Krysko, Ravichandran and Vandenabeele, 2018). Dying cells also release several DAMPs. The secretion of adenosine triphosphate (ATP) attracts monocytes via binding the P2Ys purinoceptor (Martins *et al.*, 2009). During late apoptosis, high mobility group box 1 (HMGB1) is released which binds TLR2 and TLR4 to promote DC pro-inflammatory cytokine production and assists in antigen presentation to cytotoxic T cells (Saenz *et al.*, 2014)(Sistigu *et al.*, 2014).

1.3 Molecular regulation of Autophagy

1.3.1 What is autophagy?

Autophagy is an evolutionarily-conserved process, used to preserve cell homeostasis in response to stressful stimuli such as nutrient deprivation or damage to organelles. Derived from the Greek for self (auto) and eat (phagein), autophagy directly translates to 'eat oneself'. The process involves the generation of a double membrane bound vesicle, termed an autophagosome, which engulfs cargo and fuses with a lysosome to degrade it's intravesicular cargo. Years of research into autophagy have revealed it to be a regulated, context-dependent process, with biological roles beyond those of survival and homeostasis. Autophagy has been shown to play a key role in neurodegenerative diseases such as Alzheimer's, in immune responses and cancer. The role of autophagy as a key biological process with implications in human health and disease was highlighted with the awarding of the 2016 Nobel prize in physiology or medicine to Yoshinori Ohsumi for his work on autophagy mechanisms in yeast.

1.3.2 Types of autophagy

Different types of autophagy exist, varying in how they uptake cargo, but all of which cumulate in lysosomal degradation. The most well characterised form of autophagy is termed macro-autophagy. In the literature, macro-autophagy is termed autophagy unless otherwise stated. This involves the de-novo generation of an autophagosome which sequesters its cargo for transport to the lysosome. In contrast to macro-autophagy, micro-autophagy circumvents the need for an autophagosome by directly sequestering cargo into the lysosome for degradation. This type of autophagy is generally non-selective, although there are some exceptions. Chaperone-mediated

autophagy (CMA) is highly selective, whereby cargo labelled with a unique pentapeptide motif (KFERQ) are recognised by HSP70 and transported to the lysosome. Here, HSP70 interacts with the lysosomal membrane protein LAMP-2A to translocate cargo into the lysosome for hydrolytic degradation (Cuervo and Wong, 2013).

1.3.3 Autophagic vesicle formation and trafficking

1.3.3.1 Formation of the autophagosome

In mammalian cells, autophagosome formation, initiated by a stimulus such as nutrient deprivation, is generally accepted to occur on the endoplasmic reticulum membrane via the formation of an Omegasome. Phagophore formation begins when the ULK1/2 kinase complex (consisting of ULK1, ULK2, ATG13, FIP200 and ATG101) becomes activated. Activation of the ULK1/2 complex results in its translocation to the ER, at a site denoted by ATG9 (Yu, Chen and Tooze, 2017). Next, the class III phosphatidylinositol 3-kinase (PtdIns3-kinase) complex is recruited, resulting in the generation of ER domains or the Omegasome, containing PtdIns3P. These ER domains are highly curved areas, favouring the recruitment of the PtdIns3K complex I, facilitating changes to the lipid structure to form the phagophore. This curved shape also serves to aid the clustering of PtdIns3P, allowing the recruitment of WIPI2B and in turn the recruitment of the ATG12–ATG5-ATG16L1 E3-like complex (Dooley *et al.*, 2014). Besides the endoplasmic reticulum, organelle membranes, such as the mitochondrial membrane, have been shown to play a role in autophagosome formation, where ATG components such as ATG14 and the Q-snare protein STX17 accumulate. The Golgi is also a purported site of origin for autophagosomes during

non-canonical autophagy (see later). The so called ATG9 compartment, an evolutionarily conserved cluster of vesicles, can be mobilised under stressful conditions and fuse with the growing phagophore (Mari *et al.*, 2010).

1.3.3.2 Autophagosome elongation

Following exposure to a stressful stimulus, ULK proteins are phosphorylated and undergo a conformational change to phosphorylate Atg13 and FIP200 (Chan, Longatti *et al.*, 2009; Jung, Jun et *al.*, 2009). Activation of the class III PI3K complex (composed of vps34, vps15, beclin-1 and Atg14) then occurs following phosphorylation of AMBRA1 by the ULK/Atg1 complex. The PI3K complex controls vesicle elongation via recruiting two essential ubiquitin-like conjugation systems to the phagophore in a sequential manner. Firstly, the Atg12-Atg5 complex is formed when Atg12, activated by Atg7 (E1-like activating enzyme), is conjugated to Atg5 by Atg10 (E2-like conjugating enzyme). This complex interacts with Atg16 to form a tetrameric Atg12-Atg5-Atg16 complex. This structure then attaches to the phagophore, resulting in its expansion around target substrates (Geng and Klionsky, 2008).

The Atg8-PE conjugation system is the second ubiquitin-like mechanism required for autophagosome formation. Atg8 is a homologue of mammalian LC3 (microtubule-associated protein 1 light chain 3), which resides in the cytosol under normal conditions and is recruited to the phagophore in response to stressful stimuli. The c-terminus of LC3 I is cleaved by Atg4 to expose a glycine residue, which is subsequently conjugated to phosphatidylethanolamine (PE) in the autophagosome membrane bilayer to form LC3II (Glick, Barth and Macleod, 2010). The presence of

LC3II on the mature double membraned autophagosome is considered one of the most reliable markers of autophagy. LC3II is reported to play roles in membrane tethering and in selecting cargo for degradation.

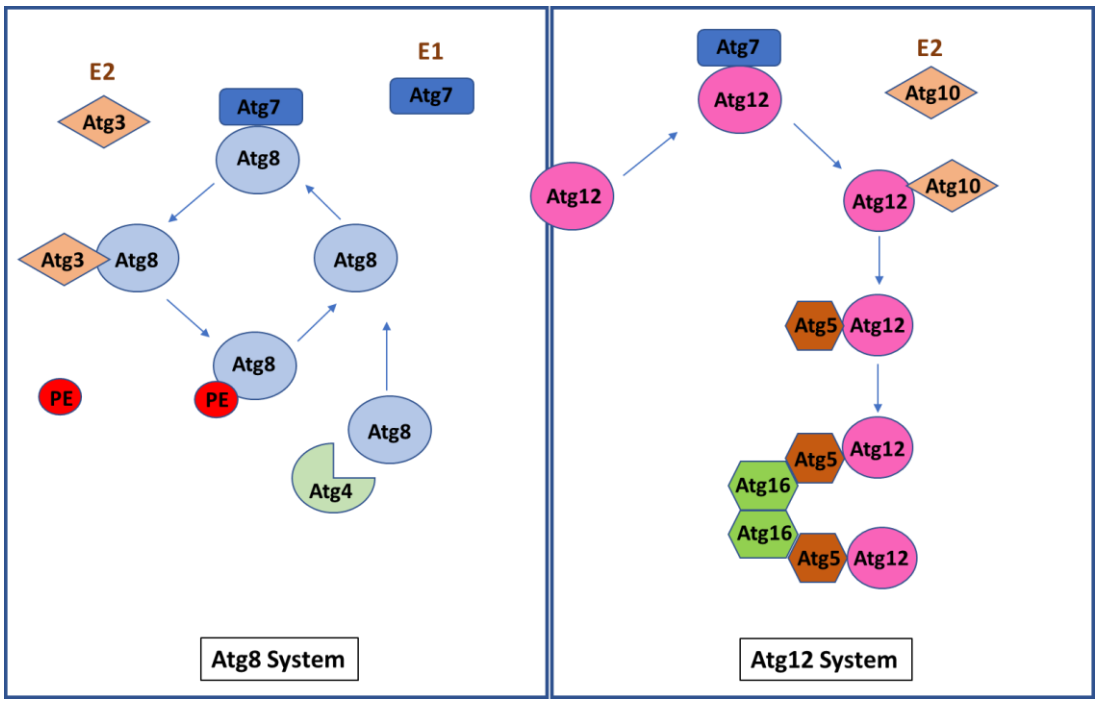

Figure 1.5: Schematic depiction of the autophagy ubiquitin-like conjugation systems, the Atg8 system and the Atg12 system. During the Atg8 system, Atg8 is cleaved by Atg4, transferred on to Atg7(E1) and Atg3(E2) and binds with is substrate phosphatidylethanolamine (PE). The Atg8-PE conjugate functions in the autophagosome membrane. Atg8-PE can then be deconjugated by Atg4, and Atg8 is recycled. Atg12 is activated by Atg7 (E1) and conjugated to Atg5 by Atg10(E2). The Atg5-12 complex interacts with Atg16 to form the Atg12-Atg5-Atg16 complex, which aids phagophore expansion.

1.3.3.3 Autophagosome/Lysosome tethering and fusion

To enable the mature autophagosome to fuse with a lysosome, they need to be in close proximity. Stressful stimuli, such as starvation, results in a clustering of lysosomes in the perinuclear region of the cell. Microtubules, particularly the microtubule motor dynein, facilitate the transport of autophagosomes to perinuclear lysosomes. The HOPs complex, consisting of vacuolar protein sorting 11 (VPS11), Vps16, VPS18, Vps33A, VPS39, and Vps41, play a core role in tethering (Seals *et al.*, 2000)(Wurmser, Sato and Emr, 2000). Additionally, RAB proteins, particularly Rab7, are small GTPases which interact with the HOPS complex and bind to other membrane anchored proteins, thus allowing the fusion of opposing membranes. Another key aspect to autophagosome/lysosome fusion is the generation of a SNARE complex. The force necessary to facilitate adjacent membranes fusing is driven by the assembly of an R-SNARE and a Q-SNARE protein into a trans-snare complex. In mammalian cells, the Q-SNARE protein STX17 interacts with the R-SNARE VAMP8 to mediate autophagosome/lysosome fusion (Itakura, Kishi-Itakura and Mizushima, 2012).

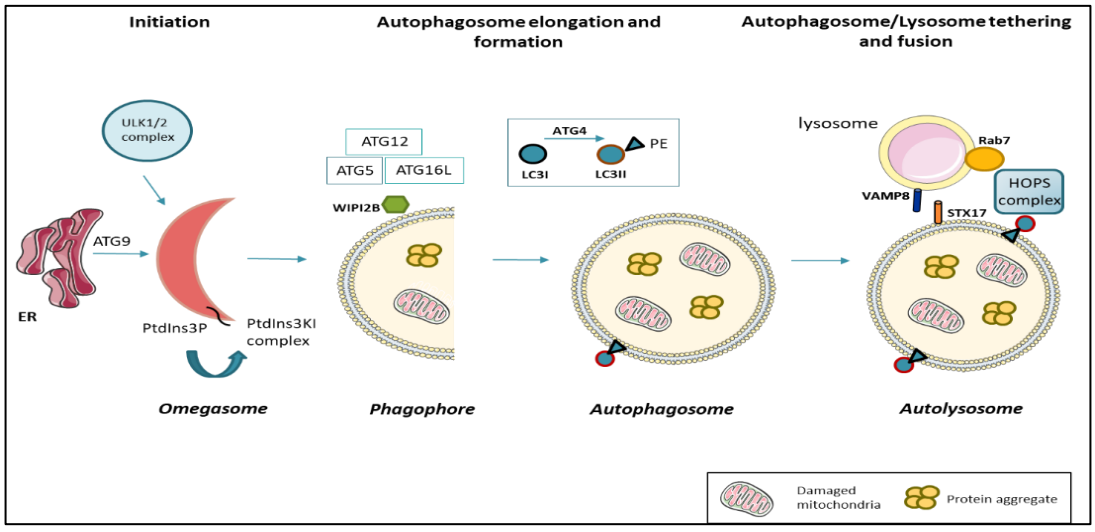

Figure 1.6: Illustration of the autophagic pathway, from generation of the phagophore, elongation and completion of the autophagosome, to fusion with the lysosome. Details of each step are provided in the text, section 1.3.3.

1.3.4 Signalling pathways regulating autophagy

1.3.4.1 PI3K/AKT/mTOR signalling

When is a cell is not under nutritive stress and has a plentiful supply of nutrients and amino acids, inducible autophagy is supressed via activation of the class I PI3K/AKT/mTOR pathway. In contrast, under conditions of nutrient depravation, the PI3K/AKT/mTOR pathway is deactivated, resulting in autophagy activation.

The mechanistic target of rapamycin (mTOR) is an evolutionarily conserved serine/threonine protein kinase, belonging to the PI3K-related kinase family (PIKK). mTOR responds to extracellular and intracellular stimuli, including growth factors, nutrients, energy status and cellular stress. mTOR and its associated proteins form two distinct complexes, mTORC1 and mTORC2. The two complexes differ in their composition, activation and also in their sensitivity to rapamycin. While mTOR in both complexes interacts with DEPTOR and mLST8, only mTORC1 interacts with RAPTOR and PRAS40, while mTORC2 interacts with rapamycin-insensitive companion of mTOR (RICTOR) and mSIN1 (H. Yang *et al.*, 2013)(P. Liu *et al.*, 2015).

mTORC1 activation involves the guanosine triphosphatases (GTPases) RAG and RHEB (Ras homolog enriched in brain). RAG exists as a heterodimer attached to the lysosome membrane and is activated in the presence of nutrients (Bar-Peled *et al.*, 2012). Following RAG activation, mTORC1 is recruited to the lysosome membrane where it meets RHEB. RHEB activation is negatively controlled by tuberous sclerosis 1 and 2 (TSC1/2). The phosphorylation of TSC1/2 is a key regulatory step dictating mTOR activation in response to upstream signals. Growth factor induced PI3K/AKT signalling activates TSC2 via S939/T1462 phosphorylation, resulting in RHEB activation and thus mTORC1 activation. In contrast, nutrient deprivation activates

adenosine monophosphate protein kinase (AMPK), leading to TSC2 phosphorylation (T1227/S1387), enhanced TSC1/2 activity and mTOR inhibition (Yu and Cui, 2016).

1.3.4.2 AMPK

AMP-activated protein kinase (AMPK) is a metabolic sensor which plays a key role in maintaining energy homeostasis by responding to stress factors such as exercise, ischemia, redox imbalance changes in cellular pH and nutrient deprivation. All of these stressors result in the depletion of intracellular ATP levels, with the subsequent increase in the ratio of AMP:ATP resulting in the activation of AMPK (Yung, Ngan and Chan, 2016). AMPK is characterised by a catalytic α-subunit and regulatory β/γ subunits, and upon activation is phosphorylated at Thr-172 within the activation domain of the α-subunit by the kinases LKB1 and CaMKKβ (Yung, Ngan and Chan, 2016). The role of AMPK in autophagy initiation is well established. Under conditions of glucose starvation, AMPK activates Ulk1, a component of the autophagy machinery. The activation of AMPK can also phosphorylate and activate TSC2 which in turn can suppress mTORC1 and activate autophagy (Jang *et al.*, 2018). It is only recently that AMPK has been shown to contribute to autophagosome maturation and lysosomal fusion. Knockout of the AMPK subunit AMPK α1 under starvation impaired autophagosome formation, with LC3-puncta positively stained with LAMP1 observed in few AMPK α1 knockout cells. Impairment of AMPK signalling also resulted in the repression of autophagic flux (Jang *et al.*, 2018).

1.3.4.3 TFEB (transcription factor EB)

Transcription factor EB (TFEB) is a master regulator of autophagy, which is responsible for the transcription of genes involved in autophagy and lysosome biogenesis (Sha *et al.*, 2017). After phosphorylation by mTOR, TFEB is inactive and remains in the cytosol. Conversely, inhibition of mTORC1 results in dephosphorylation of TFEB, which becomes active and translocates to the nucleus where it upregulates transcription of its target genes (Sha *et al.*, 2017). A recent study has identified a role for the ubiquitin-proteasome pathway in the regulation of autophagy and lysosomal functions through its regulation of TFEB activity. A chaperone-dependent E3 ubiquitin ligase, STUB1 (STIP1 homology and U-Box containing protein 1), has been shown to preferentially target inactive phosphorylated TFEB for degradation by the ubiquitin-proteasome pathway. An accumulation of phosphorylated TFEB in STUB1-deficient cells results in decreased autophagy and mitochondrial biogenesis (Sha *et al.*, 2017). Therefore, the ubiquitin-proteasome pathway is involved in the regulation of autophagy and lysosomal functions through its regulation of TFEB activity.

1.3.4.4 P53

The autophagy and p53 pathways are functionally linked, where autophagy suppresses p53 and in turn, p53 activates autophagy (White, 2016). It is believed that the activation of autophagy is part of the ‘protective function’ of p53 in response to various stresses such as DNA damage, metabolic and oxidative stress. The absence of p53 itself may also create stress, resulting in the activation of autophagy. The regulation of autophagy through nuclear transactivation occurs through several pathways. These include the pro-autophagic factors TSC2, PTEN and AMPK, with

further signalling then mediated via mTOR inhibition (Mrakovcic and Frohlich, 2018). A more direct method of autophagy activation by p53 is through the upregulation of DRAM (damage-related autophagy modulator), which represents a lysosomal protein that can interfere with various stages of autophagosome formation (Mrakovcic and Frohlich, 2018). In addition, the downregulation of BCL-2, BCL-xL and MCL-1 or upregulation of BAX, BAD, BNIP3 or PUMA by p53 releases Beclin 1 and initiates autophagy. The cellular location of p53 also plays a crucial role in autophagy, with p53 proteins located in the cytosol having an inhibitory effect on autophagy. The mechanism by which cytosolic p53 exerts an inhibitory effect on autophagy remains to be fully elucidated. FIP200 (ATG17) has been identified as a cytoplasmic binding partner of p53 which may aid in the negative regulation of autophagy (Morselli *et al.*, 2011).

1.4 Selective Autophagy

Originally thought to be a bulk degradative process, research into autophagy has identified highly selective processes, including but not limited to, mitophagy, nucleophagy, xenophagy and aggrephagy. This selectivity is in part mediated by specific adaptor proteins – which selectively bind to cargo – and to LC3.

1.4.1 Mitophagy

Mitophagy is one of the best characterised types of selective autophagy. It serves to eliminate damaged mitochondria from the cell. Targeting of damaged mitochondria for elimination via autophagy involves two key genes, PINK1 and PARK2. When mitochondrial protein transport is disrupted, PINK1 is stabilised on the outer

mitochondrial membrane in a complex of TOM proteins. Stabilisation of PINK results in phosphorylation of pre-existing ubiquitin molecules on the mitochondrial surface, to which PARKIN (an E3 ligase) is recruited and tethered to the membrane where it is then phosphorylated by PINK1 (Youle and Narendra, 2011). The adaptor proteins NDP52 and OPTN were found to be required for mitophagy, binding the ubiquitinated cargo and linking them to the autophagosome for degradation (Heo *et al.*, 2015). BNIP3 (BCL2 and adenovirus E1B 19 kDa-interacting protein 3) and BNIP3-like (BNIP3L), also referred to as NIX, have been reported to induce mitophagy in response to hypoxia. Screening for autophagy receptors revealed the ability of NIX to interact with LC3 and GABARAP via its LC3 interaction region (LIR) motif. Competition by BNIP3 or NIX for Bcl-2 binding may liberate Beclin 1 from inhibitory BCl-2 complexes, resulting in autophagy activation (Bellot *et al.*, 2009). A third mechanism proposed for BNIP3 in autophagy activation is via mTOR inhibition. BNIP3 can bind to and deactivate RHEB, an upstream activator of mTOR (Li *et al.*, 2007).

1.4.2 Nucleophagy

First described in yeast, nucleophagy describes the sequestration and degradation of nuclear material. Termed 'piecemeal autophagy of the nucleus' in yeast, small pieces of the nuclear envelope are engulfed via invaginations of the vacuolar membrane and degraded by luminal hydrolases (Roberts *et al.*, 2003). Degradation of whole nuclei has also been reported in the fungus *Aspergillus Oryzae* (Rello-Varona *et al.*, 2012). Previous studies have evidenced a role for autophagy in the maintenance of genomic integrity. Micronuclei, damaged DNA arising from the mis-segregation of chromosomes via a cell cycle perturbation, are tagged with p62 and subject to

degradation by autophagosomes (Rello-Varona *et al.*, 2012). Interestingly, these micronuclei are positive for Ku70 and RAD51, markers of DNA repair, implying these micronuclei tried and failed to repair their DNA (Erenpreisa *et al.*, 2002)(Erenpreisa *et al.*, 2011). As demonstrated by Erenpreisa *et al*. (2011), micronuclei can re-join the main nucleus, where they can participate in DNA repair. Failure to repair appears to trigger their pinching away from the nucleus, where nucleophagy is activated. Autophagy has also been shown to degrade chromatin during cellular senescence. Cytoplasmic chromatin fragments arise during cell senescence, where chromatin pieces bud off from the nucleus, in a form of 'terminal cell-cycle arrest'(Dou *et al.*, 2017). During oncogene induced cellular senescence, such as RAS activation, LC3 binds to lamin binding domains present on chromatin (Dou *et al.*, 2015). Lamin B1 and associated histones shuttle from the nucleus to the cytoplasm for degradation via lysosomes. Attenuation of the interaction between LC3 and lamin B1, or indeed inhibition of autophagy, prevents lamin loss thus mitigating oncogene induced senescence (Dou *et al.*, 2015).

1.4.3 Aggrephagy

Aggrephagy describes the elimination of ubiquitinated and aggregated proteins by macroautophagy. Protein aggregates form when misfolded proteins are not dealt with by chaperons and the ubiquitin-proteasome system (UPS). The ubiquitination of misfolded proteins is a key feature enabling the selection and degradation of protein aggregates via aggrephagy. Several receptors in mammalian cells, which possess LC3 interaction regions (LIRs) and a ubiquitin binding domain, facilitate the interaction between LC3 members and ubiquitinated substrates (Lamark and Johansen, 2012). The histone deacetylase HDAC6, p62 and dynein all play critical roles in aggresome

formation. HDAC6 can bind to polyubiquitinated misfolded proteins, along with dynein motors, allowing the transport of misfolded proteins to the aggresome (Kawaguchi *et al.*, 2003). BCL-2-associaated athanogene 3 (BAG3), in conjunction with the chaperones HSP70 and HSPB8, and p62, targets aggregated proteins for autophagic degradation (Stürner and Behl, 2017).

1.5 Other forms of autophagy

1.5.1 Non-canonical autophagy

It is now clear that variations on this macroautophagic pathway exist. The typical non-canonical pathway described differs from traditional autophagy only in that it is independent of Beclin 1. A second type of non-canonical autophagy, termed Atg 5/ 7 independent autophagy, relies on Beclin 1, but as the name infers, is independent of Atg5 and Atg7. Unlike the other forms of autophagy, this pathway does not require lipidation of LC3 on the mature autophagosome. Instead, Rab9-positive vesicles fuse with lysosomes to degrade intra-vesicular cargo. This type of autophagy was first described in ATG5 null MEFs, which could still form autophagosomes following treatment with etoposide, a DNA damaging agent (Arakawa *et al.*, 2017). Another key feature which distinguishes Atg5/7-independent autophagy from the Beclin 1 independent and conventional autophagy pathways is the origin of the autophagosome membrane components. While subject to some debate, the ER is generally accepted to be involved in the generation of autophagosomes. Double-FYVE-containing protein 1, an ER localised protein, was found on the surface of pre-autophagosome structures termed “omegasomes” (Axe *et al.*, 2008). Mitochondrial and plasma membranes have also been reported as origin material for autophagosome generation (Tooze and

Yoshimori, 2010). In contrast to the multiple sources of membrane material reported in conventional autophagy, the Atg5/7-independent pathway appears to derive its source material exclusively from the Golgi. This is supported with key observations made by Nishida *et al*. (2009), where autophagic vacuoles were almost always located proximal to the Golgi, while autophagosomes and autolysosomes displayed trans-Golgi proteins. Golgi ministack formation was always found to precede autophagosome generation, and most importantly, the depletion of Golgi proteins inhibited this non-canonical pathway, but not conventional autophagy (Nishida *et al.*, 2009). The lipidation of LC3 on the mature autophagosome in conventional autophagy does not occur in this non-canonical pathway. The GTPase Rab9, which traffics proteins from late endosomes to the Golgi membrane, was demonstrated to be critical in the formation of isolation membranes. GFP-Rab9 was shown to be colocalised with autolysosomes in etoposide treated ATG5 deficient MEFs. siRNA knockdown of Rab9 decreased the number of autophagosomes and increased the number of isolation membranes, indicating a role for Rab9 in the elongation and closure of isolation membranes. In terms of the biological role of non-canonical autophagy, further studies are required. However, it has been shown to play a role in mitochondrial clearance during pluripotent stem cell differentiation, and like conventional autophagy, can be induced in response to DNA damage (Ma *et al.*, 2015)(Nishida *et al.*, 2009). We are the first to investigate a potential role for non-canonical autophagy in OC cells in response to paclitaxel treatment.

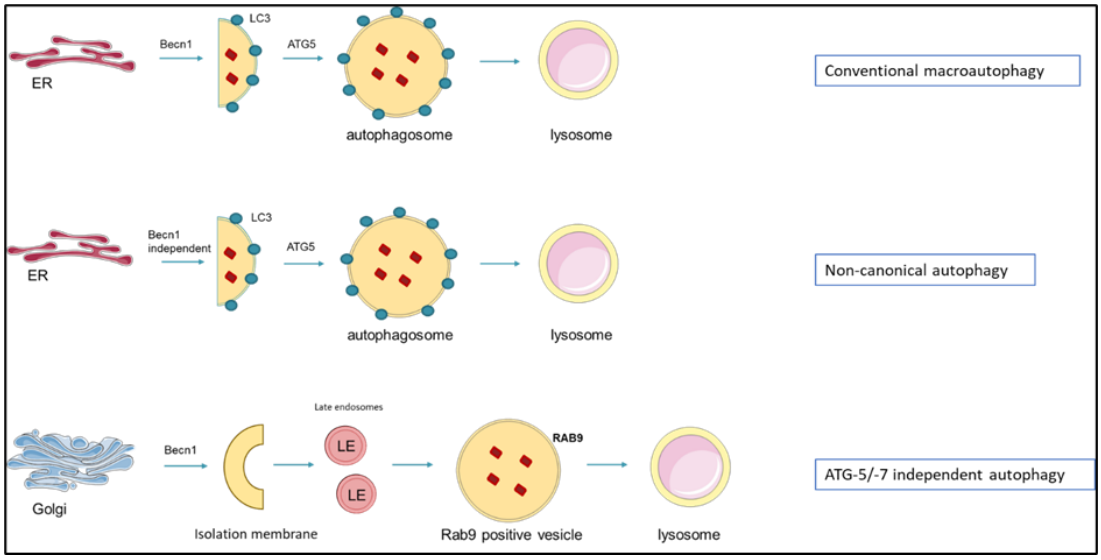

Figure 1.7: Schematic outlining the different macroautophagic pathways, which vary in the proteins involved but all culminate with lysosome degradation (A) conventional macroautophagy, which utilises Beclin 1 and Atg5, with lipidated LC3 found on the mature autophagosome (B) the non-canonical autophagy pathway differs from canonical autophagy in that Beclin 1 is not required for initiation (C) the Atg5/7-independent pathway requires Beclin 1 for initiation, but unlike the previous pathways described, does not utilise Atg5 or Atg7 for conjugation. The Golgi is an exclusive membrane source for autophagosome generation which occurs when late endosomes fuse with isolation membranes (derived from the *trans*-Golgi cisternae). Rab9 is required to facilitate the extension and closure of the alternative autophagosome.

1.5.2 LC3-associated phagocytosis

As mentioned in section 1.5.1 above, various non-canonical functions for autophagy exist which are distinct in their mechanisms and functions. One such function is LC3-associated phagocytosis (LAP), which is involved in immune regulation and disease. Unlike canonical autophagy, LAP is not dependent on the AMPK-mTORC1-ULK1 pathway and does not respond to nutrient depletion or intra-cellular stress (Heckmann and Green, 2019). The hallmark of LAP is conjugation of LC3 to the phagosome membrane, and as such, the activation stimulus occurs from the cell exterior upon phagocytosis. Surface receptors including pattern recognition receptors (PRR), Toll-like receptors (TLR) and immunoglobulin receptors (IgG) can activate LAP, however it remains unclear how these interactions lead to the recruitment of LAP regulators to the phagosome.

LAP is unique in three aspects: it is characterised by a single membrane phagosome; the P13KC3 complex involved in LAP contains UVRAG and RUBCN which is unique and indispensable; and an intermediate stage requiring the production of ROS (reactive oxygen species) is necessary for LAP, prior to LC3 lipidation but subsequent to P13KC3 assembly. NOX2 is a protein complex which associates with the phagosome membrane whose activity is also required to recruit the LC3 conjugation machinery. Evidence is also emerging which suggests LAP differs in LC3 lipidation, with a rapid rate of LC3 lipidation observed after sealing of the phagosome membrane (Heckmann and Green, 2019).

In terms of its physiological effects, LAP has been shown to play an important role in regulating the immune system. LAP is obligatory for the immunologically silent process of efferocytosis to occur, by preventing the secretion of pro-inflammatory cytokines. Efferocytosis describes the process whereby apoptotic cells are engulfed by

macrophages to prevent an autoimmune response. Phosphatidylserine (PtdSer) on the surface of dead cells interacts with TIM4 and triggers LAP (Martinez *et al.*, 2011). In the tumour microenvironment, LAP can prevent the mounting of an effective anti-tumour immune response, via the secretion of anti-inflammatory cytokines. LAP activation in tumour associated macrophages (TAMs) polarizes them toward a pro-tumour M2 phenotype, resulting in impaired T lymphocyte function and immune tolerance (Cunha *et al.*, 2018).

1.6 Unconventional protein secretion

1.6.1 Secretory autophagy

The majority of secreted eukaryotic proteins are tagged with N-terminal peptides, permitting entry to the ER, where they follow a defined secretory pathway through the Golgi and are released via secretory vesicles at the plasma membrane [reviewed in (Cotzomi-Ortega *et al.*, 2018)]. Unconventional secretion describes the extracellular secretion of proteins which lack signal peptides and thus are unable to enter the ER.

Secretory autophagy can be classed as a form of unconventional secretion. Secretory autophagy describes the process by which the canonical autophagy pathway participates in the secretion of proteins via transporting them within an autophagosome to the plasma membrane, to multivesicular bodies (MVB) or secretory lysosomes for extracellular expulsion. The prototypical cargo for autophagic secretion is IL-1β. IL-1β was found to translocate to the lumen of a vesicle carrier, facilitated by heat shock protein HSP90, which later becomes a phagophore, then an autophagosome or fuses with them. Following generation of the double membrane autophagosome, IL-1β localises between the inner and outer membranes (M. Zhang

et al., 2015). This can explain how IL-1β escapes autolysosomal degradation and can be transported to the plasma membrane, where the IL-1β containing autophagosome can fuse with the plasma membrane, or via an MVB first. Rab8a, which regulates polarized membrane trafficking and plasma membrane fusion of vesicular carriers, was reported to regulate the initiation of secretory autophagy and the release of IL-1 β (Dupont *et al.*, 2011).

Disruption of degradative autophagy may divert autophagosomal organelles into the secretory autophagy pathway. This is supported by a study where pharmacological inhibition of autophagosome-lysosome fusion with Bafilomycin A1 could enhance α-synuclein secretion, a constituent of protein aggregates known as Lewy bodies, while knockdown of Atg5 could attenuate secretion. Likewise, increased microtubule acetylation, caused by downregulation of HDAC6, resulted in decreased autophagosome lysosome fusion and increased α-synuclein secretion (Ejlerskov *et al.*, 2013).

1.6.2 Exosome secretion

Exosomes are nano-sized extracellular vesicles, less than 150nm in diameter, which originate from the endocytic pathway. During multivesicular body (MVB) formation, cells internalise macromolecules, membranes and fluids via invagination of the plasma membrane to form intraluminal vesicles (ILVs). The ESCRT machinery, consisting of four protein complexes ESCRT-o, -I, -II, -III and the AAA ATPase Vps4 complex, play an important role in formation of ILVs and sorting of cargo (Baixauli, López-Otín and Mittelbrunn, 2014). For exosomes to be released, ILVs within MVBs must be transported to and fuse with the plasma membrane (Alenquer and Amorim, 2015).

Exosomes contain a mixture of both soluble and membrane bound proteins, DNA and microRNA. Uptake of cargo can occur in a bulk nonselective manner or selectively via ubiquitination of substrates (Smith, Jackson and Schorey, 2015).

Tumour derived exosomes have been shown to play a significant role in facilitating cell to cell communication, immune regulation and metastatic spread. Exosomes derived from ovarian cancers contain a host of bioactive molecules which favour tumour progression and treatment resistance. Annexin A3 can be detected within exosomes derived from cisplatin resistant OC cell lines and in tumour samples from platinum resistant OC patients (Yin *et al.*, 2012) (Yan *et al.*, 2010). Human peritoneal mesothelial cells (HPMCs) treated with ovarian cancer-derived exosomes had a significantly enhanced invasion capacity, via exosomal transfer of CD44, enhancing the secretion of matrix-metalloprotinease-9 (MMP-9). Ovarian cancer derived exosomes have also been found to contain a range of miRNA which contribute to drug resistance. MiR-21, found in exosomes isolated from OC cancer associated adipocytes and fibroblasts, is transferred to the cancer cells where it can supress apoptosis and confer chemoresistance (Au Yeung *et al.*, 2016). MicroRNA have also been implicated in mediating crosstalk between exosome release and autophagy, resulting in a phenomenon termed bystander autophagy. Bystander autophagy describes the activation of autophagy in distant cells which have not directly received treatment. Exosomes derived from irradiated brain tissue were found to contain high levels of miR-7. Following tail vein injection into mice, these exosomes travelled through the blood stream to the lung, where upon internalisation, could enhance the expression of autophagy markers LC3B and Beclin 1 via miR-7 inhibition of Bcl-2 (Cai *et al.*, 2017).

1.7 Autophagy and Cancer

When describing the complex dynamics between autophagy and tumour biology, the phrase ‘double edged word’ is frequently and aptly used. The role of autophagy in the cancer setting is dependent on a range of factors, including tumour type, stage and the genetic landscape. Autophagy has primarily evolved as a cytoprotective mechanism, to enable a cell to maintain homeostasis. As our knowledge of this process expands, it is evident that cancer cells can use this process to their advantage, meaning targeting autophagy could be clinically useful.

1.7.1 Autophagy as a tumour suppressor

Knockout of BECN1, which increased spontaneous tumour formation in mice, was the first indication of a tumour suppressive function of autophagy (Yue *et al.*, 2003). A key tumour suppressive function of autophagy is its ability to remove reactive oxygen species (ROS). ROS act as key drivers of mutagenesis via activation of oncogenes and driving inflammation (Goetz and Luch, 2008). Additionally, mitochondria are key producers of ROS, so their elimination via mitophagy plays a crucial role in preventing oncogenesis. Conversely, a lack of autophagy can fuel malignant progression if ROS are not removed. Autophagic removal of protein aggregates also mediates an anti-tumour response, as accumulation of such aggregates can lead to increased ROS production, ER stress and activation of the DNA damage response (Mathew *et al.*, 2009). Autophagy can promote apoptotic death of tumour cells via degradation of inhibitor of apoptosis (IAP) proteins (Xu *et al.*, 2016). Supporting a tumour suppressive role for autophagy, deletion of proteins which positively regulate autophagy, including UVRAG and Bif-1, lead to increased cancer cell proliferation in breast, colon and prostate tumours (Morselli *et al.*, 2009).

1.7.2 Autophagy in tumour progression

Healthy cells use autophagy at basal levels to maintain cellular homeostasis, whereas malignant cells can elevate their autophagy levels. Particularly in the context of an oncogenic RAS mutation, cancer cells have been described as 'autophagy addicted' (Mancias and Kimmelman, 2011). Cancer cells typically have higher proliferation rates than their non-malignant counterparts, coupled with higher metabolic requirements. These requirements can be met by inducing high levels of autophagy, to produce ATP and other metabolic building blocks. Autophagy plays a diverse role in regulating cancer cell metabolism. Even in the presence of oxygen, sufficient to support oxidative phosphorylation, cancer cells favour the metabolism of glucose to lactate, a phenomenon dubbed the Warburg effect. Pyruvate kinase M2 (PKM2) is a key enzyme in the glycolytic pathway, preventing the accumulation of glycolytic intermediates. Inhibition of PKM2 results in an accumulation of glycolytic intermediates. Cancer cells utilise chaperone mediated autophagy to degrade PKM2, leading to an increase in glycolytic intermediates which can be used in biosynthetic pathways to support tumour growth (Lv *et al.*, 2011). Conversely, the utilisation of autophagy to supress glycolysis can also be beneficial to cancer cells. Under acute stress conditions, cancer cells will slow down their proliferation rate in order to survive. The degradation of hexokinase-2 (HK2) by autophagy downregulates glycolysis, thus slowing down proliferation (Jiao *et al.*, 2018).

One of the hallmarks of cancer is its ability to evade the immune response, a hallmark which autophagy has been implicated in. Granzyme B, a serine protease used by natural killer (NK) cells to lyse their target, has been shown to be degraded via autophagy (Viry *et al.*, 2014). Interestingly, autophagy has also been linked to the regulation of immune checkpoints, prominent targets for immunotherapies. Activation

of autophagy via mTOR inhibition was found to decrease the expression of PD-L1 in lung cancer cells, while mTOR activation resulted in increased PD-L1 expression (Lastwika *et al.*, 2016). In a feed-forward loop PD-L1 can activate mTOR, which in turn upregulates PD-L1 expression. Of note, this feed-forward loop proceeded via mTORC1 and not mTORC2. In line with this, melanoma and ovarian cancer cells with low autophagy flux were found to have higher expression of PD-L1 compared to cells which displayed high autophagy flux (Clark *et al.*, 2016).

Autophagy has also been linked to tumour invasion and metastasis. One study reported that ULK2, which promotes autophagy by phosphorylating the initiation complex, downregulates E-cadherin, promoting cell motility (Kim *et al.*, 2016). During metastasis, cells that travel to distant organs must be able to resist cell death which occurs due to the loss of contact with the extracellular matrix (ECM), termed anoikis. Autophagy has been shown to contribute to anoikis resistance and lung colonization in hepatocellular carcinoma cells (HCC) both *in-vitro* and *in-vivo*. Attenuation of autophagy via miR-30a overexpression could significantly reduce lung metastasis (Fu *et al.*, 2018).

1.7.3 Modulating autophagy for cancer treatment

Given that autophagy generally plays a protective role in established tumours, inhibitors of autophagy are being trialled in patients. The anti-malarial drug hydroxychloroquine (HCQ), which prevents lysosomal turnover of autophagic substrates, is the most extensively trialled autophagic modulator. Several trials are underway in pancreatic cancer, combining HCQ with chemotherapies such as gemcitabine and abraxane (NCT01128296, NCT01506973). Promising results have

been obtained in breast and lung cancer patients with brain metastases, whereby the addition of HCQ lead to a one year increase in progression free survival in 83% of patients trialled, compared to 53% in the placebo group (Rojas-Puentes *et al.*, 2013). In contrast, inducers of autophagy have been trialled to a lesser extent. Temsirolimus, an mTOR inhibitor, significantly improved progression free survival compared to standard of care chemotherapy regimens in patients with mantle cell lymphoma (Hess *et al.*, 2009). A novel aspect of this study aimed to evaluate the chemosensitising ability of the autophagy modulating drug lithium, FDA approved for bipolar disorder. Given that both inhibiting and promoting autophagy can be beneficial, a one size fits all approach will not work. If autophagy modulation is to be successfully implemented into clinical regimens, the autophagy status of each cancer must be carefully assessed.

Cancer type	Autophagy modulators	Trial phase	Clinicaltrials.gov reference
Advanced and metastatic pancreatic adenocarcinoma	HCQ + Gemcitabine/abraxane	I/II	NCT01506973
Metastatic pancreatic adenocarcinoma	Trametinib + HCQ	I	NCT03825289
KRAS-mutated pancreatic adenocarcinoma, colorectal adenocarcinoma, and histology agnostic adenocarcinoma	Cobimetinib, Atezolizumab, Hydroxychloroquine	I/II	NCT04214418
Advanced or metastatic breast cancer	CQ + taxane	II	NCT01446016
Oligometastatic prostate cancer	HCQ	II	NCT04011410
Multiple Myeloma	Carfilzomib + HCQ	I	NCT04163107
Platinum resistant epithelial ovarian cancer	Itraconazole + HCQ	I/II	NCT03081702
Advanced HCC	Sorafenib + HCQ	II	NCT03037437
Small cell lung cancer	Gemcitabine/carboplatin + HCQ	II	NCT02722369

Table 1.4: Table summarising autophagy modulators in clinical trials for cancer therapy.

1.7.4 Autophagy in ovarian cancer

The role for autophagy in OC is diverse and can play both tumour suppressive and tumour promoting roles, depending on disease stage. Studies suggest that autophagy is generally suppressed in OC, which likely facilitates tumourigenesis. A recent study published by Delaney *et al.* (2017) has provided a genetic rationale for the study of autophagy in OC. Haploinsufficiency network analysis was used to identify pathways which are most disrupted by somatic copy number alterations (SCNAs), the most prevalent genetic alteration in OC. Of all KEGG (Kyoto Encyclopedia of Genes and Genomes) pathways analysed, autophagy was found to be the most severely disrupted. Monoallelic deletions in BECN1 and/or LC3 were found in 94% of the TCGA tumours analysed. In addition, autophagy genes such as Atg10, GAPARAPL2 and ULK2 were commonly lost in OV (Delaney *et al.*, 2017). Despite this, numerous studies have shown that autophagy is readily inducible in OC cells in response to treatment. Autophagy induction, either by thioredoxin domain containing 17 (TXNDC17), ERK signalling or YAP activation promoted cisplatin resistance in various OC cell lines (S.-F. Zhang *et al.*, 2015)(Wang and Wu, 2014)(Xiao *et al.*, 2016). A role for autophagy in promoting OC cancer stem cell survival is also described in section 1.1.8.2.2. Thus, autophagy appears to take on a tumour supportive role in the established tumour where it confers a significant survival advantage.

Metastasis is a key process in tumour progression, as it allows cancer cells to disseminate from the site of origin. The most common route of metastasis in OC is via peritoneal seeding, and autophagy has been shown to aid in this process. A study by Kuo *et al*. (2019) revealed that autophagy plays a key role in selecting metastatic cells which can thrive in the peritoneum. OC cells were injected into mice, peritoneal metastases were harvested, cultured and implanted into new hosts. The selection

process was repeated three times to generate sublines. The metastases derived sublines were found to not only be enriched for autophagy genes but were more capable of inducing autophagy in response to stress (i.e. serum starvation or cisplatin treatment) than the parental cell lines. Inhibition of autophagy via ATG5 knockdown could also significantly impede the growth of the metastases derived sublines (Kuo *et al.*, 2019). This study suggests that upregulation of autophagy confers a survival advantage to metastatic cells, meaning targeting autophagy may be clinically useful to tackle peritoneal metastases in OC.

Analysis of the expression of autophagy markers may also be useful as a prognostic tool in OC. Expression of ATG9A, a key protein in autophagosome biogenesis, was analysed in tissue samples taken from 160 ovarian adenocarcinoma patients. High ATG9A expression correlated with higher clinical stage and relapsed disease (Dai, Zhang and Chen, 2014). A recent study developed a novel scoring system which could accurately predict the outcome for advanced OV patients after chemotherapy, using a panel of 43 ATG genes. The authors developed a training dataset using TCGA data to allow analysis of overall survival and recurrence-free survival (RFS). While the ATG score could not predict primary chemoresponse, following first line treatment, a higher ATG score was associated with shorter RFS (68.3% v 47.2%) (Niu *et al.*, 2019). A higher ATG score was also correlated with poor overall survival, regardless of residual diseases status, a key clinical feature when predicting patient outcomes following treatment. Similarly, a paper was recently published which analysed the relationship between autophagy-related gene expression and clinical outcome of patients with ovarian serous cystadenocarcinoma. The group generated an autophagy-related risk signature containing eight genes related to autophagy: BLOC1S1, IL24, NRG4, PDK4, PEX3, PRKG1, SIRT2, and WDR45L. This autophagy-related risk signature

was found to be an independent prognostic indicator for serous ovarian cancer (An *et al.*, 2018).

Targeting autophagy is an attractive target for the clinical management of OC, to tackle chemoresistance and metastasis, and as a prognostic biomarker. However, given the complex role of autophagy in regulating multiple facets of tumour biology, a better understanding of the molecular pathways regulating autophagy in OC is required. This study aimed to assess, for the first time, the presence of more than one autophagy pathway in OC cells. By answering these questions, it is aimed to develop a therapeutic strategy involving autophagy that can improve OC patient outcomes.

1.8 Thesis hypothesis and aims

Hypothesis: Autophagy is used by ovarian cancer cells to facilitate recovery and regrowth following treatment with clinically relevant chemotherapy drugs.

Aims:

- **1 (A):** To evaluate the sensitivity of a panel of ovarian cancer cell lines to paclitaxel and carboplatin
- **1 (B)** To characterize the ability of ovarian cancer cell lines to undergo apoptosis and induce autophagy
- **2 (A):** To assess the effect of chloroquine and lithium on the chemosensitivity of ovarian cancer cells
- **2 (B):** To evaluate the effect of brefeldin A on basal and drug induced autophagy
- **3:** To assess the importance of autophagy in the ability of ovarian cancer cells to recover from paclitaxel treatment
- **4:** To elucidate whether OC cells can recover their DNA content following drug treatment, and to assess whether autophagy contributes to this recovery

1.9 References

Abraham, A. G. and O'Neill, E. (2014) 'PI3K/Akt-mediated regulation of p53 in cancer', Biochemical Society Transactions, 42(4), p. 798 -803.

Acheson, E. D. et al. (1982) 'Mortality of two groups of women who manufactured gas masks from chrysotile and crocidolite asbestos: a 40-year follow-up', British journal of industrial medicine, 39(4), pp. 344–348.

Adkins, I. et al. (2014) 'Physical modalities inducing immunogenic tumor cell death for cancer immunotherapy.', Oncoimmunology, p. e968434.

Aghajanian, C. et al. (2012) 'OCEANS: A randomized, double-blind, placebo-controlled phase III trial of chemotherapy with or without bevacizumab in patients with platinum-sensitive recurrent epithelial ovarian, primary peritoneal, or fallopian tube cancer', Journal of Clinical Oncology, 30(17), pp. 2039–2045.

Alenquer, M. and Amorim, M. J. (2015) 'Exosome Biogenesis, Regulation, and Function in Viral Infection', Viruses, 7(9), pp. 5066–5083.

An, Y. *et al.* (2018) 'Development of a Novel Autophagy-related Prognostic Signature for Serous Ovarian Cancer', Journal of Cancer, 9(21), pp. 4058–4071.

Anglesio, M. S. et al. (2011) 'Clear cell carcinoma of the ovary: A report from the first Ovarian Clear Cell Symposium, June 24th, 2010', Gynaecologic Oncology, pp. 407–415.

Arakawa, S. et al. (2017) 'Molecular mechanisms and physiological roles of Atg5/Atg7-independent alternative autophagy', Proceedings of the Japan Academy. Series B, Physical and biological sciences, 93(6), pp. 378–385.

Arend, R. C. et al. (2018) 'Molecular Response to Neoadjuvant Chemotherapy in High-Grade Serous Ovarian Carcinoma', Molecular Cancer Research, 16(5), p. 813 -824.

Armstrong, D. K. *et al.* (2006) 'Intraperitoneal cisplatin and paclitaxel in ovarian cancer.', The New England journal of medicine, 354(1), pp. 34–43.

Au Yeung, C. L. et al. (2016) 'Exosomal transfer of stroma-derived miR21 confers paclitaxel resistance in ovarian cancer cells through targeting APAF1.', Nature communications, 7, p. 11150.

Axe, E. L. et al. (2008) ‘Autophagosome formation from membrane compartments enriched in phosphatidylinositol 3-phosphate and dynamically connected to the endoplasmic reticulum’, The Journal of Cell Biology, 182(4), pp. 685–701.

Baixauli, F., López-Otín, C. and Mittelbrunn, M. (2014) ‘Exosomes and autophagy: coordinated mechanisms for the maintenance of cellular fitness’, Frontiers in immunology, 5, p. 403.

Bao, L. et al. (2015) ‘Induction of autophagy contributes to cisplatin resistance in human ovarian cancer cells.’, Molecular medicine reports, 11(1), pp. 91–98.

Bar-Peled, L. et al. (2012) ‘Ragulator is a GEF for the rag GTPases that signal amino acid levels to mTORC1.’, Cell, 150(6), pp. 1196–1208.

Bellot, G. et al. (2009) ‘Hypoxia-Induced Autophagy Is Mediated through Hypoxia-Inducible Factor Induction of BNIP3 and BNIP3L via Their BH3 Domains’, Molecular and Cellular Biology, 29(10), p. 2570-2581.

Beral, V. et al. (2008) ‘Ovarian cancer and oral contraceptives: collaborative reanalysis of data from 45 epidemiological studies including 23 257 women with ovarian cancer and 87 303 controls’, The Lancet, 371(9609), pp. 303–314.

Bixel, K. and Hays, J. L. (2015) ‘Olaparib in the management of ovarian cancer’, Pharmacogenomics and Personalized Medicine, 8, pp. 127–135.

Burger, R. A. et al. (2011) ‘Incorporation of Bevacizumab in the Primary Treatment of Ovarian Cancer’, New England Journal of Medicine, 365(26), pp. 2473–2483.

Buys, S. S. *et al.* (2011) ‘Effect of Screening on Ovarian Cancer Mortality: The Prostate, Lung, Colorectal and Ovarian (PLCO) Cancer Screening Randomized Controlled Trial’, *JAMA*, 305(22), pp. 2295–2303.

Cai, S. et al. (2017) ‘Exosomal miR-7 Mediates Bystander Autophagy in Lung after Focal Brain Irradiation in Mice’, International journal of biological sciences, 13(10), pp. 1287–1296.

Callahan, M. J. et al. (2007) ‘Primary fallopian tube malignancies in BRCA-positive women undergoing surgery for ovarian cancer risk reduction’, Journal of Clinical Oncology, 25(25), pp. 3985–3990.

Carden, C. P. (2012) ‘The Association of PI3 Kinase Signaling and Chemoresistance in Advanced Ovarian Cancer’, pp. 1609–1617.

Cardenas, C. et al. (2017) ‘Adipocyte microenvironment promotes Bclxl expression and confers chemoresistance in ovarian cancer cells’, Apoptosis, 22(4), pp. 558–569.

Chan, E. Y. W. et al. (2009) ‘Kinase-inactivated ULK proteins inhibit autophagy via their conserved C-terminal domains using an Atg13-independent mechanism.’, Molecular and cellular biology, 29(1), pp. 157–171.

Chang, C. et al. (2017) ‘MicroRNA-134-3p is a novel potential inhibitor of human ovarian cancer stem cells by targeting RAB27A’, Gene, 605, pp. 99–107.

Chen, M.-W. et al. (2017) ‘The STAT3-miRNA-92-Wnt Signaling Pathway Regulates Spheroid Formation and Malignant Progression in Ovarian Cancer’, Cancer Research, 77(8), p. 1955-1967.

Chen, S. and Parmigiani, G. (2007) ‘Meta-analysis of BRCA1 and BRCA2 penetrance’, Journal of Clinical Oncology, 25(11), pp. 1329–1333.

Clark, C. A. et al. (2016) ‘Tumor-Intrinsic PD-L1 Signals Regulate Cell Growth, Pathogenesis, and Autophagy in Ovarian Cancer and Melanoma.’, Cancer research, 76(23), pp. 6964–6974.

Cotzomi-Ortega, I. et al. (2018) ‘Autophagy and Its Role in Protein Secretion: Implications for Cancer Therapy’, Mediators of inflammation. p. 4231591.

Cuervo, A. M. and Wong, E. (2013) ‘Chaperone-mediated autophagy: roles in disease and aging’, Cell Research. Shanghai Institutes for Biological Sciences, Chinese Academy of Sciences, 24, p. 92.

Cunha, L. D. et al. (2018) ‘LC3-Associated Phagocytosis in Myeloid Cells Promotes Tumor Immune Tolerance’, Cell, 175(2), p. 429–441.

Curiel, T. J. et al. (2004) ‘Specific recruitment of regulatory T cells in ovarian carcinoma fosters immune privilege and predicts reduced survival’, Nature Medicine, 10, p. 942.

Dabholkar, M. et al. (1994) ‘Messenger RNA levels of XPAC and ERCC1 in ovarian cancer tissue correlate with response to platinum-based chemotherapy.’, Journal of Clinical Investigation, pp. 703–708.

Dai, F., Zhang, Y. and Chen, Y. (2014) ‘Involvement of miR-29b signaling in the sensitivity to chemotherapy in patients with ovarian carcinoma’, Human Pathology, 45(6), pp. 1285–1293.

David, Y. Ben et al. (2002) ‘Effect of BRCA mutations on the length of survival in epithelial ovarian tumors’, Journal of Clinical Oncology, 20(2), pp. 463–466.

Delaney, J. R. et al. (2017) ‘Haploinsufficiency networks identify targetable patterns of allelic deficiency in low mutation ovarian cancer’, Nature communications, 8, p. 14423.

Dhuriya, Y. K. and Sharma, D. (2018) ‘Necroptosis: a regulated inflammatory mode of cell death’, Journal of Neuroinflammation, 15(1), p. 199.

Dimopoulos, M. A. et al. (2004) ‘Treatment of ovarian germ cell tumors with a 3-day bleomycin, etoposide, and cisplatin regimen: A prospective multicenter study’, Gynaecologic Oncology, 95(3), pp. 695–700.

Disis, M. L. *et al.* (2019) ‘Efficacy and Safety of Avelumab for Patients With Recurrent or Refractory Ovarian Cancer: Phase 1b Results From the JAVELIN Solid Tumor Trial’, JAMA Oncology, 5(3), pp. 393–401.

Dooley, H. C. et al. (2014) ‘WIPI2 links LC3 conjugation with PI3P, autophagosome formation, and pathogen clearance by recruiting Atg12-5-16L1’, Molecular cell, 55(2), pp. 238–252.

Dou, Z. et al. (2015) ‘Autophagy mediates degradation of nuclear lamina’, Nature, 527, p. 105.

Dunn, G. P. et al. (2014) ‘In vivo multiplexed interrogation of amplified genes identifies GAB2 as an ovarian cancer oncogene’, Proceedings of the National Academy of Sciences of the United States of America, pp. 1102–1107.

Dupont, N. et al. (2011) ‘Autophagy-based unconventional secretory pathway for extracellular delivery of IL-1β’, The EMBO journal, 30(23), pp. 4701–4711.

Ejlerskov, P. et al. (2013) ‘Tubulin polymerization-promoting protein (TPPP/p25alpha) promotes unconventional secretion of alpha-synuclein through exophagy by impairing autophagosome-lysosome fusion.’, The Journal of biological chemistry, 288(24), pp. 17313–17335.

Erenpreisa, J. et al. (2002) ‘Nuclear envelope-limited chromatin sheets are part of mitotic death’, Histochemistry and Cell Biology, 117(3), pp. 243–255.

Erenpreisa, J. et al. (2011) ‘Polyploid tumour cells elicit paradiploid progeny through depolyploidizing divisions and regulated autophagic degradation’, Cell Biology International, 35(7), pp. 687–695.

Eskander, R. N. *et al.* (2019) 'JAVELIN ovarian PARP 100 study design: Phase III trial of avelumab + chemotherapy followed by avelumab + talazoparib maintenance in previously untreated epithelial ovarian cancer.', Journal of Clinical Oncology. American Society of Clinical Oncology, 37(8_suppl), pp. TPS9-TPS9.

Etemadmoghadam, D. et al. (2009) 'Integrated Genome-wide DNA Copy Number and Expression Analysis Identifies Distinct Mechanisms of Primary Chemo-resistance in Ovarian Carcinomas', Clinical cancer research: an official journal of the American Association for Cancer Research, pp. 1417–1427.

Fathalla, M. F. (2013) 'Incessant ovulation and ovarian cancer - a hypothesis re-visited.', Facts, views & vision in ObGyn. Vlaamse Vereniging voor Obstetrie en Gynaecologie, 5(4), pp. 292–7.

Ferlazzo, G. et al. (2002) 'Human Dendritic Cells Activate Resting Natural Killer (NK) Cells and Are Recognized via the NKp30 Receptor by Activated NK Cells', The Journal of Experimental Medicine, pp. 343–351.

Fu, X.-T. et al. (2018) 'MicroRNA-30a suppresses autophagy-mediated anoikis resistance and metastasis in hepatocellular carcinoma', Cancer Letters, 412, pp. 108–117.

Fujiwara, K. *et al.* (2011) 'A randomized Phase II/III trial of 3 weekly intraperitoneal versus intravenous carboplatin in combination with intravenous weekly dose-dense paclitaxel for newly diagnosed ovarian, fallopian tube and primary peritoneal cancer.', Japanese journal of clinical oncology, 41(2), pp. 278–282.

Galluzzi, L. et al. (2014) 'Molecular mechanisms of regulated necrosis', Seminars in Cell & Developmental Biology, 35, pp. 24–32.

Galluzzi, L. et al. (2017) 'Immunogenic cell death in cancer and infectious disease.', Nature reviews. Immunology, 17(2), pp. 97–111.

Galluzzi, L. et al. (2018) 'Molecular mechanisms of cell death: recommendations of the Nomenclature Committee on Cell Death 2018', Cell Death & Differentiation, 25(3), pp. 486–541.

Gao, Y. et al. (2015) 'LncRNA-HOST2 regulates cell biological behaviours in epithelial ovarian cancer through a mechanism involving microRNA let-7b', Human Molecular Genetics, 24(3), pp. 841–852.

Garg, A. D. et al. (2017) ‘Trial watch: Immunogenic cell death induction by anticancer chemotherapeutics.’, Oncoimmunology, 6(12), p. e1386829.

Gartner, C. et al. (2012) ‘Knock-down of endothelial connexins impairs angiogenesis.’, Pharmacological research, 65(3), pp. 347–357.

Geisler, J. P. *et al.* (2007) ‘Nutritional assessment using prealbumin as an objective criterion to determine whom should not undergo primary radical cytoreductive surgery for ovarian cancer.’, Gynecologic oncology, 106(1), pp. 128–131.

Geller, M. A. et al. (2017) ‘Combination therapy with IL-15 superagonist (ALT-803) and PD-1 blockade enhances human NK cell immunotherapy against ovarian cancer’, Gynaecologic Oncology, 145, p. 19.

Geng, J. and Klionsky, D. J. (2008) ‘The Atg8 and Atg12 ubiquitin-like conjugation systems in macroautophagy. “Protein modifications: beyond the usual suspects” review series’, EMBO reports, 9(9), pp. 859–864.

Gershenson, D. M. (2007) ‘Management of ovarian germ cell tumors’, Journal of Clinical Oncology, pp. 2938–2943.

Glick, D., Barth, S. and Macleod, K. F. (2010) ‘Autophagy: cellular and molecular mechanisms’, The Journal of Pathology, 221(1), pp. 3–12.

Goetz, M. E. and Luch, A. (2008) ‘Reactive species: A cell damaging rout assisting to chemical carcinogens’, Cancer Letters, 266(1), pp. 73–83.

Goff, B. (2012) ‘Symptoms Associated with Ovarian Cancer’, Clinical Obstetrics and Gynecology, 55(1), pp. 36–42.

Golstein, P. and Kroemer, G. (2007) ‘Cell death by necrosis: towards a molecular definition’, Trends in Biochemical Sciences, 32(1), pp. 37–43.

Graybill, W. et al. (2015) ‘State of the science: Emerging therapeutic strategies for targeting angiogenesis in ovarian cancer’, Gynaecologic Oncology, 138(2), pp. 223–226.

Green, D. R. and Llambi, F. (2015) ‘Cell Death Signaling’, Cold Spring Harbor perspectives in biology, 7(12), p. a006080.

Hagemann, T. et al. (2006) ‘Ovarian Cancer Cells Polarize Macrophages Toward a Tumor-Associated Phenotype’, The Journal of Immunology, 176(8), p. 5023-5032.

Hallamaa, M. *et al.* (2012) 'Serum HE4 concentration is not dependent on menstrual cycle or hormonal treatment among endometriosis patients and healthy premenopausal women.', Gynecologic oncology, 125(3), pp. 667–672.

Hansen, J. M., Coleman, R. L. and Sood, A. K. (2016) 'Targeting the tumour microenvironment in ovarian cancer', European Journal of Cancer, 56, pp. 131–143.

Hassan, M. et al. (2014) 'Apoptosis and molecular targeting therapy in cancer.', BioMed research international, 2014, p. 150845.

Heckmann, B. L. and Green, D. R. (2019) 'LC3-associated phagocytosis at a glance.', Journal of cell science, 132(5).

Heo, J.-M. et al. (2015) 'The PINK1-PARKIN Mitochondrial Ubiquitylation Pathway Drives a Program of OPTN/NDP52 Recruitment and TBK1 Activation to Promote Mitophagy', Molecular cell, 60(1), pp. 7–20.

Hermans, C. et al. (2014) 'Analysis of FoxP3+ T-Regulatory Cells and CD8+T-Cells in Ovarian Carcinoma: Location and Tumor Infiltration Patterns Are Key Prognostic Markers', PLOS ONE, 9(11), p. e111757.

Hess, G. et al. (2009) 'Phase III Study to Evaluate Temsirolimus Compared with Investigator's Choice Therapy for the Treatment of Relapsed or Refractory Mantle Cell Lymphoma', Journal of Clinical Oncology, 27(23), pp. 3822–3829.

Horta, M. and Cunha, T. M. (2015) 'Sex cord-stromal tumors of the ovary: A comprehensive review and update for radiologists', Diagnostic and Interventional Radiology. Turkish Society of Radiology, 21(4), pp. 277–286.

Huang, J. et al. (2011) 'Frequent genetic abnormalities of the PI3K/AKT pathway in primary ovarian cancer predict patient outcome', Genes, chromosomes & cancer, 50(8), pp. 606–618.

Huggage, W. G. (2011) 'Morphological subtypes of ovarian carcinoma: a review with emphasis on new developments and pathogenesis', Pathology, 43(5), pp. 420–432.

Itakura, E., Kishi-Itakura, C. and Mizushima, N. (2012) 'The Hairpin-type Tail-Anchored SNARE Syntaxin 17 Targets to Autophagosomes for Fusion with Endosomes/Lysosomes', Cell, 151(6), pp. 1256–1269.

Jacobs, I. J. *et al.* (2016) 'Ovarian cancer screening and mortality in the UK Collaborative Trial of Ovarian Cancer Screening (UKCTOCS): a randomised controlled trial', The Lancet, 387(10022), pp. 945–956.

Jang, M. et al. (2018) ‘AMPK contributes to autophagosome maturation and lysosomal fusion’, Scientific Reports, 8(1), p. 12637.

Jiao, L. et al. (2018) ‘Regulation of glycolytic metabolism by autophagy in liver cancer involves selective autophagic degradation of HK2 (hexokinase 2)’, Autophagy, 14(4), pp. 671–684.

Jung, C. H. et al. (2009) ‘ULK-Atg13-FIP200 complexes mediate mTOR signaling to the autophagy machinery.’, Molecular biology of the cell, 20(7), pp. 1992–2003.

Karimi-Zarchi, M. et al. (2015) ‘Diagnostic Value of the Risk of Malignancy Index (RMI) for Detection of Pelvic Malignancies Compared with Pathology.’, Electronic physician. The Electronic Physician, 7(7), pp. 1505–10.

Karnezis, A. N. et al. (2016) ‘The disparate origins of ovarian cancers: pathogenesis and prevention strategies’, Nature Reviews Cancer, 17(1), pp. 65–74.

Kawaguchi, Y. et al. (2003) ‘The Deacetylase HDAC6 Regulates Aggresome Formation and Cell Viability in Response to Misfolded Protein Stress’, Cell, 115(6), pp. 727–738.

Kerr, J. F., Wyllie, A. H. and Currie, A. R. (1972) ‘Apoptosis: a basic biological phenomenon with wide-ranging implications in tissue kinetics’, British Journal of Cancer, 26(4), pp. 239–257.

Kim, Y. H. et al. (2016) ‘Uncoordinated 51-like kinase 2 signaling pathway regulates epithelial-mesenchymal transition in A549 lung cancer cells’, FEBS Letters, 590(9), pp. 1365–1374.

Kobel, M. et al. (2008) ‘Ovarian carcinoma subtypes are different diseases: implications for biomarker studies.’, PLoS medicine, 5(12), p. e232.

Krempski, J. et al. (2011) ‘Tumor-Infiltrating Programmed Death Receptor-1 Dendritic Cells Mediate Immune Suppression in Ovarian Cancer’, The Journal of Immunology, 186(12), p. 6905-6913.

Krishnan, V., Berek, J. S. and Dorigo, O. (2017) ‘Immunotherapy in ovarian cancer.’, Current Problems in Cancer, 41(1), pp. 48–63.

Kroeger, P. T. and Drapkin, R. (2017) ‘Pathogenesis and heterogeneity of ovarian cancer’, Current Opinion in Obstetrics & Gynecology, pp. 26–34.

Krysko, D. V, Ravichandran, K. S. and Vandenabeele, P. (2018) 'Macrophages regulate the clearance of living cells by calreticulin', Nature Communications, 9(1), p. 4644.

Kuo, C.-L. et al. (2019) 'In vivo selection reveals autophagy promotes adaptation of metastatic ovarian cancer cells to abdominal microenvironment', Cancer Science, 110(10), pp. 3204–3214.

Kuper, H., Cramer, D. W. and Titus-Ernstoff, L. (2002) 'Risk of ovarian cancer in the United States in relation to anthropometric measures: Does the association depend on menopausal status?', Cancer Causes and Control, 13(5), pp. 455–463.

Ladanyi, A. et al. (2018) 'Adipocyte-induced CD36 expression drives ovarian cancer progression and metastasis', Oncogene, 37(17), pp. 2285–2301.

Lakhani, S. R. et al. (2004) 'Pathology of Ovarian Cancers in BRCA1 and BRCA2 Carriers', Clinical Cancer Research, 10(7), p. 2473-2481.

Lamark, T. and Johansen, T. (2012) 'Aggrephagy: selective disposal of protein aggregates by macroautophagy.', International Journal of Cell Biology, 2012, p. 736905.

Lastwika, K. J. et al. (2016) 'Control of PD-L1 Expression by Oncogenic Activation of the AKT–mTOR Pathway in Non–Small Cell Lung Cancer', Cancer Research, 76(2), p. 227-238.

Ledermann, J. et al. (2014) 'Olaparib maintenance therapy in patients with platinum-sensitive relapsed serous ovarian cancer: a preplanned retrospective analysis of outcomes by BRCA status in a randomised phase 2 trial', The Lancet Oncology, 15(8), pp. 852–861.

Leonard, G. D., Fojo, T. and Bates, S. E. (2003) 'The Role of ABC Transporters in Clinical Practice', *The Oncologist*. John Wiley & Sons, Ltd, 8(5), pp. 411–424.

Lesnock, J. L. *et al.* (2013) 'BRCA1 expression and improved survival in ovarian cancer patients treated with intraperitoneal cisplatin and paclitaxel: a Gynecologic Oncology Group Study.', British journal of cancer, 108(6), pp. 1231–1237.

Li, H. et al. (1998) 'Cleavage of BID by caspase 8 mediates the mitochondrial damage in the Fas pathway of apoptosis.', Cell, 94(4), pp. 491–501.

Lilyquist, J. et al. (2017) 'Frequency of mutations in a large series of clinically ascertained ovarian cancer cases tested on multi-gene panels compared to reference controls', Gynaecologic Oncology, 147(2), pp. 375–380.

Lindor, N. M. et al. (2008) ‘Concise Handbook of Familial Cancer Susceptibility Syndromes - Second Edition’, JNCI Monographs, 2008(38), pp. 3–93.

Liu, P. et al. (2015) ‘Pten-Dependent Activation of the mTORC2 Kinase Complex’, Cancer Discovery, 5(11), p. 1194-1209.

Liu, S.-P. et al. (2013) ‘Identification of differentially expressed long non-coding RNAs in human ovarian cancer cells with different metastatic potentials’, Cancer Biology & Medicine, 10(13), pp. 138–141.

Liu, Z. et al. (2015) ‘The association between overweight, obesity and ovarian cancer: a meta-analysis.’, Japanese Journal of Clinical Oncology, 45(12), pp. 1107–15.

Lopez, J. and Tait, S. W. G. (2015) ‘Mitochondrial apoptosis: killing cancer using the enemy within.’, British Journal of Cancer, 112(6), pp. 957–962.

Low, J. J. H., Ilancheran, A. and Ng, J. S. (2012) ‘Malignant ovarian germ-cell tumours’, Best Practice and Research: Clinical Obstetrics and Gynaecology, 26(3), pp. 347–355.

Lu, K. H. and Daniels, M. (2013) ‘Endometrial and Ovarian Cancer in Women with Lynch syndrome: Update in Screening and Prevention’, Familial cancer, 12(2), p.273-277.

LUO, J. I. E. et al. (2014) ‘Role of microRNA-133a in epithelial ovarian cancer pathogenesis and progression’, Oncology Letters, pp. 1043–1048.

Lv, L. et al. (2011) ‘Acetylation targets the M2 isoform of pyruvate kinase for degradation through chaperone-mediated autophagy and promotes tumor growth’, Molecular cell, 42(6), pp. 719–730.

Ma, Y., Lu, Y. and Lu, B. (2016) ‘MicroRNA and Long Non-Coding RNA in Ovarian Carcinoma: Translational Insights and Potential Clinical Applications’, Cancer Investigation, 34(9), pp. 465–476.

Mabuchi, S., Sugiyama, T. and Kimura, T. (2016) ‘Clear cell carcinoma of the ovary: Molecular insights and future therapeutic perspectives’, Journal of Gynaecologic Oncology, 27(3), p. e31.

Mancias, J. D. and Kimmelman, A. C. (2011) ‘Targeting autophagy addiction in cancer’, Oncotarget, 2(12), pp. 1302–1306.

Mari, M. et al. (2010) ‘An Atg9-containing compartment that functions in the early steps of autophagosome biogenesis’, The Journal of cell biology, 190(6), pp. 1005–1022.

Martinez, F. O. and Gordon, S. (2014) 'The M1 and M2 paradigm of macrophage activation: time for reassessment', F1000Prime Reports, pp. 6-13.

Martinez, J. et al. (2011) 'Microtubule-associated protein 1 light chain 3 alpha (LC3)-associated phagocytosis is required for the efficient clearance of dead cells', Proceedings of the National Academy of Sciences of the United States of America, 108(42), pp. 17396–17401.

Martins, I. et al. (2009) 'Chemotherapy induces ATP release from tumor cells', Cell Cycle, 8(22), pp. 3723–3728.

Mathew, R. et al. (2009) 'Autophagy Suppresses Tumorigenesis through Elimination of p62', Cell, 137(6), pp. 1062–1075.

Matouk, I. J. et al. (2014) 'Oncofetal H19 RNA promotes tumor metastasis', Biochimica et Biophysica Acta (BBA) - Molecular Cell Research, 1843(7), pp. 1414–1426.

Matsumoto, K. et al. (2019) 'PARP inhibitors for BRCA wild type ovarian cancer; gene alterations, homologous recombination deficiency and combination therapy', Japanese Journal of Clinical Oncology, 49(8), pp. 703–707.

Matte, I. et al. (2012) 'Profiling of cytokines in human epithelial ovarian cancer ascites', American Journal of Cancer Research, pp. 566–580.

Matulonis, U. A. et al. (2019) 'Antitumor activity and safety of pembrolizumab in patients with advanced recurrent ovarian cancer: results from the phase II KEYNOTE-100 study', Annals of Oncology, 30(7), pp. 1080–1087.

Mayr, C., Hemann, M. T. and Bartel, D. P. (2007) 'Disrupting the Pairing Between let-7 and Hmga2 Enhances Oncogenic Transformation', Science, 315(5818), pp. 1576–1579.

Medeiros, F. et al. (2006) 'The tubal fimbria is a preferred site for early adenocarcinoma in women with familial ovarian cancer syndrome.', The American Journal of Surgical Pathology, 30(2), pp. 230–236.

Merritt, W. M. et al. (2008) 'Dicer, Drosha, and outcomes in patients with ovarian cancer.', The New England Journal of Medicine, 359(25), pp. 2641–2650.

Mezzanzanica, D. et al. (2010) 'Role of microRNAs in ovarian cancer pathogenesis and potential clinical implications', The International Journal of Biochemistry & Cell Biology, 42(8), pp. 1262–1272.

Mikula-Pietrasik, J. et al. (2017) ‘The Proangiogenic Capabilities of Malignant Ascites Generated by Aggressive Ovarian Tumors’, Biomed Research International, 2017.

Moore, K. *et al.* (2018) ‘Maintenance Olaparib in Patients with Newly Diagnosed Advanced Ovarian Cancer.’, The New England journal of medicine, 379(26), pp. 2495–2505.

Moore, R. G. *et al.* (2009) ‘A novel multiple marker bioassay utilizing HE4 and CA125 for the prediction of ovarian cancer in patients with a pelvic mass.’, Gynecologic oncology, 112(1), pp. 40–46.

Morselli, E. et al. (2009) ‘Anti- and pro-tumor functions of autophagy’, Biochimica et Biophysica Acta (BBA) - Molecular Cell Research, 1793(9), pp. 1524–1532.

Morselli, E. et al. (2011) ‘p53 inhibits autophagy by interacting with the human ortholog of yeast Atg17, RB1CC1/FIP200.’, Cell Cycle, 10(16), pp. 2763–2769.

Mrakovcic, M. and Frohlich, L. F. (2018) ‘p53-Mediated Molecular Control of Autophagy in Tumor Cells.’, Biomolecules, 8(2).

Muscat, J. E. and Huncharek, M. S. (2008) ‘Perineal talc use and ovarian cancer: a critical review.’, European journal of cancer prevention: the official journal of the European Cancer Prevention Organisation (ECP), 17(2), pp. 139–46.

Mutch, D. G. and Prat, J. (2014) ‘2014 FIGO staging for ovarian, fallopian tube and peritoneal cancer’, Gynecologic Oncology, 133(3), pp. 401–404.

Naomi, N. et al. (2010) ‘Gene amplification CCNE1 is related to poor survival and potential therapeutic target in ovarian cancer’, Cancer, 116(11), pp. 2621–2634.

Nelson, B. E., Rosenfield, A. T. and Schwartz, P. E. (1993) ‘Preoperative abdominopelvic computed tomographic prediction of optimal cytoreduction in epithelial ovarian carcinoma.’, Journal of clinical oncology: official journal of the American Society of Clinical Oncology, 11(1), pp. 166–172.

Nieman, K. M. et al. (2011) ‘Adipocytes promote ovarian cancer metastasis and provide energy for rapid tumor growth’, Nature medicine, 17(11), pp. 1498–1503.

Nishida, Y. et al. (2009) ‘Discovery of Atg5/Atg7-independent alternative macroautophagy’, Nature, 461(7264), p. 654.

Niu, Y. et al. (2019) ‘A novel scoring system for pivotal autophagy-related genes predicts outcomes after chemotherapy in advanced ovarian cancer patients’, Cancer Epidemiology Biomarkers & Prevention, 28(12), p. 2106-2114.

Nowak, M. *et al.* (2015) ‘Current clinical application of serum biomarkers to detect ovarian cancer’, Menopause review, 14(4), pp. 254–259.

Opara, E. I. and Zaidi, J. (2007) ‘The interpretation and clinical application of the word “parity”: a survey’, BJOG: An International Journal of Obstetrics & Gynaecology, 114(10), pp. 1295–1297.

Oza, A. M. et al. (2015) ‘Standard chemotherapy with or without bevacizumab for women with newly diagnosed ovarian cancer (ICON7): overall survival results of a phase 3 randomised trial.’, The Lancet. Oncology, 16(8), pp. 928–36.

Pagotto, A. et al. (2017) ‘Autophagy inhibition reduces chemoresistance and tumorigenic potential of human ovarian cancer stem cells’, Cell Death & Disease, 8(7), p. e2943.

Paik, E. S. et al. (2018) ‘Molecular Signature for Lymphatic Invasion Associated with Survival of Epithelial Ovarian Cancer’, Cancer Research and Treatment: Official Journal of Korean Cancer Association, 50(2), pp. 461–473.

Pampena, M. B. and Levy, E. M. (2015) ‘Natural Killer Cells as Helper Cells in Dendritic Cell Cancer Vaccines’, Frontiers in Immunology, 2015, p. 6-13.

Parikh, A. et al. (2014) ‘microRNA-181a has a critical role in ovarian cancer progression through the regulation of the epithelial–mesenchymal transition’, Nature Communications, 5(2977).

Park, E. J. et al. (2016) ‘Chloroquine enhances TRAIL-mediated apoptosis through up-regulation of DR5 by stabilization of mRNA and protein in cancer cells.’, Scientific reports. 6, p. 22921.

Parsons, S. L., Lang, M. W. and Steele, R. J. C. (1996) ‘Malignant ascites: a 2-year review from a teaching hospital’, European Journal of Surgical Oncology, 22(3), pp. 237–239.

Perren, T. J. et al. (2011) ‘A Phase 3 Trial of Bevacizumab in Ovarian Cancer’, New England Journal of Medicine, 365(26), pp. 2484–2496.

Pfeffer, C. M. and Singh, A. T. K. (2018) ‘Apoptosis: A Target for Anticancer Therapy.’, International Journal of Molecular Sciences, 19(2).

Pinsky, P. F. *et al.* (2016) 'Extended mortality results for ovarian cancer screening in the PLCO trial with median 15years follow-up', Gynecologic oncology, 143(2), pp. 270–275.

Pogge von Strandmann, E. et al. (2017) 'Tumor-Host Cell Interactions in Ovarian Cancer: Pathways to Therapy Failure.', Trends in cancer, 3(2), pp. 137–148.

Prat, J. et al. (2015) 'Figo's staging classification for cancer of the ovary, fallopian tube, and peritoneum: Abridged republication', Journal of Gynaecologic Oncology, 26(2), pp. 87–9.

Prat, J., Ribe, A. and Gallardo, A. (2005) 'Hereditary ovarian cancer', Journal of Clinical Oncology, 36(8), pp. 861–870.

Pujade-Lauraine, E. et al. (2014) 'Bevacizumab combined with chemotherapy for platinum-resistant recurrent ovarian cancer: The AURELIA open-label randomized phase III trial', Journal of Clinical Oncology, 32(13), pp. 1302–1308.

Quarato, G. et al. (2016) 'Sequential Engagement of Distinct MLKL Phosphatidylinositol-Binding Sites Executes Necroptosis.', Molecular Cell, 61(4), pp. 589–601.

Rautela, J. and Huntington, N. D. (2017) 'IL-15 signaling in NK cell cancer immunotherapy.', Current Opinion in Immunology, 44, pp. 1–6.

Ray-Coquard, I. et al. (2014) 'Gynaecologic Cancer InterGroup (GCIG) Consensus Review for Ovarian Sex Cord Stromal Tumors', International Journal of Gynaecological Cancer, 24, pp. S42–S47.

Reid, B. M., Permuth, J. B. and Sellers, T. A. (2017) 'Epidemiology of ovarian cancer: a review.', Cancer Biology & Medicine, 14(1), pp. 9–32.

Rello-Varona, S. et al. (2012) 'Autophagic removal of micronuclei', Cell Cycle, 11(1), pp. 170–176.

Roberts, P. et al. (2003) 'Piecemeal microautophagy of nucleus in Saccharomyces cerevisiae', Molecular biology of the cell. The American Society for Cell Biology, 14(1), pp. 129–141.

Rojas-Puentes, L. L. et al. (2013) 'Phase II randomized, double-blind, placebo-controlled study of whole-brain irradiation with concomitant chloroquine for brain metastases', Radiation Oncology, 8(1), p. 209.

Rubin, S. C. et al. (1996) 'Clinical and pathological features of ovarian cancer in women with germ-line mutations of BRCA1.', The New England Journal of Medicine, 335(19), pp. 1413–6.

Saenz, R. et al. (2014) ‘TLR4-dependent activation of dendritic cells by an HMGB1-derived peptide adjuvant’, Journal of translational medicine, 12, p. 211.

Sakai, K. et al. (2017) ‘Clonal composition of human ovarian cancer based on copy number analysis reveals a reciprocal relation with oncogenic mutation status’, Cancer Letters, 405, pp. 22–28.

Salazar, C., Campbell, I. G. and Gorringe, K. L. (2018) ‘When Is “Type I” Ovarian Cancer Not “Type I”? Indications of an Out-Dated Dichotomy’, Frontiers in Oncology, p. 654.

Samimi, G. *et al.* (2003) ‘Increase in Expression of the Copper Transporter ATP7A during Platinum Drug-Based Treatment Is Associated with Poor Survival in Ovarian Cancer Patients’, Clinical Cancer Research, 9(16), p. 5853 LP-5859.

Samimi, G. *et al.* (2004) ‘Modulation of the Cellular Pharmacology of Cisplatin and Its Analogs by the Copper Exporters ATP7A and ATP7B’, Molecular Pharmacology, 66(1), p. 25 LP-32.

Sasada, A., Abe, M. and Abe, H. (2017) ‘A case of advanced ovarian cancer effectively treated with a combination of multi-peptide dendritic cell immunotherapy, surgery, and chemotherapy’, Personalized Medicine Universe, 6, pp. 28–30.

Schiff, P. B., Fant, J. and Horwitz, S. B. (1979) ‘Promotion of microtubule assembly in vitro by taxol.’, Nature, 277(5698), pp. 665–667.

Seals, D. F. et al. (2000) ‘A Ypt/Rab effector complex containing the Sec1 homolog Vps33p is required for homotypic vacuole fusion’, Proceedings of the National Academy of Sciences of the United States of America, 97(17), pp. 9402–9407.

Sedlakova, I. *et al.* (2015) ‘Clinical significance of the resistance proteins LRP, Pgp, MRP1, MRP3, and MRP5 in epithelial ovarian cancer.’, International journal of Gynecological cancer: official journal of the International Gynecological Cancer Society, 25(2), pp. 236–243.

Seifert, L. and Miller, G. (2017) ‘Molecular Pathways: The Necrosome—A Target for Cancer Therapy’, Clinical Cancer Research, 23(5), p. 1132-1136.

Selvakumaran, M. et al. (2003) ‘Enhanced Cisplatin Cytotoxicity by Disturbing the Nucleotide Excision Repair Pathway in Ovarian Cancer Cell Lines’, Cancer Research, 63(6), p. 1311-1316.

Serrano-del Valle, A. et al. (2019) ‘Immunogenic Cell Death and Immunotherapy of Multiple Myeloma’, Frontiers in Cell and Developmental Biology, 7, p. 50.

Sha, Y. et al. (2017) ‘STUB1 regulates TFEB-induced autophagy-lysosome pathway.’, The EMBO Journal, 36(17), pp. 2544–2552.

Shell, S. et al. (2007) ‘Let-7 expression defines two differentiation stages of cancer’, Proceedings of the National Academy of Sciences of the United States of America, 104(27), pp. 11400–11405.

Shukla, G. C., Singh, J. and Barik, S. (2011) ‘MicroRNAs: Processing, Maturation, Target Recognition and Regulatory Functions’, Molecular and cellular pharmacology, pp. 83–92.

Singh, R., Letai, A. and Sarosiek, K. (2019) ‘Regulation of apoptosis in health and disease: the balancing act of BCL-2 family proteins’, Nature Reviews Molecular Cell Biology, 20(3), pp. 175–193.

Sistigu, A. et al. (2014) ‘Cancer cell–autonomous contribution of type I interferon signaling to the efficacy of chemotherapy’, Nature Medicine, 20, p. 1301.

Smith, V. L., Jackson, L. and Schorey, J. S. (2015) ‘Ubiquitination as a Mechanism to Transport Soluble Mycobacterial and Eukaryotic Proteins to Exosomes’, The Journal of Immunology, 195(6), p. 2722-2730.

Soslow, R. A. (2008) ‘Histologic Subtypes of Ovarian Carcinoma’, International Journal of Gynaecological Pathology, PAP (14), pp. 161–174.

Spisek, R. et al. (2007) ‘Bortezomib enhances dendritic cell (DC)–mediated induction of immunity to human myeloma via exposure of cell surface heat shock protein 90 on dying tumor cells: therapeutic implications’, Blood, 109(11), p. 4839-4845.

Strathdee, G. et al. (1999) ‘A role for methylation of the hMLH1 promoter in loss of hMLH1 expression and drug resistance in ovarian cancer’, Oncogene, 18, p. 2335.

Stronach, E. et al. (2011) ‘DNA-PK Mediates AKT Activation and Apoptosis Inhibition in Clinically Acquired Platinum Resistance’. Neoplasia, 13(11), p. 1069-1080.

Stürner, E. and Behl, C. (2017) ‘The Role of the Multifunctional BAG3 Protein in Cellular Protein Quality Control and in Disease’, Frontiers in Molecular Neuroscience, 10, p. 177.

Tan, G. et al. (2015) ‘A novel role for microRNA-129-5p in inhibiting ovarian cancer cell proliferation and survival via direct suppression of transcriptional co-activators YAP and TAZ’, Oncotarget, pp. 8676–8686.

Testa, U. et al. (2018) ‘Ovarian Cancers: Genetic Abnormalities, Tumor Heterogeneity and Progression, Clonal Evolution and Cancer Stem Cells’. Medicines, 5(1).

Tewari, K. S. et al. (2019) ‘Final Overall Survival of a Randomized Trial of Bevacizumab for Primary Treatment of Ovarian Cancer.’, Journal of Clinical Oncology, 37(26), pp. 2317–2328.

Todd, R. C. and Lippard, S. J. (2009) ‘Inhibition of transcription by platinum antitumor compounds’, Metallomics: integrated biometal science, 1(4), pp. 280–291.

Tooze, S. A. and Yoshimori, T. (2010) ‘The origin of the autophagosomal membrane’, Nature Cell Biology, 12, p. 831.

Tothill, R. W. et al. (2008) ‘Novel Molecular Subtypes of Serous and Endometrioid Ovarian Cancer Linked to Clinical Outcome’, Clinical Cancer Research, 14(16), p. 5198-5208.

Tripathi, D. N. et al. (2013) ‘Reactive nitrogen species regulate autophagy through ATM-AMPK-TSC2–mediated suppression of mTORC1’, Proceedings of the National Academy of Sciences, 110(32), p. E2950-E2957.

Van Nagell, J. R. et al. (2011) ‘Long-term survival of women with epithelial ovarian cancer detected by ultrasonographic screening.’, Obstetrics and Gynecology, 118(6), pp. 1212–21.

Venkatesan, P. (2017) ‘Possible origin of ovarian cancer in the fallopian tubes’, The Lancet Oncology, 18(12), p. e714.

Viry, E. et al. (2014) ‘Autophagic degradation of GZMB/granzyme B: a new mechanism of hypoxic tumor cell escape from natural killer cell-mediated lysis’, Autophagy, 10(1), pp. 173–175.

Vitale, I. et al. (2011) ‘Mitotic catastrophe: a mechanism for avoiding genomic instability.’, Nature reviews. Molecular cell biology, pp. 385–392.

Walker, J. L. *et al.* (2019) ‘Randomized Trial of Intravenous Versus Intraperitoneal Chemotherapy Plus Bevacizumab in Advanced Ovarian Carcinoma: An NRG Oncology/Gynecologic Oncology Group Study.’, Journal of clinical oncology : official journal of the American Society of Clinical Oncology, 37(16), pp. 1380–1390.

Wang, J. and Wu, G. S. (2014) 'Role of Autophagy in Cisplatin Resistance in Ovarian Cancer Cells', The Journal of Biological Chemistry, pp. 17163–17173.

Wang, X., Ivan, M. and Hawkins, S. M. (2017) 'The role of MicroRNA molecules and MicroRNA-regulating machinery in the pathogenesis and progression of epithelial ovarian cancer', Gynaecologic Oncology, 147(2), pp. 481–487.

Wang, Y. et al. (2015) 'HOTAIR is a potential target for the treatment of cisplatin resistant ovarian cancer.', Molecular medicine reports, 12(2), pp. 2211–2216.

Wang, Y. K. et al. (2017) 'Genomic consequences of aberrant DNA repair mechanisms stratify ovarian cancer histotypes', Nature Genetics, 49, p. 856.

White, E. (2016) 'Autophagy and p53.', Cold Spring Harbor Perspectives in Medicine, 6(4), p. a026120.

Williams, S. et al. (1994) 'Adjuvant therapy of ovarian germ cell tumors with cisplatin, etoposide, and bleomycin: a trial of the Gynaecologic Oncology Group.', Journal of clinical oncology: Official Journal of the American Society of Clinical Oncology, 12(4), pp. 701–6.

Wright, A. A. *et al.* (2016) 'Neoadjuvant Chemotherapy for Newly Diagnosed, Advanced Ovarian Cancer: Society of Gynecologic Oncology and American Society of Clinical Oncology Clinical Practice Guideline', Journal of clinical oncology : official journal of the American Society of Clinical Oncology, 34(28), pp. 3460–3473.

Wurmser, A. E., Sato, T. K. and Emr, S. D. (2000) 'New component of the vacuolar class C-Vps complex couples nucleotide exchange on the Ypt7 GTPase to SNARE-dependent docking and fusion', The Journal of Cell Biology, 151(3), pp. 551–562.

Xiang, L., Rong, G., Zhao, J., Wang, Z., Shi, F. (2018) 'Identification of candidate genes associated with tubal origin of high-grade serous ovarian cancer.', Oncology Letters, 15(5), pp. 7769–7775.

Xiao, L. et al. (2016) 'YAP induces cisplatin resistance through activation of autophagy in human ovarian carcinoma cells.', OncoTargets and Therapy, 9, pp. 1105–1114.

Xiao, M. et al. (2017) 'Let-7e sensitizes epithelial ovarian cancer to cisplatin through repressing DNA double strand break repair', Journal of Ovarian Research, 10, p. 24.

Xu, J. et al. (2016) 'Autophagy-Mediated Degradation of IAPs and c-FLIP(L) Potentiates Apoptosis Induced by Combination of TRAIL and Chal-24', Journal of Cellular Biochemistry, 117(5), pp. 1136–1144.

Yan, X. et al. (2010) ‘Increased expression of annexin A3 is a mechanism of platinum resistance in ovarian cancer.’, Cancer Research, 70(4), pp. 1616–1624.

Yang, H. et al. (2013) ‘mTOR kinase structure, mechanism and regulation.’, 497(7448), pp. 217–223.

Yi, S. et al. (2017) ‘Antiangiogenic drugs used with chemotherapy for patients with recurrent ovarian cancer: a meta-analysis.’, OncoTargets and Therapy, 10, pp. 973–984.

Yin, J. et al. (2012) ‘Secretion of annexin A3 from ovarian cancer cells and its association with platinum resistance in ovarian cancer patients.’, Journal of cellular and molecular medicine, 16(2), pp. 337–348.

Yin, M. et al. (2016) ‘Tumor-associated macrophages drive spheroid formation during early transcoelomic metastasis of ovarian cancer’, The Journal of Clinical Investigation, pp. 4157–4173.

Youle, R. J. and Narendra, D. P. (2011) ‘Mechanisms of mitophagy’, Nature reviews. Molecular cell biology, 12(1), pp. 9–14.

Yu, J. S. L. and Cui, W. (2016) ‘Proliferation, survival and metabolism: the role of PI3K/AKT/mTOR signalling in pluripotency and cell fate determination’, Development, 143(17), p. 3050-3060.

Yu, L., Chen, Y. and Tooze, S. A. (2017) ‘Autophagy pathway: Cellular and molecular mechanisms’, Autophagy, 14(2), pp. 207–215.

Yue, Z. et al. (2003) ‘Beclin 1, an autophagy gene essential for early embryonic development, is a haploinsufficient tumor suppressor’, Proceedings of the National Academy of Sciences of the United States of America, 100(25), pp. 15077–15082.

Zeller, C. et al. (2012) ‘Candidate DNA methylation drivers of acquired cisplatin resistance in ovarian cancer identified by methylome and expression profiling’, Oncogene, 31, p. 4567.

Zhang, L. et al. (2016) ‘UCA1 overexpression predicts clinical outcome of patients with ovarian cancer receiving adjuvant chemotherapy’, Cancer Chemotherapy and Pharmacology, 77(3), pp. 629–634.

Zhang, M. et al. (2015) ‘Translocation of interleukin-1beta into a vesicle intermediate in autophagy-mediated secretion.’, eLife, 4.

Zhang, S.-F. et al. (2015) ‘TXNDC17 promotes paclitaxel resistance via inducing autophagy in ovarian cancer’, Autophagy, 11(2), pp. 225–238.

Zhu, Z. *et al.* (2015) ‘CYP1B1 enhances the resistance of epithelial ovarian cancer cells to paclitaxel in vivo and in vitro’, International journal of molecular medicine, 35(2), pp. 340–348.

Chapter Two: Evaluation of the response of a panel of ovarian cancer cell lines to paclitaxel and carboplatin

2.1 Abstract

Ovarian cancer is the seventh most commonly diagnosed cancer among women worldwide. Most women have an excellent response to first line chemotherapy however disease recurrence is a major clinical challenge. In order to gain an insight into the mechanisms driving resistance, we investigated the response of a panel of ovarian cancer cell lines to two clinically relevant drugs, paclitaxel and carboplatin. Induction of apoptosis was evident only in response to paclitaxel, and to varying levels amongst the cell line panel. The murine ID8-luc2 cell line expressed the lowest active caspase-3 levels (3%), with the human OVCAR-3 cell line expressing the highest (40%). Importantly this activity was significantly reduced in all cell lines tested following recovery of surviving clones from a single round of treatment.

We have also investigated expression of key autophagy proteins (Beclin 1, Atg5/12, and LC3I/II) and the capacity of all cell lines to undergo autophagy in the presence or absence of drugs. Each of the cell lines expressed the key autophagy proteins, although to varying levels, and importantly, protein expression did not correlate with the cells ability to undergo autophagy. Two subgroups of cells could be distinguished from this study, based on their drug sensitivity and their apoptotic and autophagic competency. The OVCAR-3 and -4 cells were most sensitive to both drugs, displayed the highest levels of apoptosis and low autophagy induction levels. By comparison, the OVCAR-5 and -8 cell lines were more drug resistant, with low levels of apoptosis and high autophagy induction.

The findings from this chapter have clinically significant implications, suggesting that apoptosis can be diminished following re-challenge with paclitaxel. As ovarian cancer patients typically receive multiple rounds of chemotherapy, this signifies autophagy as a clinically relevant target when conventional therapies are failing to induce cell

death. The use of a cell line panel in this study enabled the characterisation of cells with differing drug sensitivities, which may be linked to their apoptotic/autophagic competency. Such characterisation is important for the development of effective chemosensitising strategies in the face of considerable heterogeneity which exists among patients.

2.2 Introduction

Ovarian cancer remains the leading cause of death from gynaecological malignancies among women worldwide. Due to the benign nature of the disease symptoms, diagnoses are often made at a late stage resulting in poor survival outcomes for women. The standard of care for the clinical management of ovarian cancer has remained largely unchanged, with surgery and a dual taxane/platinum chemotherapy regimen utilised. Patients will typically receive an intravenous paclitaxel/carboplatin infusion every three weeks for up to 6 cycles (Boyd and Muggia, 2018). Disease recurrence is the major clinical challenge faced in the treatment of OC. The implementation of PARP inhibitors such as Olaparib, which are indicated as a maintenance monotherapy for women with complete or partial response to platinum chemotherapy, have improved progression free survival (O'Cearbhaill, 2018). Despite this, there is a need to further elucidate the molecular mechanisms driving resistance in order to improve patient outcomes.

An area which has gained interest as a potential therapeutic target to overcome resistance is autophagy. Autophagy is an evolutionary conserved catabolic process, enabling the degradation and recycling of intracellular components. While autophagy primarily functions to promote healthy cell survival and homeostasis, it can also be utilised by cancer cells to confer a survival advantage. Cancer cells can use autophagy to thrive in the harsh tumour microenvironment and to withstand chemotherapeutic insult. Studies have reported that autophagy can contribute to both cisplatin and paclitaxel resistance (Kulshrestha *et al.*, 2019); (Wang and Wu, 2014); (S.-F. Zhang *et al.*, 2015).

Ovarian cancers comprise a group of five pathologically and histologically distinct malignancies, as discussed in depth in section 1.1.3 of Chapter one. Serous cancers

are the most common, with high grade serous tumours accounting for over 70% of ovarian cancer deaths (Kim *et al.*, 2018). A panel of four human cell lines (OVCAR-3, -4, -5, -8) and one murine (ID8-luc2) cell line, all of which represent the serous subtype, were assessed for their response to paclitaxel and carboplatin.

A recent haploinsufficiency study identified autophagy as the most severely disrupted pathway among ovarian cancer cohorts, with monoallelic deletions in key autophagy genes including BECN1 and LC3 also reported in the OVCAR-3 cell line (Delaney *et al.* 2017). Levels of apoptosis competency have also been reported to vary widely among ovarian cancer cell lines. Therefore, in this study, we assessed a panel of OC cell lines for their ability to undergo apoptosis and autophagy in response to standard chemotherapeutic agents.

2.3 Materials and Methods

2.3.1 Cell culture and Reagents

Established human ovarian cancer cell lines OVCAR-3, OVCAR-4, OVCAR-5 and OVCAR-8 were obtained directly from the NCI Frederick Cancer DCTC Tumor/Cell Line Repository. Murine ID8-luc2 cells were obtained from the Mayo Clinic. All human OVCAR cell lines were maintained in RPMI-1640 media. Due to a slow rate of growth in media supplemented with 10% (v/v) foetal calf serum (FCS), OVCAR-3 and OVCAR-4 cultures were supplemented with 20% (v/v) (FCS). OVCAR-5 and OVCAR-8 cultures were supplemented with 10% (v/v) foetal calf serum. Murine ID8-luc2 cells were cultured using Dulbecco's Modified Eagles Medium (DMEM) containing 10% (v/v) foetal calf serum. All cultures were supplemented with 1% penicillin/streptomycin (Gibco Life Technologies, Cat # 15070-063). Cells were grown in T75cm^2 flasks (Sarstedt) and maintained at 37°C, 5% CO_2. The OVCAR-3 cell line was established by Hamilton and colleagues in 1983, from the malignant ascites of an ovarian adenocarcinoma patient treated with cisplatin, adriamycin and cyclophosphamide (Hamilton *et al.*, 1983). The OVCAR-4 cell line was also derived from the metastatic ascites of a HGSOC cisplatin refractory patient (Hamilton, Young and Ozols, 1984). The OVCAR-5 cell line was derived from ascites of a treatment naïve patient, while the OVCAR-8 cell line originated from the tumour tissue of a high dose carboplatin refractory patient (Hamilton, Young and Ozols, 1984). These cell lines were selected after a review of the literature was conducted, as they most likely represent the high grade serous subtype of OC. Microscopic analysis of OVCAR-3,-4, -5 and -8 derived xenografts revealed histology consistent with that of HGSOC tumours (Mitra *et al.*, 2015). A study published in 2013 also ranked the OVCAR-3, -4 and -8 cell lines as likely HGSOC, based on the fraction of their genome altered and

the number of copy number alterations, which were consistent with TCGA patient data (Domcke *et al.*, 2013). All four OVCAR cell lines were also identified as high grade serous by (Anglesio *et al.*, 2013). A number of functional characteristics, including migration, invasion and cisplatin sensitivity, of the OVCAR-4, -5 and -8 cell lines was conducted by (Haley *et al.*, 2016). OVCAR-3 cells have been reported to have monoallelic deletions of BECN1 and LC3, with the OVCAR-5 and -8 cell lines having allelic gains in these genes (Delaney *et al.*, 2017). Little is known about the status of these genes in the OVCAR-4 and ID8-luc2 cell lines. Each of the OVCAR cell lines is BRCA1/2 wildtype, however the OVCAR-8 cell line has hypermethylation of BRCA1. The OVCAR-8 cell line also has a hyperdiploid karyotype. The murine ID8 cell line was derived from spontaneously transformed mouse surface epithelial cells (MOSE) by (Roby *et al.*, 2000). They were included in the study in anticipation of future *in vivo* studies, as these cells form tumours within the peritoneal cavity of mice resembling stage III or IV cancers in women.

2.3.2 Drug treatments

Paclitaxel (Cat # T7402) and carboplatin (Cat # C2538) were both purchased from Sigma Aldrich. Paclitaxel was reconstituted in dimethyl sulfoxide (DMSO) to give 58.55mM stock. Aliquots were prepared and stored at -20^{0}C. Working concentrations of paclitaxel were prepared fresh in media on the day of treatment. Carboplatin was reconstituted in water to give a 26.93mM stock, aliquoted and stored in the dark at room temperature. Working concentrations were prepared in media on the day of treatment. Cells received a 48 hour treatment with both paclitaxel and carboplatin unless otherwise stated. A working stock of chloroquine (CQ) was prepared in media

(1mM) on the day of treatment and added to the cells at the desired concentration of 10μM, 2 hours prior to any other drug treatment.

For clonogenic recovery assays, cells were treated for 24 or 48 hours with paclitaxel or carboplatin and subsequently reseeded for colony regrowth. For caspase-3 assays, cells also received a 24 or 48 hour treatment with paclitaxel or carboplatin, after which cells were probed and assessed by flow cytometry.

For autophagy assays, cells were treated with paclitaxel or carboplatin +/-CQ (10μM) for 24 or 48 hours. Media containing drugs was then removed and replaced with new drug free media. Cells were allowed to recover for 24 hours and prepared for western blot, Cyto-ID autophagy assay or immunofluorescence. A 24 hour recovery period was added in an effort to mimic the clinical scenario, whereby the patient receives a treatment free interval.

The process of generating OVCAR clones is described in figure 2.1 below.

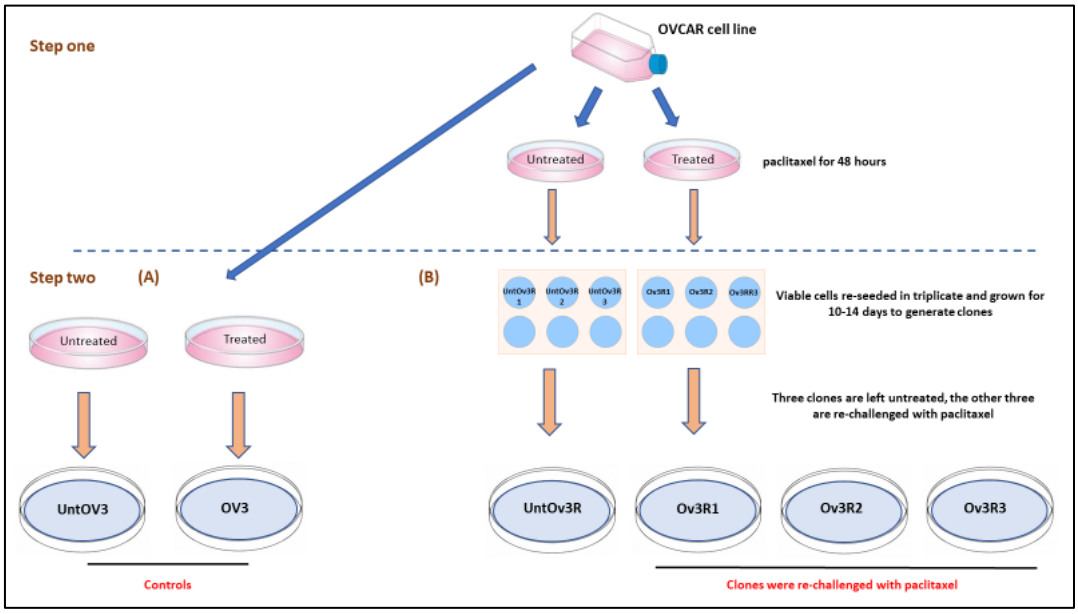

Figure 2.1. Schematic illustrating the process of generating OVCAR clones. **Step one** of the process involves treating the OVCAR cell line (either 3, 4 or 5) with paclitaxel for 48 hours, along with untreated cells. Caspase activity was assessed after 48 hours. Cells were then seeded into six well plates in triplicate and allowed to recover for 10-14 days in drug-free media. Each well of the triplicate represents a different clone. **Step two (B)** After the recovery period, viable cells from each clone (Ov3R1, Ov3R2, Ov3R3) were re-challenged with paclitaxel for 48 hours or remained untreated (UntOv3R). Cells were re-seeded and allowed to recover in drug-free media for 10-14 days. This represents the rounds of standard treatment as described in section 2.2. **Step two (A)** In addition to the clones, OVCAR cells were seeded and received either no treatment or paclitaxel for 48 hours, followed by a recovery in drug-free media for 10-14 days.

2.3.3 Colony formation assay

Colony formation (clonogenic) assays were used to determine the ability of single cells to recover from a drug treatment and re-establish colonies. Following treatment with paclitaxel or carboplatin, the cells were trypsinised using 500µl Trypsin EDTA (Sigma Aldrich, Cat # T4049) and viable cells counted using the automated cell counter, NucleoCounter NC-100 (Chemometec). For the OVCAR-5, OVCAR-8 and ID8-luc2 cell lines, 1,500 viable cells were re-seeded into their respective wells on a six-well plate (Nunc™ Thermo Scientific, Cat # 140685) (in triplicate). For the OVCAR-3 and OVCAR-4 cell lines, 2,500 cells were re-seeded in the same manner as these cell lines were much slower to replicate. Cells were allowed to recover for 10-14 days in drug-free medium, until control cells reached a minimum confluency of 70%, and then prepared for staining. Media was aspirated, and cells were washed once with PBS before fixing in methanol for 5 minutes. Cells were then stained with Pro-diff solution C (Braidwood Laboratories E310) for 5 minutes. Plates were rinsed with water to remove excess stain and allowed to air-dry overnight. Plates were scanned and quantified using the Odyssey IR imaging system (Li-Cor, Cambridge, United Kingdom). For each cell line, we have looked for concentrations of both drugs that would reduce colony regrowth by over 50%.

2.3.4 Evaluation of morphology

Treated cells were cytospun and allowed to air dry for 5 minutes. Cells were then fixed using methanol and stained using May Grunwald Giemsa (DiaPath). Cells were identified as apoptotic based on the presence of two or more of the following morphological features: cell shrinkage, chromatin condensation or DNA fragmentation into ‘apoptotic bodies’. Images were acquired using a DP70 digital

microscope camera and Olympus DP-Soft 823 version 3.2 software (Mason Technologies Dublin, Ireland).

2.3.5 Evaluation of caspase-3 activity by flow cytometry

Treated cells were trypsinised using 500µl Trypsin EDTA (Sigma Aldrich, Cat # T4049) and neutralised with 1ml of media, saving the supernatant. Cells were subsequently fixed in 4% paraformaldehyde (PFA) for 45 minutes at 4^0C, washed in a permeabilisation buffer (0.1% Triton X-100, 0.1% sodium azide, 10 mM HEPES, 4 % FCS, 150 mM NaCl) and incubated with anti-active caspase-3 antibody (BD Biosciences, Cat # 559565) for 1 hour at 4°C. Cells were detected using an Alexa flour 488 secondary antibody (Life Technologies, Cat # A11034). Analysis was performed using the BD LSR II flow cytometer and BD FACS Diva software.

2.3.6 Western Blotting

Total cellular protein was extracted by trypsinisation of cells followed by lysing in 10-25µl modified RIPA buffer (50 mM Tris HCl (pH 7.4), 150 mM NaCl, 0.25% sodium deoxycholate, 1% Igepal, 1 mM EDTA, 1x Pefabloc, 1x protease inhibitor cocktail, 1 mM Na_3VO_4, 1 mM NaF), depending on pellet size. Samples (75 µg) were separated on NuPAGE 4–12% Bis-Tris gels (Invitrogen Life Technologies, Cat # NP0322) and electrophoretically transferred onto a PVDF membrane using the iBlot gel transfer system (Invitrogen IB1001). Membranes were blocked for one hour at room temperature using Odyssey blocking buffer (Li-Cor, Cat # 927-40100), and incubated overnight at 4°C using: anti-LC3 (Cat # MBL-PD014), anti- ATG5 (Novus, Cat # NB110-53818), anti-Beclin-1 (Novus, Cat # NB500-249). Anti-β-actin (loading

control) (Sigma, Cat # A5441) was incubated at room temperature, rocking, for one hour. IR-Dye conjugated secondary antibodies (Rockland) were utilised for protein detection. Membranes were analysed using the Odyssey Infra-red imaging system (Li-Cor, Cambridge, United Kingdom).

2.3.7 Cyto-ID Autophagy Detection kit

Treated cells were trypsinised using 500µl of Trypsin EDTA (Sigma Aldrich, Cat # T4049) and stained using the Cyto-ID autophagy detection kit (Enzo Life Sciences, Cat # ENZ-51031-K200) according to the manufacturer's instructions. Cyto-ID is a cationic amphiphilic tracer dye which selectively accumulates within autophagic vesicles. An increase in autophagic vacuole accumulation will result in an increase in fluorescence in the 488-2 channel. Samples were run on the BD LSRII flow cytometer with FACS Diva acquisition and analysis software. FlowJo data analysis software was used for gating and generating overlay histograms. Data is presented as Mean Fluorescence Intensity (MFI).

2.3.8 Immunofluorescence

Prior to treatment, cells were seeded directly onto coverslips in the well of a six well plate (Nunc™ Thermo Scientific, Cat # 140685). Following treatment (previously described), cells were washed with PBS, fixed (4 % PFA/PBS), washed 3 times with PBS and permeabilised in 100% cold methanol for 10 minutes at -20℃. Cells were again washed 3 times with PBS and blocked for 30 minutes at room temperature (5% BSA/PBS). Cells were probed with anti-LC3 (Abgent, Cat # APG8B) in 1% BSA/PBS overnight at 4℃ and detected with an Alexa Flour 594 goat anti-rabbit secondary

antibody (Life Technologies, Cat # A11037). Cells were incubated with Nuclear ID stain (1µl per 2ml PBS) for 30 minutes at room temperature, before the slides were mounted using Pro-Long Gold anti-fade without Dapi (Invitrogen, Cat # P36970). Images were acquired using a DP70 digital microscope camera and Olympus DP-Soft823 version 3.2 software (Mason Technologies Dublin, Ireland).

2.3.9 Statistical Analysis

All data is expressed as mean ± the standard error of the mean (SEM), which represents the standard deviation of the distribution of the sample around the mean. Significance was determined by independent or paired student t-tests, which determines the difference between the means of two groups. The p-value was considered statistically significant where *$p \leq 0.05$, ** $p \leq 0.01$, *** $p \leq 0.001$. Statistical analysis was carried out and graphed using GraphPad Prism 5 software (GraphPad Software Inc., CA, USA).

2.4 Results

2.4.1 Working concentrations of paclitaxel and carboplatin were established for a panel of human and one murine ovarian cancer cell line

The sensitivity of ovarian cancer cell lines to paclitaxel and carboplatin was established using clonogenic assays. The clonogenic assay was selected as it allows the survival and proliferative capacity of a cell following treatment to be assessed. This was important for future experiments in the thesis which aimed to determine how OC cells recovered after drug treatment. To investigate cellular response to treatment, we have looked for concentrations that clearly have cytotoxic activity, reducing recovery by over 50% following withdrawal of the drug.

The ID8-luc2 cell line was treated for 24 hours with paclitaxel. Recovery was significantly impeded in a dose dependent manner at concentrations ranging from 2.5 (***p = 0.0006) – 50 μM [Figure 2.2A]. 48 hour treatments with carboplatin significantly impeded clonogenic regrowth at concentrations of 30 μM (**p = 0.001) and 40 μM [Figure 2.2B].

A panel of human ovarian cancer cell lines were also treated with both paclitaxel and carboplatin to assess their recovery over a range of concentrations. In all cell lines, dose dependent responses were evident following treatment with paclitaxel. Following 48 hour treatments, paclitaxel impeded cell recovery in the OVCAR-3 and -4 cell lines with significant loss of viability at 2 and 1.5nM (*p =0.003, ***p =0.0001, respectively) [Figure 2.3A and B, respectively]. In both the OVCAR-5 and -8 cell lines, higher concentrations of 5nM paclitaxel were required to significantly inhibit cell growth (**p = 0.002, **p = 0.001 respectively) [Figure 2.3C and D, respectively].

The OVCAR-3 and -4 cell lines were also more sensitive to carboplatin, with significantly reduced recovery evident at 0.5µM and 1µM (**p = 0.004; **p = 0.004, respectively) [Figure 2.4A and B, respectively]. In both the OVCAR-5 and -8 cell lines higher carboplatin doses of 7.5µM and 2.5µM were required to inhibit cell recovery (**p = 0.0037; ***p = 0.0005, respectively) [Figure 2.4C and D, respectively]. Based on the dose response ranges graphed in figures 2.2 to 2.4, effective concentrations of each drug were selected for use in further studies and are listed in Table 2.1.

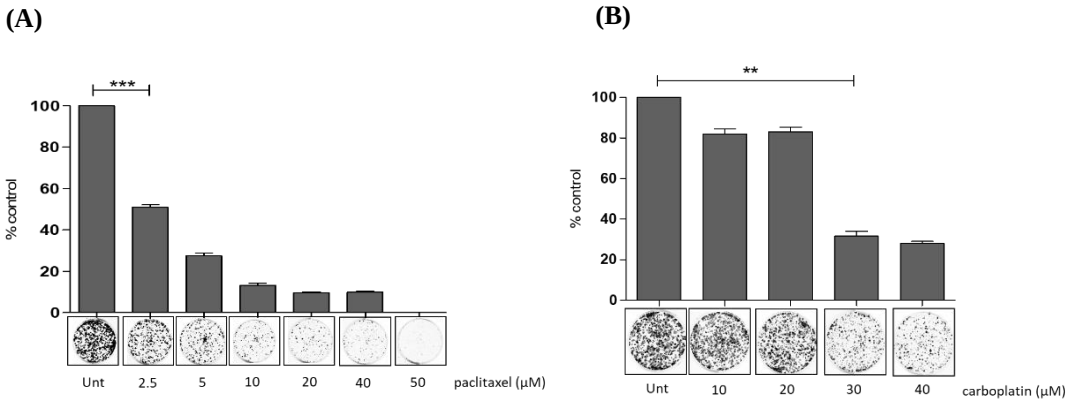

Figure 2.2. The effects of paclitaxel and carboplatin treatments on the recovery of the mouse ovarian carcinoma cell line. ID8-luc2 cells were treated with a range of **(A)** paclitaxel concentrations, for 24 hours or **(B)** carboplatin concentrations for 48 hours. Cells were re-seeded (1500 cells per well) and allowed to recover in drug free media for 10-14 days. Stained colonies were scanned, and integrated intensity values were quantified. Data is presented graphically as % control (where control = 100%) (n=3). We have looked for concentrations that would reduce recovery by at least 50%. Statistical analysis was performed using a paired students t-test and values are deemed significant where *$p \leq 0.05$, **$p \leq 0.01$.

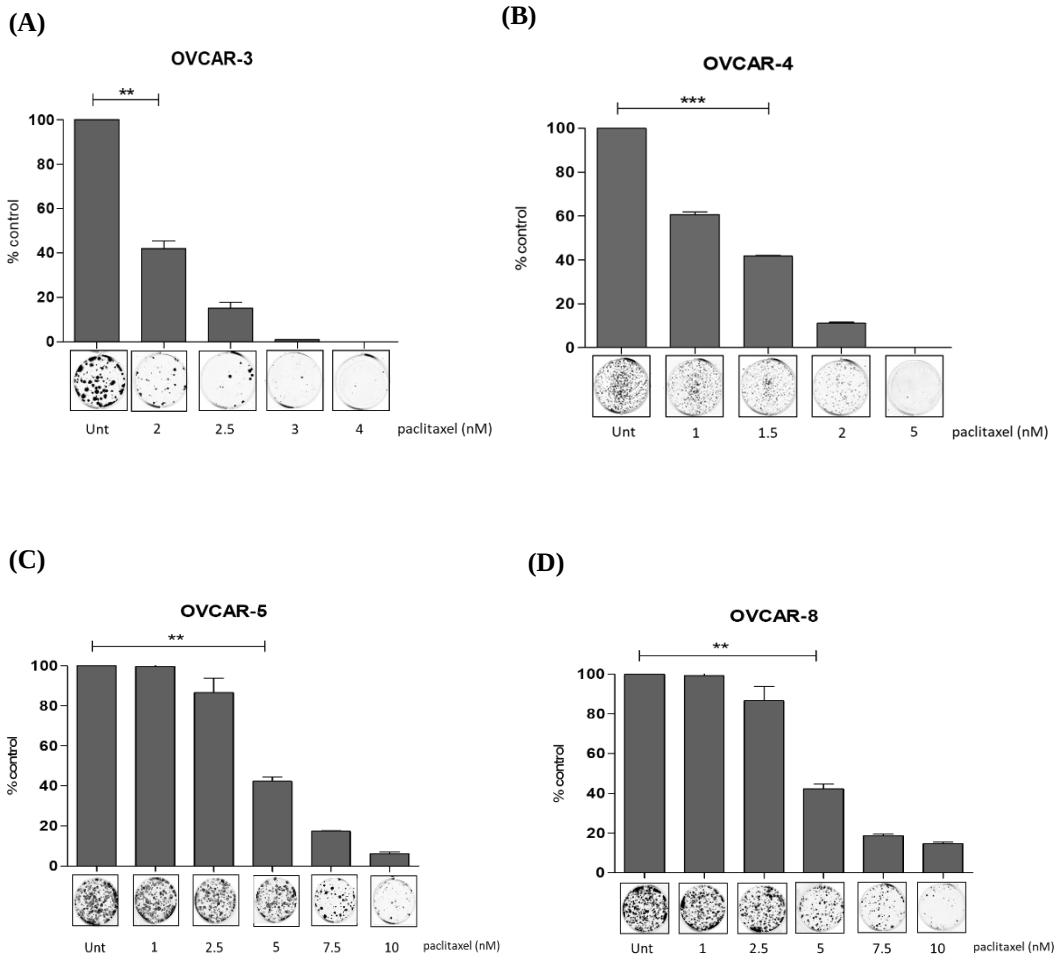

Figure 2.3. The effects of paclitaxel treatments on the recovery of the human ovarian cancer cell lines OVCAR-3, -4, -5, -8. A panel of human ovarian cancer cell lines were treated with a range of paclitaxel concentrations (nM) for 48 hours. (**A**) OVCAR-3 and (**B**) OVCAR-4 cells were seeded (2500 cells per well) and allowed to recover for 10-14 days. (**C**) OVCAR-5 and (**D**) OVCAR-8 cells were re-seeded (1500 cells per well) in drug free media and allowed 10-14 days to recover. All colonies were fixed, stained, and quantified using the Odyssey Infrared Imaging System (Li-Cor). Data is presented as % control (where control = 100%) (n=3). We have looked for concentrations that would reduce recovery by at least 50%. Statistical analysis was performed using a paired students t-test and values are deemed significant where *$p \leq 0.05$, **$p \leq 0.01$, ***$p \leq 0.001$.

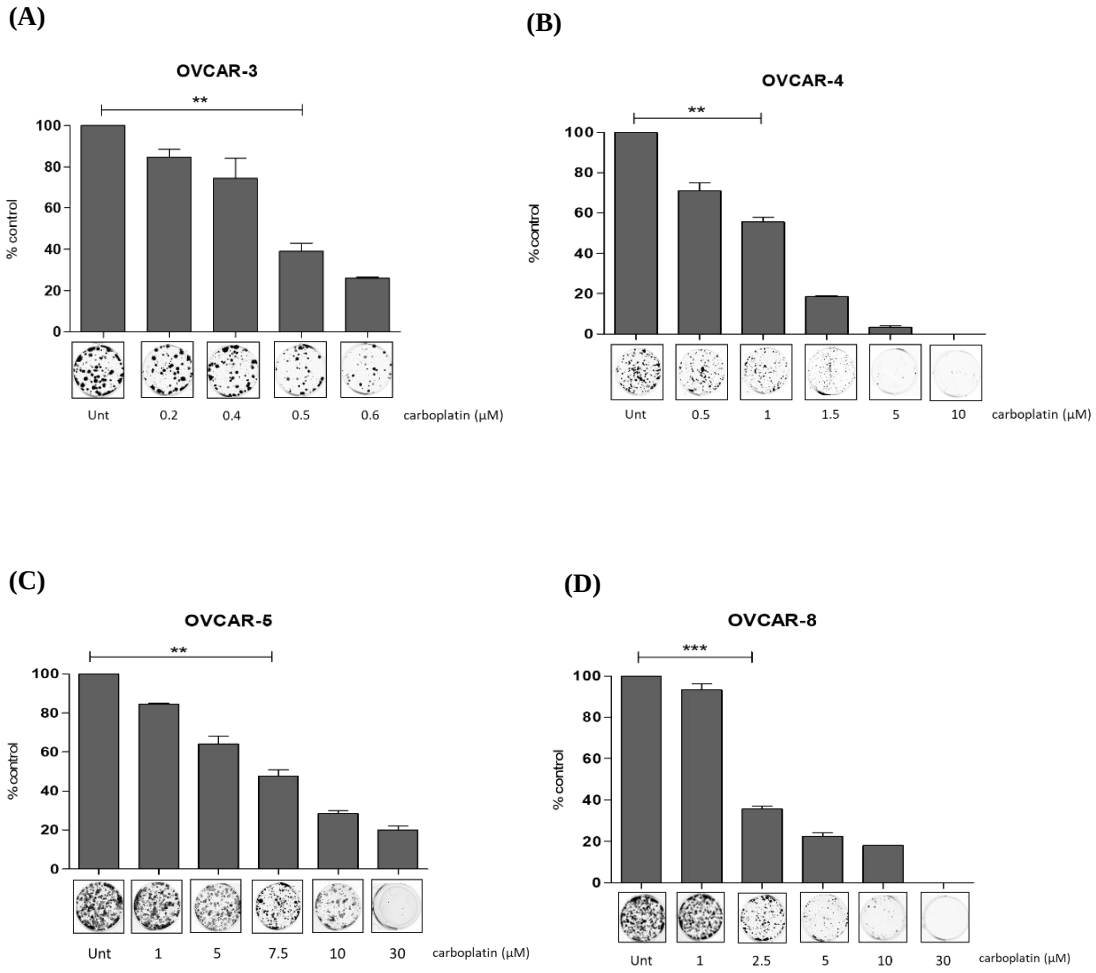

Figure 2.4. The effects of carboplatin treatments on the recovery of the human ovarian cancer cell lines OVCAR-3, -4, -5, -8. Following treatments with carboplatin (μM) for 48 hours, **(A)** OVCAR-3 and **(B)** OVCAR-4 cells were re-seeded (2500 cells per well) and allowed to recover for 10-14 days. **(C)** OVCAR-5 and **(D)** OVCAR-8 cells were re-seeded (1500 cells per well) and allowed 10-14 days to recover. All colonies were fixed, stained and integrated intensity values obtained. Data is presented as % control (where control = 100%) (n=3). We have looked for concentrations that would reduce recovery by at least 50%. Statistical analysis was performed using a paired students t-test. Values are significant where *p≤ 0.05, **p≤ 0.01, ***p ≤0.001.

Cell line	paclitaxel concentrations	carboplatin concentrations
ID8-luc2	2.5uM	40uM
OVCAR-3	2nM, 2.5nM	0.5uM, 0.6uM
OVCAR-4	1.5nM, 2nM	1uM, 1.5uM
OVCAR-5	5nM, 7.5nM	7.5uM, 10uM
OVCAR-8	5nM, 7.5nM	2.5uM, 5uM

Table 2.1. The concentrations of paclitaxel and carboplatin derived from the dose ranges in figures 2.2 to 2.4, which reduced clonogenic recovery by at least 50%, are listed. These concentrations were used for subsequent experiments.

We could also separate the human cell lines into two distinct subgroups with differential sensitivity to both drugs. The OVCAR-5 and -8 cell lines were significantly more resistant to both drugs compared to the OVCAR-3 and -4 cell lines, requiring on average 3 fold higher concentrations of paclitaxel, and 7 fold higher concentrations of carboplatin to elicit 50 % recovery.

2.4.2 Assessment of apoptosis induction in ovarian cancer cell lines following treatment with paclitaxel and carboplatin

The literature is conflicted regarding the apoptosis competency of ovarian cancer cell lines. Apoptotic cell death is the desired outcome following treatment with chemotherapeutic drugs. It was therefore important to establish if the panel of ovarian cancer cell lines were competent at inducing apoptosis in response to treatment with paclitaxel and carboplatin.

Morphology was assessed for apoptotic features including cell shrinkage, nuclear fragmentation and membrane blebbing. Active caspase-3 was also quantified using flow cytometry. Caspase-3 is a protease which is cleaved from its pro-caspase form into its active form during the execution stage of apoptosis and is a standard indicator of apoptosis.

The ID8-luc2 cell line was treated with paclitaxel (2.5µM) and carboplatin (40µM) for 24 and 48 hours, respectively. No morphological features of apoptosis were evident in treated cells [Figure 2.5A (i) and 4B (i) respectively], however mitotic catastrophe was apparent with paclitaxel, consistent with its activity as a microtubule inhibitor [Figure 2.5A (i), right panel]. Chromosome condensation (and potential mitotic catastrophe) was also evident in carboplatin treated cells (denoted with red arrows) [Figure 2.5B (i)]. A small increase in caspase-3 activity was observed following 2.5µM paclitaxel treatment (**p= 0.003), while no significant activation was observed following treatment with carboplatin (40µM) [Figure 2.5A (ii) and 2.5B (ii)].

Morphological features of apoptosis were evident in both the OVCAR-3 and -4 cell lines following 48 hour treatments with 2nM paclitaxel (black arrows, Figure 2.6A (ii) and B (ii), respectively). Following treatment with 0.5µM and 2µM carboplatin

respectively, there was no morphological evidence of apoptosis in either the OVCAR-3 or -4 cell lines, however limited necrotic features including loss of plasma membrane integrity were observed (denoted with green arrows) [Figure 2.6A (iii) and B (iii), respectively]. Consistent with the morphological evidence, both OVCAR-3 and -4 cell lines, treated with paclitaxel (2 and 2.5nM) and (1 and 1.5nM) respectively, displayed activation of active caspase-3. OVCAR-3 cells had the highest levels of active-caspase-3 at 43 % [Figure 2.6A (iv)] with the OVCAR-4 cell line showing 22 % [Figure 2.6B (iv)]. Carboplatin treatment did not activate caspase-3 in either OVCAR-3 or -4 cell lines [Figure 2.6A (iv) and Figure 2.6B (iv), respectively].

The OVCAR-5 and -8 cell lines were similarly evaluated after 48 hour treatments with both drugs. Following 5 and 7.5nM paclitaxel treatment respectively, morphological features of apoptosis were evident in both the OVCAR-5 and -8 cell lines [black arrows], Figure 2.7A (ii) and 2.7B (ii), respectively]. Following treatments with 10 and 5μM carboplatin, in the OVCAR-5 and -8 cell lines respectively, apoptotic features were not observed, however other abnormal features were, such as chromosome condensation (highlighted with red arrows), and loss of plasma membrane integrity consistent with necrosis (denoted with green arrows) [Figure 2.7A (iii) and 2.7B (iii), respectively]. Consistent with the morphological evidence, active caspase-3 expression was detected in the OVCAR-5 and -8 cell lines following 7.5nM paclitaxel treatment at 11 % and 8 % respectively [Figure 2.7A (iv) and 2.7B (iv)].

In summary, the most sensitive cell lines (OVCAR-3 and -4) displayed the highest induction of apoptosis following paclitaxel treatment and perhaps unsurprisingly, the most resistant pair (OVCAR-5 and -8) exhibited the least apoptosis induction. In contrast, treatment with carboplatin did not show any evidence of apoptosis induction

in any of the OC cell lines tested. These data highlight both a cell line dependent and drug dependent induction of apoptosis in OC cells.

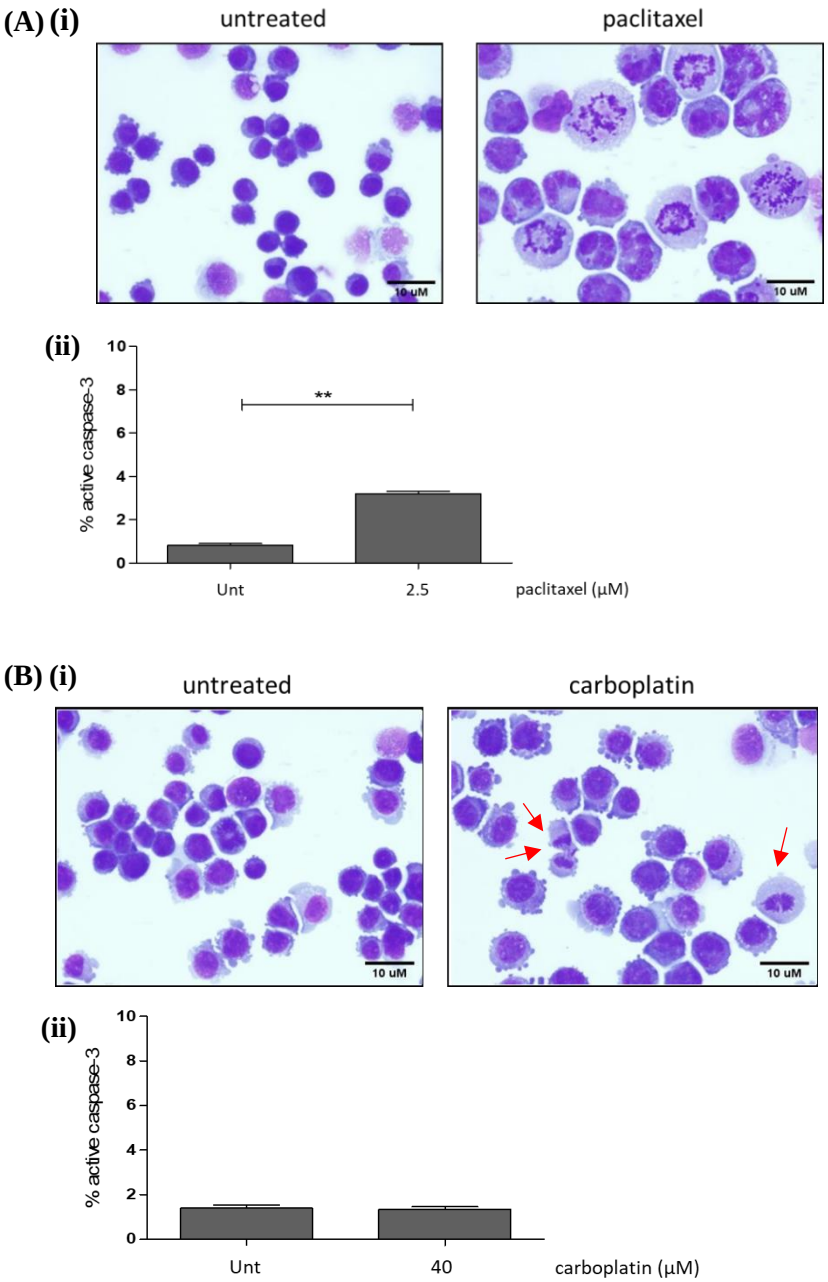

Figure 2.5. Features of apoptosis were assessed in the ID8-luc2 cell line following treatment with Paclitaxel and carboplatin (A)(i) ID8-luc2 cells were treated for 24 hours with paclitaxel (2.5 µM) and morphological features of apoptosis were assessed (not evident) (Magnification 400X) **(A)(ii)** To corroborate morphological data, active caspase-3 levels were assessed following paclitaxel treatment using flow cytometry (n=3). **(B)(i)** Morphological features of apoptosis were assessed in untreated cells (left panel) and 40 µM carboplatin treated cells (right panel). Cells with condensed chromosomes are highlighted with red arrows (Magnification 400X). **(B)(ii)** Active caspase-3 levels were assessed following carboplatin treatment using flow cytometry. All percentages of active caspse-3 are dispalyed as ± SEM (n=3). Paired students t-test were used, and values are deemed significant where, **$p \leq 0.01$.

OVCAR-3

(A)(i) **untreated**

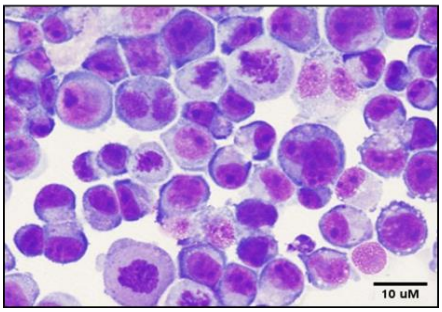

(ii) **paclitaxel**

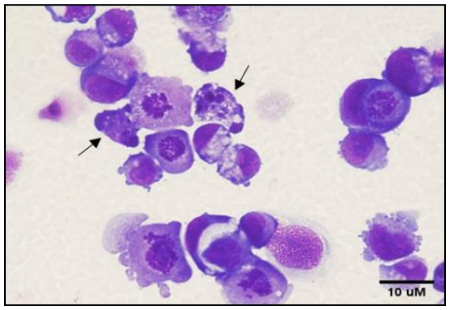

(iii) **carboplatin**

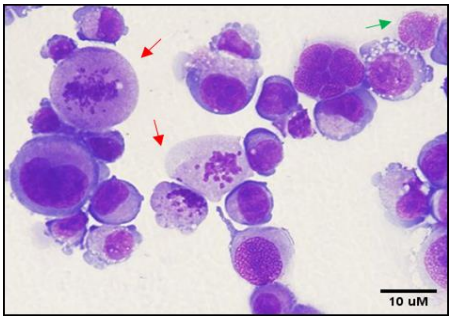

(iv)

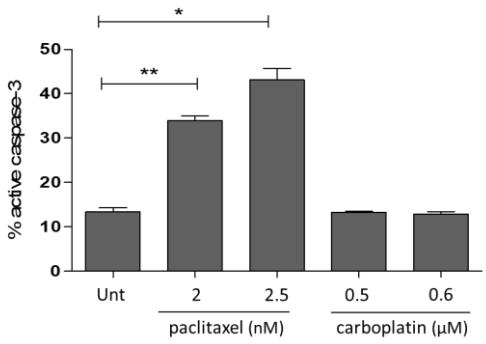

OVCAR-4

(B)(i) **untreated**

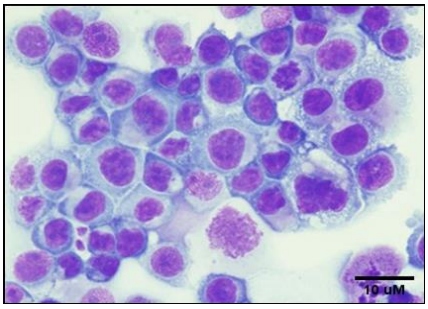

(ii) **paclitaxel**

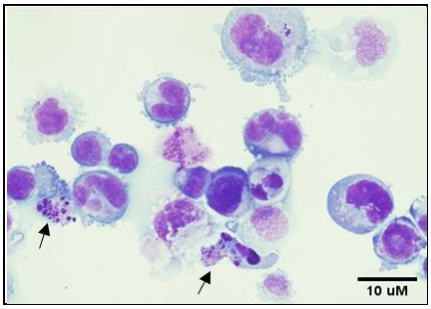

(iii) **carboplatin**

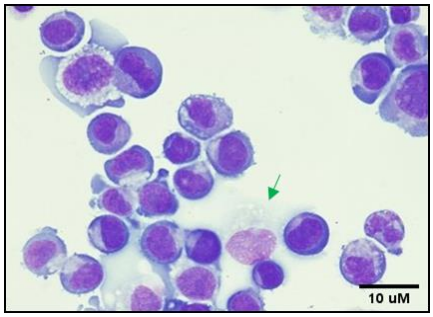

(iv)

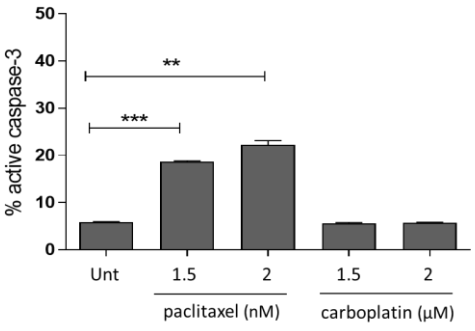

Figure 2.6. **Apoptotic features were assessed in the OVCAR-3 and -4 cell lines following 48 hour treatments with paclitaxel and carboplatin. (A)** Morphological features of OVCAR-3 cells are shown following **(ii)** paclitaxel (2nM) and **(iii)** carboplatin (0.5µM) treatment (magnification 400X). **(iv)** Analysis of active caspase 3 following treatment with both paclitaxel and carboplatin (n=3). **(B)** Morphological features of apoptosis were assessed in OVCAR-4 cells following **(ii)** paclitaxel treatment (2nM) and **(iii)** carboplatin treatment (2µM). Cells marked with black arrows display apoptotic features, cells with chromosome condensation are marked with red arrows, while cells with necrotic morphology are highlighted with green arrows (magnification 400X). **(iv)** Active caspase-3 analysis was conducted using flow cytometry to substantiate morphological data. Values are graphed ± SEM (n=3). Paired students t-test were used, and values are deemed significant where*$p \leq 0.05$, **$p \leq 0.01$, ***$p \leq 0.001$.

OVCAR-5 **OVCAR-8**

(A) (i) **untreated**

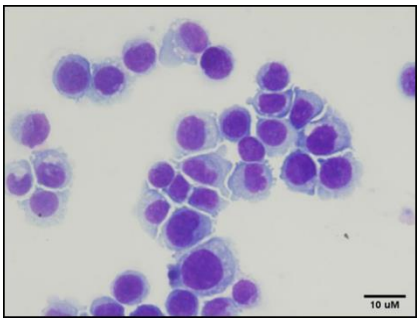

(B) (i) **untreated**

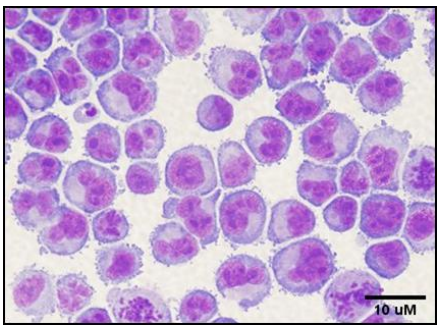

(ii) **paclitaxel**

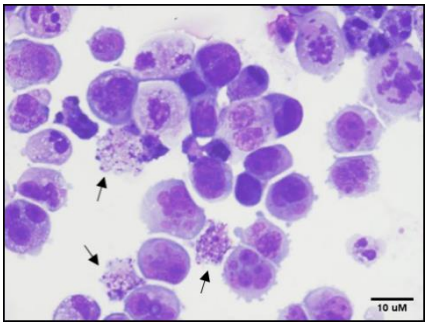

(ii) **paclitaxel**

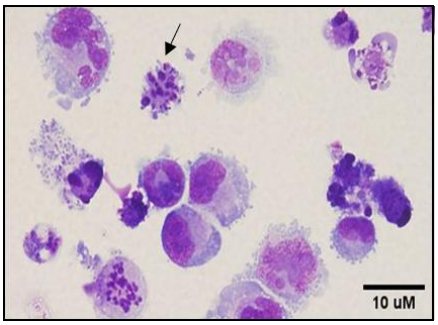

(iii) **carboplatin**

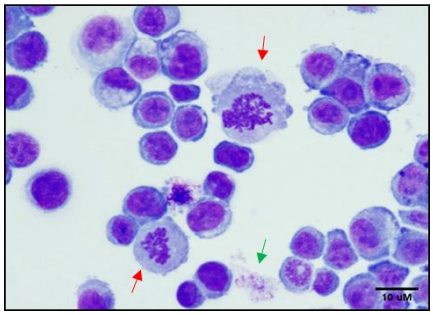

(iii) **carboplatin**

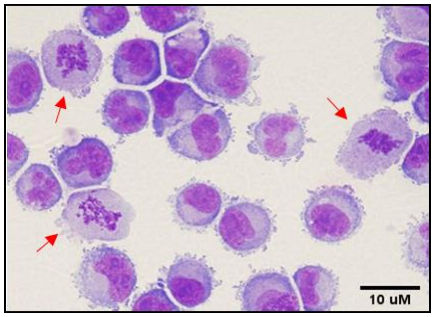

(iv)

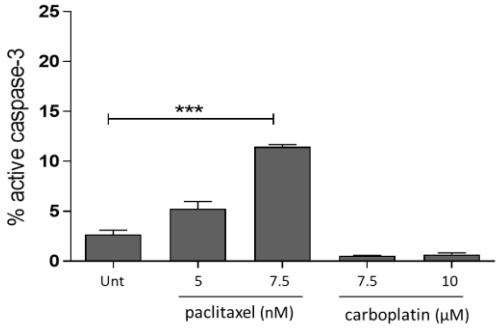

(iv)

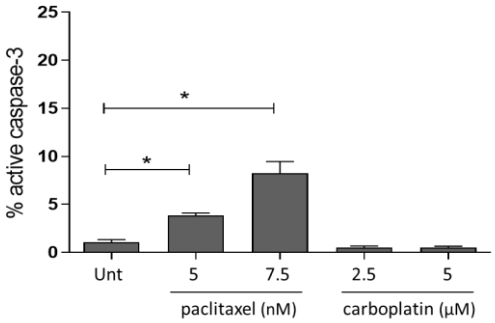

Figure 2.7. **Apoptotic features were assessed in the OVCAR-5 and -8 cell lines following 48 hour treatments with paclitaxel and carboplatin. (A)** Morphological features of OVCAR-5 cells are shown in **(i)** untreated cells and following **(ii)** paclitaxel (5nM) and **(iii)** carboplatin treatment (10μM) (magnification 400X). **(iv)** Analysis of active caspase-3 following treatment with both paclitaxel and carboplatin (n=3). **(B)** Morphological features of apoptosis were assessed in OVCAR-8 cells following **(ii)** paclitaxel treatment (7.5nM) and **(iii)** carboplatin treatment (5μM). Cells marked with black arrows display apoptotic morphology, cells with chromosome condensation are marked with red arrows, while cells with necrotic morphology are highlighted with green arrows (magnification 400X). **(iv)** Active caspase-3 analysis was conducted using flow cytometry (n=3). Paired students t-test were used, and values are deemed significant where *$p \leq 0.05$, **$p \leq 0.01$, ***$p \leq 0.001$.

2.4.3 Apoptosis is decreased, and recovery is increased, in ovarian cancer cells following a single round of paclitaxel treatment

Ovarian cancer patients often undergo successive rounds of chemotherapy, and resistance to treatment is commonly acquired. In order to mimic these clinical effects *in-vitro*, the three cell lines displaying the highest levels of active caspse-3 (OVCAR-3, -4, -5) were recovered from one round of paclitaxel treatment and then re-challenged, after which caspase-3 levels and clonogenic recovery were assessed. The OVCAR clones were generated as described in Figure 2.1.

In the OVCAR-3 cell line, all the recovered clones (Ov3R1, R2, R3) were more resistant to paclitaxel treatment, with significantly more cells recovering from the Ov3R3 clone compared to OV3 cells, which received one paclitaxel treatment (***p = 0.0002) [Figure 2.8A (i)]. The recovered clones also displayed significantly less active caspase-3 activity compared to OVCAR-3 cells receiving just one treatment (OV3) (Ov3R2 *p = 0.011, Ov3R3 *p = 0.024) [Figure 2.8A (ii)].

In the OVCAR-4 cell line, one out of three of the recovered clones had a significant increase in re-growth, as shown by the clonogenic assay, when compared to cells receiving one round of paclitaxel treatment (OV4) (Ov4R2 *p = 0.0279) [Figure 2.8B (i)]. Interestingly, two out of three clones also displayed a significant decrease in active caspase-3 activity, compared to cells receiving one round of paclitaxel treatment (Ov4R1 *p = 0.0351; Ov4R2 *p = 0.0155) [Figure 2.8B (ii)].

In the OVCAR-5 cell line, the recovered clones were all significantly more resistant to paclitaxel treatment compared to cells receiving one round of treatment, as indicated by increased re-growth of all clones in the clonogenic assay (Ov5R1 **p = 0.006, Ov5R2 ***p = 0.0001, Ov5R3 ***p = 0.0002) [Figure 2.8C (i)]. Two out of three

clones which were re-challenged with paclitaxel displayed a significant reduction in active caspase-3 activity compared to those which received just one treatment (OV5) (Ov5R2 **p = 0.002, Ov5R3 **p = 0.005) [Figure 2.8C (ii)].

These data indicate that treatment with paclitaxel results in a reduction of OC cell apoptotic competency, in at least two out of three clones from each cell line. Clones which recovered better from treatment showed a concomitant decrease in apoptosis induction.

OVCAR-3

Clonogenic Recovery **Active caspase-3**

(A) (i)

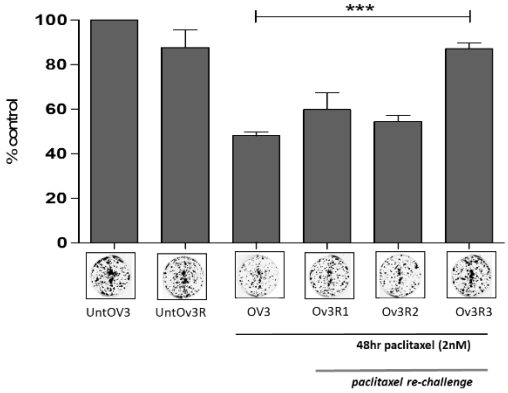

(ii)

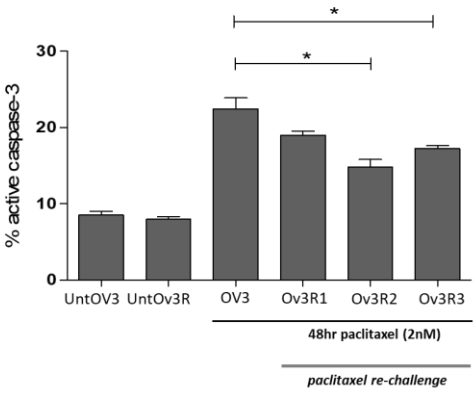

OVCAR-4

(B) (i)

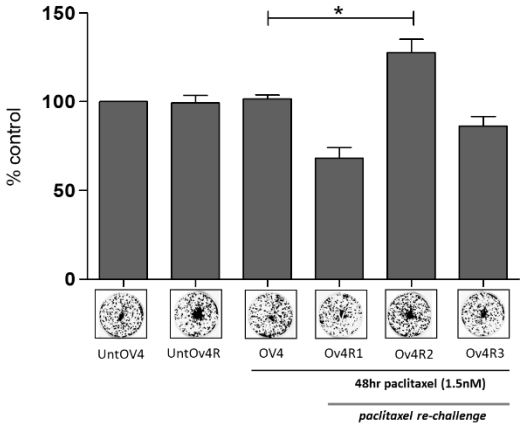

(ii)

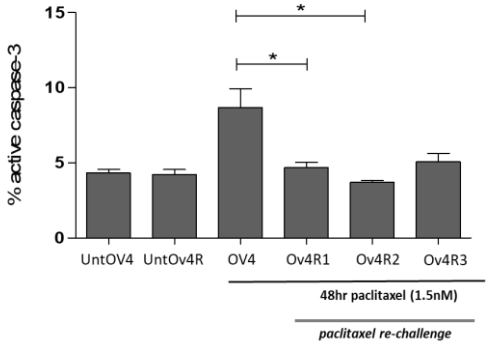

OVCAR-5

(C) (i)

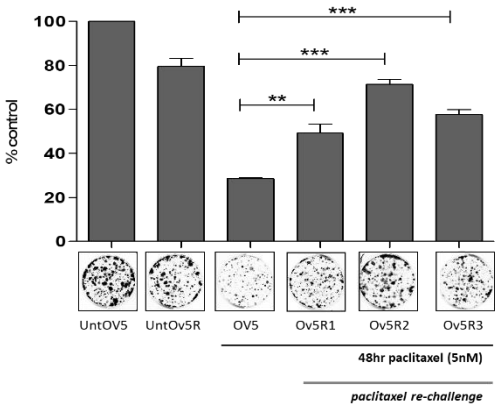

(ii)

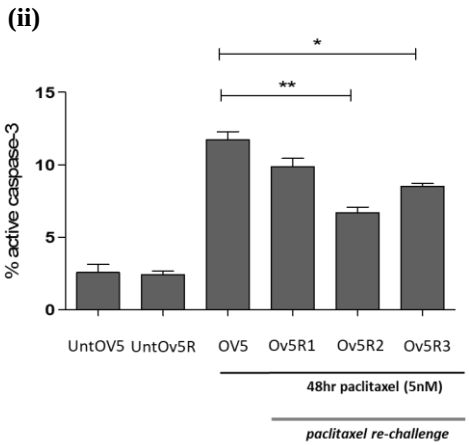

Figure 2.8. (**A**) (**i**) OVCAR-3, (**B**) (**i**) OVCAR-4 and (**C**) (**i**) OVCAR-5 cells were treated for 48 hours with 2, 1.5 and 5 nM paclitaxel, respectively. OVCAR-3 and -4 cells were then re-seeded (2500 cells per well), while OVCAR-5 cells were seeded (1500 cells per well) in drug-free media and allowed to recover for 10-14 days. Recovered clones for each cell line (labelled R1, R2 and R3) were generated by re-seeding and treating with paclitaxel at their respective concentrations for a second time. Cells were also seeded which received only one paclitaxel treatment (labelled OV3, OV4 and OV5, respectively). Recovery was assessed using clonogenic assays, integrated intensities were quantified, and data is presented as % control (where control = 100%) (n=3). (**ii**) Active caspase-3 activity was assessed by flow cytometry in all cell lines (n=3). Data is displayed as % caspase activity ± SEM. Statistical analysis was performed using an unpaired student's t-test with significance defined where *$p \leq 0.05$, **$p \leq 0.01$, ***$p \leq 0.001$.

2.4.4 Ovarian cancer cells express key autophagy proteins

Basal expression of three key autophagy proteins (Beclin 1, Atg5/12, and LC3) were assessed in untreated cells using western blotting.

Beclin 1, a key component of the PI3K complex involved in autophagosome formation, was detected in all the cell lines, producing a band 52kDa in size [Figure 2.9A (i)(ii)]. To allow LC3 lipidation during autophagosome maturation, Atg5 and 12 conjugation is necessary, producing a conjugate 55 kDa in size. Expression of the conjugate was detected in each of the cell lines [Figure 2.9B (i)(ii)]. The OVCAR-5 and -8 cell lines had the lowest expression of the conjugate, when compared to the OVCAR-3, -4 and ID8-luc2 cell lines. During autophagosome maturation, LC3I is lipidated to form LC3II and inserts into the outer membrane of the mature autophagosome. Expression of LC3II is considered one of the most reliable indicators of autophagy induction. As evident in Figure 2.9C (i)(ii), LC3I (16-18 kDa) and LC3II (14-16 kDa) were present in each of the cell lines.

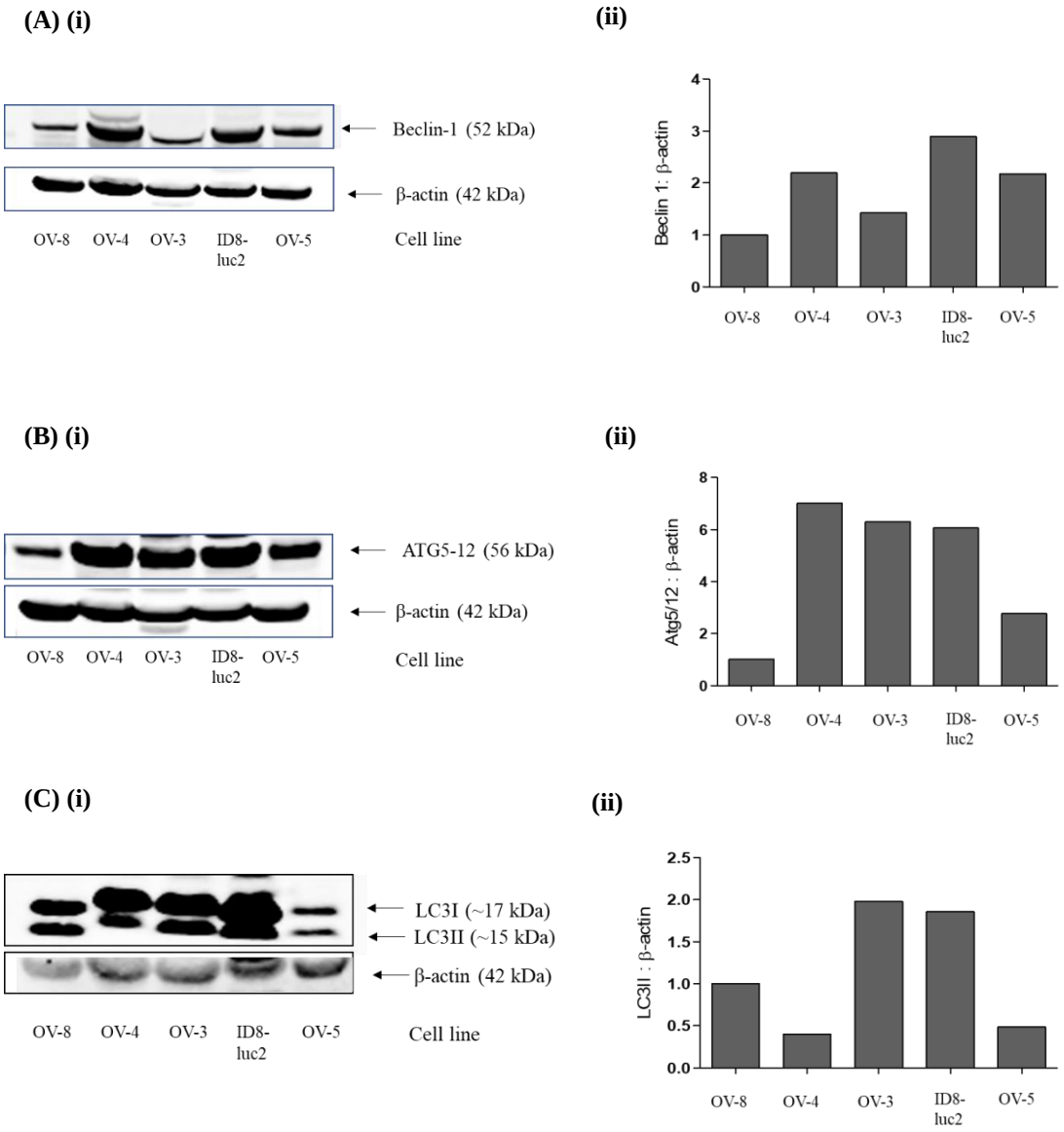

Figure 2.9. Western Blot analysis of the basal expression of key autophagy proteins. The expressions of **(A)(i)** Beclin 1, **(B)(i)** Atg5/12 and **(C)(i)** LC3II were quantified in a panel of ovarian cancer cell lines using the Li-Cor odyssey scanner and normalised to β-actin. **(ii)** Corresponding normalised integrated intensities are graphed to right of each blot (n=1).

2.4.5 Basal autophagy is present in human ovarian cancer cell lines

Having established that the panel of OC cell lines express key autophagy proteins, we tested the ability of the cell lines to undergo basal autophagy. This was evaluated by blocking autophagosome turnover with the lysomotropic agent chloroquine and assessing the amount of autophagosomes that accumulate after 24 or 48 hours. If the cell is undergoing autophagy, vesicles will accumulate due to lack of turnover.

To assess the levels of autophagic vesicles two assays were employed, the Cyto-ID autophagy detection kit and immunofluorescent imaging for LC3. Treatment with CQ (24 or 48 hours) caused a significant increase in vesicle accumulation in each of the cell lines (Figure 2.10 (i), blue overlays), ((A) ID8-luc2 *** p = 0.0007, (B) OVCAR-3 ** p = 0.001, (C) OVCAR-4 * p = 0.049, (D) OVCAR-5 ** p = 0.004, (E) OVCAR-8 *** p = 0.0009). The OVCAR-8 cell line displayed the highest accumulation of autophagosomes (4 fold increase), with a corresponding increase in red punctate LC3 staining [Figure 2.10E (i) and (ii)]. The OVCAR-5 cell line displayed a 2.3 fold increase in vesicle accumulation and increased LC3 staining [Figure 2.10D (i) and (ii)]. The murine ID8-luc2 displayed a 2 fold increase in vesicle accumulation, which appeared inconsistent with LC3 immunostaining, which was minimally affected [Figure 2.10A (i) and (ii)]. The OVCAR-3 cells also displayed a 2 fold increase in vesicle accumulation, with the OVCAR-4 cells displaying the lowest accumulation (1.4 fold increase), consistent with the corresponding LC3 immunofluorescent expression [Figure 2.10B and C (i)(ii), respectively]. These results, along with the data from section 2.4.4 above, suggest that basal autophagy is not impeded by lack of gene/protein expression. It is notable that the OVCAR-8 cells displayed the lowest levels of key autophagy proteins, but the highest levels of autophagosomes.

ID8-luc2

(A) (i) **(ii)**

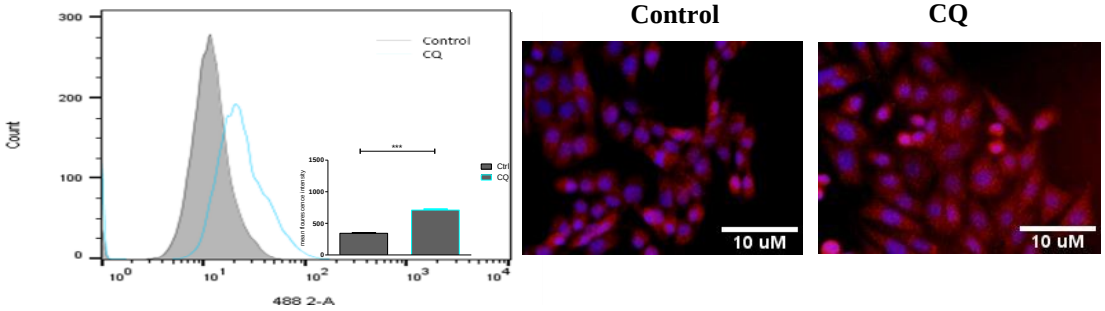

OVCAR-3

(B) (i) **(ii)**

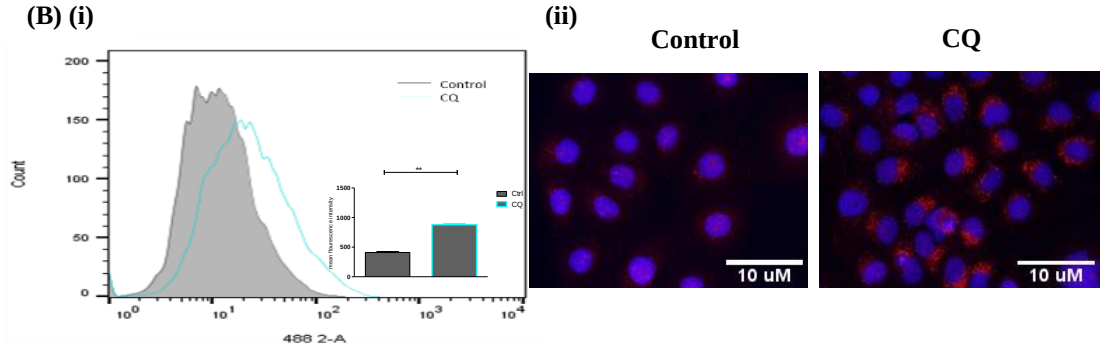

OVCAR-4

(C) (i) **(ii)**

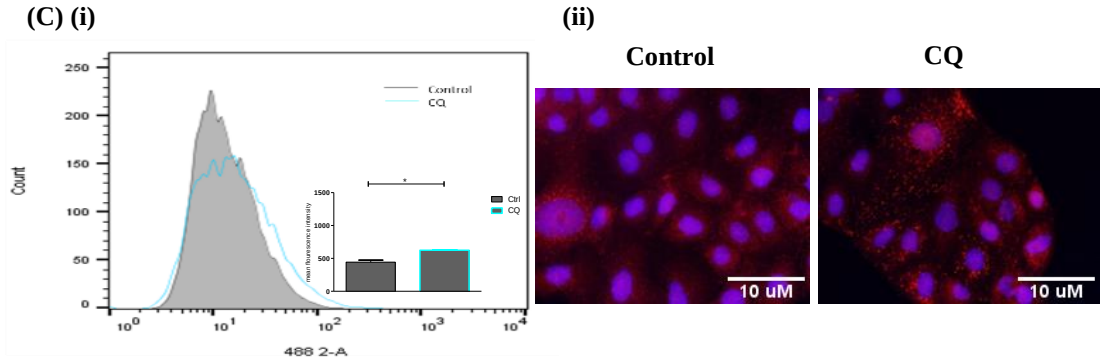

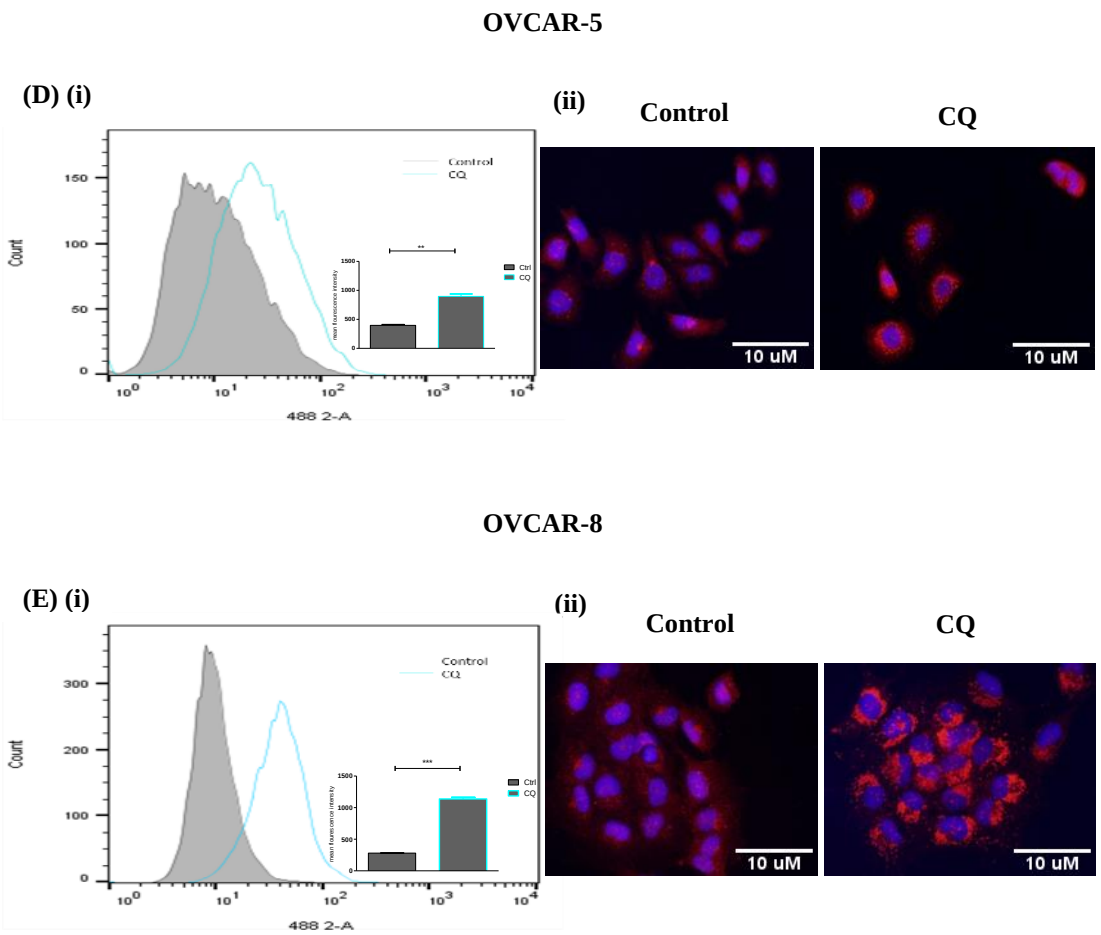

Figure 2.10. Assessment of basal autophagy in ovarian cancer cell lines. (i) The Cyto-ID autophagy detection kit was used to measure autophagic vesicle accumulation in either untreated (Control) or CQ (10µM) treated cells. Representative histogram overlays are displayed in the left-hand panels, with the corresponding mean fluorescent intensities graphed within for **(A)** ID8-luc2 **(B)** OVCAR-3 **(C)** OVCAR-4 **(D)** OVCAR-5 and **(E)** OVCAR-8 cells (n=3). **(ii)** The expression of LC3 was assessed following treatment with chloroquine in **(A)** ID8-luc2 cells (24 hours) and **(B)** OVCAR-3 **(C)** OVCAR-4 **(D)** OVCAR-5 and **(E)** OVCAR-8 cell lines (48 hours). Cells were probed with anti-LC3 antibody at 1:1000 dilution and imaged using a DP70 digital microscope camera (magnification 400X). Control cells are displayed in the left-hand panels, while CQ treated cells are on the right. Statistical analysis was performed using a paired t-test, with significance defined as *$p \leq 0.05$, **$p \leq 0.01$, ***$p \leq 0.001$. Data is displayed as ± SEM.

2.4.6 Assessment of induction of autophagic flux following drug treatment

We then assessed whether autophagy is induced following treatment with paclitaxel and carboplatin. The entire autophagy process, from cargo sequestration to degradation is termed 'flux'. Vesicle accumulation and indeed LC3II accumulation may be interpreted as either a block in the turnover of autophagosomes or an induction of the pathway. To distinguish between autophagy induction and accumulation due to blocking autophagosome turnover, cells were co-treated with CQ. ID8-luc2 cells were treated with paclitaxel alone or in combination with CQ (10μM) and allowed to recover in drug free media for 24 hours before autophagy induction was assessed. As shown in Figure 2.11A (i), treatment with paclitaxel alone (red overlay) resulted in vesicle accumulation, but the addition of CQ (green overlay) resulted in a further increase in vesicle accumulation, beyond that seen with CQ (turquoise overlay) or paclitaxel alone. This indicates an induction of autophagic flux. This was confirmed using western blot analysis of LC3II [Figure 2.11A (ii)]. The addition of CQ to paclitaxel (lanes 6-8) resulted in greater LC3II expression when compared to CQ alone (lane 2).

Autophagy induction was also evident following carboplatin treatment in the ID8-luc2 cells. Cyto-ID autophagy analysis revealed a significant increase in vesicle accumulation in cells treated with a combination of carboplatin and CQ (green overlay) when compared to either carboplatin (red overlay) or CQ alone (turquoise overlay) [Figure 2.11B (i)]. Western blot analysis of LC3II showed a greater accumulation of protein in carboplatin plus CQ treated cells (lane 4) compared to CQ alone (lane 2) [Figure 2.11 B (ii)]. These data are indicative of autophagy induction in the ID8-luc2 cells in response to both paclitaxel and carboplatin.

Vesicle accumulation was similarly assessed in all human OVCAR cell lines. As shown in Figure 2.12, the addition of CQ to (A) paclitaxel or (B) carboplatin (green overlays) in OVCAR-3 cells did not enhance vesicle accumulation beyond that with CQ alone (turquoise overlays), suggesting no autophagy flux in response to either drug. Western blot analysis revealed marginal increases in LC3II accumulation in response to paclitaxel and carboplatin following the addition of CQ [Figure 2.12C].

In the OVCAR-4 cell line the addition of CQ to paclitaxel or carboplatin (green overlays) failed to show any vesicle accumulation beyond what is induced by CQ (turquoise overlays) (Figure 2.13A and B, respectively). However, western blot analysis did reveal enhanced accumulation of LC3II when CQ was added to carboplatin (lane 9) [Figure 2.13C].

In the OVCAR-5 cell line enhanced accumulation of autophagic vesicles was detected following the addition of CQ to both paclitaxel and carboplatin (Figure 2.14A and B, green overlays) when compared to CQ (turquoise overlays) or drug (red overlays) alone. LC3II accumulation was increased following the addition of CQ to paclitaxel (lanes 4 and 6) and carboplatin (lane 10) [Figure 2.14C]. Taken together, these data suggest that autophagy is induced in the OVCAR-5 cell line in response to both paclitaxel and carboplatin.

In the OVCAR-8 cell line, the addition of CQ to both paclitaxel and carboplatin caused a significant increase in autophagic vesicle accumulation (green overlay) beyond that with CQ (turquoise overlays) or drug (red overlays) alone [Figure 2.15A and B]. Western blot analysis confirmed an increase in LC3II following paclitaxel and CQ treatment (lanes 4 and 6), however, flux was not evident in carboplatin treated cells by western blot (lanes 8 and 10) [Figure 2.15C]. The Cyto-ID autophagy assay may

be detecting autophagosomes which are not tagged with LC3, resulting in increased autophagosome accumulation which was not detected via western blotting.

(A) (i)

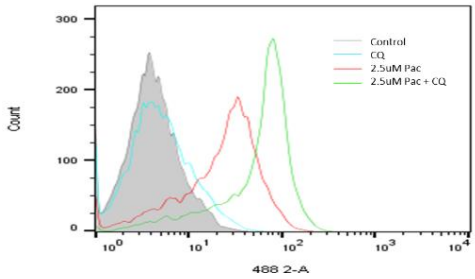
Control
CQ
2.5uM Pac
2.5uM Pac + CQ
Count
488 2-A

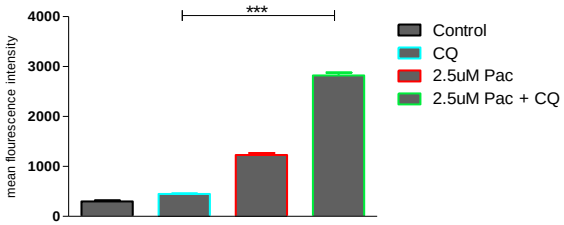
***
mean flourescence intensity
Control
CQ
2.5uM Pac
2.5uM Pac + CQ

(ii)

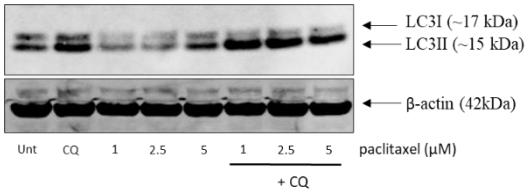
LC3I (~17 kDa)
LC3II (~15 kDa)
β-actin (42kDa)
Unt CQ 1 2.5 5 1 2.5 5
paclitaxel (μM)
+ CQ

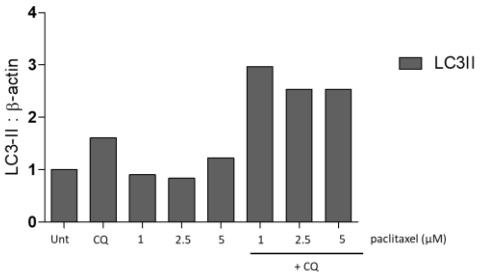
LC3-II : β-actin
LC3II
Unt CQ 1 2.5 5 1 2.5 5
paclitaxel (μM)
+ CQ

(B) (i)

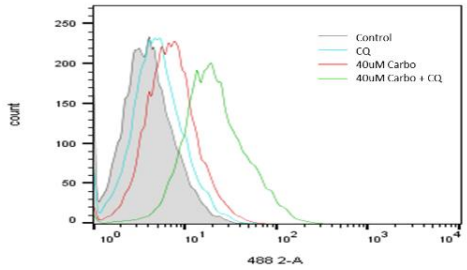
Control
CQ
40uM Carbo
40uM Carbo + CQ
count
488 2-A

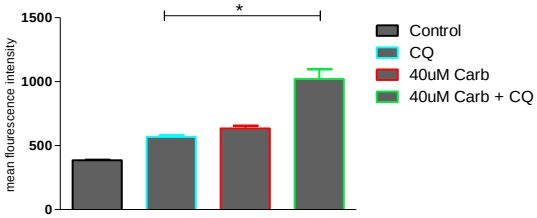
*
mean flourescence intensity
Control
CQ
40uM Carb
40uM Carb + CQ

(ii)

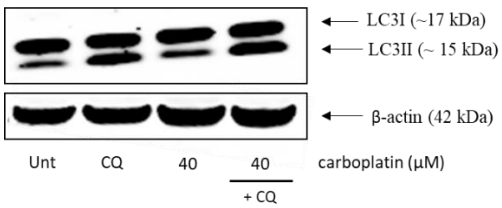
LC3I (~17 kDa)
LC3II (~ 15 kDa)
β-actin (42 kDa)
Unt CQ 40 40
carboplatin (μM)
+ CQ

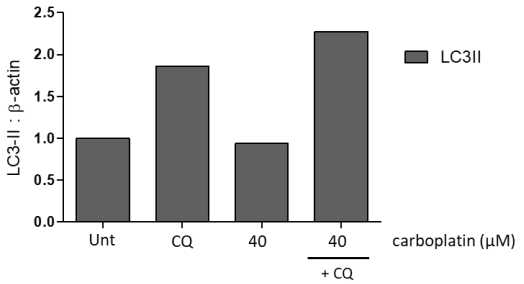
LC3-II : β-actin
LC3II
Unt CQ 40 40
carboplatin (μM)
+ CQ

Figure 2.11. Assessment of autophagy in the ID8-luc2 cell line after treatment with paclitaxel and carboplatin +/- CQ, followed by a 24 hour recover period. Cells were treated with paclitaxel (1, 2.5 or 5μM) +/- CQ (10μM) or carboplatin +/- CQ (40μM) for 24 and 48 hours respectively and allowed to recover in drug free media for a further 24 hours. Cyto-ID analysis by flow cytometry was utilised to assess autophagy induction after a 24 hour recovery period following **(A)(i)** paclitaxel or **(B)(i)** carboplatin treatment. A representative histogram overlay is presented to the left, while corresponding mean fluorescent intensities are graphed to the right (n=3). LC3II protein expression was measured via western blotting after the recovery period following **(A)(ii)** paclitaxel or **(B)(ii)** carboplatin treatment. Bands were quantified and normalised to β-actin, with the corresponding normalised integrated intensity values graphed to the right (n=1). Differences between means were analysed using a paired t-test, with significance defined as *$p \leq 0.05$, ***$p \leq 0.001$.

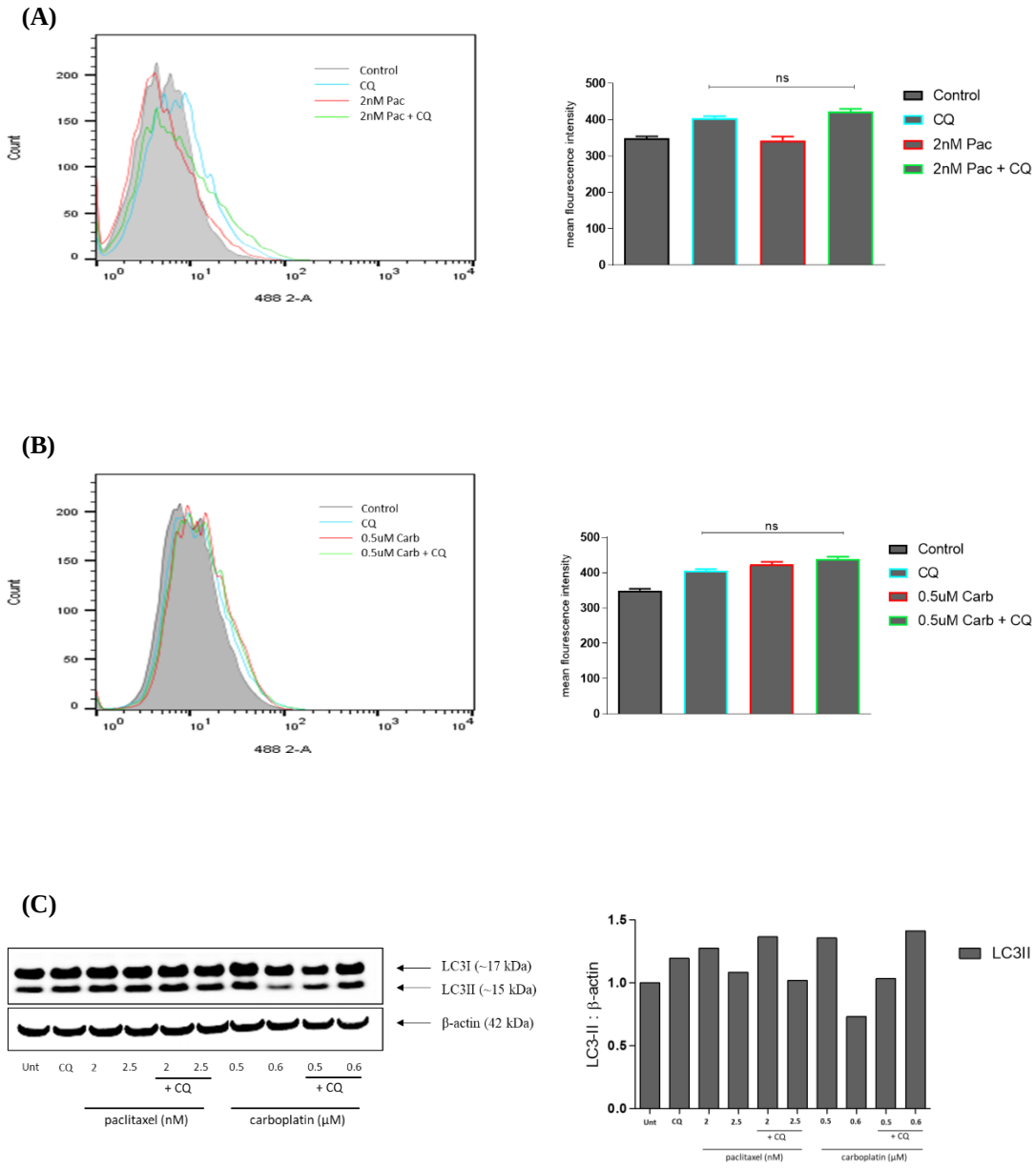

Figure 2.12. Assessment of autophagy in the OVCAR-3 cell line after treatment with paclitaxel and carboplatin +/-CQ, followed by a 24 hour recover period. (A) Following a 48 hour treatment with paclitaxel +/- CQ (10μM), or **(B)** carboplatin +/- CQ, cells were allowed 24 hours in drug free media to recover. Cyto-ID autophagy detection kit was used to assess autophagic vesicle accumulation. A representative histogram overlay is shown to the left, with corresponding mean fluorescent intensities graphed to the right (n=3). **(C)** Following the same treatment conditions, cells were probed for LC3II to assess autophagy induction. Blots were quantified and normalised to β-actin. Normalised integrated intensity LC3II values are graphed to the right of the blot image (n=1).

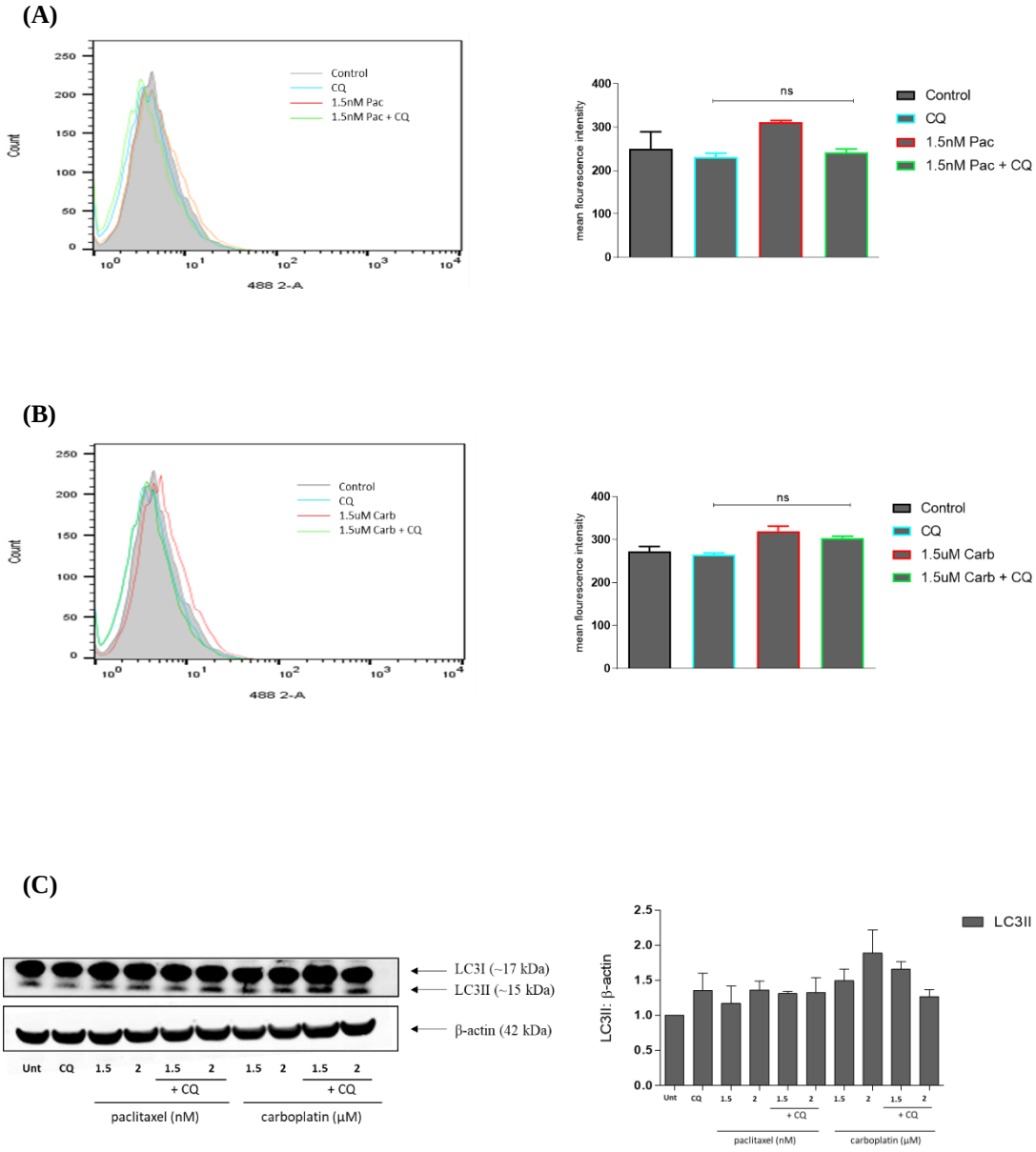

Figure 2.13. Assessment of autophagy in the OVCAR-4 cell line after treatment with paclitaxel and carboplatin +/- CQ, followed by a 24 hour recover period. Following a 48 hour treatment with **(A)** paclitaxel +/- CQ (10μM) or **(B)** carboplatin +/- CQ, cells were allowed 24 hours in drug free media to recover. Cyto-ID autophagy detection kit was used to assess vesicle accumulation. Representative histogram overlays are presented to the left, alongside corresponding mean fluorescent intensity values to the right (n=3). **(C)** Following the same treatment condition, western blot analysis was performed to assess LC3II accumulation. Blots were scanned and quantified using the Odyssey Li-Cor Infrared scanning system and normalised to β-actin. Normalised integrated intensity values are graphed to the right of the blot image (n=2).

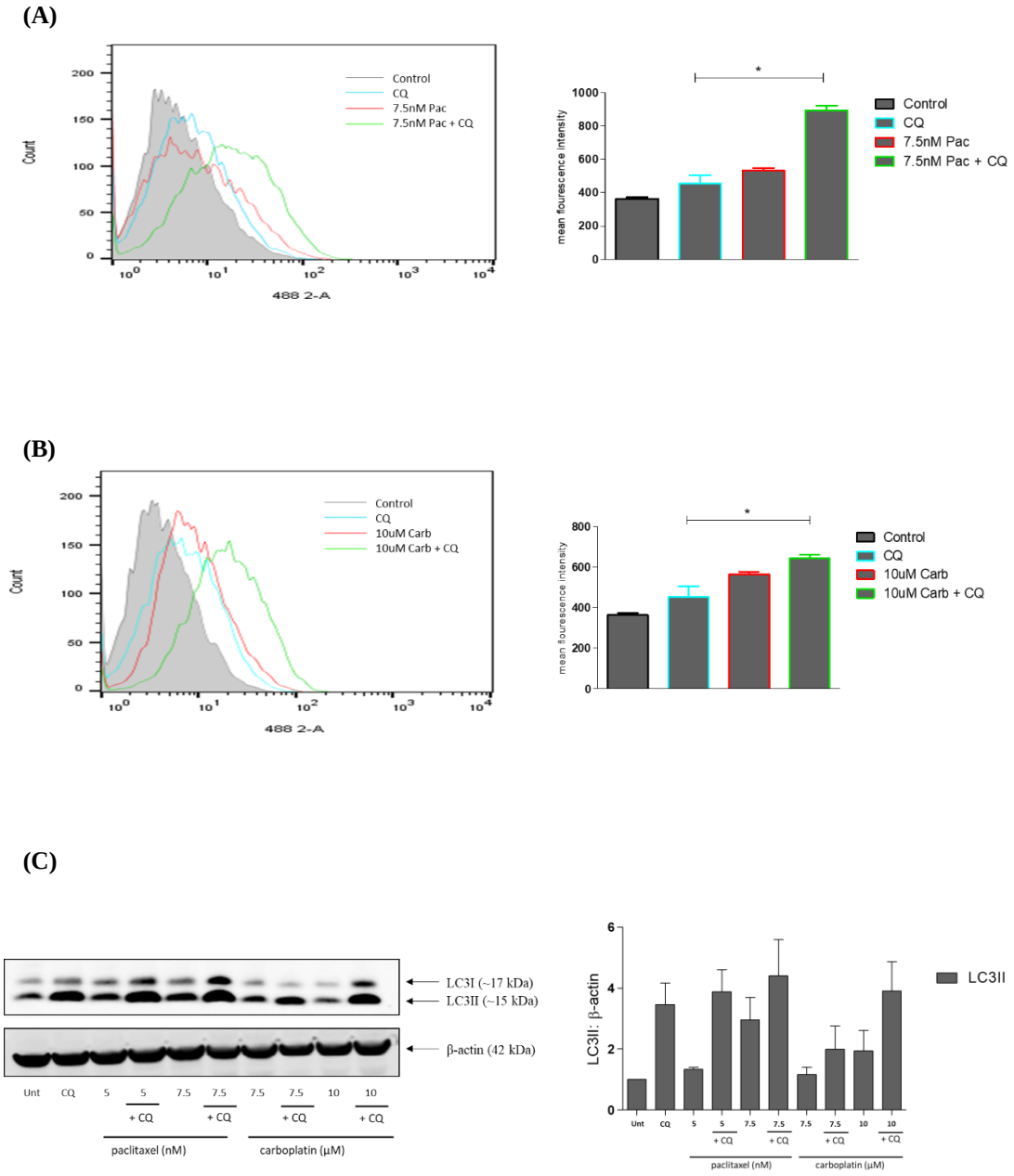

Figure 2.14. Assessment of autophagy in the OVCAR-5 cell line 24 hours after withdrawal of paclitaxel and carboplatin +/- CQ. Cyto-ID analysis by flow cytometry was utilised to assess autophagic vesicle accumulation following a 24 hour recovery following **(A)** paclitaxel +/- CQ (10μM) or **(B)** carboplatin +/- CQ treatment. Representative histogram overlays are presented to the left with their corresponding mean fluorescent intensity values presented to the right (n=3). **(C)** Western blot analysis of LC3II following withdrawal of paclitaxel and carboplatin was assessed. Blots were scanned and quantified using the Odyssey Li-Cor Infrared scanner. Integrated intensities are graphed as LC3II normalised to β-actin (n=3). Paired t-test was used to assess significance, defined as *$p \leq 0.05$.

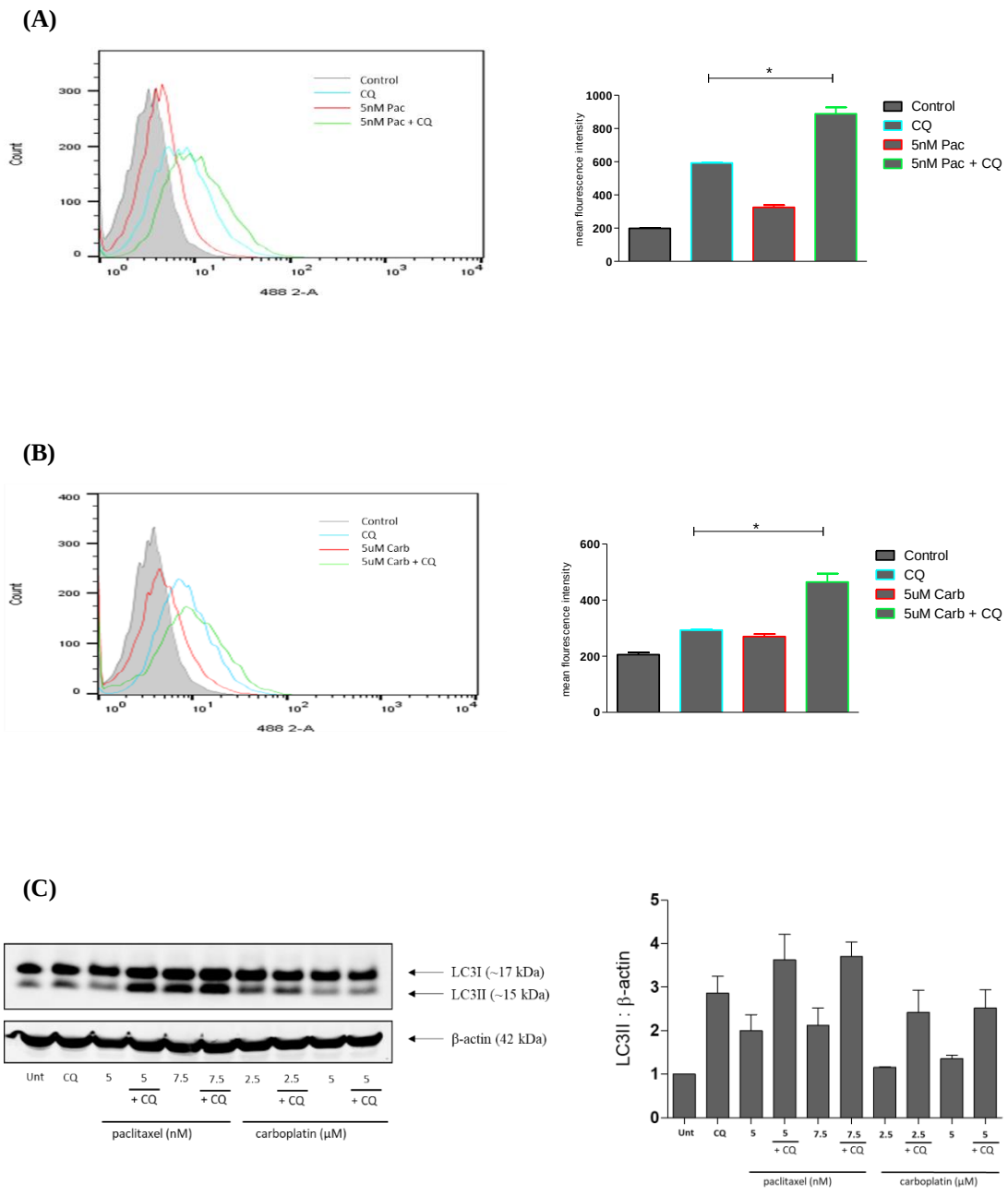

Figure 2.15. OVCAR-8 cells were assessed for autophagy induction following a 24 hour recovery from paclitaxel and carboplatin treatment +/- CQ. Cyto-ID autophagy assay was used to assess autophagosome accumulation following a 24 hour recovery period from treatment with **(A)** paclitaxel +/- CQ (10μM) and **(B)** carboplatin +/- CQ. Histogram overlays are shown to the left, with corresponding mean fluorescent intensities graphed to the right (n=3) **(C)** Western blot analysis of LC3II was performed to further assess autophagy induction (n=3). Data is presented as LC3II normalised to β-actin. Differences in means were determined to be significant where *p≤0.05, **p≤0.01.

Taking the results from this study together, we can separate the cell lines based on their drug sensitivity, autophagy and apoptotic levels. The cell lines which had the lowest levels of basal and drug induced autophagy (OVCAR-3 and OVCAR-4), also displayed the highest levels of apoptosis, and were most sensitive to both drugs. In comparison, the cells with the highest levels of basal and drug induced autophagy (OVCAR-5 and OVCAR-8), displayed the lowest levels of apoptosis and were more resistant to both drugs.

2.5 Discussion

Evidence regarding the apoptotic and autophagic competency of OC cells in the literature is conflicted. This study has characterised a panel of OC cell lines in terms of their apoptotic and autophagic response to two clinically relevant chemotherapeutics, paclitaxel, and carboplatin.

The panel of cell lines could be divided into two distinct subgroups. The ID8-luc2, OVCAR-5 and -8 cell lines were the most resistant to both drugs, while the OVCAR-3 and -4 cell lines were the most sensitive. Furthermore, the most resistant cell lines were found to have the lowest active caspase-3 levels, while the most sensitive cells displayed the highest levels of active caspase-3. Despite seeing a visible reduction in clonogenic recovery in the ID8-luc2 cell line following treatment with paclitaxel and carboplatin, paclitaxel induced a small increase in caspase-3 cleavage (3%), while carboplatin did not induce any caspase-3 cleavage. It is possible that these cells have lost apoptosis, however, caspase-3 activation has previously been reported in the ID8 cell line (Said and Motamed, 2005). Morphological analysis of ID8-luc2 cells treated with paclitaxel revealed features of mitotic catastrophe, such as G2/M arrest and micronucleation. It is possible that ID8 cells undergo caspase-independent mitotic death (CIMD), previously reported to occur in colon cancer cells following paclitaxel treatment (Niikura *et al.*, 2007). Caspase-3 activation was not evident in any of our OC cells in response to carboplatin treatment. This suggests that the cytotoxic effects of carboplatin observed in the panel of OC cell lines is non-apoptotic. In contrast to our data, a study by Abed *et al.* (2016) reported increased caspase-3 activation in OVCAR-3, -4 and -8 cells following carboplatin treatment. This study however, used a significantly higher concentration of carboplatin, 66μM (Abed, Abdullah and Richardson, 2016). A postulated mechanism of action for carboplatin's induction of

apoptosis is via ROS generation, reported only to occur at high concentrations (> 50μM) in cardiomyocytes and human laryngeal carcinoma cells (Cheng *et al.*, 2008) (Brozovic *et al.*, 2013). Platinum salts, such as carboplatin, elicit their cytotoxic mechanisms via two methods: direct covalent bonding of the salt to the DNA resulting in adducts, or via the generation of ROS which form DNA adducts (Nunes and Serpa, 2018). Supporting this observation, high levels of glutathione, a ROS scavenger, have been implicated in resistance to carboplatin. Thus, it is possible, that the low concentrations of carboplatin used in our study are insufficient for ROS generation and apoptosis induction, although we have not assessed this. In agreement with our findings, a recent study showed that carboplatin treatment in OVCAR-3 cells lead to Akt phosphorylation and XIAP stabilisation, resulting in the inhibition of caspase-3 and -7 activation and lack of apoptosis induction (Zhang *et al.*, 2018). Limited necrotic morphology was evident in OVCAR-3, -4 and -5 cells following carboplatin treatment. Supporting this observation, a recent study reported the induction of necroptosis in a carboplatin resistant OC cell line EFO-21, whereas apoptosis was induced in carboplatin sensitive OC cells IGROV-1 and A2780S (Thibault *et al.*, 2018). Necroptosis may be induced in our cells in response to carboplatin, however, this would need to be confirmed with specific markers, such as activation of RIPK3. Cancer cells use multiple pathways to evade drug induced death, including the upregulation of drug efflux pumps such as P-glycoprotein, leading to drug resistance. While each of the OVCAR cell lines have wild type BRCA, the promoter region of BRCA1 is hypermethylated in the OVCAR-8 cell line. A patient with extensive BRCA1 methylation was found to have lost this methylation during disease relapse after combination carboplatin treatment (Patch *et al.*, 2015). Epigenetic alterations to BRCA genes after treatment may also contribute to resistance.

Further investigation into the cell death pathways underlying response to carboplatin in OC cells is necessary.

We have demonstrated for the first time that apoptosis is reduced in OC cells following a re-challenge with paclitaxel, and that these cells are more resistant. This could have significant implications for the clinical management of OC, given that OC patients undergo multiple rounds of chemotherapy. Our results were obtained following a single paclitaxel treatment; however, it implies that apoptosis is likely abrogated following multiple treatments. Thus, targeting this pathway may be ineffective in the long term, which is consistent with the attainment of resistance in most patients.

We have confirmed that the panel of OC cell lines express key autophagy proteins Beclin 1, Atg5/12 and LC3, and importantly, we have shown that the cell lines express varying levels of each protein. Furthermore, we have demonstrated that high protein expression levels are not predictive of a cells tendency to undergo autophagy. While the OVCAR-8 cells displayed the lowest expression of Beclin 1 and Atg5/12, they had the highest induction of basal autophagy. In OC, autophagy was found to be the most severely disrupted pathway by coincident gene deletions (Delaney *et al.*, 2017). Despite this, each cell line in our panel was found to express key autophagy proteins and autophagy was readily inducible. In agreement with our findings, a previous study revealed that while a monoallelic deletion in BECN1 was found in OVCAR-8 cells, protein expression remained stable (Correa *et al.*, 2015). Studies to date have focused on the prognostic value of autophagy biomarkers, as opposed to a 'predictive' biomarker, to stratify patients who will respond to a given treatment. A combination of autophagy markers, including LC3 and Beclin 1, have previously been used to determine autophagy activation, and infer clinicopathologic features relating to autophagy (Masuda *et al.*, 2016) (Wolpin *et al.*, 2014). However, our results suggest

that caution is warranted when selecting potential autophagy biomarkers based on their expression levels.

Mirroring the caspase-3 data, the cell lines which previously displayed the lowest active caspse-3 levels (ID8-luc2, OVCAR-5 and -8) displayed the highest levels of autophagy flux in response to paclitaxel and carboplatin. The OVCAR-3 and -4 cell lines, which displayed the highest active caspase-3 levels, had the lowest levels of drug induced autophagy. Crosstalk between autophagy and apoptosis has been widely reported, with the consensus being that autophagy and apoptosis are mutually inhibitory. Autophagy can exert an inhibitory effect on apoptosis via the selective degradation of apoptotic proteins, such as caspase-8 (Hou *et al.*, 2010). If a cell reaches a point of no return, apoptosis is activated, which can lead to the suppression of autophagy. Caspases can degrade several autophagic proteins including Atg5 and Beclin 1 (You *et al.*, 2013). Caspase cleaved autophagy proteins can then acquire a pro-death role. The cleavage of Beclin 1 by caspase-3, -6 or -9 leads to the generation of a carboxy-terminal fragment downstream of its BH3 domain, which can bind to the mitochondria to mediate cytochrome c release via MOMP (Wirawan *et al.*, 2010). Upon cleavage by caspase-3, ATG4D also acquires a pro-apoptotic role and is targeted to the mitochondria (Betin and Lane, 2009). A number of studies have shown that inhibiting autophagy can potentiate apoptosis (Kim *et al.*, 2015) (Zhu *et al.*, 2018) (Lohitesh *et al.*, 2018). A study published this year found that inhibition of autophagy via microRNA targeting of LC3B, promoted apoptosis and increased the chemosensitivity of OC cells (Tang *et al.*, 2019). Another study described the interaction of p53 and RAS signalling networks in mediating OC cisplatin resistance via modulation of both apoptosis and autophagy. P53 induction, along with the introduction of ERK active RAS mutants inhibited apoptosis and promoted autophagy

in OC cells, conferring cisplatin resistance, while AKT active RAS mutants had less autophagy, more apoptosis and were sensitive to cisplatin (Zhang *et al.*, 2019). In these studies, autophagy played a cytoprotective role, suggesting that inhibition of autophagy may be a useful strategy in sensitising cells to treatment. Expression of key proteins which regulate autophagy may also account for the different levels of autophagy observed. In agreement with our observations, the OVCAR-3 cells, which displayed low autophagic flux in this study, have been reported to express high levels of mTOR, which supresses autophagy (Zhou *et al.*, 2018).

In summary, this study has shown that a panel of OC cells differ significantly in their response to chemotherapy. To our knowledge, this is the first study to assess a panel of OC cell lines in terms of their apoptotic and autophagic response to chemotherapeutic drugs. By using of a panel of OC cell lines, generated from different patient types, it is more representative of the heterogeneity which exists among patients in the clinic. This data also supports a personalised medicine approach and highlights a current unmet need in OC for biomarkers to predict treatment response.

2.6 References

Abed, M. N., Abdullah, M. I. and Richardson, A. (2016) 'Antagonism of Bcl-XL is necessary for synergy between carboplatin and BH3 mimetics in ovarian cancer cells', Journal of Ovarian Research, 9(1), p. 25.

Anglesio, M. S. *et al.* (2013) 'Type-specific cell line models for type-specific ovarian cancer research.', PloS one, 8(9), p. e72162.

Betin, V. M. S. and Lane, J. D. (2009) 'Caspase cleavage of Atg4D stimulates GABARAP-L1 processing and triggers mitochondrial targeting and apoptosis.', Journal of cell science, 122(Pt 14), pp. 2554–2566.

Boyd, L. R. and Muggia, F. M. (2018) 'Carboplatin/Paclitaxel Induction in Ovarian Cancer: The Finer Points.', Oncology, 32(8), pp. 418-420,422-424.

Brozovic, A. et al. (2013) 'Endoplasmic reticulum stress is involved in the response of human laryngeal carcinoma cells to Carboplatin but is absent in Carboplatin-resistant cells.', PloS One, 8(9), p. e76397.

Cheng, C.-F. et al. (2008) 'Pravastatin attenuates carboplatin-induced cardiotoxicity via inhibition of oxidative stress associated apoptosis.', Apoptosis: An International Journal on Programmed Cell Death, 13(7), pp. 883–894.

Correa, R. J. M. et al. (2015) 'Beclin-1 expression is retained in high-grade serous ovarian cancer yet is not essential for autophagy induction in vitro.', Journal of Ovarian Research, 8, p. 52.

Delaney, J. R. *et al.* (2017) 'Haploinsufficiency networks identify targetable patterns of allelic deficiency in low mutation ovarian cancer', Nature Communications, 8, p. 14423.

Domcke, S. *et al.* (2013) 'Evaluating cell lines as tumour models by comparison of genomic profiles', Nature Communications, 4(1), p. 2126.

Haley, J. *et al.* (2016) 'Functional characterization of a panel of high-grade serous ovarian cancer cell lines as representative experimental models of the disease', Oncotarget, 7(22), pp. 32810–32820.

Hamilton, T. C., Young, R. C. and Ozols, R. F. (1984) 'Experimental model systems of ovarian cancer: applications to the design and evaluation of new treatment approaches', Seminars in oncology, 11(3), pp. 285–298.

Hou, W. et al. (2010) 'Autophagic degradation of active caspase-8: a crosstalk mechanism between autophagy and apoptosis', Autophagy, 6(7), pp. 891–900.

Kim, H.-R. et al. (2015) ‘Inhibition of autophagy potentiates pemetrexed and simvastatin-induced apoptotic cell death in malignant mesothelioma and non-small cell lung cancer cells’, European Respiratory Journal, 46(suppl 59), p. PA4263.

Kim, J. *et al.* (2018) ‘Cell Origins of High-Grade Serous Ovarian Cancer’, Cancers, 10(11), p. 433.

Kulshrestha, A. *et al.* (2019) ‘Targeting V-ATPase Isoform Restores Cisplatin Activity in Resistant Ovarian Cancer: Inhibition of Autophagy, Endosome Function, and ERK/MEK Pathway’, Journal of Oncology, 2019, p. 2343876.

Lohitesh, K. et al. (2018) ‘Autophagy inhibition potentiates SAHAmediated apoptosis in glioblastoma cells by accumulation of damaged mitochondria.’, Oncology Reports, 39(6), pp. 2787–2796.

Masuda, G. O. et al. (2016) ‘Clinicopathological Correlations of Autophagy-related Proteins LC3, Beclin 1 and p62 in Gastric Cancer.’, Anticancer Research, 36(1), pp. 129–136.

Mitra, A. K. *et al.* (2015) ‘In vivo tumor growth of high-grade serous ovarian cancer cell lines.’, Gynaecologic oncology, 138(2), pp. 372–377.

Niikura, Y. *et al.* (2007) ‘BUB1 mediation of caspase-independent mitotic death determines cell fate’, The Journal of Cell Biology, 178(2), p. 283-296.

O’Cearbhaill, R. E. (2018) ‘Using PARP Inhibitors in Advanced Ovarian Cancer’, Oncology, 32(7), pp. 339–343.

Patch, A.-M. *et al.* (2015) ‘Whole-genome characterization of chemoresistant ovarian cancer.’, Nature, 521(7553), pp. 489–494.

Tang, J. et al. (2019) ‘Inhibition LC3B can increase chemosensitivity of ovarian cancer cells’, Cancer Cell International, 19(1), p. 199.

Thibault, B. et al. (2018) ‘DEBIO 1143, an IAP inhibitor, reverses carboplatin resistance in ovarian cancer cells and triggers apoptotic or necroptotic cell death’, Scientific Reports, 8(1), p. 17862.

Wang, J. and Wu, G. S. (2014) ‘Role of Autophagy in Cisplatin Resistance in Ovarian Cancer Cells’, The Journal of Biological Chemistry. 9650, pp. 17163–17173.

Wirawan, E. et al. (2010) ‘Caspase-mediated cleavage of Beclin-1 inactivates Beclin-1-induced autophagy and enhances apoptosis by promoting the release of proapoptotic factors from mitochondria.’, Cell Death & Disease, 1, p. e18.

Wolpin, B. M. et al. (2014) ‘Phase II and pharmacodynamic study of autophagy inhibition using hydroxychloroquine in patients with metastatic pancreatic adenocarcinoma’, The Oncologist, 19(6), pp. 637–638.

You, M. et al. (2013) ‘TRAIL induces autophagic protein cleavage through caspase activation in melanoma cell lines under arginine deprivation.’, Molecular and cellular biochemistry, 374(1–2), pp. 181–190.

Zhang, S.-F. *et al.* (2015) ‘TXNDC17 promotes paclitaxel resistance via inducing autophagy in ovarian cancer’, Autophagy, 11(2), pp. 225–238.

Zhang, X. et al. (2019) ‘Interaction between p53 and Ras signaling controls cisplatin resistance via HDAC4- and HIF-1alpha-mediated regulation of apoptosis and autophagy.’, Theranostics, 9(4), pp. 1096–1114.

Zhang, Y. et al. (2018) ‘Inhibition of XIAP increases carboplatin sensitivity in ovarian cancer.’, OncoTargets and Therapy, 11, pp. 8751–8759.

Zhou, H. et al. (2018) ‘Influence of carboplatin on the proliferation and apoptosis of ovarian cancer cells through mTOR/p70s6k signaling pathway.’, Journal of B.U.O.N: Official Journal of the Balkan Union of Oncology, 23(6), pp. 1732–1738.

Zhu, L. et al. (2018) ‘Autophagy is a pro-survival mechanism in ovarian cancer against the apoptotic effects of euxanthone’, Biomedicine & Pharmacotherapy, 103, pp. 708–718.

Chapter Three: Evaluation of pharmacological modulators of autophagy: chloroquine, lithium and brefeldin A, on a panel of ovarian cancer cell lines

3.1 Abstract

Five year survival rates for ovarian cancer remain poor and have not significantly improved in the last decade. The backbone of OC treatment remains cytoreductive surgery and a platinum/taxane chemotherapy doublet. Resistance to chemotherapy is a significant clinical hurdle which has yet to be overcome when treating OC. To improve patient outcomes, it is vital to elucidate novel treatment strategies to overcome chemoresistance. Autophagy has been implicated in OC chemoresistance and has gained interest as a therapeutic target. In this chapter, we aimed to assess the effect of autophagy modulators on the chemosensitivity of our panel of cell lines. Chloroquine was found to significantly reduce clonogenic recovery following drug treatment in the OVCAR-5 and -8 cell lines. In contrast, it exerted a protective effect in the OVCAR-3 and -4 cells. Lithium is a mood stabilising drug routinely used to treat bi-polar disorder; however, our group has previously shown it is an effective chemosensitising agent in both oesophageal and colon cancer. Similar to the effects of CQ, lithium could significantly sensitise OVCAR-5 and -8 cells to paclitaxel and carboplatin, but it did not sensitise OVCAR-3 cells. In addition, brefeldin A was used to block non-canonical Atg5/Atg7-independent autophagosome generation. The addition of brefeldin A to paclitaxel could significantly reduce autophagosome accumulation in ID8-luc2, OVCAR-5 and OVCAR-8 cells. While this data highlights autophagy as an attractive therapeutic target to overcome chemoresistance, it's inhibition may only be beneficial to the subgroup of patients who have autophagy dependent cancer.

3.2 Introduction

The standard of care for OC patients involves cytoreductive surgery combined with platinum and taxane chemotherapy. The combination of paclitaxel and carboplatin comprises the backbone of treatment for OC patients which is effective, well-tolerated and less toxic than other combination therapies. Although patients treated with first line paclitaxel-carboplatin achieve a good clinical response, disease recurrence rates are 25 % for those with early stage disease and 80 % for those with advanced disease (Pokhriyal *et al.*, 2019). Autophagy has been shown to play a role in chemoresistance in OC, with autophagy induction acting as a protective mechanism against cisplatin and paclitaxel (Zhan *et al.*, 2016). Thus, autophagy inhibition has emerged as an attractive therapeutic target to combat resistance in OC. During the development of novel therapies, it can take upwards of 10 years before a potential drug will reach phase I clinical trials. As such, repurposing of drugs, that are already approved, has become an area of interest, particularly for cancer treatment.

Chloroquine is one of only two autophagy modulating drugs which are FDA-approved for cancer treatment. Chloroquine and its analogues have well characterised toxicity profiles, due to their decades old use as anti-malarial agents, making them an attractive drug to target autophagy in the cancer setting. Chloroquine, which is a weak base, accumulates within acidic vesicles, such as lysosomes, where it raises intravesicular pH and impedes the function of lysosomal enzymes. This in turn impairs the fusion and digestion of autophagic vacuoles (Mauthe *et al.*, 2018).

Lithium is a mood stabilising drug, FDA approved for the treatment of bipolar disorder, with a track record of safety. The rationale for repurposing lithium as an anticancer agent came from a retrospective study of psychiatric patients receiving lithium, who displayed a significantly reduced incidence of cancer compared to their

non-lithium treated counterparts (Cohen *et al.*, 1998). More recent studies conducted have corroborated these findings (Martinsson *et al.*, 2016) (Huang *et al.*, 2016) (Pottegard *et al.*, 2016). A study published in 2019 using a systems biology approach highlighted the potential influence of lithium on cancer. Using STRING and KEGG pathway analysis, the study found mutual enrichment of STRING-derived interactomes of lithium sensitive enzymes with KEGG cancer related signaling pathways (Ge and Jakobsson, 2019). Experimental evidence also provides a rationale for using lithium to sensitise cancer cells to chemotherapy. A study by our group has shown that the addition of lithium to standard chemotherapeutic agents enhanced their cytotoxicity in oesophageal and colorectal cancer cells (O'Donovan *et al.*, 2015). Another study reported the chemosensitising effect of lithium in colorectal cancer and ovarian cancer cells (Li *et al.*, 2014). Therefore, in this study, we aimed to assess if lithium could sensitise OC cells to treatment. Although the way in which lithium exerts its cytotoxic effects remains controversial, a key pathway influenced by lithium is autophagy. Lithium has been reported to both induce and inhibit autophagy. Previous work published by our group has provided evidence to show an autophagy inhibitory effect of lithium, via lysosomal dysfunction (O'Donovan *et al.*, 2015). Thus, we also aimed to assess the effects of lithium on autophagy in our OC cells.

The Atg5/Atg7-independent autophagy pathway is a recently described alternative autophagy pathway, which can occur in the absence of Atg5 and Atg7 but requires Beclin 1. Autophagosomes formed during this pathway are thought to originate in the Golgi, as opposed to the ER during canonical autophagy. Brefeldin A, a known Golgi inhibitor, has previously been reported to inhibit this non-canonical pathway, but not canonical autophagy. In this study, we have used brefeldin A to assess the presence of Atg5/Atg7-independent autophagy, both basally and in response to treatment. A

schematic illustrating the expected effect on autophagosome accumulation via use of brefeldin A is depicted in Figure 3.1 below.

3.3 Materials and Methods

3.3.1 Cell culture and Reagents

Established human ovarian cancer cell lines OVCAR-3, OVCAR-4, OVCAR-5 and OVCAR-8 were obtained directly from the NCI Frederick Cancer DCTC Tumor/Cell Line Repository. Murine ID8-luc2 cells were obtained from Mayo Clinic. All human OVCAR cell lines were maintained in RPMI 1640 media. OVCAR-3 and OVCAR-4 cultures were supplemented with 20% (v/v) foetal calf serum, whilst OVCAR-5 and OVCAR-8 cultures were supplemented with 10% (v/v) foetal calf serum. Murine ID8-luc2 cells were cultured using Dulbecco's Modified Eagles Medium containing 10% (v/v) foetal calf serum. All cultures were supplemented with 1% penicillin/streptomycin (Gibco Life Technologies 15070-063). Cells were grown in T75cm^2 flasks (Sarstedt) and maintained at 37°C, 5% CO_2.

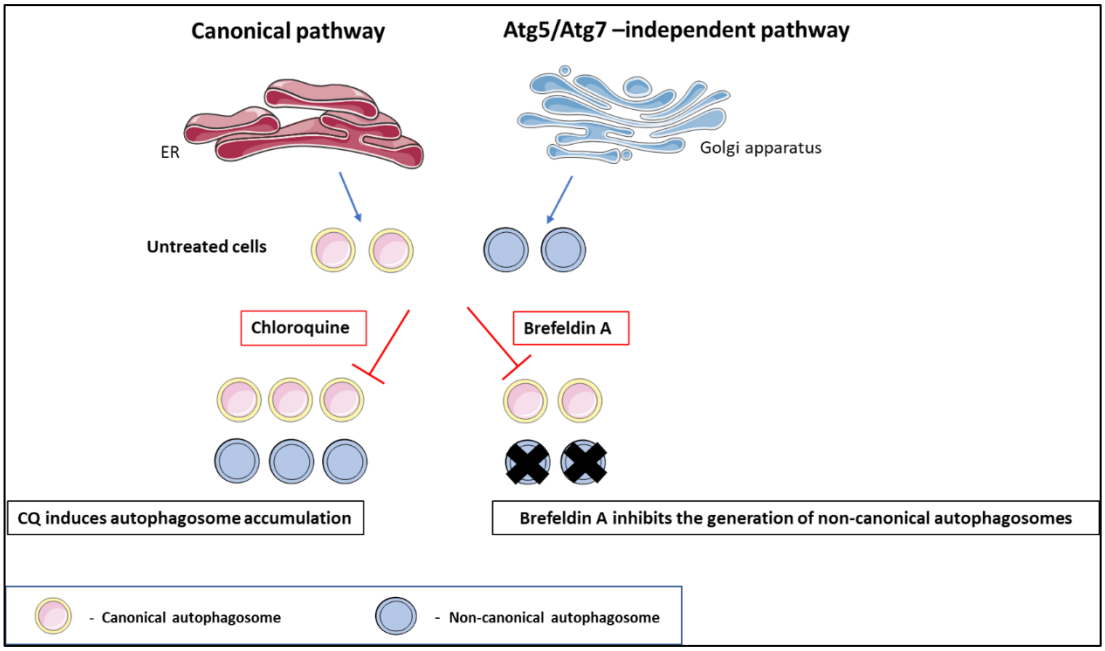

Figure 3.1. Schematic illustration of the anticipated effects of brefeldin A on autophagosome accumulation. In untreated cells, autophagosomes detected using the Cyto-ID autophagy assay may derive from both the canonical pathway and the Atg5/Atg7-independent pathway. The addition of CQ should block lysosomal fusion and lead to an accumulation of autophagosomes derived from both pathways. If basal Atg5/Atg7-independent autophagosomes are being generated, the addition of brefeldin A should prevent non-canonical autophagosome accumulation. Similarly, if chemotherapeutic treatment induces the generation of Atg5/Atg7-independent derived autophagosomes, the addition of brefeldin A should cause a decrease in the amount of autophagosomes relative to drug treated cells.

3.3.2 Drug treatments

Paclitaxel (Cat # T7402), Carboplatin (Cat # C2538), Chloroquine (Cat # C6628), Lithium Chloride (Cat # L9650) and Brefeldin A (Cat # B6542) were purchased from Sigma Aldrich. Paclitaxel was reconstituted in DMSO to give 58.55mM stock. Aliquots were prepared and stored at -20°C. Carboplatin was reconstituted in water to

give a 26.93mM stock, aliquoted and stored in the dark at room temperature. Chloroquine was reconstituted in water and stored at -20℃ in aliquots. Brefeldin A was reconstituted in 1ml of ethanol and stored at -20℃. Working concentrations of each drug were prepared in media on the day of treatment. Lithium chloride was weighed and resuspended in media to create a working stock (1mM) on the day of treatment.

For the clonogenic recovery studies assessing CQ, cells were treated with paclitaxel or carboplatin +/- CQ (10 µM) for 24 or 48 hours. CQ was added 2 hours prior to any other drug treatment and remained for the duration of treatment. Cells were subsequently re-seeded for colonies growth. For clonogenic recovery studies assessing lithium, cells were treated with paclitaxel or carboplatin +/- lithium (10 or 20mM) for 48 hours. Cells were then re-seeded for colonies growth.

To assess the effect of lithium on autophagy, cells were treated with lithium (10 or 20mM) +/-CQ (10µM) for 48 hours. Cells were then cytospun for morphological analysis, pelleted for western blots or stained with the Cyto-ID autophagy kit for flow cytometry analysis.

To evaluate the effect of brefeldin A on autophagosome accumulation, cells received CQ (10µM) for 48 hours, with brefeldin A (10µg/ml) added for the final 24 hours of treatment. Alternatively, cells were treated with paclitaxel for 48 hours, with brefeldin A (10µg/ml) added for the final 24 hours of treatment. Cells were subsequently stained using the Cyto-ID autophagy assay.

3.3.3 Colony formation assay

Colony formation (clonogenic) assays were used to determine the ability of single cells to recover from a drug treatment and re-establish colonies. Following specified treatment, cells were trypsinised using 500µl of Trypsin EDTA (Sigma Aldrich, Cat # T4049) and viable cells counted using the NucleoCounter NC-100 (Chemometec). For the OVCAR-5, OVCAR-8 and ID8-luc2 cell lines 1,500 viable cells were re-seeded into a well of a six-well plate (Nunc™ Thermo Scientific, Cat # 140685). For the OVCAR-3 and OVCAR-4 cell lines, 2,500 cells were re-seeded in the same manner. Cells were allowed to adhere and grow for between 10 and 14 days, until control wells reached at least 70% confluency. Following the recovery period, media was aspirated, and wells were washed once with PBS. Cells were then fixed in 96% ethanol for 5 minutes and stained with Pro-diff solution C (Braidwood Laboratories E310) for 5 minutes. Following a rinse with water to remove excess stain, plates were allowed to air-dry overnight. Plates were then scanned and quantified using the Odyssey IR imaging system (Li-Cor, Cambridge, United Kingdom).

3.3.4 Cyto-ID autophagy detection kit

Treated cells were trypsinised using 500µl of Trypsin EDTA (Sigma Aldrich, Cat # T4049) and stained using the Cyto-ID autophagy detection kit (Enzo Life Sciences, Cat # ENZ-51031-K200) according to the manufacturer's instructions. Cyto-ID is a cationic amphiphilic tracer dye which selectively accumulates within autophagic vesicles. An increase in autophagic vacuole accumulation will result in an increase in fluorescence in the 488-2 channel. Samples were run on the BD LSRII flow cytometer with FACS Diva acquisition and analysis software. FlowJo data analysis software was

used for gating and generating overlay histograms. Data is presented as Mean Fluorescence Intensity (MFI).

3.3.5 Western Blotting

Total cellular protein was extracted by trypsinisation of cells followed by lysing in 10-25µl of modified RIPA buffer (50 mM Tris HCl (pH 7.4), 150 mM NaCl, 0.25% sodium deoxycholate, 1% Igepal, 1 mM EDTA, 1x Pefabloc, 1x protease inhibitor cocktail, 1 mM Na_3VO_4, 1 mM NaF), depending on pellet size. Samples (75 µg) were separated on NuPAGE 4–12% Bis-Tris gels (Invitrogen Life Technologies, Cat # NP0322) and electrophoretically transferred onto a PVDF membrane using the iBlot gel transfer system (Invitrogen, Cat # IB1001). Membranes were blocked with Odyssey blocking buffer (Li-Cor, Cat # 927-40100) for 1 hour at room temperature, and incubated overnight at 4°C using: anti- ATG5 (Novus, Cat # NB110-53818), anti-Beclin 1 (Novus, Cat # NB500-249) and anti-Rab9 (Abgent, Cat # ab2810) antibodies. Anti-β-actin (loading control) (Sigma, Cat # A5441) was incubated at room temperature, rocking, for one hour. IR-Dye conjugated secondary antibodies (Rockland) were utilised for protein detection on the Odyssey Infra-red imaging system (Li-Cor, Cambridge, United Kingdom).

3.3.6 Evaluation of morphology

Treated cells were cytospun and allowed to air dry for 5 minutes. Cells were then fixed using methanol and stained using May Grunwald Giemsa (DiaPath). Cells which were apoptotic were identified based on the presence of two or more of the following morphological features: cell shrinkage, chromatin condensation or DNA

fragmentation into ‘apoptotic bodies’. Images were acquired using a DP70 digital microscope camera and Olympus DP-Soft 823 version 3.2 software (Mason Technologies Dublin, Ireland).

3.3.7 Statistical Analysis

All data is expressed as mean ± the standard error of the mean (SEM), which represents the standard deviation of the distribution of the sample around the mean. Significance was determined by independent or paired student t-tests, which determines the difference between the means of two groups. The p-value was considered statistically significant where *$p \leq 0.05$, ** $p \leq 0.01$, *** $p \leq 0.001$. Statistical analysis was carried out and graphed using GraphPad Prism 5 software (GraphPad Software Inc., CA, USA).

3.4 Results

3.4.1 Inhibition of autophagy with CQ sensitises ID8-luc2 cells to paclitaxel and carboplatin

In the previous chapter, autophagic flux, in response to paclitaxel and carboplatin was observed in the ID8-luc2 cell line. Clonogenic assays revealed that ID8-luc2 cells can recover and form colonies after paclitaxel and carboplatin treatment. The effect of chloroquine (CQ), which impedes autophagy, on chemosensitivity was therefore assessed in this cell line.

ID8-luc2 cells were treated with paclitaxel (24 hours) and carboplatin (48 hours) alone or in the presence of CQ. Following treatment, 1500 viable cells were reseeded in triplicate and allowed to recover in drug-free medium for 10-14 days. The addition of CQ to paclitaxel and carboplatin significantly reduced clonogenic recovery in the ID8-luc2 cell line following 1μM paclitaxel (*p = 0.018) and 40μM carboplatin (**p = 0.004) treatment [Figure 3.2 A and B, respectively]. A reduction in clonogenic recovery was evident following the addition of CQ to 2.5 μM paclitaxel, although it was not significant.

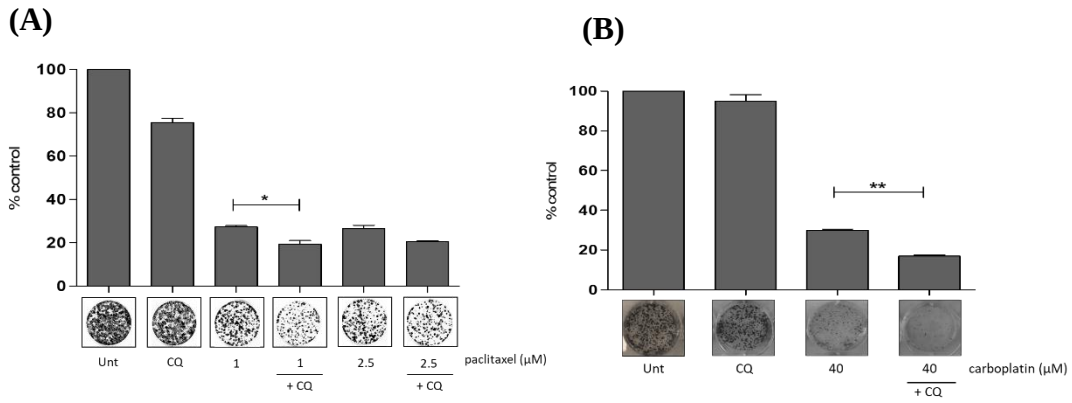

Figure 3.2. ID8-luc2 clonogenic recovery is significantly reduced following the addition of CQ to paclitaxel and carboplatin. (A) Cells were treated with 1μM and 2.5μM paclitaxel ± CQ (10 μM) for 24 hours, re-seeded (1500 cells per well) and allowed to recover for 10-14 days. **(B)** Cells were treated with 40 μM carboplatin ± CQ for 48 hours, re-seeded (1500 cells per well) and allowed to recover for 10-14 days. All colonies were stained and scanned using the Li-COR Infrared Odyssey Scanner. Integrated intensities were quantified, and data is graphed as % control (where control = 100%), (n=3). Statistical significance was defined where *$p \leq 0.05$, **$p \leq 0.01$.

3.4.2 Assessment of the effect of CQ on recovery of OVCAR-3 and OVCAR-4 cells following treatment

The addition of CQ to the OVCAR-3 cell line resulted in a significant protective effect following treatment with paclitaxel (*p = 0.010, **p = 0.001; respectively), and a moderate protective effect following treatment with carboplatin, which was not significant [Figure 3.3 A and B, respectively]. In contrast, the addition of CQ to the OVCAR-4 cell line significantly reduced clonogenic recovery following treatment with paclitaxel (*p = 0.028, *p = 0.017; respectively), while CQ protected OVCAR-4 cells from carboplatin [Figure 3.3 C and D, respectively].

OVCAR-3

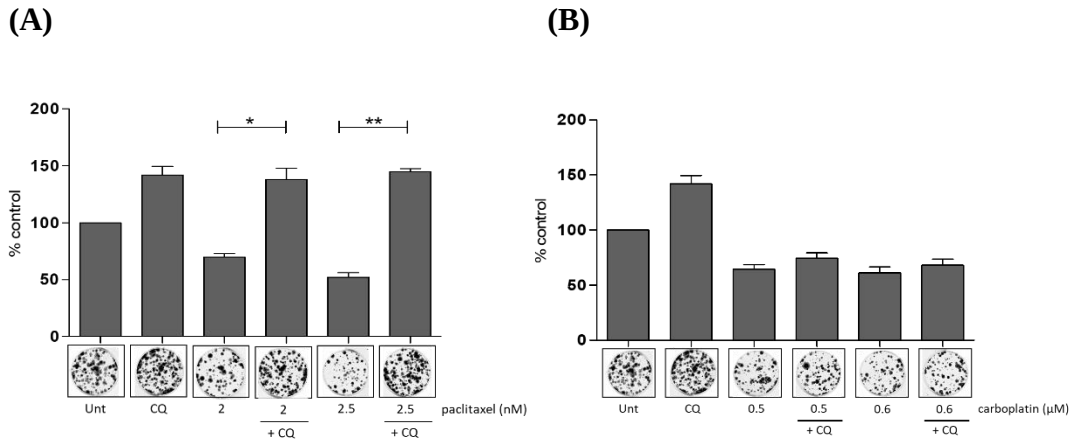

OVCAR-4

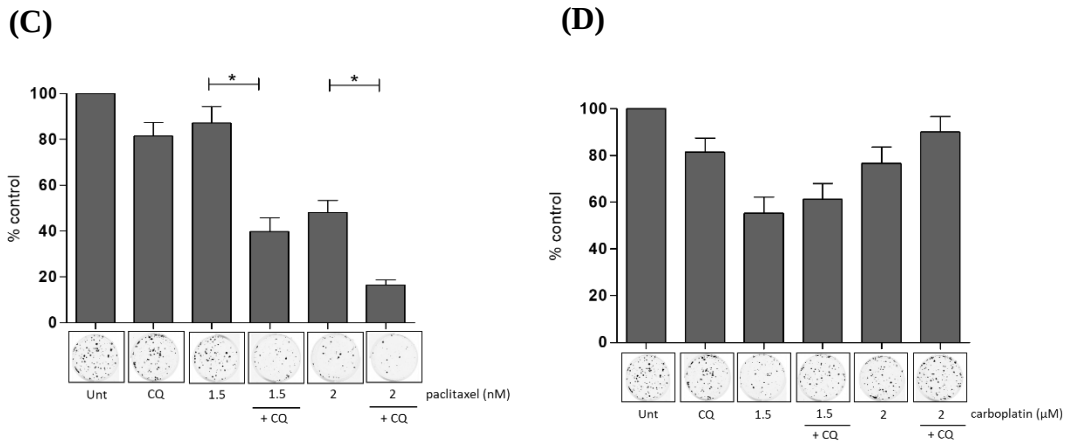

Figure 3.3. Assessment of the effect of CQ on the clonogenic recovery of OVCAR-3 and OVCAR-4 cell lines following treatment with paclitaxel and carboplatin. OVCAR-3 and -4 cells were treated with paclitaxel or carboplatin ± CQ. Following treatment viable cells were re-seeded (2500 cells per well) and clonogenic recovery was assessed. OVCAR-3 cell recovery following **(A)** paclitaxel or **(B)** carboplatin plus or minus CQ (10μM). OVCAR-4 cell recovery following **(C)** paclitaxel or **(D)** carboplatin treatment ± CQ. All colonies were fixed, stained and scanned using the Li-Cor Odyssey Infrared scanner. Integrated intensities were obtained and graphed as % control (where control = 100%) (n=3). Statistical significance is defined as *$p \leq 0.05$, **$p \leq 0.01$.

3.4.3 Inhibition of autophagy with chloroquine sensitises OVCAR-5 and OVCAR-8 cells to paclitaxel and carboplatin

In contrast to the OVCAR-3 and -4 cells, strong evidence for autophagy flux was observed by Cyto-ID or western blot in the OVCAR-5 and -8 cell lines in response to paclitaxel and carboplatin. The effect of CQ on recovery was therefore assessed in these cell lines.

The addition of CQ to paclitaxel significantly sensitised both OVCAR-5 and OVCAR-8 cells to paclitaxel treatment (*p = 0.045, *p = 0.022; *p = 0.01 respectively) [Figure 3.4A and C]. In addition, the recovery of both the OVCAR-5 and OVCAR-8 cell lines was significantly reduced by the addition of CQ following treatment with 10 and 5μM carboplatin respectively [Figure 3.4B and D]. These data would encourage the use of chloroquine as a chemosensitising agent in cancer cells that respond to chemotherapy agents with autophagy.

OVCAR-5

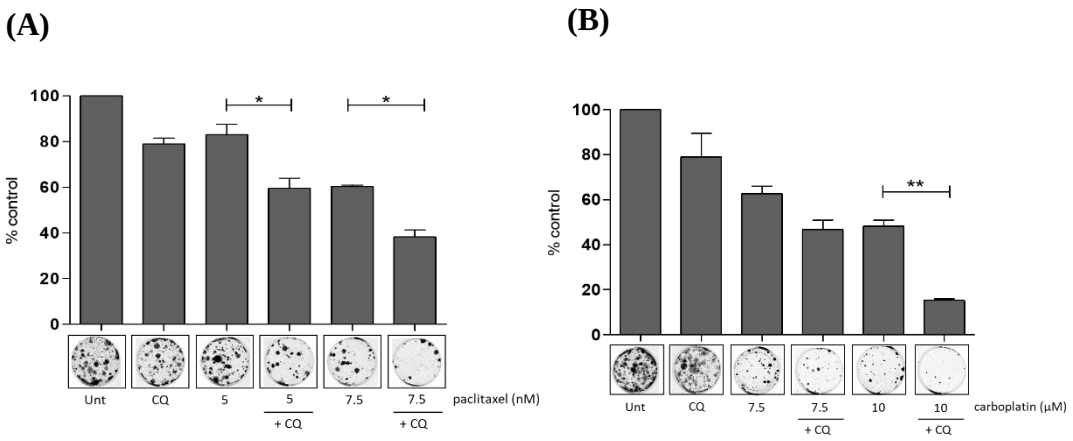

OVCAR-8

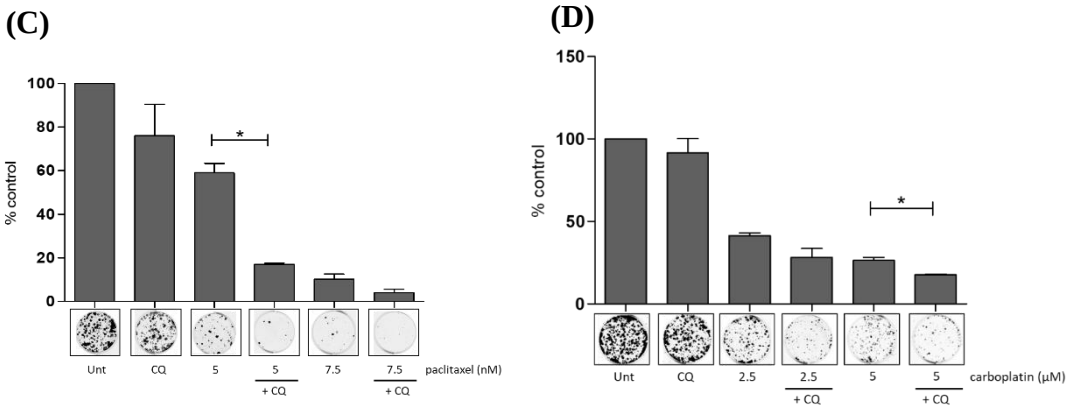

Figure 3.4. Assessment of the effect of CQ on the clonogenic recovery of OVCAR-5 and OVCAR-8 cell lines following treatment with paclitaxel and carboplatin. Following treatment with carboplatin ± CQ (10μM), OVCAR-5 and -8 cells were re-seeded (1500 cells per well) and allowed to recover for 10-14 days. OVCAR-5 cell recovery following **(A)** paclitaxel and **(B)** carboplatin ± CQ. OVCAR-8 cell recovery following **(C)** paclitaxel and **(D)** carboplatin ± CQ. All colonies were fixed, stained and scanned using the Li-Cor Odyssey Infrared scanner. Data is presented graphically as % control (where control = 100%) (n=3). Statistical significance is defined as *p $\leq$0.05, **p $\leq$ 0.01.

3.4.4 Lithium significantly enhances chemosensitivity in a panel of OC cell lines

Lithium is a mood stabilising drug commonly used in the management of bipolar disorder. Previous work by our group has demonstrated the chemo-sensitising effect of lithium in oesophageal and colorectal cancer cells (O'Donovan *et al.*, 2015). To test this in the panel of OC cell lines, cells were treated with lithium along with paclitaxel and carboplatin, and clonogenic recovery was assessed.

Treatment with lithium significantly sensitised ID8-luc2 cells to 40μM carboplatin, with no visible colonies remaining (**p = 0.003) [Figure 3.5]. Lithium did not sensitise the murine ID8-luc2 cells to paclitaxel (data not shown). The addition of lithium to paclitaxel significantly reduced clonogenic recovery in three of the OVCAR cell lines tested. Reduced clonogenic recovery in the OVCAR cell lines following treatment with lithium and paclitaxel was greater than that of either drug alone, suggesting an additive effect. A notable reduction in clonogenic recovery was evident with the OVCAR-5 and -8 cell lines following lithium addition to paclitaxel [Figure 3.6C and D, respectively]. The effect of lithium on paclitaxel sensitivity in the OVCAR-4 cell line remains to be determined.

The addition of lithium to carboplatin had no effect on the OVCAR-3 cell line and a limited effect on the OVCAR-4 cell line [Figure 3.7A and B, respectively]. The OVCAR-5 and OVCAR-8 cell lines showed significant sensitisation at both concentrations, with few visible colonies remaining [Figure 3.7C and D, respectively].

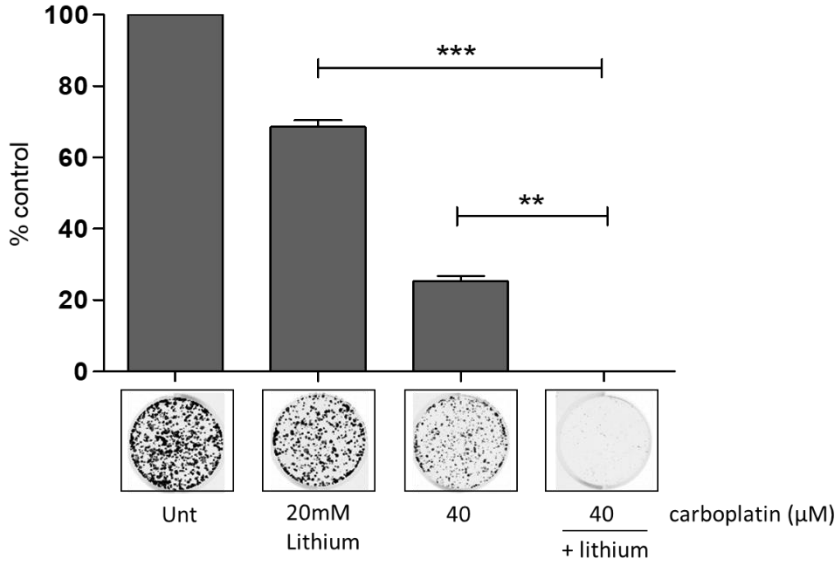

Figure 3.5. A significant reduction in recovery following treatment with lithium and carboplatin is evident in ID8-luc2 cells. To assess a potential synergistic effect between lithium and carboplatin, cells were treated with both drugs alone and in combination, and clonogenic recovery was assessed. ID8-luc2 cells were seeded (1500 cells per well) and allowed to recover. Integrated intensities were obtained and presented as % control (where control = 100%) (n=3). Statistical significance is defined as **p $\leq$ 0.01, ***p $\leq$ 0.001.

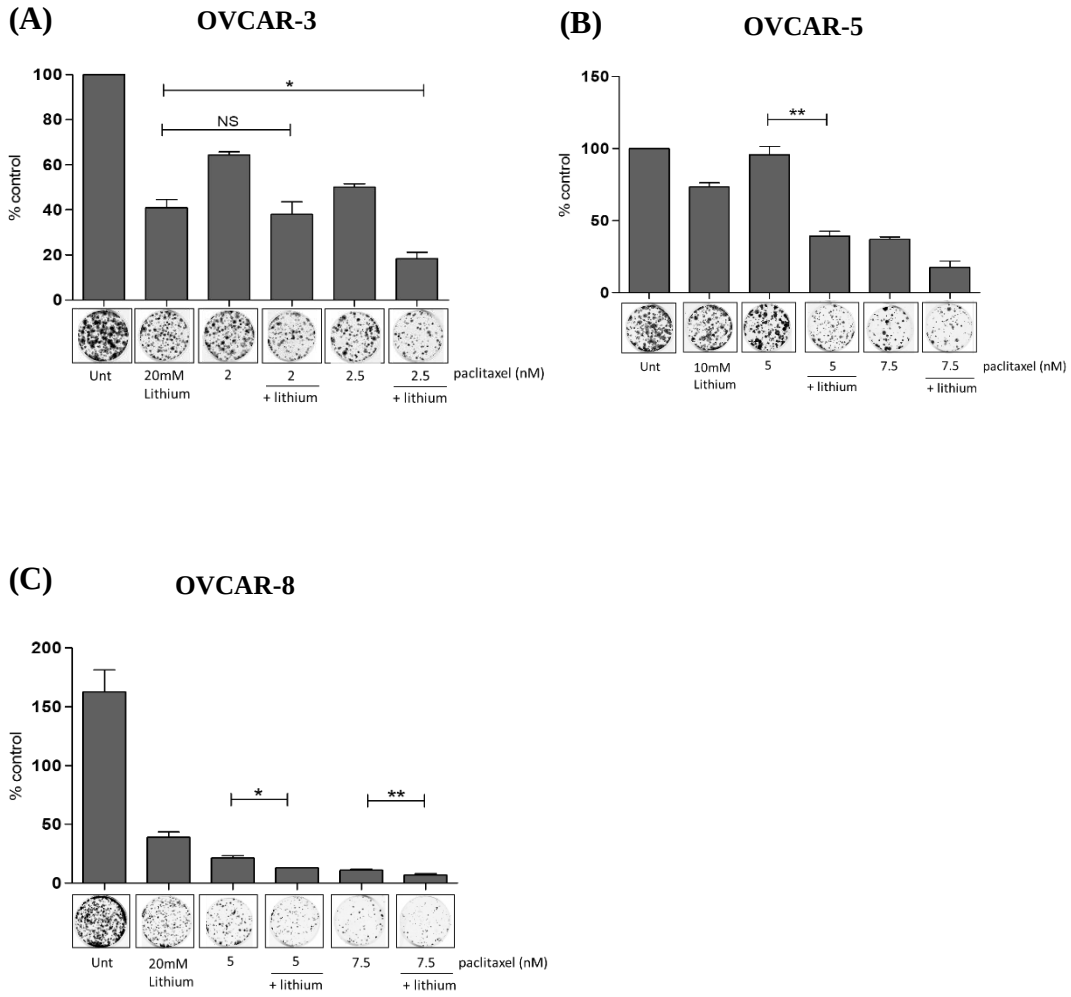

Figure 3.6. Lithium significantly sensitises OVCAR-3, -5 and -8 cells to paclitaxel. Following treatment with lithium and paclitaxel for 48 hours, clonogenic recovery was assessed. **(A)** OVCAR-3 cells were re-seeded (2500 cells per well) after treatment and recovery was assessed. **(B)** OVCAR-5 cells and **(C)** OVCAR-8 cells were seeded (1500 cells per well) and allowed to recover. All colonies were fixed, stained and scanned using the Li-Cor Odyssey Infrared scanner. Integrated intensities are graphed as % control (where control = 100%) (n=3). Statistical significance is defined as *$p \leq 0.05$, **$p \leq 0.01$.

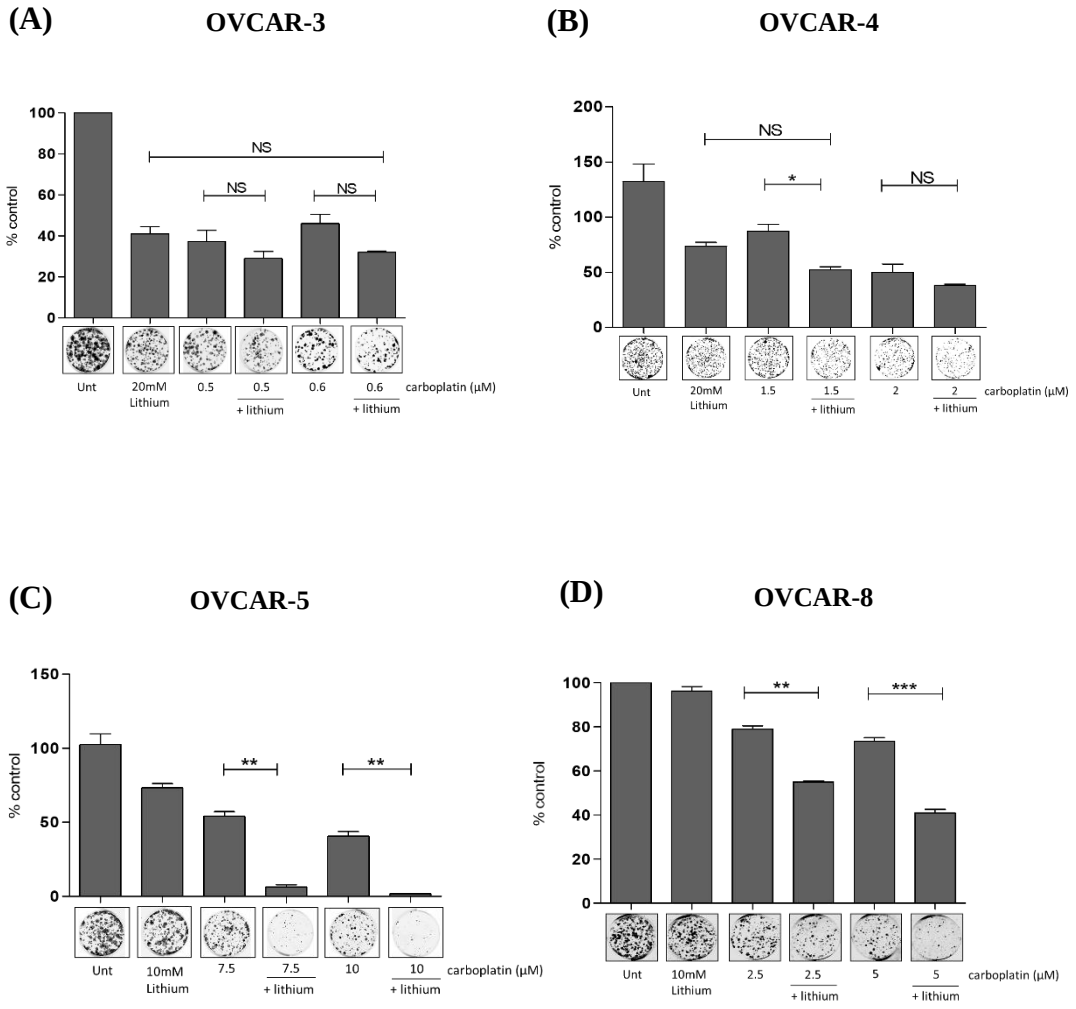

Figure 3.7. A significant reduction in recovery following combination treatment with lithium and carboplatin is evident in OVCAR-4, -5 and -8 cells. To assess a potential synergistic effect between lithium and carboplatin, cells were treated with both drugs alone and in combination, and clonogenic recovery was assessed. **(A)** OVCAR-3 and **(B)** OVCAR-4 cells were re-seeded (2500 cells per well) after treatment and recovery was assessed. **(C)** OVCAR-5 cells and **(D)** OVCAR-8 cells were seeded (1500 cells per well) and allowed to recover. All colonies were fixed, stained and scanned using the Li-Cor Odyssey Infrared scanner. Integrated intensities are graphed as % control (where control = 100%) (n=3). Statistical significance is defined as *$p \leq 0.05$, **$p \leq 0.01$.

3.4.5 Evaluation of the effects of lithium on autophagy

Previous work by our group has demonstrated a role for lithium in modulating autophagy by inhibiting turnover (O'Donovan *et al.*, 2015). The cell lines which displayed sensitivity to lithium (ID8-luc2, OVCAR-5 and -8), all displayed the highest levels of autophagic flux in chapter two. Therefore, we aimed to determine if there were any effects of lithium on autophagy in these cell lines, which may contribute to its chemosensitising effects.

3.4.5.1 Evaluation of the effects of lithium on autophagy in ID8-luc2 cells

In the ID8-luc2 cells, autophagy was assessed after 48 hour treatment. Morphology was assessed for the presence of vesicles (highlighted with black arrows). While vesicles were present in untreated cells (left hand panels), a greater accumulation of vesicles were present following 48 hour treatment with 20mM lithium (right hand panels) [Figure 3.8A]. To assess the effect of lithium on autophagic flux (described in chapter two, results section 2.4.6), cells were pre-treated with CQ alone and in combination with lithium. As shown in figure 3.8 (B), treatment with CQ alone for 48 hours resulted in an increase in vesicle accumulation (turquoise overlays), as assessed by Cyto-ID. Treatment with lithium caused a significant increase in vesicle accumulation (red overlay), which was significantly enhanced by CQ (green overlay), suggesting induction of autophagic flux (***p =0.0001). To confirm autophagy induction, LC3II expression was measured using western blotting. In contrast to the Cyto-ID data, lithium alone caused a decrease in LC3II expression. The expression of LC3II following treatment with CQ and lithium could not be quantified and would need to be repeated [Fig 3.8C]. This data suggests that in the ID8-luc2 cell line, lithium

can induce autophagosome accumulation, however we cannot conclude if the autophagosomes are LC3 dependent.

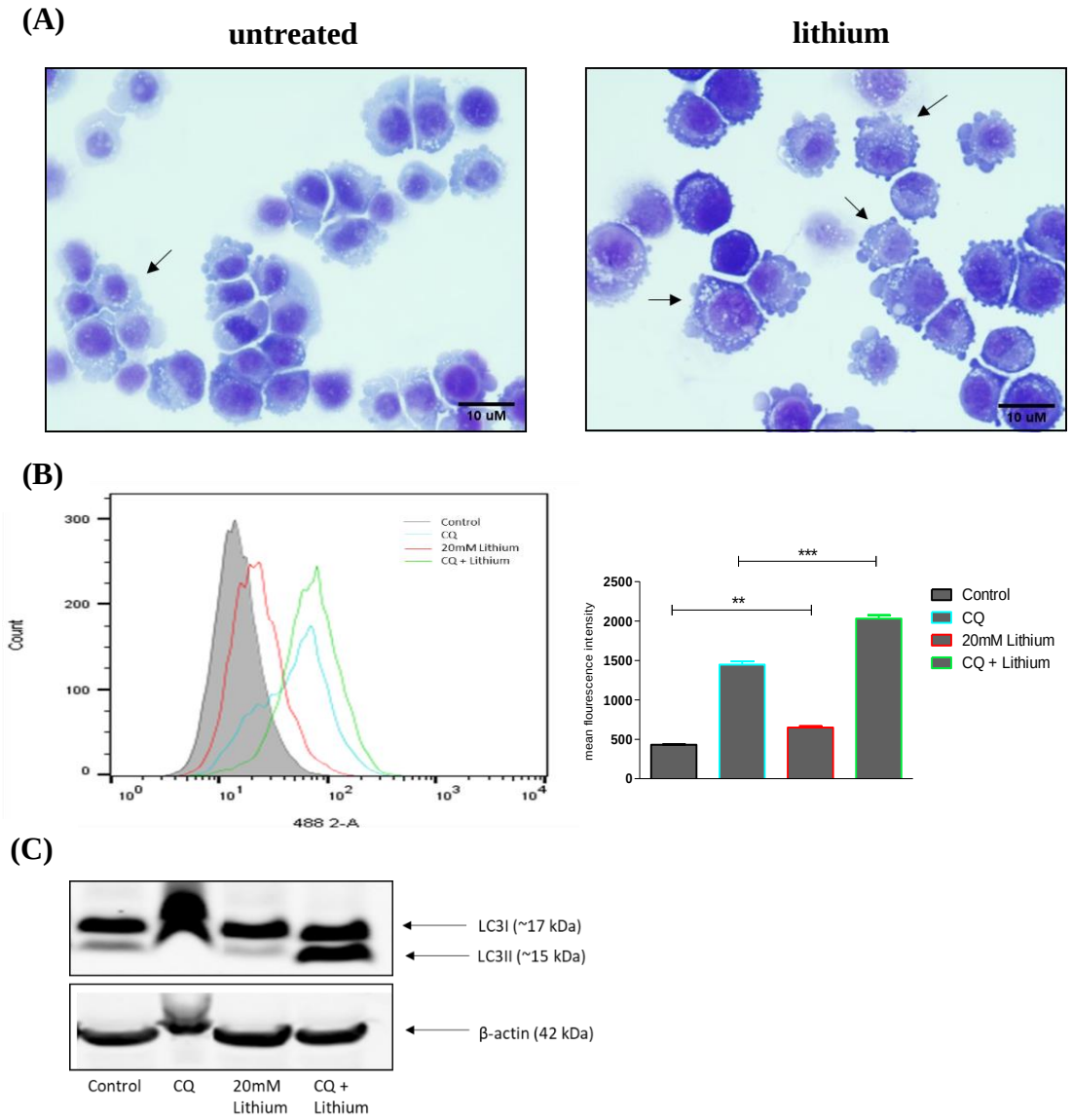

Figure 3.8. Evaluation of the effects of lithium on autophagy in ID8-luc2 cells. Cells were treated with lithium chloride (lithium) (20mM) alone and in combination with CQ (10µM) for 48 hours. **(A)** Cells were stained using Pro-diff II to assess vesicle accumulation in untreated (left hand panels) and lithium treated cells (right hand panels) (magnification 400X). Vesicles are highlighted with black arrows. **(B)** Cyto-ID analysis was used to assess vesicle accumulation following 48 hour treatment with lithium ± CQ. Mean fluorescent intensities are graphed ± SEM (n=3), to the right of the representative histogram overlays. **(C)** Western blot analysis of LC3I and LC3II following 48 hour treatment with lithium +/- CQ. Blots were scanned using the Odyssey Infrared Imaging system (Li-Cor) (n=1). Values were statistically significant when ** $p \leq 0.01$, ***$p \leq 0.001$.

3.4.5.2 Evaluation of the effects of lithium on autophagy in OVCAR-5 and -8 cells

OVCAR-5 cells received treatment with 10mM lithium. Morphological analysis of OVCAR-5 cells revealed enhanced cytoplasmic accumulation of vesicles following 48 hour lithium treatment (right hand panels) compared to untreated cells (left hand panels) [Figure 3.9A]. Features of apoptosis (described in methods section 5.3.4 and indicated with green arrows) were evident 48 hours post lithium treatment. Cyto-ID analysis revealed enhanced vesicle accumulation following 48 hour lithium treatment (red overlay) (**p = 0.005) or CQ alone (turquoise overlay) [Figure 3.9B]. The combination of both further enhanced accumulation although it was not statistically significant (green overlay) [Figure 3.9 B]. Analysis of LC3II expression revealed a modest increase in expression following treatment with lithium at 48 hours, which was not enhanced by the addition of CQ [Fig 3.9C].

In the OVCAR-8 cell line, vesicle accumulation (indicated with black arrows) was enhanced following a 48 hour treatment with lithium [Figure 3.10A]. Features of apoptosis (indicated with green arrows) were present 48 hours post lithium treatment (top right hand panel) [Figure 3.10A]. Cyto-ID analysis revealed a slight accumulation of autophagic vesicles after lithium treatment (red overlay), which was further increased, although not significantly, by CQ (green overlay), suggesting moderate flux [Figure 3.10B]. Western blot analysis of LC3II expression showed no increase in LC3II levels following 48 hour lithium treatment, with no increase in expression following the addition of CQ [Figure 3.10C]. Taken together, this data implies lithium induces autophagosome accumulation and moderate turnover (flux), not dependent on LC3.

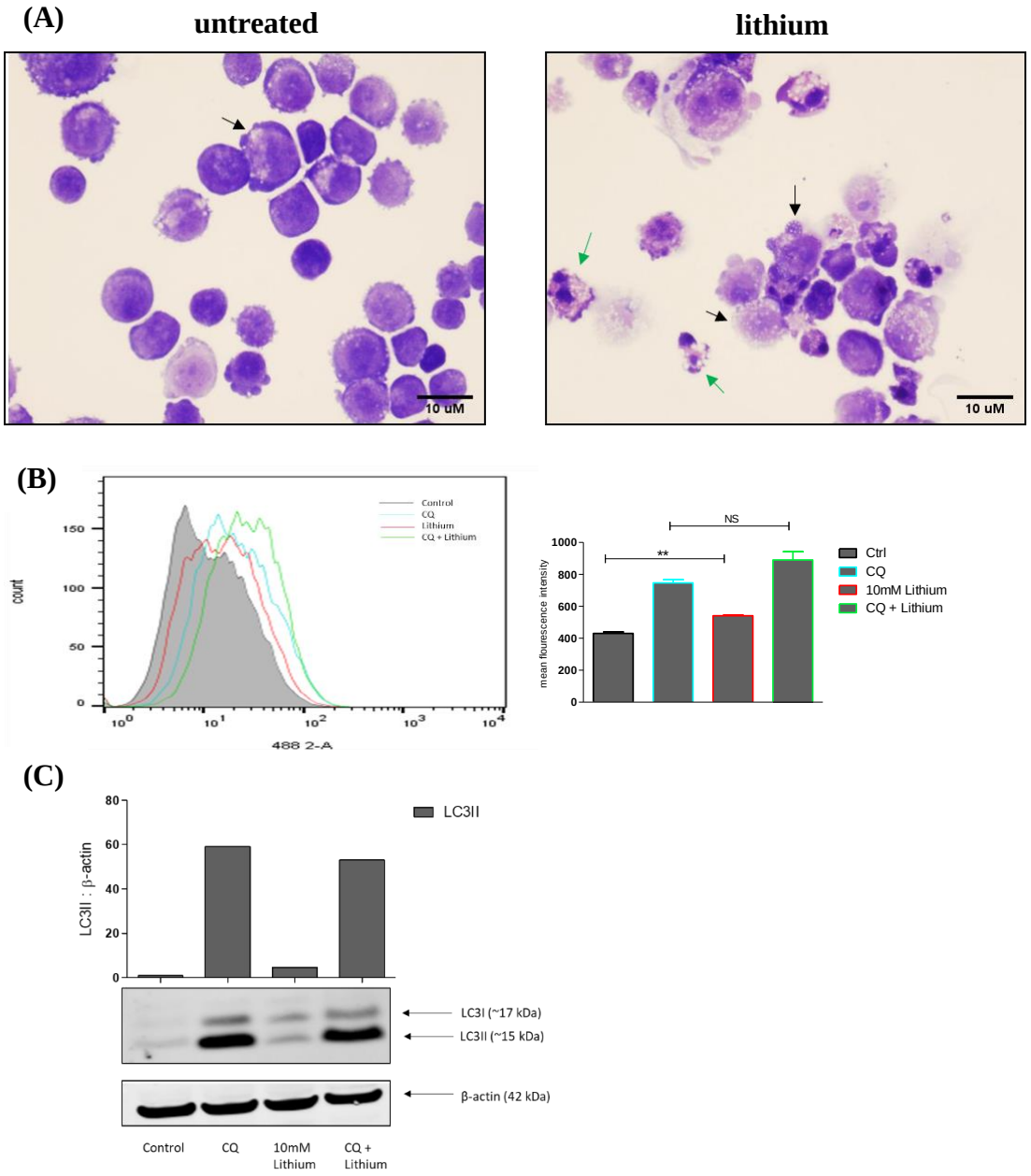

Figure 3.9. Evaluation of the effects of lithium in OVCAR-5 cells. Cells were treated with lithium chloride (lithium) (10mM) alone and in combination with CQ (10µM) for 48 hours. **(A)** Cells were stained using Pro-diff II to assess vesicle accumulation in untreated (left hand panels) and lithium treated cells (right hand panels) (magnification 400X). Vesicles are highlighted with black arrows. Cells displaying apoptotic features following lithium treatment are indicated with green arrows. **(B)** Cyto-ID analysis was used to assess vesicle accumulation following 48 hour treatment with lithium ± CQ. Mean fluorescent intensities are graphed ± SEM (n=3), beside the representative histogram overlays. **(C)** Western blot analysis of LC3I and LC3II following 48 hour treatment. Bands were quantified, normalised to β-actin and integrated intensities graphed (n=1). Values were statistically significant when **p $\leq$ 0.01, ***p $\leq$ 0.001.

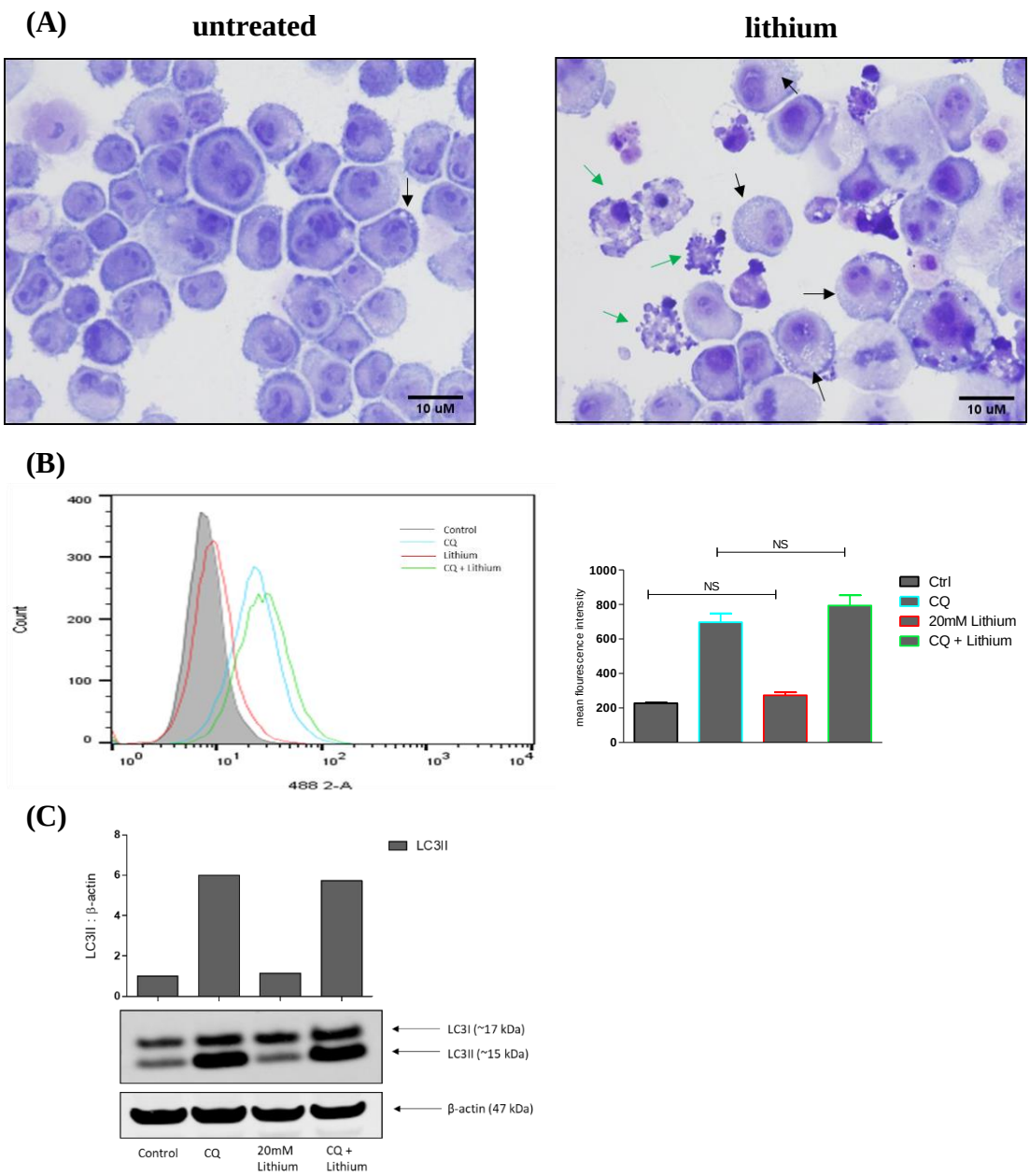

Figure 3.10. Evaluation of the effects of lithium in OVCAR-8 cells. Cells were treated with lithium (20mM) alone and in combination with CQ (10µM) for 48 hours. **(A)** Cells were stained using Pro-diff II to assess vesicle accumulation in untreated (left hand panels) and lithium treated cells (right hand panels) (magnification 400X). Vesicles are highlighted with black arrows. Cells displaying apoptotic features following lithium treatment are indicated with green arrows. **(B)** Cyto-ID analysis was used to assess vesicle accumulation following 48 hour treatment with lithium ± CQ. Mean fluorescent intensities are graphed ± SEM, to the right of representative histogram overlays (n=3). **(C)** Western blot analysis of LC3I and LC3II following 48 hour treatment. Bands were quantified using the Odyssey Infrared Imaging system (Li-Cor), normalised to β-actin and integrated intensities graphed (n=1).

3.4.6 Non-canonical autophagy may contribute to basal autophagy in OVCAR-5 and OVCAR-8 cells

The Atg5/Atg7 independent non-canonical autophagy pathway has recently been described, and has been shown to be induced following chemotherapy treatment (Arakawa *et al.,* 2017). We therefore wanted to assess whether this non-canonical pathway was present in our cells. Autophagosomes generated during Atg5/Atg7 independent non-canonical autophagy have been reported to originate from the Golgi apparatus and brefeldin A has been shown to inhibit this type of autophagy (illustrated in figure 3.1 of section 3.3) (Grose and Klionsky, 2016), (Nishida *et al.,* 2009). To assess the accumulation of autophagosomes originating from the Golgi, brefeldin A was used.

Basal accumulation of non-canonical derived autophagosomes was first assessed. Cells were treated with chloroquine for 48 hours ± brefeldin A (10µg/ml), with brefeldin A added for the final 24 hours of treatment. As evident in Figure 3.11A and B respectively, the addition of brefeldin A (red overlays) could significantly reduce basal autophagic vesicle levels in the OVCAR-5 (**p = 0.004) and OVCAR-8 (**p = 0.002) cell lines. Brefeldin A could also significantly reduce CQ-dependent autophagic vesicle accumulation in the OVCAR-5 (**p = 0.008) and OVCAR-8 (*p = 0.025) cell lines, providing further evidence that non-canonical autophagy is contributing to overall accumulation. Non-canonical derived autophagosomes were similarly assessed in OVCAR-3 and -4 cells. Brefeldin A reduced autophagosome accumulation alone and when added with CQ in OVCAR-3 and -4 cells, although this reduction was significant in the OVCAR-4 cells only [Supplementary figure 1]. These data suggest the presence of basal levels of non-canonical derived autophagosomes.

OVCAR-5

(A)

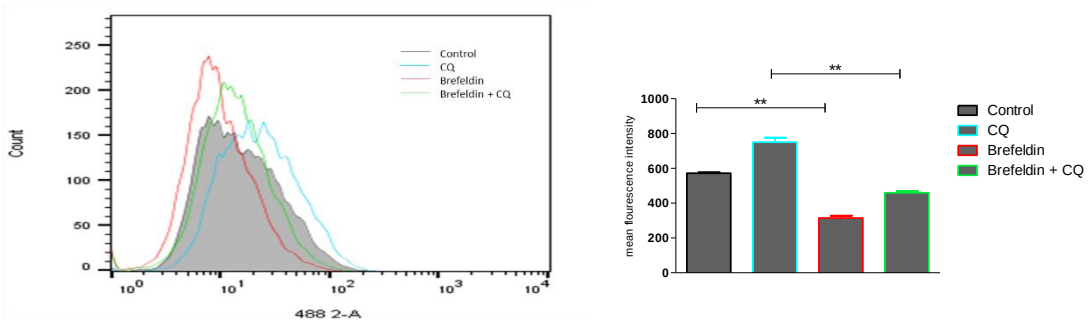

OVCAR-8

(B)

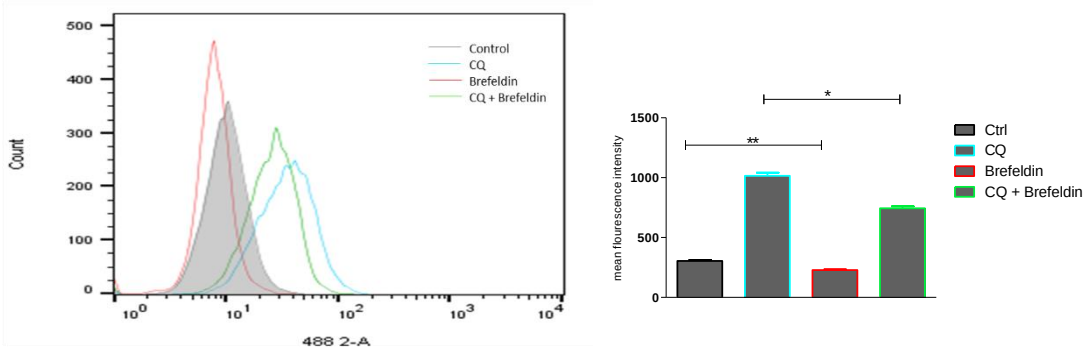

Figure 3.11. Assessment of the presence of basal non-canonical autophagy in OVCAR-5 and OVCAR-8 cells. The OVCAR-5 and -8 cells were treated for 48 hours with CQ (10µM), with brefeldin A (10µg/ml) added for the final 24 hours of treatment. Cyto-ID autophagy assay was used to assess autophagy levels in **(A)** OVCAR-5 and **(B)** OVCAR-8 cells. Representative histogram overlays are presented to the left, with mean fluorescent intensities graphed to the right (n=3). A paired t-test was used to assess significance, which was defined as *$p \leq 0.05$, **$p \leq 0.01$.

3.4.7 Non-canonical autophagy may contribute to the response to paclitaxel in OVCAR-5 and OVCAR-8 cells

We then assessed the effect of brefeldin A on paclitaxel dependent autophagosome accumulation. Following a 48 hour treatment with paclitaxel, OVCAR-5 and OVCAR-8 cells were placed in paclitaxel free media which contained brefeldin A (10µg/ml) for a further 24 hours. Autophagosome accumulation was assessed using the Cyto-ID autophagy assay. Treatment with brefeldin A significantly reduced paclitaxel induced vesicle accumulation in OVCAR-5 (**p = 0.003) and OVCAR-8 (**p =0.005) cell lines [Figure 3.12A and B respectively]. Similar effects of brefeldin A on non-canonical autophagosome accumulation following paclitaxel treatment were observed in OVCAR-3 and -4 cells [Supplementary figure 2]. These data indicate that both canonical and non-canonical autophagosomes are generated in response to paclitaxel.

(A) **OVCAR-5**

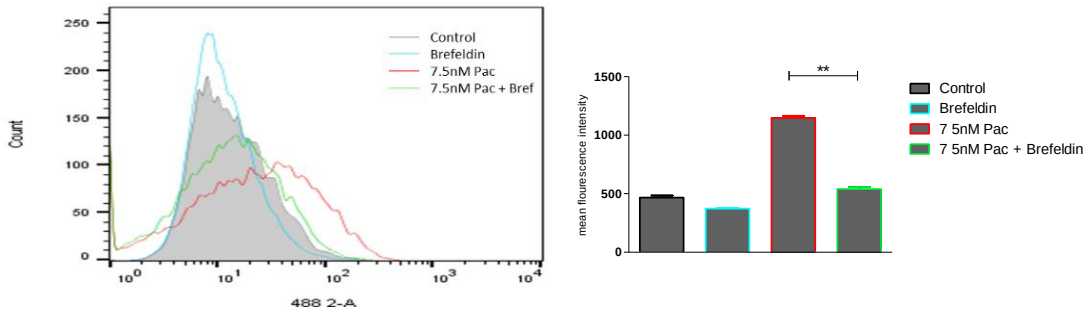

(B) **OVCAR-8**

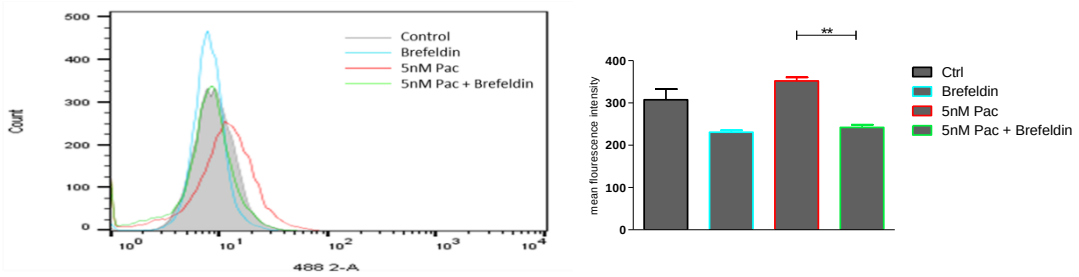

Figure 3.12. Evaluation of the presence of non-canonical autophagy following treatment with paclitaxel in OVCAR-5 and OVCAR-8 cells. The Cyto-ID autophagy detection kit was used to measure autophagosome accumulation after treatment with paclitaxel ± brefeldin A (10µg/ml). Representative histogram overlays are shown in the left-hand panels for **(A)** OVCAR-5 and **(B)** OVCAR-8 cells, with corresponding mean fluorescent intensities from triplicate samples graphed to the right (n=3). Asterisks indicate a significant difference between paclitaxel alone versus paclitaxel plus brefeldin A (*$p \leq 0.05$, **$p \leq 0.01$).

3.5 Discussion

Here we have evaluated the chemosensitising effects of autophagy modulators in our panel of OC cell lines. We have observed that CQ exerts a protective effect in two of our cell lines, OVCAR-3 and -4. The protective effect of CQ on the OVCAR-3 cell line observed in our study may be attributable to caspase inhibitory effects. CQ is widely used as an inhibitor of autophagic flux, however, autophagy-independent functions of CQ, such as apoptosis modulation, have been described. CQ has been reported to elicit both pro- and anti-apoptotic effects. It can enhance TRAIL mediated apoptosis via upregulation of death receptor 5 (DR5) (Park *et al.*, 2016). CQ can act as a DNA intercalator, and has been reported to induce apoptosis via p53 activation, potentially by causing structural DNA perturbations which upregulate p53 signalling (Tan *et al.*, 2012) (Kim *et al.*, 2010). In contrast, CQ was also found to impede apoptosis by reducing caspase-3 levels in OVCAR-3 cells (Lang *et al.*, 2015). The protective effect of CQ on the OVCAR-3 cell line observed in our study may therefore be attributable to such caspase inhibitory effects, and further work would be needed to confirm this.

The addition of CQ to paclitaxel and carboplatin had a chemosensitising effect in both the OVCAR-5 and -8 cell lines, which displayed higher levels of autophagy. It is possible that the enhanced cytotoxicity is related to a higher dependency on autophagy. In agreement with our study, pre- treatment with CQ was found to increase paclitaxel sensitivity in lung cancer cells via inhibition of autophagy (Datta *et al.*, 2019). Similarly, CQ could sensitise paclitaxel-resistant ovarian, lung and sarcoma cells to treatment via autophagy inhibition, and via inhibition of drug efflux transporters on the cell membrane (Gao, Xu and Qiu, 2015). Another study reported that cytoprotective autophagy was induced in OC cells via Akt/mTOR activation in

response to cisplatin. The addition of CQ led to an inhibition of autophagy and sensitised the cells to cisplatin (Zhu *et al.*, 2017). Studies have also shown that CQ mediated autophagy inhibition can enhance apoptosis. This was reported in osteosarcoma cells, whereby the addition of chloroquine could enhance apoptosis by inhibiting autophagy (Ishibashi *et al.*, 2019). Another study showed that apoptosis induced by cisplatin in gastric cancer cells could be enhanced via the addition of CQ, and this effect was due to the inhibition of autophagy (Jin *et al.*, 2014). In our cell lines which demonstrated enhanced chemosensitivity following the addition of CQ, drug induced apoptosis levels were low with paclitaxel and absent with carboplatin, as discussed in chapter two. It is possible that CQ is increasing apoptosis in these cells or another cell death mechanism, mediating the enhanced toxicity observed. It will be important going forward to test the effect of CQ on apoptosis in all of the cell lines.

CQ can also elicit its cytotoxic effects independently of caspase mediated apoptosis via lysosomal cell death (LCD). LCD is executed via lysosomal membrane permeabilisation (LMP). During LMP, lysosomal proteases, such as cathepsins, are released from the lysosome, where they can mediate both caspase-dependent and independent cell death mechanisms, including necrosis (Aits and Jäättelä, 2013). Thus in apoptosis deficient cells, CQ may sensitise cells to treatment via activating other cell death pathways, as was reported by Circu et al in non-small-cell lung cancer cells, which underwent cathepsin-mediated death (Circu *et al.*, 2018). Another study reported lysosomal mediated death following CQ treatment in metastatic breast cancer cells, which was dependent on glucose (Gallagher *et al.*, 2017). Alternative cell death induced by CQ may also be important for sensitising OC cells to chemotherapy, given that we have demonstrated diminished apoptosis in OC cells following re-challenge with paclitaxel in chapter two.

Multiple clinical trials are underway assessing the efficacy of CQ (and its derivative hydroxychloroquine) in combination with chemotherapies (Duffy *et al.*, 2015). The HYDRA-1 study is a phase I/II trial investigating the tolerability and efficacy of combining hydroxychloroquine with Itraconazole for platinum resistant epithelial OC patients (NCT03081702). Given that we have shown a protective effect of CQ in the OVCAR-3 and OVCAR-4 cells in response to chemotherapeutic drugs, our results suggest that caution is warranted when using CQ to treat OC patients in the clinic. Its use could be detrimental to some patients rather than beneficial. Further studies are needed to elucidate the effect of CQ on OC cells to enable its effective implementation into current treatment strategies.

Like CQ, we have shown that lithium can significantly sensitise three of our five cell lines OC cells to both paclitaxel and carboplatin (ID8-luc2, OVCAR-5 and -8). In contrast to our results, a study reported that lithium significantly increased resistance to cisplatin in OC cells (Cai *et al.*, 2007). Similarly, the addition of lithium to two high grade serous OC cell lines did not elicit a chemosensitising effect (Novetsky *et al.*, 2013). However, the study by Novetsky *et al*. (2013) used 1mM lithium, 10 times less than that used in our study suggesting dose dependent effects of lithium, which has been reported in other studies. In breast cancer MCF-7 cells, it was found that at low lithium concentrations (1-10mM), cells were protected from apoptosis via reductions in caspase-2 and -7 and increases in anti-apoptotic proteins such as BAX (Suganthi *et al.*, 2012). Similarly, another study using PC12 neural cells found that a higher concentration of lithium (9.6 mM) was found to decrease cell viability, while at a lower concentration (2.4mM) cell viability was not affected (Sahebgharani *et al.*, 2008). Comparable to our study, lithium was found to significantly inhibit the growth

of SKOV3 OC cells *in vitro* and *in vivo*, when SKOV3 cells were xenografted into mice (Cao, Lu and Feng, 2006).

Our study revealed that in the OVCAR-3 cells there was no benefit to adding lithium to both drugs. We have previously characterised this cell lines as having low autophagy levels. By comparison, significant chemosensitisation was evident following the addition of lithium to both drugs in the OVCAR-5 and OVCAR-8 cell lines, which displayed high levels of autophagy. This suggests that lithium's chemosensitising ability may be autophagy dependent. The role of lithium in modulating autophagy is conflicting, with studies reporting both inhibition and promotion of autophagy. Induction of autophagy via lithium has been reported to elicit a variety of neuroprotective functions primarily via the clearance of aggregate proteins. Lithium has been reported to induce autophagy by inhibiting inositol monophosphatase (IMPase), resulting in a decrease of free inositol and myo-inositol-1,4,5-triphosphate (IP_3). This inhibitory effect of IMPase by lithium increased the cellular clearance of mutant huntingtin fragments by induction of autophagy (Sarkar *et al.*, 2005). Lithium has also been shown to exert autophagy inhibitory effects (Li *et al.*, 2010). In our analysis, lithium treatment caused an increase in vesicles in the ID8-luc2, OVCAR-5 and -8 cells, as evident by the Cyto-ID autophagy assay, while observational analysis of morphology also revealed enhanced vesicle accumulation. However, in the OVCAR-5 and -8 cell lines, the addition of CQ to lithium-treated cells did not significantly enhance the accumulation of autophagosomes, suggesting compromised flux. We hypothesised that if lithium impedes autophagic flux, it may explain why our cells which previously exhibited the greatest autophagy flux were the most sensitive to lithium. In line with this, our group has previously suggested that compromised flux, due to lysosomal dysfunction, may contribute to lithium's

cytotoxic effects (O'Donovan *et al.*, 2015). In addition to compromised flux, lithium can also inhibit autophagy via inhibition of GSK-3β, leading to mTOR activation (Sarkar *et al.*, 2008).

Several studies also describe lithium's modulating effects on apoptosis, with both pro and anti-apoptotic effects reported. In colon cancer cells, the addition of lithium to cisplatin increased caspse-3 activity and reduced cell viability (Bao *et al.*, 2014). In contrast, lithium has also been reported to exert anti-apoptotic effects. Lithium was found to reverse propofol-induced caspase 3 activation, while a separate study reported diminished caspase 3 expression in a rat model of brain injury, which was attributed to upregulation of the anti-apoptotic protein XIAP (Straiko *et al.*, 2009) (Li *et al.*, 2010). In our study, morphological features of apoptosis were evident in OVCAR-5 and -8 cells following lithium treatment, which may be attributable to its cytotoxicity. Future work will aim to elucidate a mechanism of action for lithium. Apoptosis assays will be conducted, as well as western blotting and flow cytometry to assess the effect of lithium on lysosome function. Future work will also evaluate the chemosensitising ability of lithium in xenograft models and *in vivo* models. Given that we have shown significant chemosensitising effects of lithium, a drug known to be safe and well tolerated, it provides a plausible additional therapeutic option for OC patients.

We have demonstrated that brefeldin A significantly reduces basal and paclitaxel-induced autophagosome accumulation, suggesting that a non-canonical brefeldin A-sensitive autophagy may be present in OC cells. To our knowledge this has not previously been reported. During our study, we also performed clonogenic assays with the addition of brefeldin A to assess any chemosensitising effects in our cells. However, due to high toxicity of brefeldin A alone, any sensitising effects when

combined with chemotherapeutics could not be determined. Future studies will be repeated with lower doses, or reduced treatment times. Other studies however have reported the benefit of pharmacological modulation with brefeldin A to sensitise OC cancer cells. Brefeldin A has been reported to inhibit migration and invasion and to induce intrinsic apoptosis and caspase-8 activation in OVCAR-3 cells (Lee, Kim and Lee, 2013). In line with its potential as an anti-cancer agent, efforts are being made to develop brefeldin A analogues with enhanced pharmacological properties and anti-proliferative activity (Paek, 2018).

The results from this study may have important clinical ramifications. While these data highlight autophagy modulation as an attractive therapeutic target to overcome chemoresistance for some patients, it may not provide any benefit to others. Cell line dependent effects of CQ and lithium were observed, with chemosensitising effects evident only in the cell lines which displayed low apoptosis and high autophagy levels. This highlights the patient specific approach which must therefore be undertaken when pharmacologically modulating autophagy and the need for biomarkers to predict response.

3.6 References

Aits, S. and Jäättelä, M. (2013) 'Lysosomal cell death at a glance', Journal of Cell Science, 126(9), p. 1905-1912.

Bao, H. et al. (2014) 'Delayed administration of a single dose of lithium promotes recovery from AKI.', Journal of the American Society of Nephrology: JASN, 25(3), pp. 488–500.

Cai, G. et al. (2007) 'Phosphorylation of glycogen synthase kinase-3 beta at serine 9 confers cisplatin resistance in ovarian cancer cells.', International Journal of Oncology, 31(3), pp. 657–662.

Cao, Q., Lu, X. and Feng, Y.-J. (2006) 'Glycogen synthase kinase-3β positively regulates the proliferation of human ovarian cancer cells', Cell Research, 16(7), pp. 671–677.

Circu, M. et al. (2018) 'Modulating lysosomal function through lysosome membrane permeabilization or autophagy suppression restores sensitivity to cisplatin in refractory non-small-cell lung cancer cells, PLoS ONE, 12(9), pp.e0184922.

Cohen, Y. et al. (1998) 'Cancer morbidity in psychiatric patients: influence of lithium carbonate treatment.', Medical Oncology, 15(1), pp. 32–36.

Datta, S. et al. (2019) 'Autophagy inhibition with chloroquine reverts paclitaxel resistance and attenuates metastatic potential in human nonsmall lung adenocarcinoma A549 cells via ROS mediated modulation of beta-catenin pathway.', Apoptosis: An International Journal on Programmed Cell Death, 24(5–6), pp. 414–433.

Duffy, A. et al. (2015) 'Autophagy modulation: a target for cancer treatment development.', Cancer Chemotherapy and Pharmacology, 75(3), pp. 439–447.

Gallagher, L. E. et al. (2017) 'Lysosomotropism depends on glucose: a chloroquine resistance mechanism', Cell Death & Disease, 8(8), pp. e3014–e3014.

Gao, M., Xu, Y. and Qiu, L. (2015) 'Enhanced combination therapy effect on paclitaxel-resistant carcinoma by chloroquine co-delivery via liposomes.', International Journal of Nanomedicine, 10, pp. 6615–6632.

Ge, W. and Jakobsson, E. (2019) 'Systems Biology Understanding of the Effects of Lithium on Cancer', Frontiers in Oncology, 9(296), p. 296.

Huang, R.-Y. et al. (2016) 'Use of lithium and cancer risk in patients with bipolar disorder: population-based cohort study.', The British journal of psychiatry: The Journal of Mental Science, 209(5), pp. 393–399.

Ishibashi, Y. et al. (2019) ‘Chloroquine Enhances Rapamycin-induced Apoptosis in MG63 Cells.’, Anticancer Research, 39(2), pp. 649–654.

Jin, Z. X. et al. (2014) ‘The Effect of Chloroquine on the Apoptosis Induced by Cisplatin in Human Gastric Cancer BGC823 Cells’, Advanced Materials Research, 926–930, pp. 1124–1127.

Kim, E. L. et al. (2010) ‘Chloroquine activates the p53 pathway and induces apoptosis in human glioma cells’, Neuro-Oncology, 12(4), pp. 389–400.

Lang, F. et al. (2015) ‘Apoptotic Cell Death Induced by Resveratrol Is Partially Mediated by the Autophagy Pathway in Human Ovarian Cancer Cells’, PloS One, 10(6), pp. e0129196–e0129196.

Lee, S. A., Kim, Y. J. and Lee, C. S. (2013) ‘Brefeldin a induces apoptosis by activating the mitochondrial and death receptor pathways and inhibits focal adhesion kinase-mediated cell invasion.’, Basic & Clinical Pharmacology & Toxicology, 113(5), pp. 329–338.

Li, H. et al. (2014) ‘Lithium chloride suppresses colorectal cancer cell survival and proliferation through ROS/GSK-3β/NF-κB signaling pathway’, Oxidative Medicine and Cellular Longevity, 2014, p. 241864.

Li, Q. et al. (2010) ‘Lithium reduces apoptosis and autophagy after neonatal hypoxia-ischemia.’, Cell death & disease, 1(7), p. e56.

Martinsson, L. et al. (2016) ‘Lithium treatment and cancer incidence in bipolar disorder.’, Bipolar Disorders, 18(1), pp. 33–40.

Mauthe, M. et al. (2018) ‘Chloroquine inhibits autophagic flux by decreasing autophagosome-lysosome fusion’, Autophagy, 14(8), pp. 1435–1455.

Novetsky, A. P. et al. (2013) ‘Lithium Chloride and Inhibition of Glycogen Synthase Kinase 3β as a Potential Therapy for Serous Ovarian Cancer’, International Journal of Gynaecologic Cancer, 23(2), p. 361-366.

O’Donovan, T. R. et al. (2015) ‘Lithium Modulates Autophagy in Esophageal and Colorectal Cancer Cells and Enhances the Efficacy of Therapeutic Agents In Vitro and In Vivo.’, PloS One, 10(8), p. e0134676.

Paek, S.-M. (2018) ‘Recent Synthesis and Discovery of Brefeldin A Analogs.’, Marine Drugs, 16(4), p.133.

Park, E. J. et al. (2016) ‘Chloroquine enhances TRAIL-mediated apoptosis through up-regulation of DR5 by stabilization of mRNA and protein in cancer cells.’, Scientific Reports, 6, p. 22921.

Pokhriyal, R. et al. (2019) ‘Chemotherapy Resistance in Advanced Ovarian Cancer Patients’, Biomarkers in Cancer’, 11, p. 1179-1198.

Pottegard, A. et al. (2016) ‘Long-term use of lithium and risk of colorectal adenocarcinoma: a nationwide case-control study.’, British Journal of Cancer, 114(5), pp. 571–575.

Sahebgharani, M. et al. (2008) ‘Lithium chloride protects PC12 pheochromocytoma cell line from morphine-induced apoptosis.’, Archives of Iranian Medicine, 11(6), pp. 639–648.

Sarkar, S. et al. (2005) ‘Lithium induces autophagy by inhibiting inositol monophosphatase’, The Journal of Cell Biology, 170(7), pp. 1101–1111.

Sarkar, S. et al. (2008) ‘A rational mechanism for combination treatment of Huntington’s disease using lithium and rapamycin.’, Human Molecular Genetics, 17(2), pp. 170–178.

Straiko, M. M. W. et al. (2009) ‘Lithium protects against anaesthesia-induced developmental neuroapoptosis.’, Anaesthesiology, 110(4), pp. 862–868.

Suganthi, M. et al. (2012) ‘Biphasic Dose-Dependent Effect of Lithium Chloride on Survival of Human Hormone-Dependent Breast Cancer Cells (MCF-7)’, Biological Trace Element Research, 150(1), pp. 477–486.

Tan, H. K. et al. (2012) ‘Interference of intrinsic curvature of DNA by DNA-intercalating agents.’, Organic & Biomolecular Chemistry, 10(11), pp. 2227–2230.

Zhan, L. et al. (2016) ‘Autophagy as an emerging therapy target for ovarian carcinoma’, Oncotarget, 7(50), pp. 83476–83487.

Zhu, J. et al. (2017) ‘Low concentration of chloroquine enhanced efficacy of cisplatin in the treatment of human ovarian cancer dependent on autophagy’, American Journal of Translational Research, 9(9), pp. 4046–4058.

3.7 Supplementary figures

(A) **OVCAR-3**

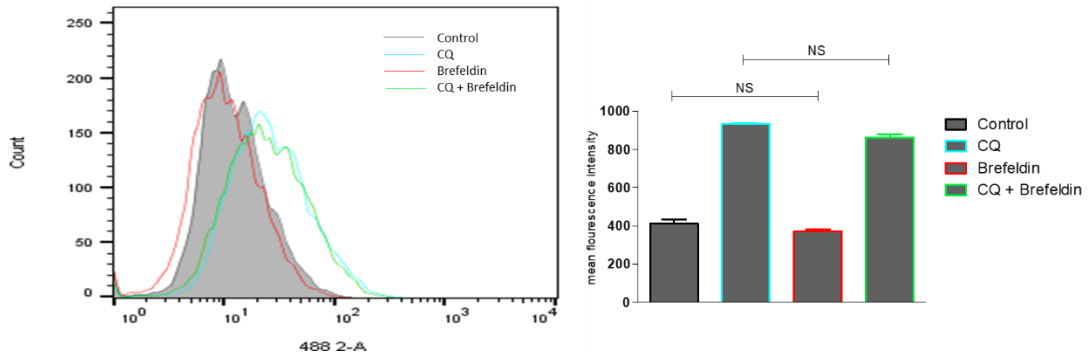

(B) **OVCAR-4**

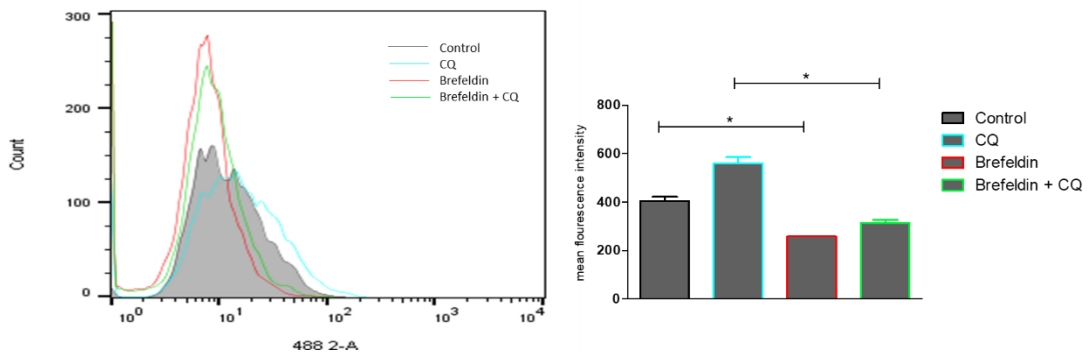

Supplementary figure 1: Assessment of the presence of basal non-canonical autophagy in OVCAR-3 and OVCAR-4 cells. Cyto-ID autophagy assay was used to assess autophagy levels in **(A)** OVCAR-3 and **(B)** OVCAR-4 cells, following treatment with CQ (10μM) (turquoise overlays) for 48 hours, with brefeldin A (10μg/ml) (red overlays) added for the final 24 hours of treatment. Representative histogram overlays are presented to the left, with mean fluorescent intensities graphed to the right (n=3). The addition of brefeldin A to CQ (green overlay) significantly reduces autophagosome accumulation in OVCAR-4 cells. A paired t-test was used to assess significance, which was defined as *$p \leq 0.05$.

(A) **OVCAR-3**

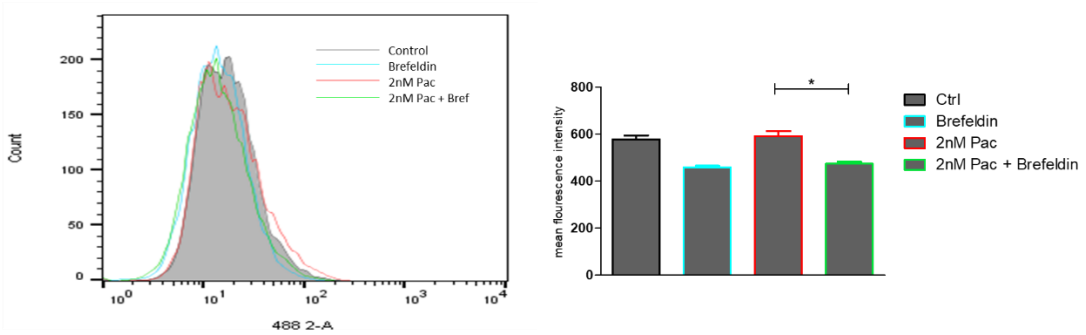

(B) **OVCAR-4**

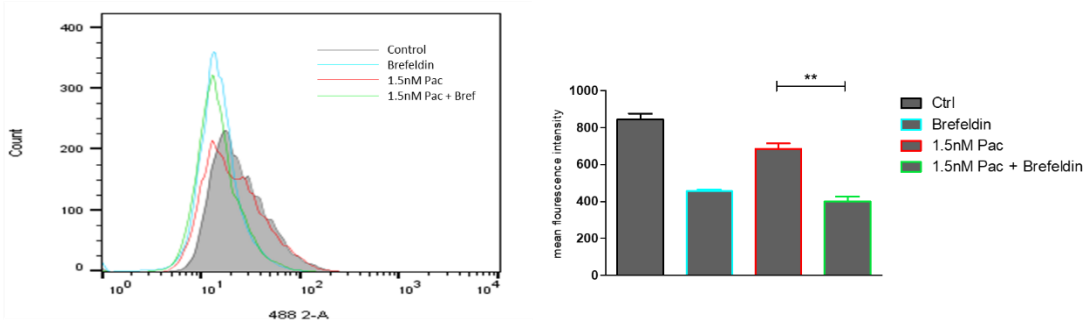

Supplementary figure 2: Evaluation of the presence of non-canonical autophagy following treatment with paclitaxel +/- brefeldin A in OVCAR-3 and OVCAR-4 cells. Brefeldin A significantly reduces autophagosome accumulation following treatment with paclitaxel in OVCAR-3 and OVCAR-4 cells. The Cyto-ID autophagy detection kit was used to measure autophagosome accumulation after treatment with paclitaxel (red overlays) ± brefeldin A (10µg/ml) (turquoise overlays) in **(A)** OVCAR-3 and **(B)** OVCAR-4 cells. Brefeldin A addition to paclitaxel (green overlays) significantly reduces autophagosome accumulation in both cell lines. Representative histogram overlays are shown in the left-hand panels with corresponding mean fluorescent intensities are graphed to the right (n=3). Asterisks indicate a significant difference between paclitaxel alone versus paclitaxel plus brefeldin A (*p≤0.05, **p≤0.01).

Chapter Four: Inhibition of autophagy reduces recovery and enhances chemo-sensitivity in ovarian cancer cells following treatment with paclitaxel

4.1 Abstract

Advances in targeted therapies have decreased the reliance on toxic chemotherapies in a number of cancers, such as breast and prostate cancer. The backbone of OC treatment, however, remains cytoreductive surgery and a platinum/taxane chemotherapy doublet. Resistance to chemotherapy is a significant clinical hurdle which has yet to be overcome when treating OC. To improve patient outcomes, it is vital to elucidate the molecular determinants which underpin chemoresistance. In chapters two and three, we observed high levels of autophagy in the ID8-luc2, OVCAR-5 and -8 cells, and recovery of these cells was significantly reduced by the autophagy inhibitor chloroquine. To further establish a role for autophagy in chemoresistance, siRNA knockdown of two key autophagy genes, BECN1 and ATG5, was performed in these cell lines. Knockdown of these genes could significantly reduce ID8-luc2 and OVCAR-8 cell recovery following paclitaxel treatment, and reduce OVCAR-5 cell recovery, despite optimal knockdown not being achieved. These data highlight a role for autophagy in recovery following treatment. The reduction of autophagosomes in chapter three following brefeldin A treatment suggested the presence of an additional brefeldin A-sensitive autophagy pathway, which may be the non-canonical Atg5/7-independent autophagy pathway. To further assess the contribution of this non-canonical pathway in response to treatment, siRNA knockdown of a gene involved in non-canonical autophagy, Rab9, was performed along with BECN1. Knockdown of Rab9 significantly impeded the recovery of OVCAR-8 cells following treatment with paclitaxel. Although not statistically significant, reduction in Rab9 expression could also reduce clonogenic recovery of OVCAR-5 cells following paclitaxel treatment. To our knowledge, this is the first study to demonstrate a potential role for non-canonical autophagy pathway in the

resistance of OC cells to paclitaxel. This data provides a rationale for inhibiting autophagy to combat chemoresistance in OC.

4.2 Introduction

Over 70% of women diagnosed with OC present with late stage disease which is difficult to treat. The backbone of OC treatment involves surgical debulking and intravenous administration of a carboplatin/paclitaxel doublet for 6 cycles, which was developed based on the results of the GOG 158 study (Ozols *et al.*, 2003). Although most patients will achieve an excellent clinical response following first line treatment, disease relapse is a common occurrence. This is the most significant clinical challenge yet to be met in the treatment of OC. In those patients with advanced disease, relapse can occur within just 2 years of receiving initial treatment. Resistance to chemotherapies occurs generally via two mechanisms: (A) intrinsic chemo-resistance- whereby the cancer cells are inherently resistant or (B) acquired resistance- where the cancer cells utilise biological functions such as increased drug efflux, inhibition of apoptosis or autophagy (Pokhriyal *et al.*, 2019). The excellent efficacy of first line treatment observed in patients, and the subsequent high rates of disease recurrence, warrants a better understanding of the mechanisms behind acquired resistance in order to tackle the high rates of recurrence.

In chapter three, CQ could significantly sensitise ID8-luc2, OVCAR-5 and -8 cells to paclitaxel, suggesting a role for autophagy paclitaxel resistance. However, CQ is not specific to the autophagy pathway, and can mediate other processes important in drug response, including apoptosis. Therefore, to confirm a role for autophagy in response to treatment, siRNA knockdown of key autophagy genes, BECN1 and ATG5 was

performed. Beclin 1 is a Bcl-2-homology (BH)-3 domain only protein which plays an important role in localising autophagic proteins to a pre-autophagosomal structure (PAS). It is mainly localised within the cytoplasm in places such as the endoplasmic reticulum (ER), mitochondria and perinuclear membrane (Kang *et al.*, 2011). Beclin 1 can mediate every major step in autophagic pathways, from autophagosome formation to autophagosome maturation. Atg5 plays a key role in autophagosome formation. The conjugation of ATG5-ATG12-ATG16L1 allows phagophore membrane elongation and facilitates autophagosome-lysosome fusion by binding to TECPR1 (Zheng *et al.*, 2019) (Ye, Zhou and Zhang, 2018).

The Atg5/Atg7-independent autophagy pathway is a recently described alternative autophagy pathway, which can occur in the absence of Atg5 and Atg7 but requires Beclin 1. Autophagosomes formed during this pathway derive from the Golgi, as opposed to the ER during canonical autophagy, and LC3 is not required. Rab9 is required to facilitate membrane extension and closure by fusing isolation membranes with vesicles from the trans-Golgi and late endosomes. Physiological roles for Atg5/Atg7-independent autophagy include mitochondrial clearance in stem cells and clearance of erythrocytes (reviewed by (Shimizu, 2018). While the non-canonical Atg5/Atg7-independent autophagy pathway has been reported to be induced following treatment with etoposide, there is no known role for Atg5/Atg7-independent autophagy in chemoresistance (Arakawa *et al.*, 2017). In chapter three, we have shown that brefeldin A can significantly reduce paclitaxel induced autophagosome accumulation. To assess a potential role for non-canonical autophagy in response to treatment, Rab9 was knocked down along with BECN1 and recovery was assessed.

4.3 Materials and Methods

4.3.1 Cell culture and Reagents

Established human ovarian cancer cell lines OVCAR-5 and OVCAR-8 were obtained directly from the NCI Frederick Cancer DCTC Tumor/Cell Line Repository. Murine ID8-luc2 cells were obtained from Mayo Clinic. All human OVCAR cell lines were maintained in RPMI 1640 media. OVCAR-5 and OVCAR-8 cultures were supplemented with 10% (v/v) foetal calf serum. Murine ID8-luc2 cells were cultured using Dulbecco's Modified Eagles Medium containing 10% (v/v) foetal calf serum. All cultures were supplemented with 1% penicillin/streptomycin (Gibco Life Technologies 15070-063). Cells were grown in T75cm^2 flasks (Sarstedt) and maintained at 37°C, 5% CO_2.

4.3.2 siRNA transfection

Cells were reverse transfected for 24 hours, prior to any drug treatment, with gene specific siRNAs and non-specific scramble controls using Lipofectamine 2000 transfection reagent (Life technologies, Cat # 11668500) according to instructions from the manufacturer. Depending on the cell line, knockdown efficiency was validated at either 48 or 72 hours, to coincide with drug treatment duration. On-Target plus smartpool siRNA were purchased from Dharmacon for both mouse (Beclin-1: Cat # L-055895-00-0005, ATG5: Cat # L-064838-00-0005, Rab9: Cat # L-040861-01-0005) and human cell lines (Beclin-1: Cat # L-010552-00-0005, ATG5: Cat # L-004374-00-0005, Rab9A: Cat # L-004177-00-0005) . A Non-specific target control was also purchased from Dharmacon (Non-targeting siRNA #1: Cat # D-001810-01-20).

4.3.3 Drug treatments

Paclitaxel (Cat # T7402) and carboplatin (Cat # C2538) were purchased from Sigma Aldrich. Paclitaxel was reconstituted in DMSO to give 58.55mM stock. Aliquots were prepared and stored at -20°C. Working concentrations of paclitaxel were prepared fresh in media on the day of treatment. Carboplatin was reconstituted in water to give a 26.93mM stock, aliquoted and stored in the dark at room temperature. Working concentrations were prepared in media on the day of treatment. ID8-luc2 cells received a 24 hour treatment with both paclitaxel and carboplatin, while the human OVCAR cell lines received a 48 hour treatment. Chemotherapeutic drugs were added 24 hours post transfection to all cell lines.

4.3.4 Colony formation assay

Colony formation (clonogenic) assays were used to determine the ability of single cells to recover from a drug treatment and re-establish colonies. Following specified treatments, cells were trypsinised using 500µl of Trypsin EDTA (Sigma Aldrich, Cat # T4049) and viable cells counted using the NucleoCounter NC-100 (Chemometec). For the OVCAR-5, OVCAR-8 and ID8-luc2 cell lines 1,500 viable cells were re-seeded into a well of a six-well plate (Nunc™ Thermo Scientific, Cat # 140685). For the OVCAR-3 and OVCAR-4 cell lines, 2,500 cells were re-seeded in the same manner. Cells were allowed to adhere and grow for between 10 and 14 days, until control cells reached at least 70% confluency. Following the recovery period, media was aspirated, and wells were washed once with PBS. Cells were then fixed in 96% ethanol for 5 minutes and stained with Pro-diff solution C (Braidwood Laboratories E310) for 5 minutes. Plates were rinsed with water to remove excess stain and air-dried

overnight. Plates were scanned and quantified using the Odyssey IR imaging system (Li-Cor, Cambridge, United Kingdom).

4.3.5 Western Blotting

Total cellular protein was extracted by trypsinisation of cells followed by lysing in 10-25µl of modified RIPA buffer (50 mM Tris HCl (pH 7.4), 150 mM NaCl, 0.25% sodium deoxycholate, 1% Igepal, 1 mM EDTA, 1x Pefabloc, 1x protease inhibitor cocktail, 1 mM Na_3VO_4, 1 mM NaF), depending on pellet size. Samples (75 µg) were separated on NuPAGE 4–12% Bis-Tris gels (Invitrogen Life Technologies, Cat # NP0322) and electrophoretically transferred onto a PVDF membrane using the iBlot gel transfer system (Invitrogen IB1001). Membranes were blocked with Odyssey blocking buffer (Li-Cor, Cat # 927-40100) for 1 hour at room temperature. Membranes were then incubated overnight at 4°C using: anti- ATG5 (Novus, Cat # NB110-53818), anti-Beclin 1 (Novus, Cat # NB500-249) and anti-Rab9 (Abgent, Cat # ab2810) antibodies overnight at 4°C. Anti-β-actin (loading control) (Sigma, Cat # A5441) was incubated at room temperature, rocking, for one hour. IR-Dye conjugated secondary antibodies (Rockland) were utilised for protein detection on the Odyssey Infra-red imaging system (Li-Cor, Cambridge, United Kingdom).

4.3.6 Statistical Analysis

All data is expressed as mean ± the standard error of the mean (SEM), which represents the standard deviation of the distribution of the sample around the mean. Significance was determined by independent or paired student t-tests, which determines the difference between the means of two groups. The p-value was considered statistically

significant where *$p \leq 0.05$, ** $p \leq 0.01$, *** $p \leq 0.001$. Statistical analysis was carried out and graphed using GraphPad Prism 5 software (GraphPad Software Inc., CA, USA).

4.4 Results

4.4.1 Inhibition of autophagy demonstrates its role in chemoresistance in ID8-luc2 cells

In chapter two, autophagic flux, in response to paclitaxel and carboplatin was observed in the ID8-luc2 cell line. Clonogenic assays revealed recovery and colony regrowth of up to 50% in ID8-luc2 cells after paclitaxel and carboplatin treatment. To assess the involvement of autophagy in this recovery, key autophagy regulators BECN1 and ATG5 were knocked down and recovery was assessed.

ID8-luc2 cells were transfected with 30nM of BECN1 and ATG5 siRNA either alone or in combination. Protein expression following knockdown of BECN1 alone was reduced to 58% (lane 2) and when combined with Atg5 was reduced to 33% (lane 4) compared to a scrambled control (lane 1) [Figure 4.1A]. Transfection of ID8-luc2 cells with an siRNA targeted to ATG5 reduced protein expression to 66% (lane 2), with a minimal reduction in Atg5/12 expression evident when combined with a BECN1 siRNA (lane 3) [Figure 4.1B].

Following reverse transfection with the targeted siRNAs for 24 hours, ID8-luc2 cells were treated with 2.5μM paclitaxel for 24 hours, re-seeded and clonogenic recovery assessed. Transfection with each siRNA alone resulted in small reductions in clonogenic recovery, which were not significant. However, a significant reduction in recovery was found following double knockdowns of BECN1 & ATG5 (*$p = 0.027$) [Figure 4.1C]. Although optimal knockdowns were not achieved, recovery was still significantly reduced, suggesting that autophagy does play a role in recovery following drug treatment.

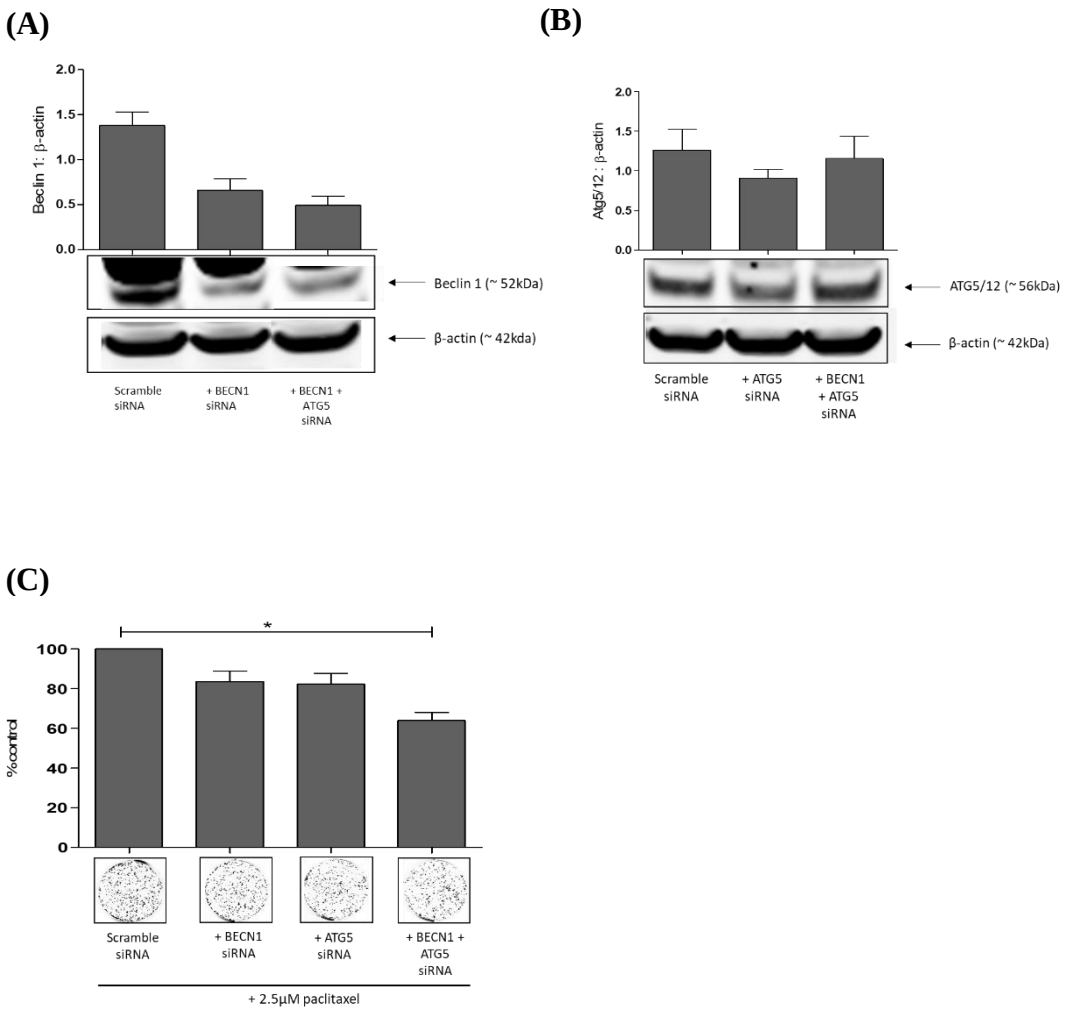

Figure 4.1. Knockdown of BECN1 in combination with ATG5 significantly reduces ID8-luc2 recovery following paclitaxel treatment. ID8-luc2 cells were transfected for 24 hours with 30nM siRNA. 24 hours post transfection, media was removed, and cells were treated with 2.5μM paclitaxel for a further 24 hours, before cells were reseeded for clonogenic recovery (48 hours post transfection). Western blot was used to assess **(A)** Beclin 1 and **(B)** Atg5/12 expression (48 hours post transfection). All blots were scanned, quantified and values normalised to β-actin. Integrated intensities are graphed ±SEM (n=2). **(C)** Following knockdown with specific siRNAs and 24 hour treatment with 2.5μM paclitaxel, ID8-luc2 cells were re-seeded and recovery assessed. All colonies were fixed, stained and scanned using the Li-Cor Odyssey Infrared scanner. Integrated intensities are graphed as % control (where control = 100%) (n=2). Statistical significance is defined as *$p \leq 0.05$.

4.4.2 Knockdown of key autophagy genes BECN1 and ATG5 sensitises OVCAR-5 and OVCAR-8 cells to paclitaxel

We have demonstrated that autophagic flux is induced following paclitaxel treatment in OVCAR-5 and OVCAR-8 cells, and that these cells exhibited up to 50% colony regrowth. We have also shown the ability of CQ to significantly sensitise these cells to treatment, indicating a role for autophagy in recovery. To confirm this, two key autophagy regulators, BECN1 and ATG5, were transiently knocked down using siRNA. Cells were then treated for 48 hours with paclitaxel and recovery was assessed.

The OVCAR-5 cell line was transfected with 20 nM of specific siRNA targeted to BECN1 and ATG5, either alone or combined as a double knockdown. Western blot analysis showed a reduction in Beclin 1 expression to 25% (lane 2) and to 37% (lane 3) following single and double knockdown respectively, 72 hours post knockdown [Figure 4.2A]. ATG5 protein expression was reduced to 40% (lane 2), and to 60% (lane 3) following single and double knockdown respectively [Figure 4.2B].

Knockdown of ATG5 alone and in combination with BECN1 reduced recovery of OVCAR-5 cells following paclitaxel treatment, although it was not statistically significant [Figure 4.2C]. It is possible that a greater knockdown is required to impede autophagy.

The OVCAR-8 cell line was transfected with 30nM of siRNA targeted to BECN1 and ATG5, either alone or in combination. Western blot analysis revealed a reduction in Beclin 1 expression to just 10% (lane 2), and 25% (lane 3) in the single and double knockdown cells respectively, 72 hours post transfection [Figure 4.3A]. Atg5 protein expression levels were reduced to just 14% in the single knockdown (lane 2) and 36% in the double knockdown cells (lane 3) [Figure 4.3B].

Single or double knockdown of BECN1 and ATG5 resulted in a significant inhibition of OVCAR-8 cell recovery following treatment with paclitaxel (*p = 0.008, *p = 0.08, *p = 0.031, respectively) [Figure 4.3C]. Taken together, these data highlight a role for autophagy in the recovery of OVCAR-5 and OVCAR-8 cell lines following paclitaxel treatment. It is likely that sufficient knockdown is required in order to achieve an impediment in autophagy. Where this is achieved in the OVCAR-8 cells, the importance of autophagy for recovery following drug treatment is evident.

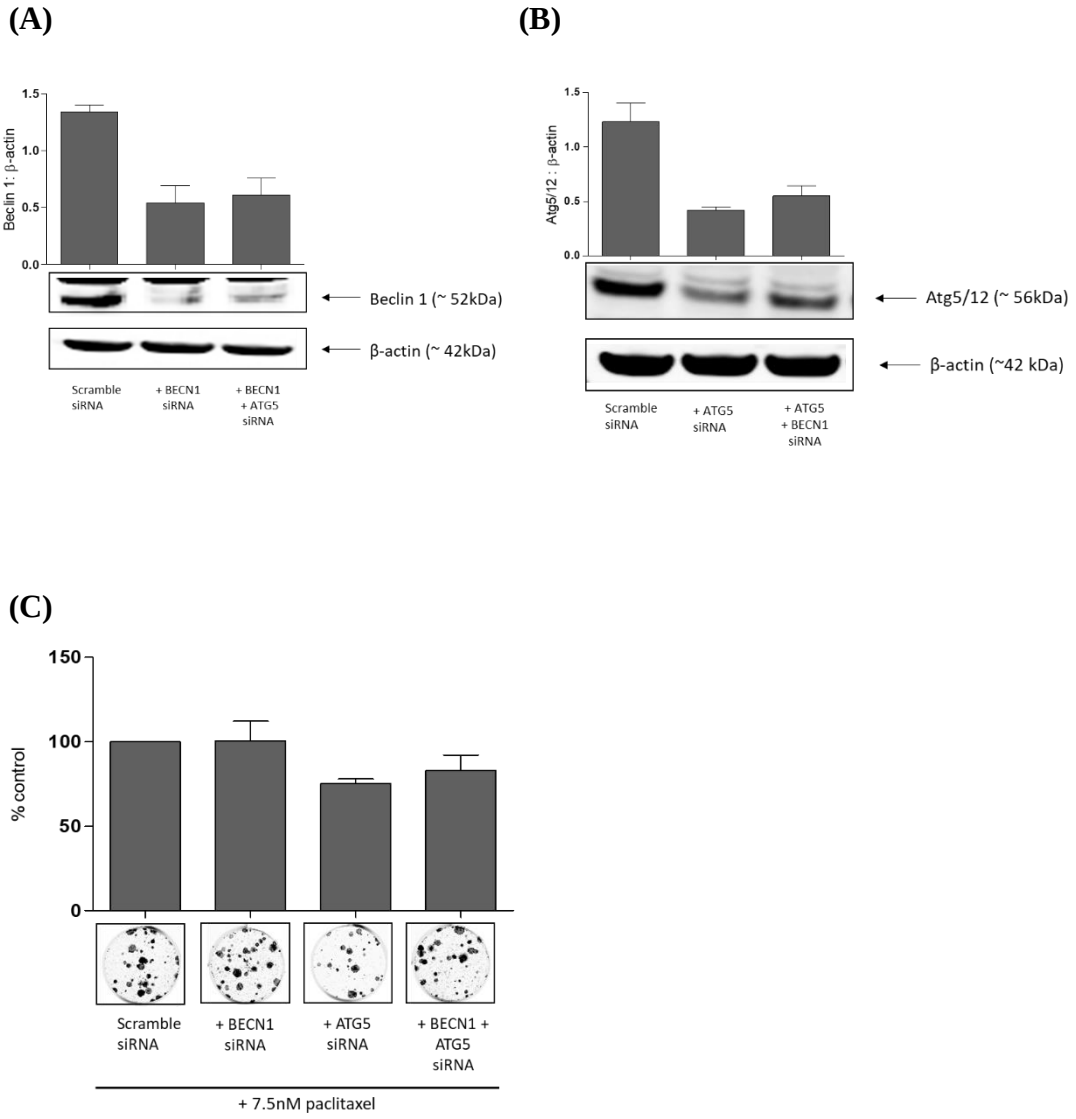

Figure 4.2. ATG5 knockdown alone and combined with BECN1 reduces recovery of OVCAR-5 cells following paclitaxel treatment (A) Reduction in expression of Beclin 1 and **(B)** Atg5/12 was shown using western blotting 72 hours post transfection (n=2) **(C)** 24 hours after siRNA transfection, cells were treated with 5nM paclitaxel for a further 48 hours and cells were reseeded for colony regrowth (72 hours post transfection). Colonies were fixed, stained and scanned using the Li-Cor Odyssey Infrared scanner. Integrated intensities are graphed as % control (where control = 100%) (n=2).

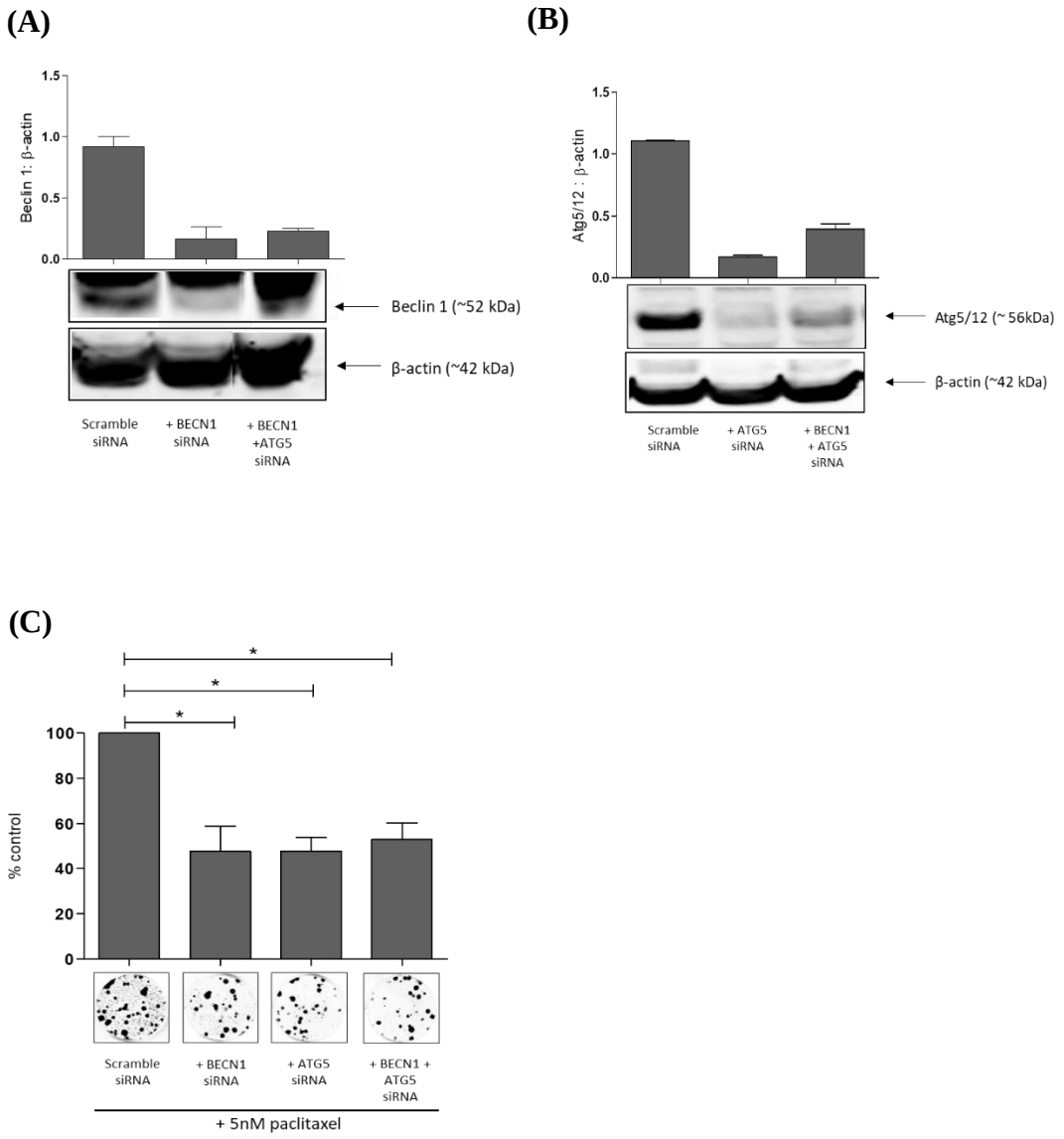

Figure 4.3. BECN1 and ATG5 knockdown significantly reduces OVCAR-8 cell recovery following paclitaxel treatment (A) Reduction in the expression of Beclin 1 and **(B)** Atg5/12 was demonstrated using western blotting (n=2). **(C)** 24 hours after siRNA transfection, cells were treated with 5nM paclitaxel for 48 hours and reseeded for clonogenic recovery (72 hours post transfection). Colonies were fixed, stained and scanned using the Li-Cor Odyssey Infrared scanner. Integrated intensities are graphed as % control (where control = 100%) (n=2). Statistical significance is defined as *p $\leq$ 0.05 **p $\leq$ 0.01.

4.4.3 Knockdown of Rab9 and BECN1 sensitises OVCAR-5 and OVCAR-8 cells to paclitaxel

In chapter three, the addition of brefeldin A could significantly reduce basal and drug induced autophagosomes, suggesting the presence of a non-canonical brefeldin A-sensitive autophagy pathway, which may be Atg5/Atg7-independent autophagy. To further assess a role for this pathway in recovery from paclitaxel, Rab9 was knocked down alone and in combination with BECN1. Autophagosomes generated during the Atg5/Atg7-independent non-canonical pathway require Rab9 for extension and closure of phagophores (Nishida *et al.*, 2009). Rab9 is GTPase with multiple functions in the endolysosomal system, including lysosome biogenesis and transport from the trans-Golgi network to late endosomes (Kucera, Bakke and Progida, 2016). BECN1 is also involved in the initiation of this non-canonical pathway.

OVCAR-5 cells were transfected for 24 hours with 20nM of BECN1, and 40nM of Rab9 siRNA. Beclin 1 expression was reduced to 56% following knockdown of BECN1 alone (lane 2) and to 61% when used in combination with Rab9 (lane 3) [Figure 4.4A]. The Rab9 knockdown was not as effective, with protein expression reduced to only 80% and 70% following single knockdown (lane 2) and double knockdown with BECN1 (lane 3) respectively [Figure 4.4B]. Despite not achieving optimal knockdown, the reductions in Beclin 1 and Rab9 protein expression did reduce the recovery of OVCAR-5 cells following paclitaxel treatment, although this did not reach significance [Figure 4.4C]. It remains possible that non canonical autophagy may contribute to response to paclitaxel, however more efficient knockdown of Rab9 would be required to demonstrate this.

OVCAR-8 cells were transfected for 24 hours with 30nM of BECN1 and Rab9 siRNA. Beclin 1 expression was reduced to 10% following single knockdown (lane 2), and

just 25% when part of a double knockdown with Rab9 (lane 3) [Figure 4.5A]. Following transfection with 30nM siRNA, Rab9 expression was reduced to 30% when knocked down alone (lane 2), and to 32% when combined with a BECN1 targeted siRNA (lane 3) [Figure 4.5B]. After 48 hour treatment with 5nM paclitaxel, knockdown of BECN1 and Rab9 significantly reduced clonogenic recovery (*p = 0.022) [Figure 4.5C]. These data indicate that a non-canonical brefeldin A-sensitive autophagy pathway may also play a role in the recovery of OVCAR-8 cells following paclitaxel treatment.

Collectively, these data suggest that both canonical and non-canonical pathways are likely to be involved in the recovery of OVCAR-5 and OVCAR-8 cells following treatment with paclitaxel.

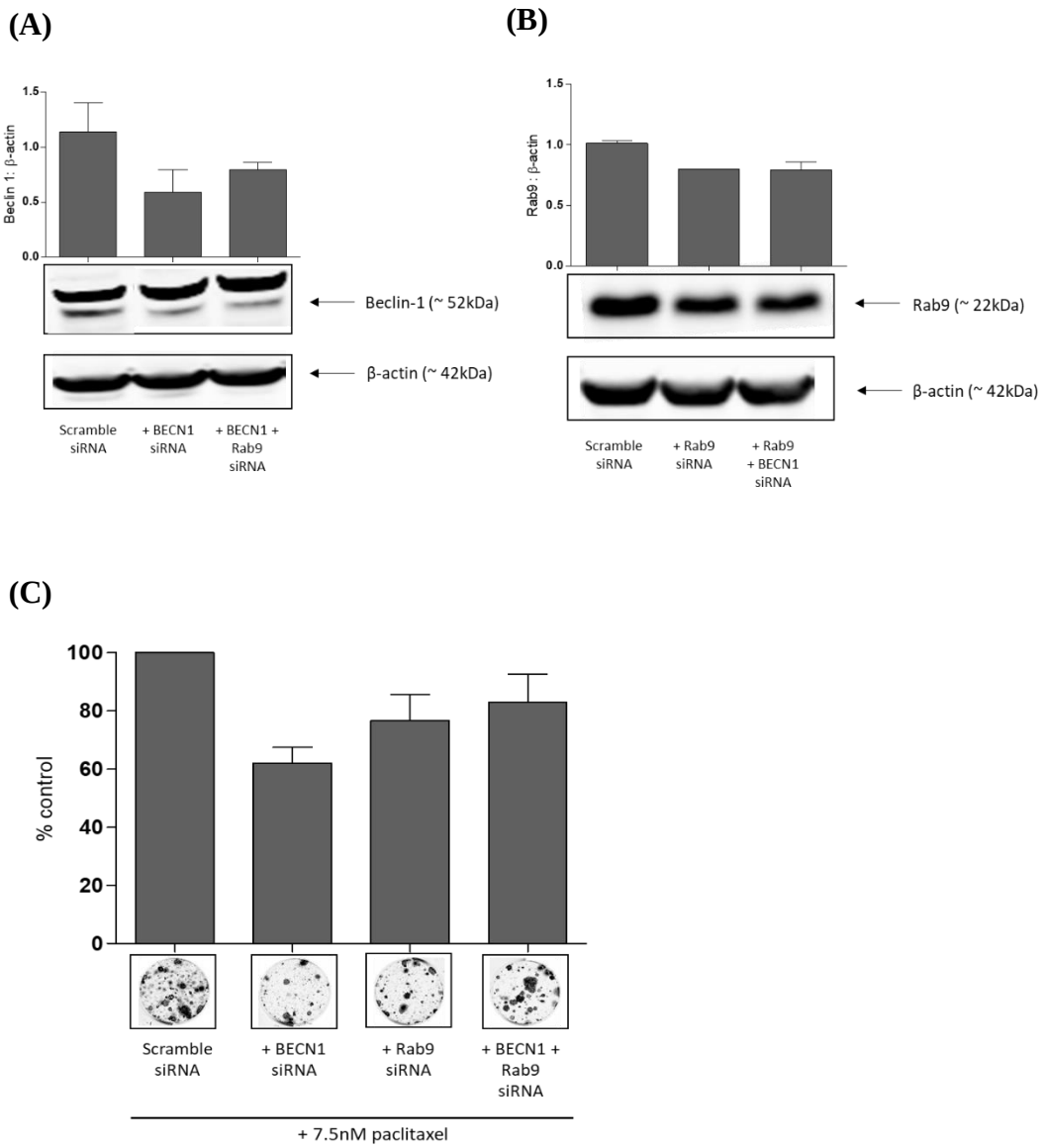

Figure 4.4. Evaluation of the effect of BECN1 and Rab9 knockdown on OVCAR-5 cell recovery following paclitaxel treatment. OVCAR-5 cells were transfected for 24 hours with targeted siRNA, treated for 48 hours with 7.5nM paclitaxel and clonogenic recovery was assessed. **(A)** Western blot analysis of Beclin 1 and **(B)** Rab9 72 hours after siRNA knockdown. All blots were scanned, quantified and values normalised to β-actin. Integrated intensities are graphed ±SEM (n=2). **(C)** Following knockdown with specific siRNAs and 48 hour treatment with paclitaxel, OVCAR-5 cells were re-seeded (1500 cells/well) and recovery assessed. All colonies were fixed, stained and scanned using the Li-Cor Odyssey Infrared scanner. Integrated intensities are graphed ± SEM as % control (n=2).

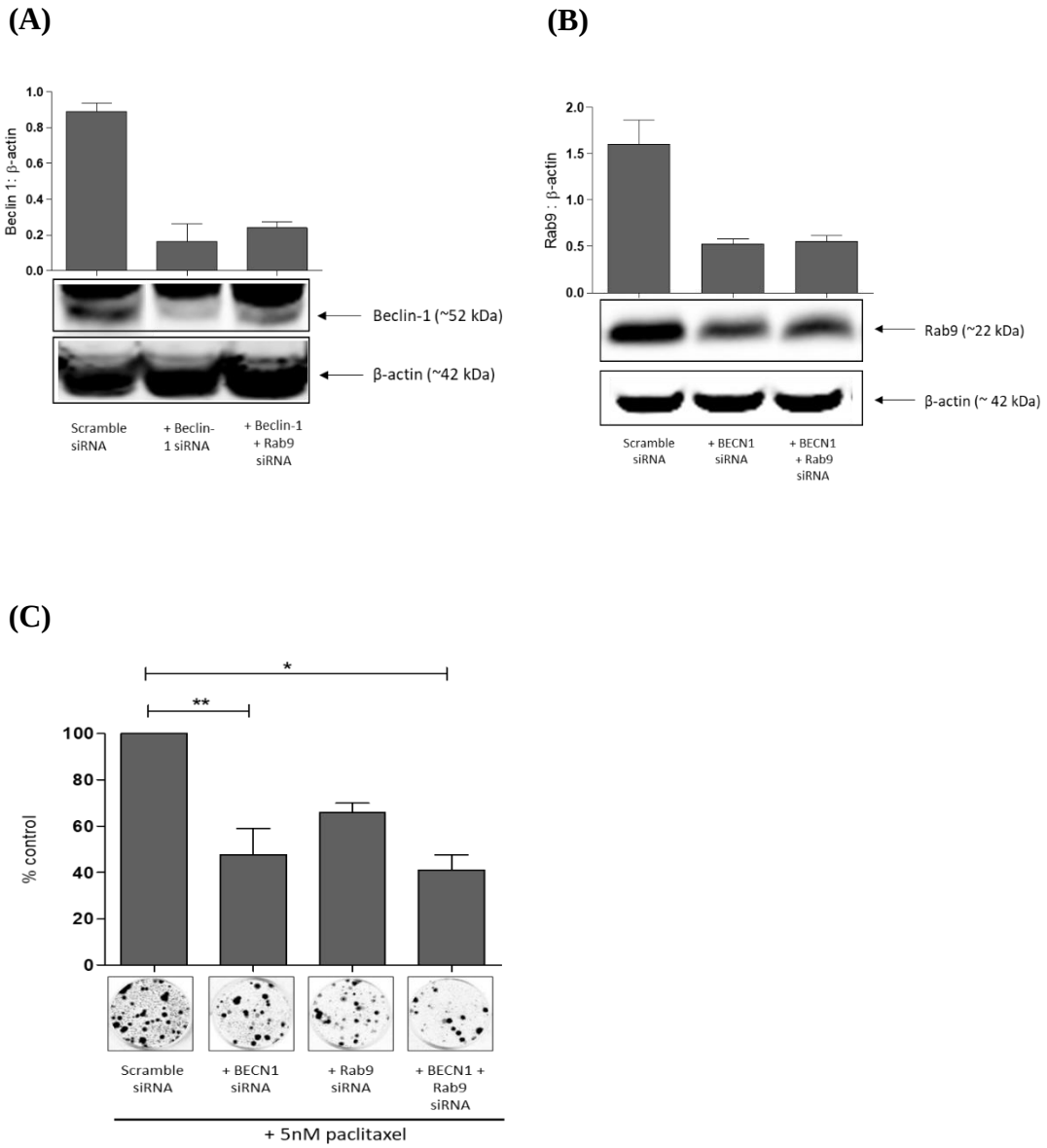

Figure 4.5. Reducing the expression of Beclin 1 and Rab9 significantly impedes OVCAR-8 recovery following paclitaxel treatment. OVCAR-8 cells were transfected for 24 hours with 30nM siRNA, treated for 48 hours with 5nM paclitaxel and clonogenic recovery was assessed. **(A)** Western Blot analysis of Beclin 1 and **(B)** Rab9 knockdown was confirmed 72 hours post transfection. Blots were scanned, quantified and values normalised to β-actin. Integrated intensities are graphed ± SEM (n=2). **(C)** Following knockdown with specific siRNAs and 48 hour treatment with paclitaxel, OVCAR-8 cells were re-seeded (1500 cells/well) and recovery assessed. All colonies were fixed, stained and scanned using the Li-Cor Odyssey Infrared scanner. Integrated intensities were obtained and are graphed as % control (with the control being 100%) ± SEM (n=2). Paired t-test was used to assess significance, defined as *$p \leq 0.05$ **$p \leq 0.01$.

4.5 Discussion

In this study, siRNA knockdown of key genes BECN1 and ATG5 significantly reduced clonogenic recovery in ID8-luc2 and OVCAR-8 cells. While not significant, reductions in Beclin 1 and Atg5 expression could also reduce OVCAR-5 cell recovery. The ID8-luc2 and the OVCAR-5 cell line were generally more difficult cell lines in which to achieve knockdown. Higher concentrations of siRNA, used for the OVCAR-8 cells, were tested in OVCAR-5 cells, however no improvement, or reduced knockdown efficiency was obtained. Further optimisation of the transfection procedure in OVCAR-5 cells would be required, which was not feasible during this study. Alternatively, other strategies could be employed to reduce the expression of autophagy proteins. Lentiviral transfection of short hairpin RNA (shRNA) provides a more durable knockdown. CRISPRi technology, which allows gene silencing at the DNA level, can also provide a more robust knockdown with less off target effects. More robust and sustained knockdown of autophagy genes will also allow more accurate assessment of the role of autophagy in recovery. The half-life of siRNA can be anywhere from 3 to 6 days, meaning that the effects of the siRNA are likely reduced by the end of the clonogenic recovery. The knockdown achieved with OVCAR and ID8-luc2 cells indicates that autophagy plays a role in the recovery of OC cells following paclitaxel treatment. This finding is in line with several studies which also implicate autophagy in chemoresistance in OC cells. One study reported that knockdown of ATG5 in OV433 OC cells inhibited cell growth following cisplatin treatment (Wang et al 2014), while another study demonstrated that ATG5 knockdown could enhance the chemosensitivity of OC stem cells to carboplatin treatment (Pagotto et al 2017). Similarly, knockdown of BECN1 in A2780cp cisplatin resistant OC cells

enhanced cisplatin mediated cell death (Bao et al 2015). Further studies with a platinum based drug in our cell lines would therefore be interesting.

Knockdown of the non-canonical gene Rab9 with BECN1 reduced the recovery of OVCAR-5 and -8 cells following paclitaxel treatment, highlighting a potential role for brefeldin A-sensitive autophagy, such as the Atg5/Atg7-independent pathway, in response to treatment. Biological functions of Atg5/Atg7-independent autophagy have only begun to be elucidated. Roles in erythrocyte maturation, mitochondrial clearance during stem cell differentiation, and anti-inflammatory functions have all been reported (Honda *et al.*, 2014) (Ma *et al.*, 2015) (Ra *et al.*, 2016). To date, only one other study has reported the presence of Atg5/Atg7-independent autophagy in response to a chemotherapeutic agent. Arakawa et al reported the accumulation of autophagic structures in Atg 5 deficient MEFs following treatment with etoposide, a DNA topoisomerase inhibitor (Arakawa *et al.*, 2017). To our knowledge, ours is the first study to provide evidence that a non-canonical brefeldin A-sensitive autophagy pathway may contribute to paclitaxel resistance in OC cells. However, to confirm the presence of the Atg5/7-independent autophagy pathway, further experiments are required to assess autophagosome accumulation in Atg5/7 deficient cells. Immunofluorescence analysis of LAMP2, and its colocalisation with Rab9, following paclitaxel treatment in Atg5/7 deficient cells will also be performed. This data also highlights the possibility that more than one autophagy pathway may be present in OC cells and that this could also contribute to resistance to chemotherapy. This may have clinical significance when identifying therapeutic targets to tackle chemoresistance in OC. It is likely that targeting multiple pathways will be necessary. However, the full contribution and molecular regulation of this non-canonical pathway remains to be elucidated and warrants further investigation.

In summary, we have demonstrated a role for autophagy in response to paclitaxel in OC cells. Our data also supports a potential role for non-canonical Atg5/Atg7-independent autophagy in chemoresistance.

4.6 References

Arakawa, S. et al. (2017) ‘Molecular mechanisms and physiological roles of Atg5/Atg7-independent alternative autophagy’, Proceedings of the Japan Academy. Series B, Physical and Biological Sciences, 93(6), pp. 378–385.

Bao, L. et al. (2015) ‘Induction of autophagy contributes to cisplatin resistance in human ovarian cancer cells.’, Molecular Medicine Reports, 11(1), pp. 91–98.

Honda, S. et al. (2014) ‘Ulk1-mediated Atg5-independent macroautophagy mediates elimination of mitochondria from embryonic reticulocytes.’, Nature Communications, 5, p. 4004.

Kang, R. et al. (2011) ‘The Beclin 1 network regulates autophagy and apoptosis’, Cell death and Differentiation, 18(4), pp. 571–580.

Kucera, A., Bakke, O. and Progida, C. (2016) ‘The multiple roles of Rab9 in the endolysosomal system’, Communicative & integrative biology, 9(4), pp. e1204498–e1204498.

Ma, T. et al. (2015) ‘Atg5-independent autophagy regulates mitochondrial clearance and is essential for iPSC reprogramming’, Nature Cell Biology, 17, p. 1379.

Ozols, R. F. *et al.* (2003) ‘Phase III trial of carboplatin and paclitaxel compared with cisplatin and paclitaxel in patients with optimally resected stage III ovarian cancer: a Gynecologic Oncology Group study.’, Journal of clinical oncology: official journal of the American Society of Clinical Oncology, 21(17), pp. 3194–3200.

Pagotto, A. et al. (2017) ‘Autophagy inhibition reduces chemoresistance and tumorigenic potential of human ovarian cancer stem cells’, Cell Death & Disease, p. e2943.

Pokhriyal, R. et al. (2019) ‘Chemotherapy Resistance in Advanced Ovarian Cancer Patients’, Biomarkers in Cancer, 11, p. 1179-1198.

Ra, E. A. et al. (2016) ‘TRIM31 promotes Atg5/Atg7-independent autophagy in intestinal cells.’, Nature Communications, 7, p. 11726.

Shimizu, S. (2018) ‘Biological Roles of Alternative Autophagy’, Molecules and cells. 2018/01/23. Korean Society for Molecular and Cellular Biology, 41(1), pp. 50–54.

Wang, J. and Wu, G. S. (2014) ‘Role of Autophagy in Cisplatin Resistance in Ovarian Cancer Cells’, The Journal of Biological Chemistry. 9650, pp. 17163–17173.

Ye, X., Zhou, X.-J. and Zhang, H. (2018) ‘Exploring the Role of Autophagy-Related Gene 5 (ATG5) Yields Important Insights into Autophagy in Autoimmune/Autoinflammatory Diseases’, Frontiers in Immunology, 9, p. 2334.

Zheng, W. et al. (2019) ‘ATG5 and ATG7 induced autophagy interplays with UPR via PERK signaling’, Cell Communication and Signaling, 17(1).

Appendix 1:

Uncropped western blots

1. Uncropped western blots

Western blots showing how each relevant band (Beclin 1; ATG5/12 and Rab9) was identified. A molecular weight protein ladder was run alongside the samples in order to identify the proteins of interest based on their predicted size (kDa), which is stated on each blot.

(A)

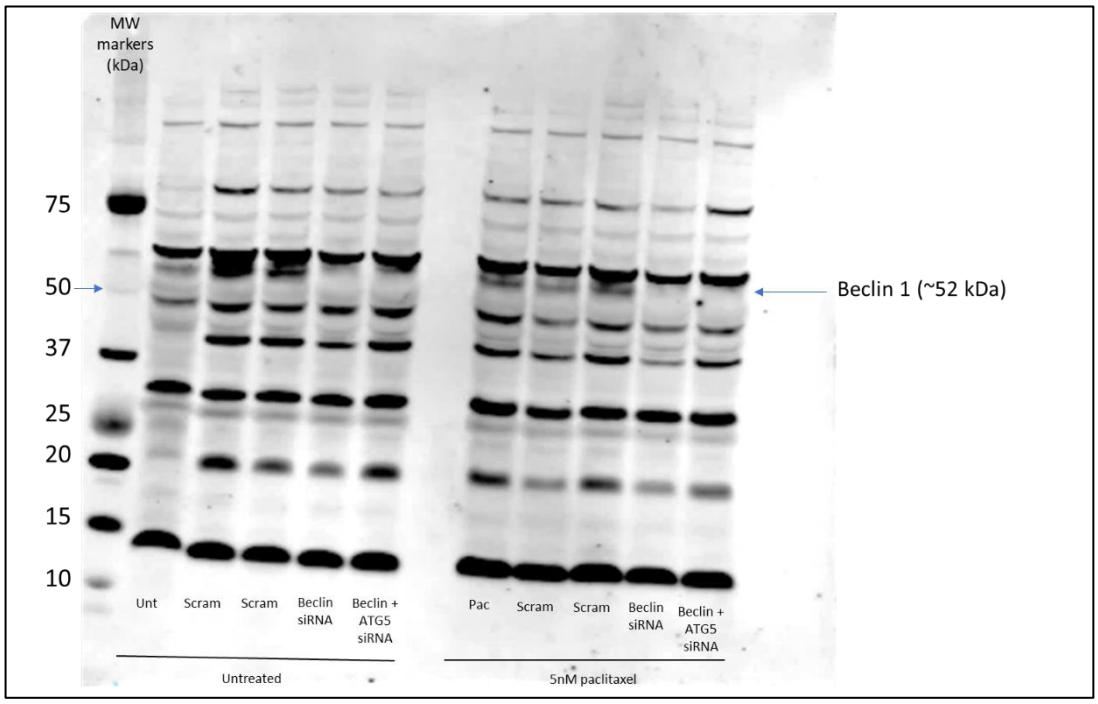

(B)

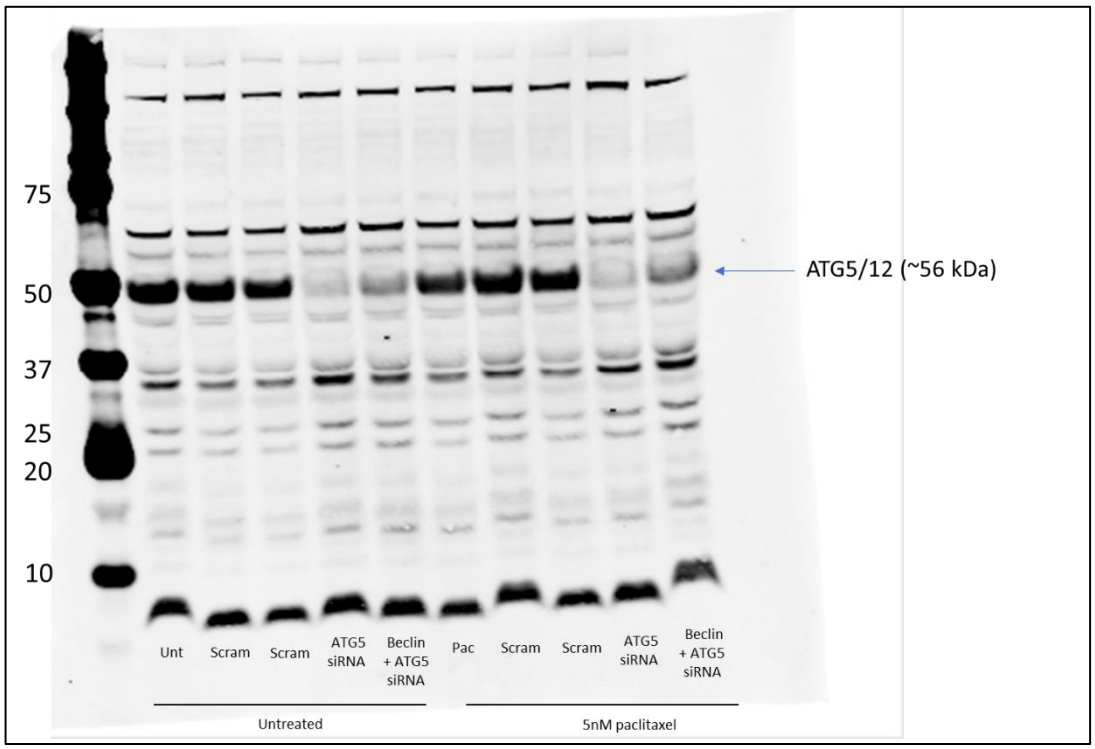

(C)

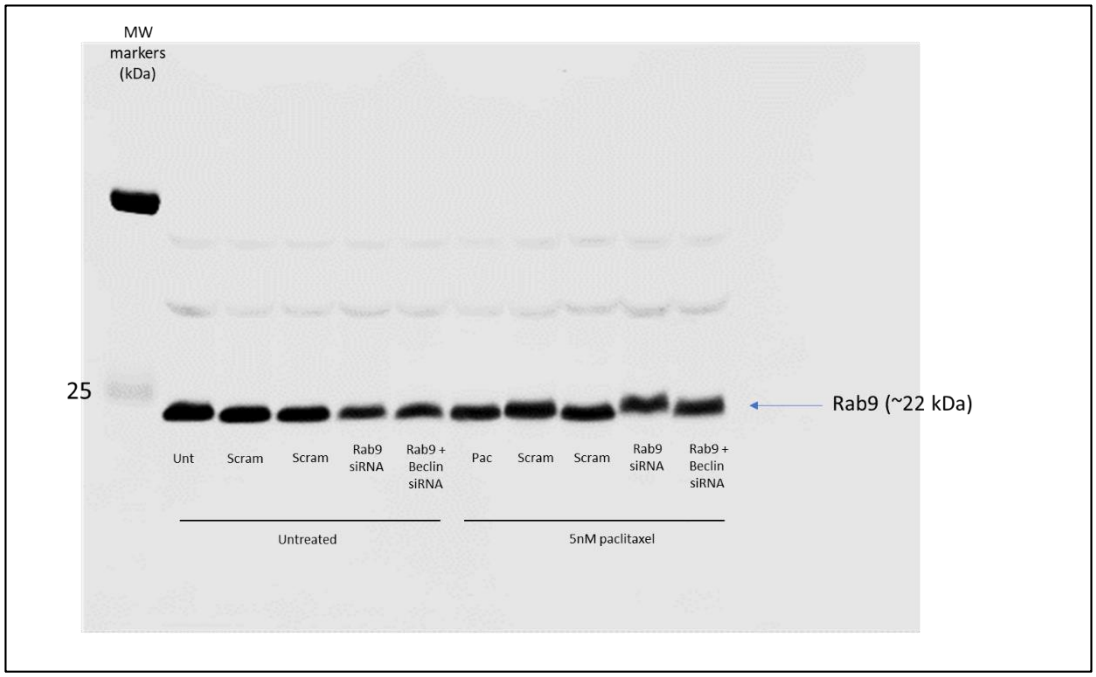

Uncropped western blots for OVCAR-8 cells. Western blots are shown for OVCAR-8 cells probed for **(A)** Beclin 1 **(B)** ATG5/12 and **(C)** Rab9, following no treatment (untreated) or paclitaxel (5nM) treatment (pac). Cells were transfected for 24 hours with targeted siRNA or scramble control (scram). Predicted size in kDa is indicated on each blot.

Chapter Five: Autophagy is involved in the recovery of DNA content following paclitaxel treatment

5.1 Abstract

Ovarian cancer is the sixth most common cancer in women, with over 70% of women diagnosed with late stage disease. Paclitaxel is routinely used in the clinical management of OC. Despite its efficacy as a first line treatment, resistance and disease recurrence are common. Paclitaxel functions as a microtubule stabiliser, resulting in segregation errors and karyotype abnormalities which typically leads to apoptosis. Despite this, we have shown that OC cells can recover from paclitaxel treatment, and that autophagy contributes to this recovery. In this chapter, we aimed to assess the impact of paclitaxel on the cell cycle profile of ID8-luc2 and OVCAR-8 cells and assess if there may be a role for autophagy in the recovery of a normal DNA content. Treatment with paclitaxel resulted in a G2/M arrest and an accumulation of polyploid cells. Following 5 and 7 day recovery periods after paclitaxel treatment, ID8-luc2 and OVCAR-8 cells displayed a remarkable ability to recover their original cell cycle profile. The addition of CQ during the recovery period impeded ID8-luc2 cell cycle recovery, suggesting a role for autophagy. In addition, in OVCAR-8 cells, knockdown of BECN1 and ATG5 enhanced accumulation of polypoid cells, further supporting a role for autophagy in the recovery of a 'normal' DNA profile. We have shown that DNA fragments produced following paclitaxel treatment interact with autophagy markers LC3 and LAMP1 in ID8-luc2 and OVCAR-8 cells. Taken together, these data suggest that a selective type of autophagy, termed nucleophagy, may contribute to the recovery of nuclear integrity in paclitaxel treated OC cells.

5.2 Introduction

The standard of care for OC treatment has remained unchanged over the last few decades, comprising of surgical debulking and chemotherapy. Although most patients will achieve an excellent clinical response following first line treatment, disease relapse occurs in the majority of women. This is the most significant clinical challenge yet to be met in the treatment of OC.

Paclitaxel is a widely utilised taxane in the management of OC, which functions as a microtubule stabiliser. Paclitaxel causes segregation errors, resulting in striking nuclear fragmentation and the partition of genetic material into micronuclei (MN). MN typically originate from acentric chromosome or whole chromosome fragments which, after failing to be incorporated into the nucleus during telophase, become enclosed within a nuclear membrane (Fenech *et al.*, 2011). Ovarian cancers have been reported to be predisposed to MN formation, facilitating genomic adaption following genotoxic insult, which may contribute to resistance and disease recurrence (Tang *et al.*, 2018). Additionally, maintenance of genomic integrity is essential for cell survival and the presence of genomic abberations typically leads to cell death.

Recently, studies have emerged linking autophagy to the maintenance of genome integrity. This was first evidenced in cancer cells deficient in the key autophagy gene Beclin 1, which displayed increased markers of DNA damage and aneuploidy (Karantza-Wadsworth *et al.*, 2007). Since then studies have detailed the complex crosstalk between autophagy and DNA damage response (DDR) pathways, including homologous recombination (E. Y. Liu *et al.*, 2015). In addition to its links to DDR responses, autophagic machinery has also been reported to selectively eliminate nuclear material, a process termed nucleophagy. Nucleophagy was first described in the budding yeast *saccharomyces cerevisiae* and termed piecemeal micro autophagy

of the nucleus (PMN) (Roberts *et al.*, 2003). PMN occurs when small pieces of nucleus are extruded at nucleus-vacuole (NV) junctions into vacuolar membranes, which are then released into the vacuolar lumen and degraded by luminal hydrolases (Kvam and Goldfarb, 2007). In mammalian cells, mouse embryonic fibroblasts (MEFs) were found to contain autophagosomes positive for LC3 close to the nucleus. The autophagosomes were also positive for LAMP2, and colocalised with histone H1 and γH2AX, indicative of chromatin within the autophagosome (Park *et al.*, 2009). Autophagy has also been shown to eliminate micronuclei. In a study by Rello-Varona *et al*. (2012), micronuclei colocalised with LC3 positive vesicles and stained positive for the autophagy adaptor protein p62. These co-localisations were lost upon knockdown of Atg5 or Atg7, supporting a role for autophagy in MN degradation (Rello-Varona *et al.*, 2012).

In this study, we have performed cell cycle analysis to assess the recovery of OC cell's DNA profile following paclitaxel treatment. To assess a role for autophagy in recovery of the DNA profile, CQ was used to impede autophagy. To further evaluate a role for autophagy, siRNA knockdown of BECN1 and ATG5 was also performed. We have used confocal imaging to assess the localisation of autophagy markers with nuclear material, which may indicate the presence of nucleophagy in OC cells.

5.3 Materials and Methods

5.3.1 Cell culture and Reagents

OVCAR-8 were obtained directly from the American Type Culture Collection (ATCC) and maintained in RPMI 1640 media, supplemented with 10% (v/v) foetal calf serum. Murine ID8-luc2 cells were obtained from the Mayo Clinic and cultured in DMEM containing 10% (v/v) foetal calf serum. All cultures were maintained in T75cm^2 flasks (Sarstedt) supplemented with 1% penicillin/streptomycin (Gibco Life Technologies, Cat # 15070-063) and maintained at 37°C, 5% CO_2.

5.3.2 Drug treatments

Paclitaxel (Cat # T7402) and carboplatin (Cat # C2538) were both purchased from Sigma Aldrich. Paclitaxel was reconstituted in DMSO to give 58.55mM stock. Aliquots were prepared and stored at -20^{0}C. Working concentrations of Paclitaxel were prepared fresh in media on the day of treatment. Carboplatin was reconstituted in water to give a 26.93mM stock, aliquoted and stored in the dark at room temperature. Working concentrations were prepared in media on the day of treatment. CQ was prepared in media on the day of treatment (1mM) and added to the cells 2 hours prior to any other drug treatment.

For the cell cycle profile experiments, cells were treated with paclitaxel or carboplatin +/- CQ (10µM) for 24 or 48 hours. To assess cell cycle recovery, drugs were removed, and cells received new drug-free media, and were allowed to recover for up to 7 days. To assess the effect of CQ on cell cycle recovery, cells received media containing CQ (10µM), which was replenished three times over the 7 day recovery period, every 48 hours.

For immunofluorescence experiments, cells were treated paclitaxel or carboplatin for 24 or 48 hours, followed by a further 24 hour recovery period in drug free media.

For transfection experiments, cells received a 24 or 48 hour treatment with paclitaxel or carboplatin.

5.3.3 Immunofluorescence

Prior to treatment, cells were seeded directly onto coverslips in the well of a six well plate (Nunc™ Thermo Scientific, Cat # 140685). Following treatment, cells were washed using PBS, fixed (4 % PFA/PBS), and washed 3 times with PBS and permeabilised in 100% cold methanol for 10 minutes at -20°C. Cells were washed 3 times with PBS and blocked for 30 minutes at room temperature (5% BSA/PBS). Cells were probed with anti-LC3 (Abgent, Cat # APG8B) and anti-LAMP1 antibodies (Abcam, Cat # Ab25245) in 1% BSA/PBS overnight at 4°C and detected by

Alexa Flour 594 goat anti-rabbit and Alexa Flour 633 goat anti-rat secondary antibodies (Life Technologies, Cat # A11037 and A21094, respectively). Cells were incubated with Nuclear ID stain (1µl per 2ml PBS) for 30 minutes at room temperature, before the slides were mounted using Pro-Long Gold anti-fade without Dapi (Invitrogen, Cat # P36970). Images were acquired using the Olympus Fluoview1000 Confocal Laser Imaging System.

5.3.4 siRNA transfection

Cells were reverse transfected for 24 hours using gene specific siRNAs and non-specific scramble controls using Lipofectamine 2000 transfection reagent (Life

technologies, Cat # 11668500) according to instructions from the manufacturer. On-Target plus smartpool siRNA were purchased from Dharmacon for both mouse (Beclin-1: Cat # L-055895-00-0005, ATG5: Cat # L-064838-00-0005) and human cell lines (Beclin-1: Cat # L-010552-00-0005, ATG5: Cat # L-004374-00-0005). A Non-specific target control was also purchased from Dharmacon (Non-targeting siRNA #1: Cat # D-001810-01-20).

5.3.5 Cell Cycle Analysis

After designated treatment, 500,000 cells were pelleted and resuspended in 500µl PBS. Cells were fixed by adding 1,167µl of 100% ethanol dropwise while gently vortexing, to a final concentration of 70% and stored at -20°C until the day of analysis. A minimum of 24 hours fixation at -20°C was found to yield sharper peaks in the cell cycle profiles. On the day of analysis, cells were pelleted and washed with PBS. Propidium Iodide (20µg/ml) and Rnase A (200mg/ml) were prepared in PBS, added to the samples, and incubated at room temperature in the dark for 1 hour. PI is a DNA intercalator, which binds to DNA stoichiometrically. As cells residing in different phases of the cell cycle contain differing DNA contents, cells with higher contents (e.g. G2/M phase – 4N content, and aneuploid – >4N content) will have the highest fluorescence. As PI can also bind to RNA, Rnase A is added to remove RNA, allowing more accurate analysis. Data was acquired and analysed using the BD LSR II flow cytometer and BD FACS Diva acquisition and analysis software.

5.4 Results

5.4.1 ID8-luc2 cells recover a typical DNA profile following paclitaxel and carboplatin treatment, and this is impeded by chloroquine

Paclitaxel functions as a microtubule stabiliser, leading to aberrant segregation of chromosomes, G2/M arrest, formation of micronuclei and mitotic catastrophe. Despite this, we have shown that ID8-luc2 cells can recover and regrow following treatment. The effect of paclitaxel on the cell cycle profile of ID8-luc2 cells, which have a near tetraploid karyotype, following treatment and a subsequent recovery period in drug free media, was assessed by flow cytometry.

The top panel of Figure 5.1 shows representative histograms of paclitaxel treated cells. Cells with ≥2N DNA content were gated and denoted as % (of parent population) within the histograms. Following 24 hour paclitaxel treatment (upper second panel) a G2/M arrest was evident. Increased accumulation of polyploid cells (with >4N DNA content) was also evident after treatment (upper middle panel) [Figure 5.1 (i)]. 5 days after withdrawal of drug, cells recovered their DNA profile, with the majority returning to the G0 phase with a decrease in cells with ≥2N DNA content (upper right panel) [Figure 5.1 (i)]. To assess the potential contribution of autophagy to this recovery, autophagy was inhibited using CQ (bottom panel outlined in red) [Figure 5.1 (ii)]. Cells were treated with 2.5μM paclitaxel plus or minus CQ for 24 hours, reseeded and allowed to recover for up to 5 days in paclitaxel free media. To maintain the effect of CQ, it was supplemented into the media every 48 hours throughout the recovery period. Cells treated for 24 hours with paclitaxel in the presence of CQ still accumulated in the G2/M phase [lower middle panel, Figure 5.1 (ii)]. However, cells recovered for 5 days following paclitaxel treatment in the presence of CQ maintained G2/M accumulation [right lower panel, Figure 5.1 (ii)]. The addition of CQ also

impeded the clearance of cells with >4N DNA content after a 5 day recovery period. These data suggest that impeding autophagy does not interfere with the G2/M arrest, but it does impede the recovery of a pre-treatment DNA profile.

Cell cycle was similarly assessed in ID8-luc2 cells following carboplatin treatment. The top panel of Figure 5.2 shows representative histograms of carboplatin treated cells. Control cells displayed higher accumulation in the G0 and G2/M phases, compared to those from Figure 5.1, which may be due to the longer growth time. Following 48 hour carboplatin treatment (top middle panel) a G2/M arrest was evident. Increased accumulation of polyploid cells (with >4N DNA content) was also evident after treatment (upper middle panel) [Figure 5.2 (i)]. 7 days after withdrawal of drug, cells can recover their DNA profile, with a reduction in cells with ≥2N DNA content evident (upper right panel) [Figure 5.2 (i)]. To assess the potential contribution of autophagy to this recovery, autophagy was inhibited using CQ (bottom panel outlined in red) [Figure 5.2 (ii)]. Cells were treated with 40μM carboplatin plus or minus CQ for 48 hours, reseeded and allowed to recover for up to 7 days in carboplatin free media. To maintain the effect of CQ, it was supplemented into the media throughout the recovery period. Cells treated for 48 hours with paclitaxel in the presence of CQ still accumulated in the G2/M phase (lower middle panel), while an increase in polyploid cells was also evident [Figure 5.2 (ii)]. However, following a 7 day recovery after paclitaxel treatment, in the presence of CQ, cells with ≥2N DNA content were minimally reduced and the clearance of polyploid cells was impeded (lower right panel) [Figure 5.2 (ii)]. This data suggests that impeding autophagy prevents the recovery of a pre-treatment DNA profile.

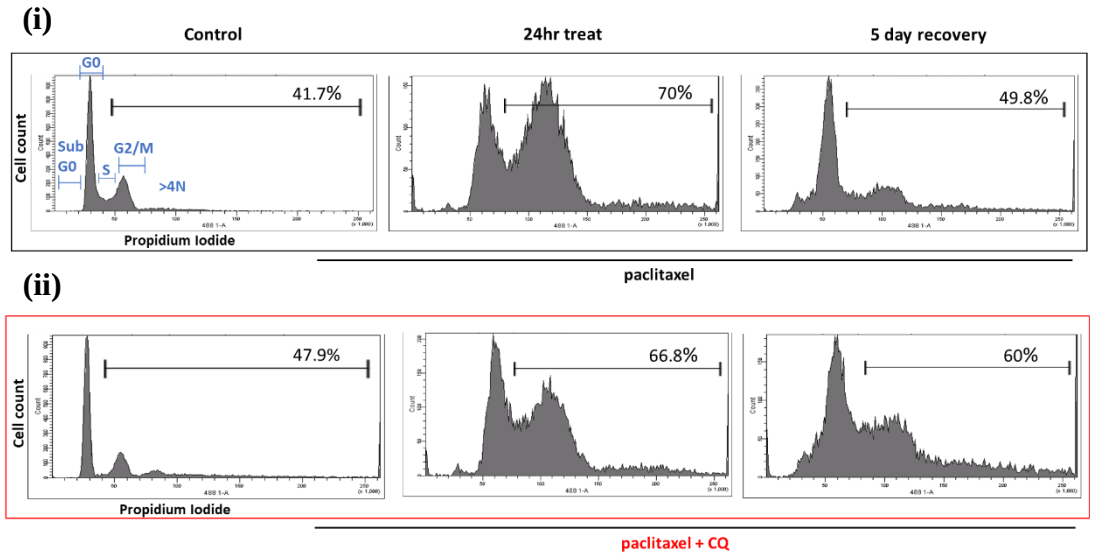

Figure 5.1. Assessment of the cell cycle profile of ID8-luc2 cells following treatment with paclitaxel and CQ. (i) Cells were treated with paclitaxel (2.5µM) for 24 hours, and viable cells re-seeded and allowed to recover for 5 days. **(ii)** Cells were pre-treated with chloroquine (10µM) for 2 hours, prior to the addition of paclitaxel, for 24 hours. Viable cells were re-seeded and allowed to recover for 5 days in the presence of chloroquine. Cells were stained with propidium iodide (20µg/ml) and analysed via flow cytometry (n=1).

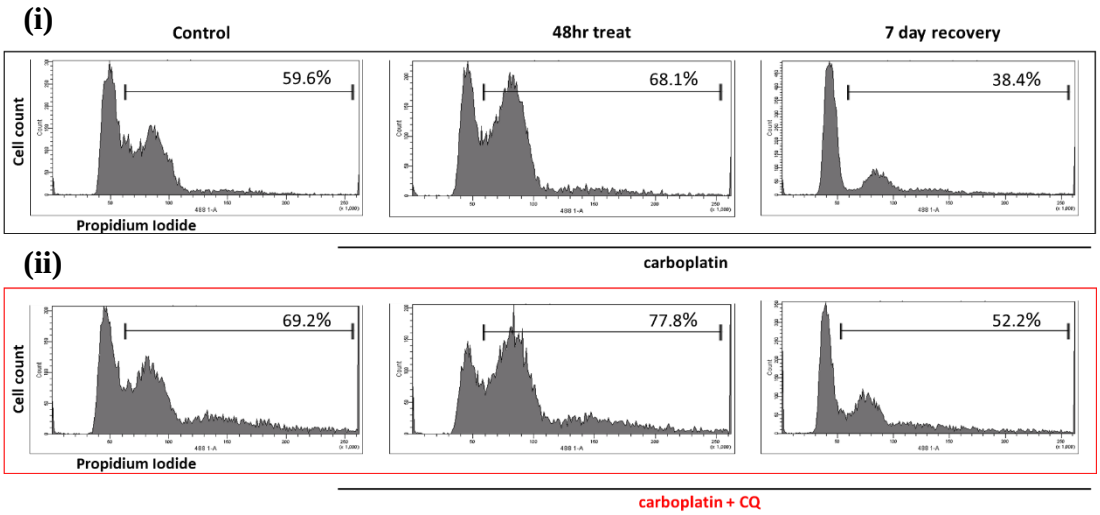

Figure 5.2. Evaluation of the cell cycle profile of ID8-luc2 cells following treatment with carboplatin and CQ. (i) Following treatment with carboplatin (40µM) for 48 hours, viable cells were re-seeded and allowed to recover for 7 days. **(ii)** Cells were pre-treated with chloroquine (10µM) for 2 hours, prior to the addition of carboplatin, for 48 hours. Viable cells were re-seeded and allowed to recover for 7 days in the presence of chloroquine. Cells were stained with propidium iodide (20µg/ml) and analysed via flow cytometry (n=1).

5.4.2 Nuclear material colocalises with LC3 and LAMP1 after paclitaxel treatment in ID8-luc2 cells

Nucleophagy, a specific type of autophagy, is involved in the degradation of nuclear components. Removal of damaged nuclear material and micronuclei contributes to genome stability, which may enable cell recovery following treatment with chemotherapeutics. To assess the presence of nucleophagy, immunofluorescence analysis was performed following a 24 hour paclitaxel treatment and subsequent 24 hour recovery in drug free media. The interaction between the autophagy marker LC3 (green) and lysosomal marker LAMP1 (red) with DNA was assessed. Nuclei were visualised using the blue Nuclear-ID stain.

In control cells (upper panel) the nuclei appeared intact, with little nuclear colocalisation between LC3 and LAMP1 [Figure 5.3]. In contrast, paclitaxel treated cells displayed marked nuclear fragmentation (lower panel). This fragmented nuclear material was colocalised with LC3, producing a cyan blue colour, highlighted with white arrows [lower middle left panel, Figure 5.3]. Fragmented nuclear material also colocalised with LAMP1, producing a magenta pink colour, also denoted with white arrows [lower middle right panel, Figure 5.3]. Yellow punctate foci, resulting from LC3 and LAMP1 colocalising, also associated with fragmented nuclear material, denoted with white arrows [lower right panel, Figure 5.3]. Taken together, these data suggest that autophagy may be involved in the elimination of micronuclei/DNA fragments in ID8-luc2 cells following paclitaxel treatment.

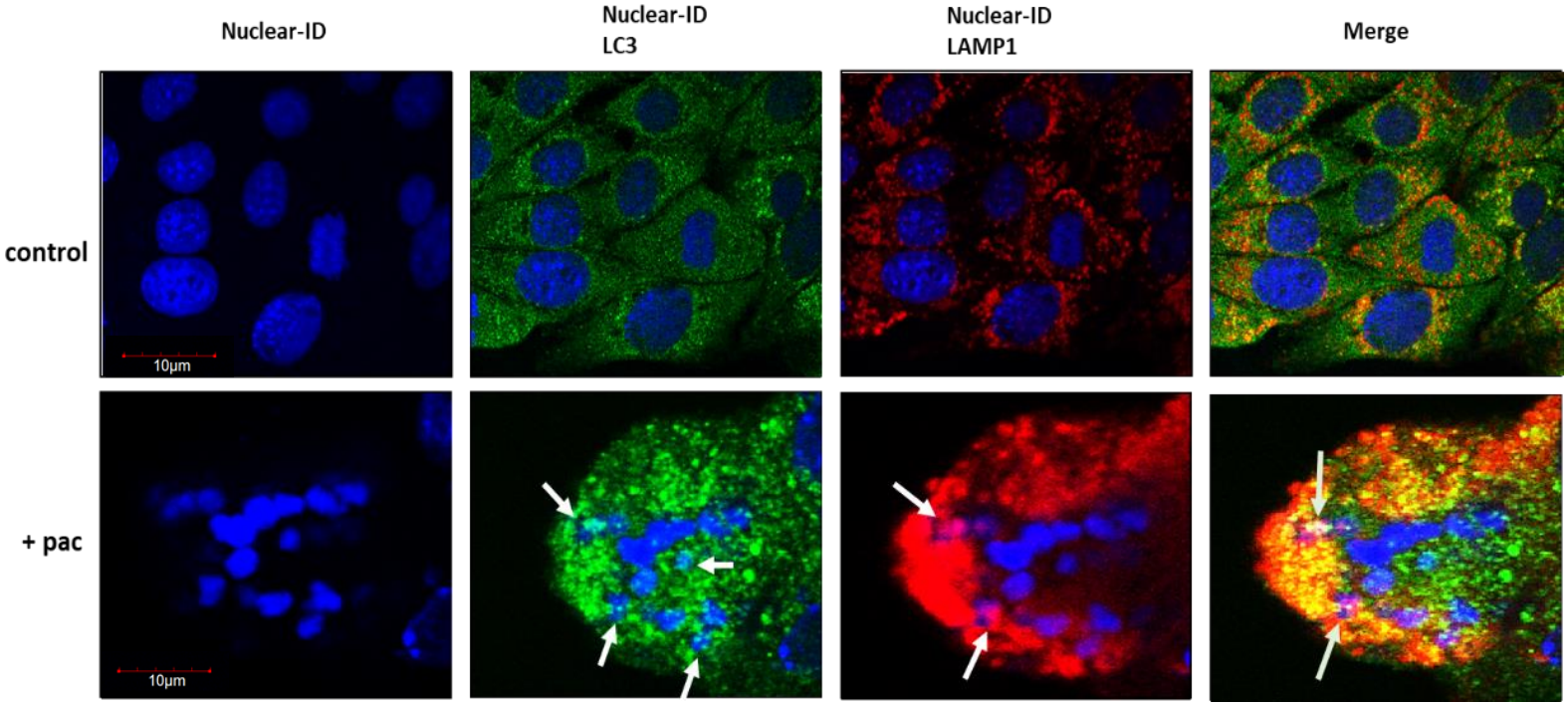

Figure 5.3. Confocal Image analysis of ID8-luc2 cells following paclitaxel treatment. Following a 24 hour treatment with paclitaxel (2.5µM) and a subsequent 24 hour recovery in drug free media, cells were stained with antibodies against LC3 (green punctate foci) and LAMP1 (red punctate foci). Control cells are presented in the top panels (magnification 100X), while a paclitaxel treated single cell is shown in the bottom panels (magnification 100X; zoom 4X) (n=2). Nuclei were stained using the Nuclear-ID stain. In control cells (top panels), nuclei appear whole and intact, with LC3 staining predominantly cytoplasmic. Areas of colocalisation between DNA and LC3 appears as a cyan colour, while colocalisation with LAMP1 appear as magenta colour. Areas of LC3 and LAMP1 appear as yellow punctate staining and localise with fragmented nuclear material. Images were acquired using Olympus Fluoview1000 Confocal Laser Imaging System.

5.4.3 OVCAR-8 cells can recover a typical DNA profile following paclitaxel treatment, which is not impeded by CQ

We then assessed the effect of paclitaxel on the cell cycle profile of human OVCAR-8 cells, which have a hyperdiploid karyotype. Following a 48 hour paclitaxel treatment (5nM) (top second panel), a G2/M arrest was evident, as was an accumulation of cells with >4N DNA content [Figure 5.4 (i)]. Following a 5 day recovery in drug free media, OVCAR-8 cells can recover a cell cycle profile similar to untreated cells, with the majority of cells returning to the G0 phase and cells with >4N DNA content were cleared [Figure 5.4 (i)]. To evaluate a role for autophagy in this recovery, autophagy was impeded using CQ. The addition of CQ to paclitaxel had a minimal effect on recovery. At 5 day recovery, a minimal increase in cells with >4N DNA content was present [Figure 5.4 (ii)]. More selective targeting of autophagy in OVCAR-8 cells may be required to elicit an effect on cell cycle recovery.

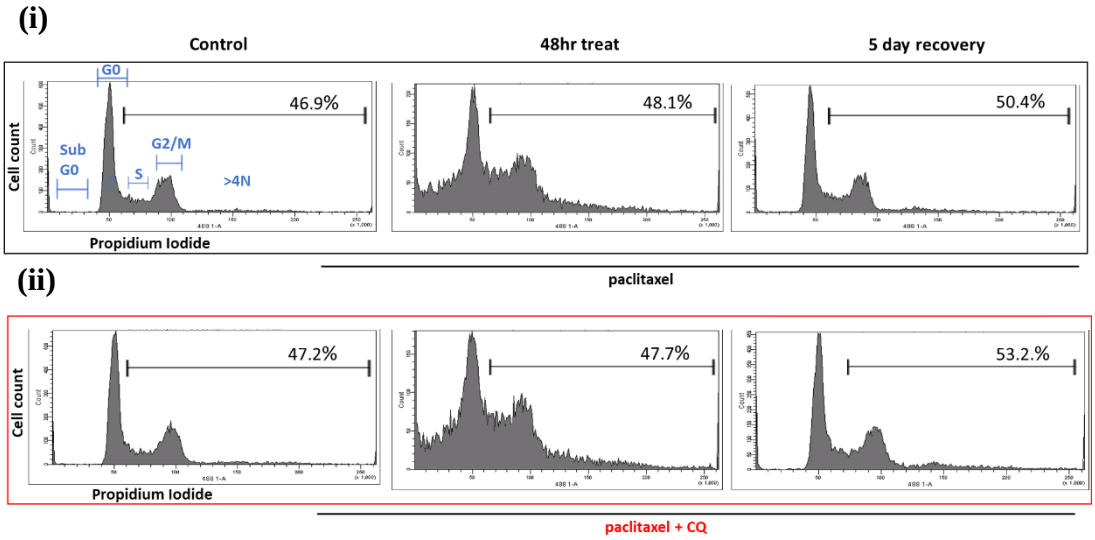

Figure 5.4. Assessment of the cell cycle profile of OVCAR-8 cells following treatment with paclitaxel and CQ. Following 48 hour treatments with (**i**) paclitaxel (5nM) (**ii**) plus CQ (10µM), cells were re-seeded and allowed to recover for 5 days. Cells were stained with propidium iodide (20µg/ml) and analysed via flow cytometry (n=1). Cells with ≥ 2N cells were gated, quantified and written as % (of parent population) within the histograms.

5.4.4 Nuclear material colocalises with LC3 and LAMP1 after paclitaxel treatment in OVCAR-8 cells

To assess the presence of nucleophagy, cells were treated with paclitaxel for 48 hours, followed by a subsequent 24 hour recovery period in drug free media. Cells were then probed for LC3 and LAMP1. Nuclei were visualised using a blue Nuclear-ID stain. In control untreated cells, displayed in the top panels, nuclei appeared intact, with little nuclear colocalisation of LC3. In contrast, paclitaxel treated cells (lower panels) displayed nuclear fragmentation, and these fragments were closely associated with LC3 (denoted with yellow arrows) [Figure 5.5]. In control cells probed with LAMP1, nuclei were intact, with LAMP1 primarily cytoplasmic (top panels) [Figure 5.6]. Following paclitaxel treatment, fragmentation of the nucleus was evident, highlighted with yellow arrows (lower left hand panel). Fragmented nuclear material colocalised with LAMP1, producing a magenta colour, as highlighted with yellow arrows (lower right hand panel) [Figure 5.6]. Due to weaker staining of LAMP1 in the OVCAR-8 cells, colocalisation between LC3 and LAMP1 could not be visualised.

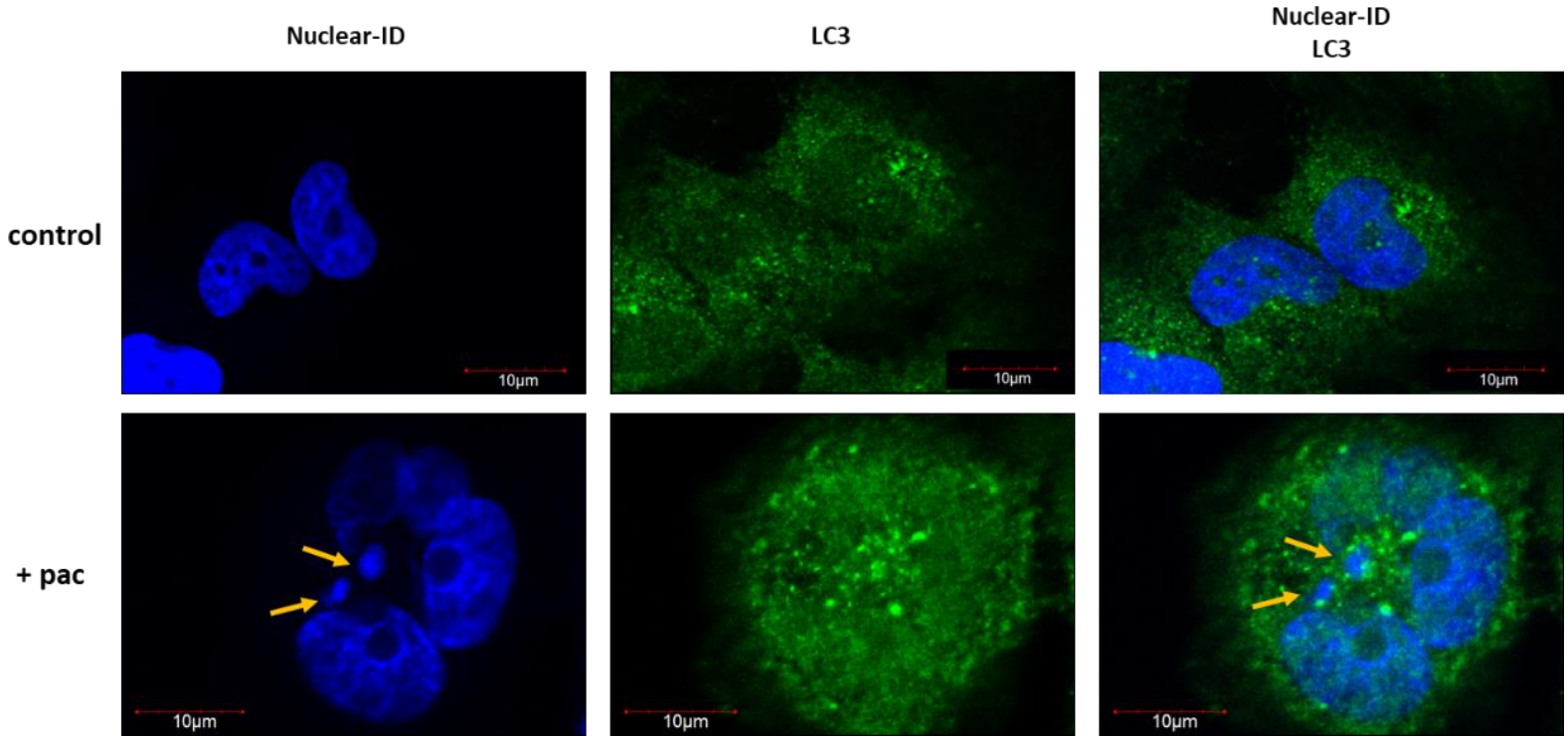

Figure 5.5. Confocal Image analysis of OVCAR-8 cells following paclitaxel treatment. Following a 48 hour treatment with paclitaxel (5nM) and a subsequent 24 hour recovery in drug free media, cells were stained with antibodies against LC3 (green punctate staining) and LAMP1 (red punctate staining). Nuclei were stained using the blue Nuclear-ID stain. Control untreated cells are displayed upper panel (magnification 100X), while cells treated with paclitaxel (5nM) are displayed in the lower panel (magnification 100X; zoom 4X) (n=2). Co-localisation of LC3 with fragmented nuclear material produces a cyan stain, denoted with yellow arrows. Images were acquired using Olympus Fluoview1000 Confocal Laser Imaging System.

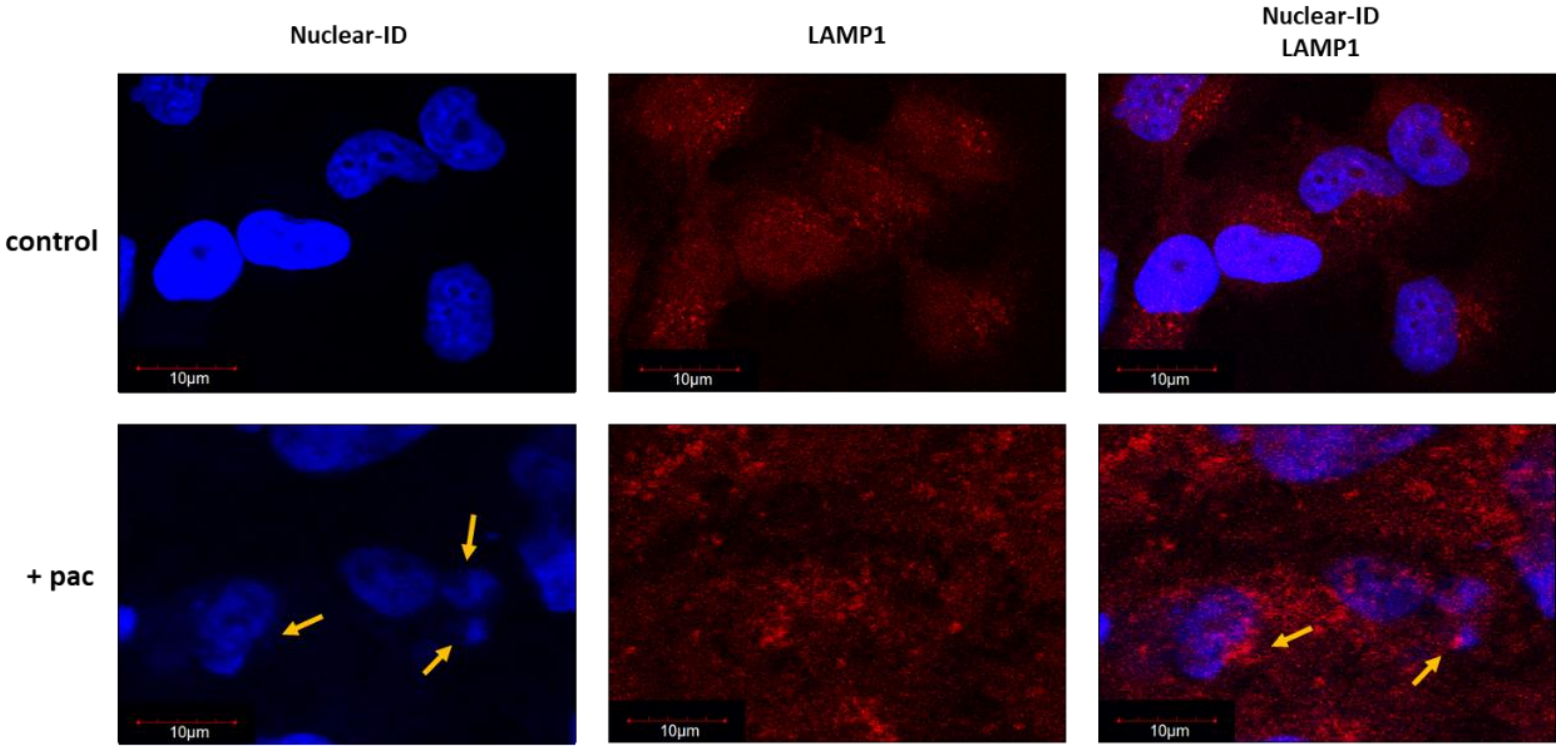

Figure 5.6. Confocal Image analysis of OVCAR-8 cells following paclitaxel treatment. Following a 48 hour treatment with paclitaxel (5nM) and a subsequent 24 hour recovery in drug free media, cells were stained with an antibody against LAMP1 (red punctate staining). Nuclei were stained using the blue Nuclear-ID stain. Control cells are displayed in the upper panel (magnification 100X), while paclitaxel treated cells are displayed in the lower panel (magnification 100X; zoom 3X) (n=2). Colocalisation of LAMP1 with fragmented nuclear material produces a magenta stain, denoted with yellow arrows. Images were acquired using Olympus Fluoview1000 Confocal Laser Imaging System.

5.4.5 Knockdown of key autophagy genes in OVCAR-8 cells impedes the recovery of the parental cell cycle profile

While the molecular regulators of nucleophagy are yet to be elucidated, key autophagy genes including BECN1 and members of the Atg family of proteins have been implicated in genome maintenance. Atg proteins, including Atg5 and Atg7 are present in the nucleus, while loss of Beclin 1 and Atg5 in breast epithelial cells promoted DNA damage and aneuploidy (Karantza-Wadsworth *et al.*, 2007). To elucidate a role for autophagy in the recovery of a typical cell cycle profile following treatment, siRNA knockdown of autophagy genes BECN1 and ATG5 was performed. Cells were transfected for 24 hours, after which transfection media was removed, and cells were treated with paclitaxel for 48 hours. After treatment, cells were allowed to recover in drug free media for up to 5 days.

Knockdown was confirmed via western blot at 72 hours. Transfection with an siRNA targeted to BECN1 reduced protein levels to 36%, while an ATG5 targeted siRNA reduced protein expression to 37% [Figure 5.7A (i) and (ii), respectively].

Following 48 hour paclitaxel treatment, knockdown of BECN1 and ATG5 alone or in combination had little impact on the cell cycle profile of OVCAR-8 cells [Figure 5.7B]. Cell cycle profile was also examined 5 days after withdrawal of paclitaxel. ATG5 knockdown had no impact on the recovery of the DNA profile. BECN1 alone and in combination with ATG5 reduced the clearance of polyploid cells (>4N DNA content) compared to a scrambled control [Figure 5.7C]. Several replicates of this experiment would be required to determine if these differences are significant. These data imply that autophagy may be contributing to the recovery of DNA content in OVCAR-8 cells following paclitaxel treatment.

(A) (i)

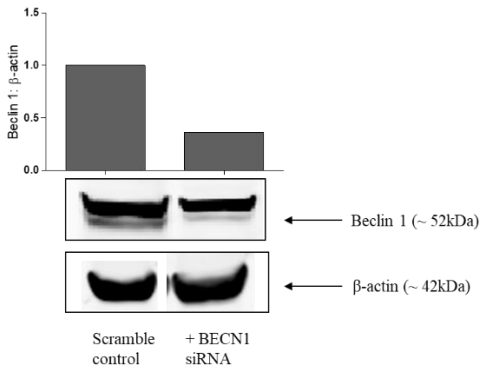

(ii)

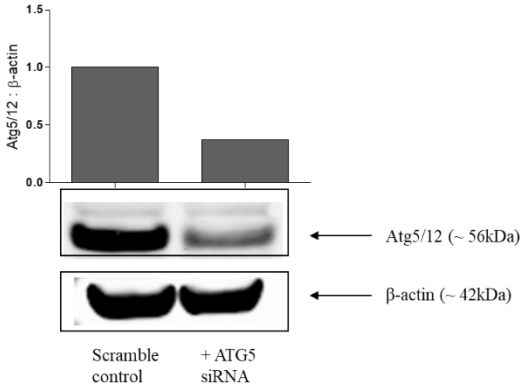

(B) **48 hour treat**

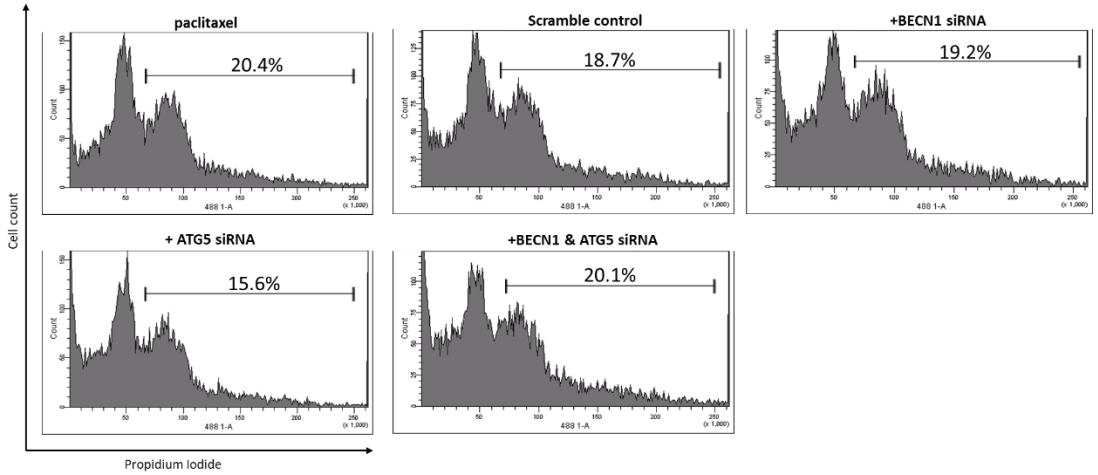

(C) **5 day recovery**

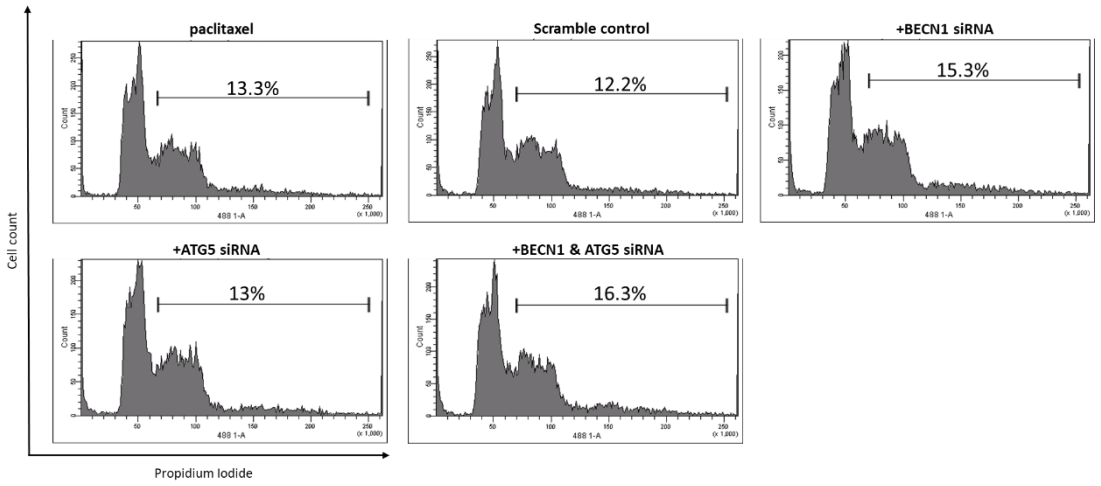

Figure 5.7. Recovery of OVCAR-8 cell cycle profile following knockdown of autophagy genes. To assess the contribution of autophagy to the recovery of a typical cell cycle profile cells received 48 hour paclitaxel treatment (5nM), autophagy genes were knocked down and flow cytometry analysis was performed. **(A)** western blot analysis was used to confirm knockdown of **(i)** BECN1 and **(ii)** ATG5, 72 hours post transfection. Blots were scanned and quantified using the Li-Cor Odyssey Infrared scanner. Bands were normalised to β-actin (n=1). Representative histograms of transfected cells following **(B)** 48 hour treatment and **(C)** 5 day recovery in paclitaxel free media (n=1). Cells with ≥ 2N DNA content were gated, quantified, and written as % (of parent population) within the histograms.

5.5 Discussion

In this study, we have shown that ovarian cancer cells can recover their DNA content profile following paclitaxel treatment and that CQ can impede this recovery. Treatment of ID8-luc2 and OVCAR-8 cells with paclitaxel causes a G2/M arrest and the accumulation of polyploid cells (>4N DNA content). Following a 5 and 7 day recovery in drug free media, the cells can recover their cell cycle profile and a reduction in polyploid cells is evident. Strikingly, the addition of CQ impeded the clearance of polyploid cells in ID8-luc2 cells. BECN1 and ATG5 knockdown in OVCAR-8 cells resulted in a modest increase in polyploid cells 5 days after withdrawal of paclitaxel. Transient knockdown with siRNA is typically lost after 3-5 days, which may account for the modest increase in polyploid cells we observed. Stable knockdown, for example using short hairpin RNA (shRNA), would provide a more robust analysis of the impact of autophagy on cell cycle recovery. Additionally, one study has reported that autophagic degradation of micronuclei occurred in approximately 2-5% of the cancer cell population (Rello-Varona *et al.*, 2012). Therefore, it is important to elucidate the full contribution of nucleophagy in OC, and these preliminary results suggest further investigation is warranted. Similar to our findings, ATG5 knockdown in mouse mammary carcinoma (MMC) cells caused an increase in polyploid cells by flow cytometry analysis following adriamycin treatment, when compared to their autophagy competent counterparts (Aqbi *et al.*, 2018).

In this study, paclitaxel treatment in OVCAR-8 cells caused the formation of micronuclei, which were tagged with LC3 and LAMP1. Paclitaxel has previously been shown to induce the formation of micronuclei (MN). An interesting theory has emerged to explain the link between autophagy and MN elimination. Erenpreisa *et al.* (2012) suggest that following a futile attempt at DNA repair, micronuclei are

eliminated via autophagy. This idea was first supported by the discovery of Rad51 positive MN in fibroblasts (Haaf *et al.*, 1999). MN can remain attached to the nucleus via extension of nuclear envelope membranes comprised of heterochromatin layers, termed envelope limited chromatin sheets (ELCS) (Erenpreisa *et al.*, 2012). ECLS allow the MN to link to new nuclear envelope sites, where their DNA can be repaired, and the MN can then be reincorporated into the nucleus. The authors then suggest that failure of repair would lead to MN budding from the nucleus and subsequent autophagic degradation (Erenpreisa *et al.*, 2012). Thus, autophagic degradation of MN serves to minimise aneuploidy arising from DNA damage, improving the overall fitness of the cell. While nucleophagy has not been well characterised in tumour cells, the evidence to date suggests that DNA damaging agents like cisplatin, used in the clinical management of OC, cleave lamins and disrupts the nuclear membrane, thereby activating nucleophagy. Li *et al.* (2019) reported that DNA damage as a result of doxorubicin treatment causes accumulation of UBC9 in the nucleus, resulting in SUMOylation of lamin A/C. Lamin A/C interacts with the autophagy protein LC3, leading to nucleophagy activation and degradation of nuclear components, including lamin A/C and leaked nuclear DNA (Li *et al.*, 2019). Another study reported that arginine reduced the lamin proteins A/C, thereby causing DNA leakage and autophagy mediated degradation of damaged nuclear DNA (Changou *et al.*, 2014). Analogous to our observations, Li *et al.* (2019) also reported colocalisation of LC3 and LAMP1 with fragmented DNA material following treatment with doxorubicin. While we have shown that LC3 associates with fragmented nuclear material in OVCAR-8 cells, further experiments, such as assessing the co-localisation of LC3 with nuclear envelope proteins, including lamin A/C and B1, would be required to further support a role for autophagy in nuclear degradation (Baron *et al.*, 2017).

Here we provide novel evidence to suggest that nucleophagy may play a role in maintaining genomic integrity in response to paclitaxel treatment in OC cells. However, the full contribution of nucleophagy in treatment response in OC cells warrants further investigation with more robust knockdown of autophagy genes. This data sheds light on the diverse role of autophagy in response to treatment in OC, making it an exciting therapeutic target.

.

5.6 References

Aqbi, H. F. et al. (2018) 'Autophagy-deficient breast cancer shows early tumor recurrence and escape from dormancy', Oncotarget, 9(31), pp.113-122.

Baron, O. et al. (2017) 'Stall in Canonical Autophagy-Lysosome Pathways Prompts Nucleophagy-Based Nuclear Breakdown in Neurodegeneration', Current Biology, 27(23), p. 3626–3642.

Changou, C. A. et al. (2014) 'Arginine starvation-associated atypical cellular death involves mitochondrial dysfunction, nuclear DNA leakage, and chromatin autophagy.', Proceedings of the National Academy of Sciences of the United States of America, 111(39), pp. 14147–14152.

Erenpreisa, J. et al. (2012) 'Macroautophagy-aided elimination of chromatin: sorting of waste, sorting of fate?', Autophagy, 8(12), pp. 1877–1881.

Fenech, M. et al. (2011) 'Molecular mechanisms of micronucleus, nucleoplasmic bridge and nuclear bud formation in mammalian and human cells', Mutagenesis, 26(1), pp. 125–132.

Haaf, T. et al. (1999) 'Sequestration of mammalian Rad51-recombination protein into micronuclei', The Journal of Cell Biology, 144(1), pp. 11–20.

Karantza-Wadsworth, V. et al. (2007) 'Autophagy mitigates metabolic stress and genome damage in mammary tumorigenesis.', Genes & Development, 21(13), pp. 1621–1635.

Kvam, E. and Goldfarb, D. S. (2007) 'Nucleus-vacuole junctions and piecemeal microautophagy of the nucleus in S. cerevisiae.', Autophagy, 3(2), pp. 85–92.

Li, Y. et al. (2019) 'Nuclear accumulation of UBC9 contributes to SUMOylation of lamin A/C and nucleophagy in response to DNA damage', Journal of Experimental & Clinical Cancer Research, 38(1), p. 67.

Liu, E. Y. et al. (2015) 'Loss of autophagy causes a synthetic lethal deficiency in DNA repair', Proceedings of the National Academy of Sciences of the United States of America, 112(3), pp. 773–778.

Park, Y.-E. et al. (2009) 'Autophagic degradation of nuclear components in mammalian cells.', Autophagy, 5(6), pp. 795–804.

Rello-Varona, S. et al. (2012) 'Autophagic removal of micronuclei', Cell Cycle, 11(1), pp. 170–176.

Roberts, P. et al. (2003) ‘Piecemeal microautophagy of nucleus in Saccharomyces cerevisiae’, Molecular Biology of the Cell, 14(1), pp. 129–141.

Tang, Z. et al. (2018) ‘Active DNA end processing in micronuclei of ovarian cancer cells’, BMC Cancer, 18(1), p. 426.

Chapter Six: General Discussion

6.1 Key findings from thesis work

Chapter 2

- OC cells exhibit differential drug sensitivities, with the most drug resistant cells (ID8-luc2, OVCAR-5 and -8) displaying low levels of caspase-3-dependent apoptosis and high levels of autophagy. In contrast, the most drug sensitive cell lines (OVCAR-3 and -4) display high levels of caspase-3-dependent apoptosis and low autophagy levels.
- Caspase-3-dependent apoptosis is significantly reduced, and recovery is significantly increased in OC cells (OVCAR-3, -4 and -5) following re-challenge with paclitaxel. This provides a novel insight into a potential mechanism of drug resistance in OC cells.
- Expression of autophagy proteins does not correlate with the ability of OC cells to undergo autophagy. This finding may be clinically relevant in the selection of biomarkers for use with autophagy modulating drugs.

Chapter 3

- CQ sensitises OC cells with high autophagy levels (ID8-luc2, OVCAR-5 and -8) to chemotherapy, but provides no benefit or exerts a protective effect in cells with low autophagy levels (OVCAR-3 and -4).
- Lithium can significantly sensitise ID8-luc2, OVCAR-5 and -8 cells to treatment, but provides no benefit to OVCAR-3 and -4 cells. Further studies are required to elucidate a mechanism.
- Brefeldin A-sensitive autophagy can be present at basal levels and in response to treatment in OC cells.

Chapter 4

- Knockdown of key autophagy genes can significantly sensitise OC cells to paclitaxel treatment, identifying a role for autophagy in paclitaxel resistance.
- Non-canonical autophagy may also contribute to paclitaxel resistance in OC cells.

Chapter 5

- OC cells can recover a pre-treatment DNA profile following recovery after paclitaxel treatment, which is impeded by inhibiting autophagy with CQ.
- Fragmented nuclear material induced by paclitaxel treatment colocalises with LC3 and LAMP1, suggesting a role for autophagic degradation of nuclear material.
- Knockdown of autophagy genes BECN1 and ATG5 marginally impeded the recovery of OC cell's DNA profile following paclitaxel treatment. Further research will be required in order to determine the role of autophagy in the maintenance of genomic integrity in OC cells.

6.2 General Discussion

Ovarian cancer is the number one cause of death from gynaecological malignancies. The benign nature of disease symptoms leads to a late stage diagnosis in most women, resulting in poor survival rates. The standard of care remains cytoreductive surgery combined with a taxane/platinum chemotherapy doublet. Carboplatin/paclitaxel is the preferred combination, given its lower toxicity profile. The introduction of targeted therapies, particularly PARP inhibitors such as Olaparib, have improved progression free survival of patients that have failed all prior lines of treatment. Despite this, the five year survival rate currently stands at 32.9%. Most women exhibit an excellent response to first line chemotherapy, however 80% of women will experience disease recurrence. Treatment resistance is the single biggest challenge which has yet to be met in the clinical management of OC. Our lack of understanding regarding the mechanisms driving chemoresistance was the impetus behind this project.

We have identified important differences in apoptosis and autophagy induction in response to chemotherapy in our panel of OC cell lines, which could be divided into two subgroups, as illustrated in Figure 1. Following paclitaxel treatment, OVCAR-3 and -4 cells displayed high levels of caspase-3 activation while ID8-luc2, OVCAR-5 and -8 cells induced low levels. None of our cell lines activated caspase-3 in response to carboplatin. Significant induction of autophagy was observed in three of our five cell lines (ID8-luc2, OVCAR-5 and -8), following treatment with paclitaxel and carboplatin.

Repopulation of OC cells following first line chemotherapy is a recognised, but poorly understood phenomenon. To balance therapeutic efficacy with unwanted toxic side effects, chemotherapy is administered in six cycles, at three week intervals, consisting of a taxane followed by a platinum agent. As a result of these intermittent periods

without treatment, and during the time from completion of first line therapy to disease relapse, OC cells can repopulate (Telleria, 2013). To mimic the clinical regimens, we treated OC cells with paclitaxel and allowed them to recover for 7 days in drug free media, before re-challenging with paclitaxel. Importantly, we found caspase-3 levels to be significantly reduced and clonogenic recovery significantly increased following a single treatment. Although we have not investigated a mechanism for this reduction in apoptosis, it provides an important insight into one of the ways OC cells may escape chemotherapy treatment. It would also support a rationale for targeting autophagy when tumours are no longer apoptosis competent to help prevent disease recurrence. As described Chapter 2 section 2.5, autophagy and apoptosis are closely linked. A better understanding of the dynamics of autophagy and apoptosis in OC may enable more timely and effective targeting for therapeutic gain.

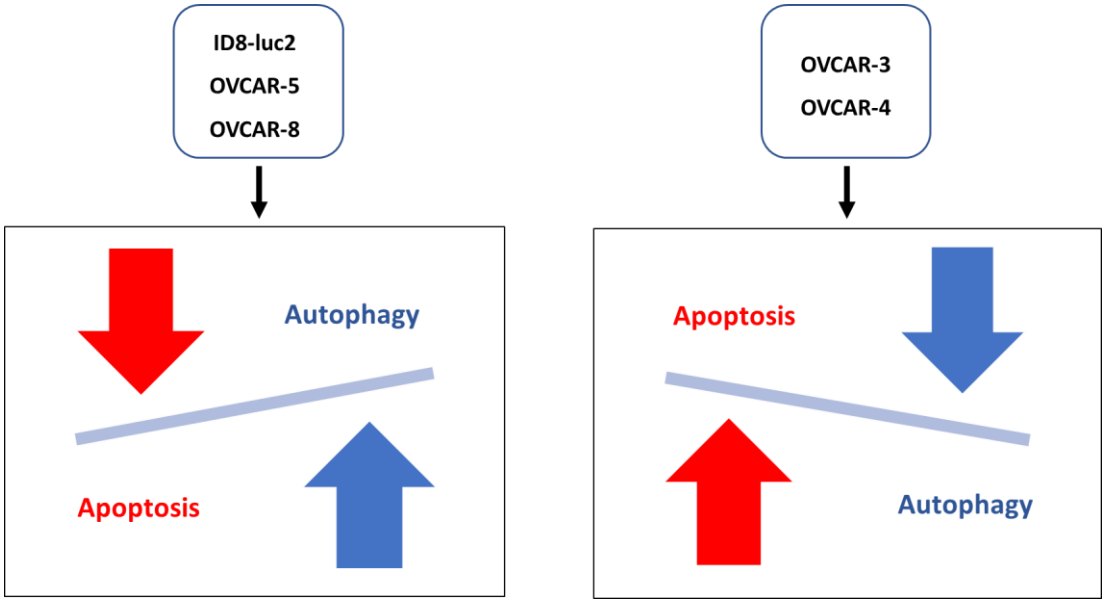

Figure 6.1. Diagram of apoptosis and autophagy induction in OC cells in response to treatment. Following paclitaxel treatment, ID8-luc2, OVCAR-5 and -8 cells induce low levels of apoptosis and high levels of autophagy. In contrast, OVCAR-3 and -4 cells have low autophagy induction and high levels of apoptosis following treatment.

We assessed the effect of autophagy modulators CQ and lithium on the chemosensitivity of our cell lines. Interestingly, we found that CQ and lithium could significantly sensitise the cells which displayed high levels of autophagy (ID8-luc2, OVCAR-5 and -8). Importantly, CQ exerted no effect or a protective effect in OVCAR-3 and -4 cells, while lithium treatment also elicited no chemosensitising effect in OVCAR-3 cells. Such differences are likely to reflect the inherent heterogeneity which exists among patients in the clinic, highlighting the need for the development of biomarkers. As we have shown with our panel of cell lines, assessing basal expression levels of autophagy proteins does not accurately reflect the autophagic capacity of a cell. Markers including LC3, Beclin 1 and Atg family members have all been suggested as biomarkers (Bortnik and Gorski, 2017). However, in our OC cell lines this would not be predictive of the ability of OC cells to undergo autophagy. The development of biomarkers to identify patients who are likely to respond to autophagy modulation will be key to the success of any new agents. By elucidating the molecular mechanisms, and the contribution of different autophagy pathways to response to treatment will aid in the identification of such biomarkers. We have identified a brefeldin A-sensitive autophagy pathway in OC cells, at basal levels and in response to paclitaxel treatment. Brefeldin A, which blocks protein transport from the Golgi, has previously been shown to inhibit non-canonical autophagy (including the Atg5/Atg7-independent pathway), but not canonical autophagy. We observed a reduction in autophagic vesicle accumulation when cells were treated with brefeldin A, suggesting a contribution of Golgi-derived autophagosomes, typical of the Atg5/Atg7-independent pathway.

In Chapter four, we identified a role for autophagy in the regulation of chemosensitivity. Knockdown of key autophagy regulators BECN1 and ATG5 significantly reduced recovery in ID8-luc2 and OVCAR-8 cells following paclitaxel treatment. In addition, we have shown that a non-canonical, brefeldin A-sensitive autophagy pathway may also contribute to chemoresistance in OC cells. The reduction in paclitaxel induced autophagosome accumulation following brefeldin A treatment in Chapter three indicated that this brefeldin A-sensitive pathway may be engaged in response to treatment. Increased sensitivity to paclitaxel following knockdown of Rab9 indicated that this pathway may be the Atg5/Atg7-independent pathway and may play a role in chemoresistance. We postulate that both canonical and non-canonical pathways may be active and contribute to resistance. This is in line with previous studies which have reported the co-operation of both pathways. One study found that the canonical and non-canonical autophagy pathways work together to maintain gut homeostasis. In response to lipopolysaccharide (LPS) stimulation, Atg5/Atg7-independent autophagy is activated and functions alongside canonical autophagy to eliminate the pathogenic bacteria *shigella* (Ra *et al.*, 2016). Similarly, mitochondrial degradation in erythrocytes is primarily mediated by non-canonical autophagy, and partly via canonical autophagy (Shimizu, 2018). While Atg5/Atg7-independent autophagy has been reported to be induced in response to the chemotherapeutic agent etoposide, we are the first to propose a role for this pathway in OC chemoresistance. Going forward, further experiments are required to elucidate an exact mechanism. Rab9, a GTPase which has functions in other pathways, is the only specific marker of the Atg5/Atg7-independent pathway identified to date, and its inhibition may be eliciting other non-autophagy related effects. To confirm the presence of the Atg5/Atg7-independent pathway, additional experiments in cells deficient in Atg5/7

are also necessary. This novel and exciting data characterises autophagy as a regulator of chemosensitivity in OC cells. We propose that the introduction of autophagy inhibitors into future treatment regimens will improve the responses of OC tumours that induce autophagy following treatment.

Preliminary data from Chapter five suggests the possibility that a selective form of autophagy, termed nucleophagy, is involved in eliminating nuclear material following paclitaxel treatment. We have demonstrated for the first time, that OC cells can recover their original DNA content following paclitaxel treatment, and that autophagy is likely to be important for this recovery. The addition of CQ to ID8-luc2 cells, and siRNA knockdown of BECN1 and ATG5 in OVCAR-8 cells, both impeded the clearance of polyploid cells. We have also found that fragmented nuclear material induced by paclitaxel associates with LC3 and LAMP1, further suggesting that autophagy may be involved in the elimination of nuclear material in OC cells. Like macroautophagy, nucleophagy induction can be described as a 'double edged sword'. In certain models, nucleophagy has been shown to induce cell death by degrading whole chromosomes in mitotic cells under oxidative stress (Sit *et al.*, 1996). In contrast, nucleophagy has also been reported to limit aneuploidy as a result of genotoxic insult. Aneuploidy exerts a toll on the cell's overall fitness, demanding higher metabolic requirements for proliferation. Thus, it is plausible to assume that tumour cells will endeavour to minimise such stress to promote cell survival and proliferation. To counteract the protective role of nucleophagy, chemotherapeutics which induce this process, such as cisplatin, could be combined with specific inhibitors of nucleophagy. In order to effectively target this pathway, it will be important to further investigate the molecular regulation of nucleophagy in OC cells. Interestingly, in a mouse model of neurodegeneration, a stall in canonical autophagy lead to the induction of non-

canonical autophagy, postulated to be Atg5/Atg7-independent autophagy, which mediated lamin degradation (Baron *et al.*, 2017). This data further supports the rationale that targeting more than one autophagy pathway is likely to be required for more effective treatment in OC patients.

Inhibition of autophagy may also provide another important benefit in OC. Ovarian cancer stem-like cells, which can be isolated from cell lines, patient derived tumours and ascites, are resistant to chemotherapy and can repopulate tumours in animal models, making them a significant target in overcoming disease recurrence (Zhang *et al.*, 2008) (Szotek *et al.*, 2006). Autophagy has emerged as a key pathway regulating the self-renewal capabilities and chemoresistance of these cells. Ovarian cancer stem cells, enriched from SKOV3 cells, were reported to have enhanced autophagic flux compared to the general population of OC cells. Impairment of autophagy, either by CQ or knockdown of ATG5, significantly enhanced the sensitivity of the cancer stem cells to paclitaxel and impeded the stem cells sphere forming ability (Peng *et al.*, 2017). Another study reported autophagy as essential for the self-renewal of ovarian cancer spheroid cells, via forming a positive feedback loop via NRF2 to activate an antioxidant response. Treatment with bafilomycin A1, impaired the OC spheroid self-renewal and inhibited tumour formation *in vivo* (Wang *et al.*, 2018). As such, targeting autophagy could negate the inherent chemoresistance of CSC's.

PARP inhibitors, such as Olaparib and Niraparib, are currently used as maintenance therapies for OC patients. While originally thought to be beneficial only in BRCA mutated patients, recent studies have supported their use in women without BRCA mutation but with mutations in other DNA repair pathways. In women who have failed all prior lines of treatment, PARP inhibitors can significantly improve progression free survival. However, as with other therapies, resistance to PARP inhibitors is inevitable.

An exciting study in published in 2019 has implicated a role for autophagy in resistance to PARP inhibitors in pre-clinical models of ovarian cancer. The group assessed the impact on autophagy of four PARP inhibitors, olaparib, niraparib, rucaparib and talazoparib in 8 ovarian cancer cell lines. The PARP inhibitors increased autophagy in each of the cell lines. The addition of CQ or targeted siRNA against ATG5 and ATG7 significantly enhanced the efficacy of the PARP inhibitors, confirming a role for autophagy in resistance to PARP inhibition (Santiago-O;Farrill *et al.*, 2019). Mechanistically, Olaparib decreases PARP activity, leading to an accumulation of DNA damage and γ-H2AX. Olaparib treatment also caused an increase in ROS accumulation and phosphorylation of ATM, while decreasing AKT and mTOR phosphorylation. Additionally, an increase in PTEN, a negative regulator of Akt, was also observed following Olaparib treatment. Given that PTEN inhibition decreases LC3 conversion, the authors suggest that PTEN may be an important regulator of olaparib-induced autophagy in OC cells. A similar study reported that the PARP inhibitor talazoparib activates autophagy in patient derived paediatric chronic myeloid leukaemia (CML) cells (Liu *et al.*, 2019). Knockdown of ATG5 significantly enhanced the efficacy of talazoparib, further highlighting a role for autophagy in PARP inhibitor resistance. These results highlight another exciting benefit of autophagy inhibition to improve OC patient outcomes.

Autophagy modulation in the cancer setting has been trialled over the last number of years, via the use of chloroquine and its derivative hydroxychloroquine (HCQ), the only FDA approved autophagy modulators. The role of autophagy in cancer is highly context dependent, with trials ongoing which both inhibit and attenuate autophagy. Based on the literature, it appears that drug induced autophagy in OC is protective, meaning that inhibiting autophagy would be beneficial. Currently, one clinical trial

involving autophagy modulation for OC is active (NCT03081702). If the cell line data is representative, it is possible that the addition of CQ would limit the efficacy of treatment and might only be beneficial in a limited number of patients. To date, there are no targeted autophagy inhibitors available. Additionally, one study reported inconsistent autophagy modulation by CQ, as determined by measuring LC3-II levels in peripheral lymphocytes (Wolpin *et al.*, 2014). As a result, more effective and less toxic CQ derivatives are also being tested, such as Lys05, a bisaminoquinoline CQ derivative. Lys05 more effectively accumulates within lysosomes and is a more potent inhibitor of autophagy. Lys05 administration in xenograft models of colon cancer and melanoma resulted in sustained autophagy inhibition using much lower doses than required with HCQ (Amaravadi and Winkler, 2012).

CQ and HCQ are the only autophagy modulators currently approved for clinical use. There is a clear need for the introduction of novel autophagy modulators which may be more effective and less toxic. Consequently, we have evaluated lithium. We have shown the efficacy of lithium as a chemosensitising agent in three of our cell lines (ID8-luc2, OVCAR-5 and -8). What remains to be elucidated are lithium's effects on autophagy in OC and how this chemosensitises the cells. Given that patients exhibit excellent initial responses to chemotherapy, resistance is likely to be acquired over multiple cycles. It could be envisioned that lithium could be administered concurrently with chemotherapy and during the three week intervals between chemotherapy cycles. Bi-polar patients receive lithium treatment for many years without adverse side effects, thus following the completion of treatment, OC patients may remain on low dose lithium treatment as a maintenance therapy (Berghöfer *et al.*, 2013). Multiple classes of chemotherapeutic drugs, including platinum agents and taxanes, count peripheral neuropathy as the main dose limiting toxicity. Taxanes such as paclitaxel,

have previously been shown to bind to neuronal calcium sensor 1 (NCS1) causing aberrant calcium signalling leading to neuropathy. Lithium has been shown to interfere with the interaction between paclitaxel, NCS1 and the inositol 1,4,5-triphosphate receptor (Mo *et al.*, 2012). A small retrospective study revealed that patients being treated with lithium while receiving chemotherapy had a reduced risk of developing chemotherapy induced peripheral neuropathy (CIPN) (Wadia *et al.*, 2017). Thus, the concurrent administration of lithium with chemotherapy could be used to greatly improve OC patient's quality of life whilst also tackling chemoresistance.

Although autophagy inhibitory drugs such as CQ are routinely used in malaria patients, chronic autophagy inhibition should be performed with caution, given the important role of autophagy in maintaining normal cell physiology. Lysosomal destruction by HCQ may interfere with other important functions such as cell signalling, secretion and metabolism. CQ has also been reported to influence the tumour microenvironment. While CQ has been shown to promote anti-tumour immunity, via polarising macrophages to an anti-tumour M1 phenotype, it has also been shown to have immune supressing functions, such as preventing the release of HGMB1 and inflammatory cytokines (Chen *et al.*, 2018) (M. Yang *et al.*, 2013) (van den Borne *et al.*, 1997). The inhibition of nucleophagy, combined with the off target DNA damaging effects of chemotherapeutics, could also lead to unwanted death of non-cancerous cells. Thus, understanding the full contribution of autophagy pathways to normal and cancer cell biology, along with elucidating the molecular regulators, should provide an improved response with reduced side effects.

In the future, the development of specific autophagy inhibitors for clinical use is needed. Several autophagy inhibitors are being tested in the laboratory but have yet to be translated for clinical use. Start-up companies have been established with the

specific aim of identifying and developing targeted autophagy inhibitors. Current efforts have focused on VPS34 inhibition, to inhibit autophagosome biogenesis. Unpublished data from one company found that in addition to its autophagy effects, VPS34 could boost inflammation in the tumour microenvironment (Dolgin, 2019). The protein kinase ULK1 is also being developed as a therapeutic target. Verteporfin is another autophagy inhibitor which may be useful. Verteporfin is reported to interfere with phagophore expansion and cargo sequestration preventing the formation of autophagosomes (Donohue *et al.*, 2011). Recently, verteporfin has been shown to inhibit OC cell proliferation, and significantly reduce tumour growth in an OVCAR-8 xenograft model, although the effects were not attributed to autophagy inhibition (Feng *et al.*, 2016). Another important question which needs to be addressed is when to administer autophagy inhibitors in the clinic. Hypothetically, autophagy inhibitors could be implemented at several different stages, as described in Figure 2. In addition, a given drug should have an accompanying biomarker to aid in the selection of patients who will benefit from the treatment. The development of such biomarkers will be crucial for the successful implementation of autophagy inhibitors into treatment regimens.

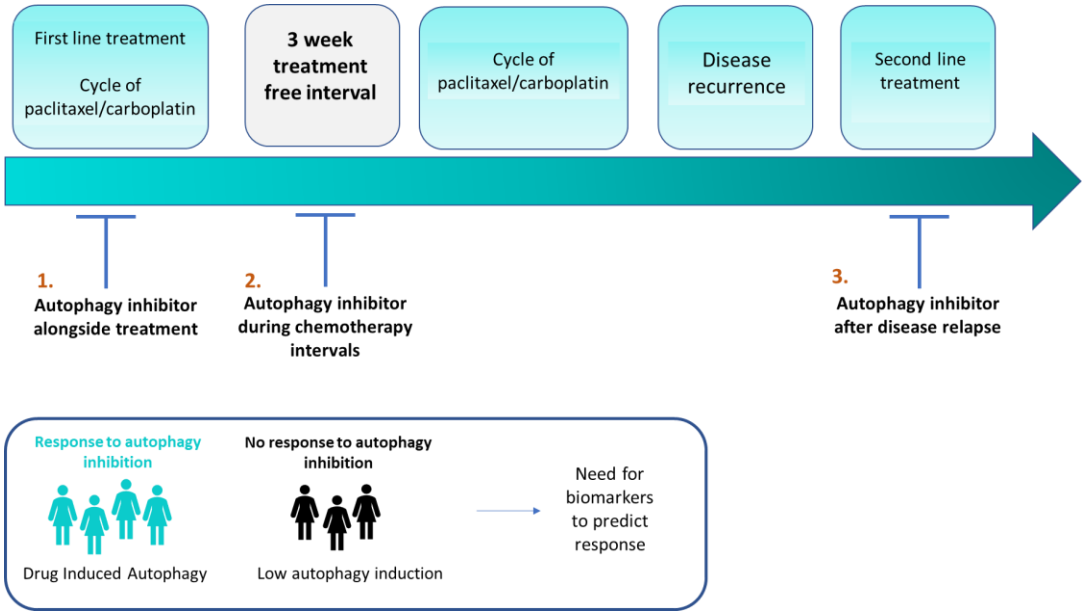

Figure 6.2. Timeline illustrating the potential implementation of autophagy inhibitors in the clinic. 1. As with current clinical trials using chloroquine, autophagy inhibitors may be administered concurrently with chemotherapy to enhance their efficacy. **2.** Ovarian cancer patients receive chemotherapy in cycles, with treatment free intervals in-between. Autophagy inhibitors may be administered during these treatment free intervals to prevent cancer cell recovery. **3.** Alternatively, inhibitors could be administered after disease relapse to re-sensitise ovarian cancer cells to second line treatment. However, the successful implementation of autophagy inhibitors will depend on the identification of biomarkers that can identify patients who will respond. Our data suggests that autophagy modulators may only be beneficial to patient tumours that induce autophagy in response to chemotherapy.

In conclusion, this research has identified a novel insight into one of the ways OC cells may become resistant to treatment, with evidence of reduced apoptosis competency and enhanced clonogenic recovery in OC cells following re-challenge with paclitaxel. We have also highlighted the significant chemosensitising ability of the autophagy modulators CQ and lithium in three of our cell lines with high autophagic flux. Importantly, we have demonstrated a role for canonical and non-canonical autophagy in paclitaxel resistance. Moreover, we have shown, for the first time, the ability of OC cells to recover their DNA content following treatment and highlighted a potential role for nucleophagy in this recovery. This thesis has shed light on the diverse roles played by autophagy in response to chemotherapy in OC cells, making it an exciting therapeutic target. It is hoped that autophagy inhibitors may be developed and incorporated into clinical regimens to prevent disease recurrence, to ultimately improve the outcome for ovarian cancer patients.

6.3 References

Amaravadi, R. K. and Winkler, J. D. (2012) 'Lys05: a new lysosomal autophagy inhibitor', Autophagy, 8(9), pp. 1383–1384.

Baron, O. et al. (2017) 'Stall in Canonical Autophagy-Lysosome Pathways Prompts Nucleophagy-Based Nuclear Breakdown in Neurodegeneration', Current Biology, 27(23), p. 3626–3642.

Berghöfer, A. et al. (2013) 'Stability of lithium treatment in bipolar disorder - long-term follow-up of 346 patients', International journal of bipolar disorders. Springer Berlin Heidelberg, 1, p. 11.

Bortnik, S. and Gorski, S. M. (2017) 'Clinical Applications of Autophagy Proteins in Cancer: From Potential Targets to Biomarkers', International journal of molecular sciences. MDPI, 18(7), p. 1496.

Chen, D. et al. (2018) 'Chloroquine modulates antitumor immune response by resetting tumor-associated macrophages toward M1 phenotype', Nature Communications, 9(1), p. 873.

Dolgin, E. (2019) 'Anticancer autophagy inhibitors attract "resurgent" interest.', Nature reviews. Drug discovery, pp. 408–410.

Donohue, E. et al. (2011) 'Inhibition of autophagosome formation by the benzoporphyrin derivative verteporfin', The Journal of biological chemistry. 2010/12/30. American Society for Biochemistry and Molecular Biology, 286(9), pp. 7290–7300.

Feng, J. et al. (2016) 'Verteporfin, a suppressor of YAP-TEAD complex, presents promising antitumor properties on ovarian cancer.', OncoTargets and therapy, 9, pp. 5371–5381.

Liu, Y. et al. (2019) 'Targeting autophagy potentiates the anti-tumor effect of PARP inhibitor in pediatric chronic myeloid leukemia', AMB Express. Springer Berlin Heidelberg, 9(1), p. 108.

Mo, M. et al. (2012) 'Prevention of paclitaxel-induced peripheral neuropathy by lithium pretreatment', FASEB journal: official publication of the Federation of American Societies for Experimental Biology. 2012/08/13. Federation of American Societies for Experimental Biology, 26(11), pp. 4696–4709.

Peng, Q. et al. (2017) 'Autophagy maintains the stemness of ovarian cancer stem cells by FOXA2.', Journal of experimental & clinical cancer research, 36(1), p. 171.

Ra, E. A. et al. (2016) 'TRIM31 promotes Atg5/Atg7-independent autophagy in intestinal cells.', Nature communications, 7, p. 11726.

Santiago-O; Farrill, J. M. et al. (2019) ‘Abstract 4768: PARP inhibitor-induced autophagy provides an adaptive mechanism of drug resistance in preclinical models of ovarian cancer’, Cancer Research, 79(13 Supplement), p. 4768-4768.

Shimizu, S. (2018) ‘Biological Roles of Alternative Autophagy’, Molecules and cells. 2018/01/23. Korean Society for Molecular and Cellular Biology, 41(1), pp. 50–54.

Sit, K.-H. et al. (1996) ‘Sequestration of mitotic (M-phase) chromosomes in autophagosomes: Mitotic programmed cell death in human Chang liver cells induced by an OH* burst from vanadyl (4)’, The Anatomical record, 245, pp. 1–8.

Szotek, P. P. et al. (2006) ‘Ovarian cancer side population defines cells with stem cell-like characteristics and Mullerian Inhibiting Substance responsiveness’, Proceedings of the National Academy of Sciences, 103(30), p. 11154 -11159.

Telleria, C. M. (2013) ‘Repopulation of ovarian cancer cells after chemotherapy’, Cancer growth and metastasis. Libertas Academica, 6, pp. 15–21.

Van den Borne, B. E. et al. (1997) ‘Chloroquine and hydroxychloroquine equally affect tumor necrosis factor-alpha, interleukin 6, and interferon-gamma production by peripheral blood mononuclear cells’, The Journal of rheumatology, 24(1), p. 55—60.

Wadia, R. J. et al. (2017) ‘The prevention of chemotherapy induced peripheral neuropathy by concurrent treatment with drugs used for bipolar disease: a retrospective chart analysis in human cancer patients’, Oncotarget, 9(7), pp. 7322–7331.

Wang, Q. et al. (2018) ‘Autophagy Is Indispensable for the Self-Renewal and Quiescence of Ovarian Cancer Spheroid Cells with Stem Cell-Like Properties.’, Oxidative medicine and cellular longevity, 2018, p. 7010472.

Wolpin, B. M. et al. (2014) ‘Phase II and pharmacodynamic study of autophagy inhibition using hydroxychloroquine in patients with metastatic pancreatic adenocarcinoma’, The Oncologist, 19(6), pp. 637–638.

Yang, M. et al. (2013) ‘Chloroquine inhibits HMGB1 inflammatory signaling and protects mice from lethal sepsis’, Biochemical pharmacology. 86(3), pp. 410–418.

Zhang, S. et al. (2008) ‘Identification and characterization of ovarian cancer-initiating cells from primary human tumors.’, Cancer research, 68(11), pp. 4311–4320.

Appendix 2: National Cancer Control Programme GP Ovarian Cancer Referral Guidelines

2. National Cancer Control Programme (NCCP) Ovarian cancer referral guidelines

The benign nature of ovarian cancer symptoms makes it extremely difficult for general practitioners (GPs) to accurately refer women for further investigation. The NCCP ovarian cancer referral guideline was developed in collaboration with the Irish college of general practitioners and a range of clinical speciality groups to facilitate the earlier detection of ovarian cancer. The guide highlights worrisome symptoms and provides a step wise algorithm for GP referral to gynaecology or radiology services.

National Cancer Control Programme

OVARIAN CANCER GP REFERRAL FOR SYPMTOMATIC WOMEN

Feidhmeannacht na Seirbhíse Sláinte
Health Service Executive

Ovarian cancer is the main cause of death from gynaecological cancer. Around 370 women are diagnosed each year; 80% are over 50 years of age. Most have advanced disease at presentation. Fewer than one-third have stage I or stage II disease at diagnosis. Survival in Ireland is poor - less than 40% at 5 years.

Data Source: National Cancer Registry Ireland

Factors that increase risk: Increasing age - most cases are post-menopausal; Lifestyle (overweight, smoking) is associated with 20%; Genetic mutations account for 10% (e.g. a woman with a first degree relative with ovarian cancer has a 3-4 fold increased risk. The known mutations, BRCA1 and BRCA2, explain less than 40% of the excess risk of familial cancer); Nulliparity; Prolonged HRT use (e.g. for more than 5 years); Unintentional infertility or use of fertility drugs.
Factors that decrease risk: Interruption of ovulation (e.g. pregnancy, oral contraceptive use, tubal ligation).

Screening of well women for ovarian cancer does not reduce mortality. It is not recommended.
Ovaries are not palpable in post-menopausal women. If they are felt, consider malignancy.

Symptoms of ovarian cancer

Ovarian cancer has few specific symptoms.

Consider ovarian cancer in women (especially aged over 50 years), who present with the following **persistent and frequent symptoms (i.e. more than 12 times per month):**

- Abdominal distension
- Early satiety
- Loss of appetite
- Pelvic or abdominal pain
- Increasing urinary urgency or frequency
- New onset Irritable Bowel Syndrome (IBS)

Consider ovarian cancer in women who present with **unexplained:**

- Ascites
- DVT
- Change in bowel habit
- Weight loss
- Fatigue

CA125

- Should not be ordered if a woman has no symptoms.
- Can be elevated in ovarian and other cancers and in many benign conditions.
- Is not an adequate ovarian cancer detection tool when used alone.
- Is raised in 80% of epithelial ovarian cancer but raised in only 50% of early stage disease.

Pelvic Ultrasound (US)

- A pelvic US is required to evaluate an ovarian mass.
- An urgent US is needed where CA125 is elevated in a symptomatic woman.
- Pre-menopausal ovarian cysts are common; almost all are benign.

A woman should be referred directly to gynaeoncology:

- If clinical findings reveal a pelvic mass or unexplained ascites (not obviously uterine fibroids)
- If an ultrasound (US) is suspicious for ovarian cancer. Please include details of where the US was carried out and a copy of the report
- If CA125 > 200kU/L
- If CA125 > 35kU/L and continues to rise on retesting but pelvic ultrasound is normal

Who can refer to gynae-oncology?

You, the GP when the patient meets the criteria in this guideline.

Another hospital based clinician (e.g. from the Emergency Department or Radiology).

When is a referral to gynae-oncology not appropriate?

If a patient has benign gynaecological conditions referral should be to the general gynaecology service.

Post-menopausal bleeding always requires an urgent referral to any gynaecology clinic

NCCP-COM-009-01(b) Draft V14: March 2016 ???????

GP REFERRAL PATHWAY FOR SYMPTOMATIC WOMEN

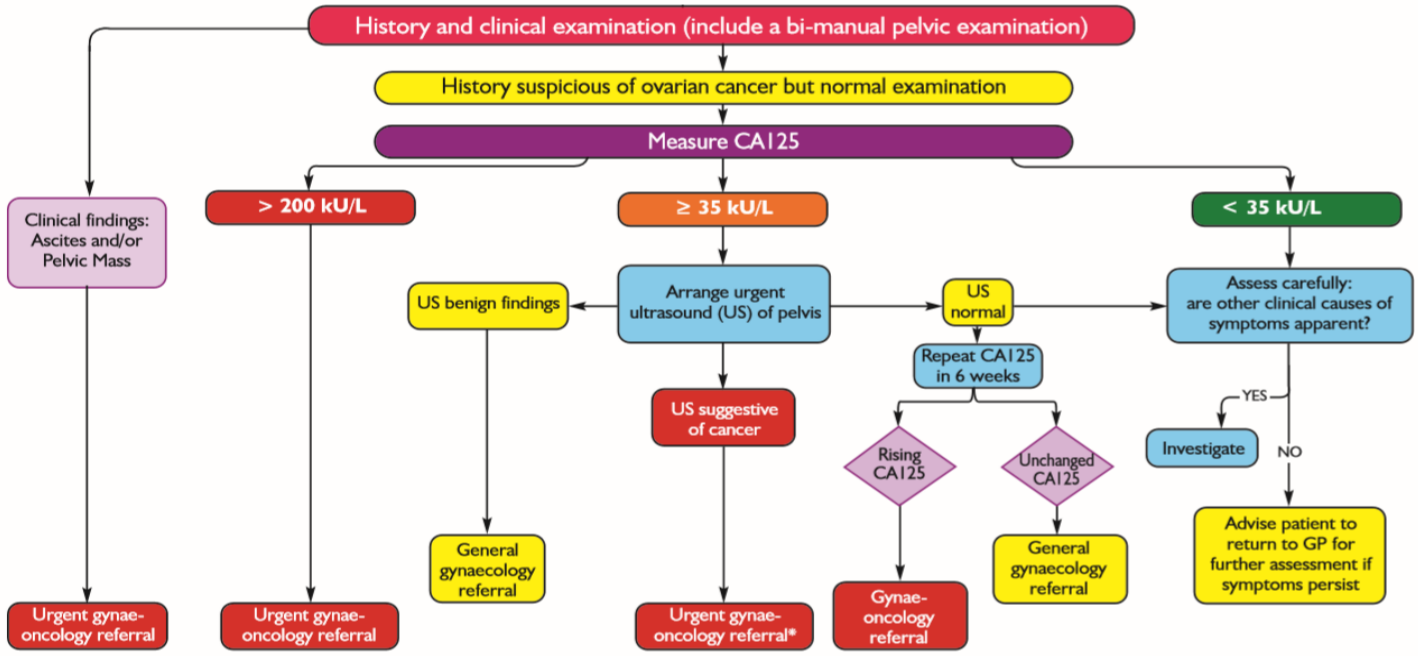

* **Note:** In some hospitals radiology may trigger a referral to gynae oncology, but this should not be assumed. In general, you (the GP) will be asked to inform the patient that they are being referred to this service

General Recommendations

This referral guideline is to prioritise women with suspected ovarian cancer. You can make a referral using the ovarian cancer referral form to one of these gynae-oncology centres.

Post-menopausal bleeding (1 year after last period) is an urgent referral to any general gynaecology clinic in your area.

Women with other gynaecology symptoms should be referred routinely to a general gynaecology clinic in your area.

Gynae-oncology centre contact details

Appendix 3: Cell line information

3. Cell Line Information

Established human ovarian cancer cell lines OVCAR-3, -4, -5 and -8 were obtained from the NCI-Frederick Cancer DCTC Tumor/Cell Line Repository (United States of America). Murine ID8 cells were obtained from the Mayo Clinic (United States of America), and were transfected in house with luciferase, to generate ID8-luc2 cells. Cell culture and culturing conditions were performed as recommended by the cell line repository.

Each cell line was passaged for no longer than six weeks. It is good practice to test for mycoplasma every six months. Mycoplasma contamination is currently assessed in the Cancer Research @ UCC lab using the PromoCell PCR Mycoplasma Test Kit I/C #PK-CA91-1024.

3.1 ID8-luc2 cell line

Cell line:	ID8-luc2
Species:	Mouse
Characteristics:	ID8 are a mouse surface ovarian epithelium (MOSE) spontaneously transformed cell line physiologically and biologically resembling human epithelial ovarian cancer.
Growth medium:	DMEM + 10% FBS+ 2 mM L-Glutamine
Mode of growth:	Adherent
Method of harvest:	Trypsin / EDTA
Source:	Dr. K. Roby
Reference:	Roby K.F., Taylor C.C., Sweetwood J.P., Cheng Y., Pace J.L., Tawfik O., Persons D.L., Smith P.G., Terranova P.F. Development of a syngeneic mouse model for events related to ovarian cancer. Carcinogenesis 21:585-591, 2000.

3.2 OVCAR-3 cell line

Designation:	OVCAR-3
Species:	Human
Histologic type:	Adenocarcinoma
Growth medium:	RPMI 1640 + 10% FBS+ 2 mM L-Glutamine
Mode of growth:	Adherent
Method of harvest:	Trypsin / EDTA
Recovery phase	P+1 5 Days T75 P+1 3 Days T25
Split ratios	P+2 1:2, 5, 10 P+3 1:5, 10, 20
Assay phase split ratios/	1:5, 10, 20
Flask Inoculation densities	1:10, 20
Approx. recovery/adaptation time & # passages:	12 Days - 2 Weeks, 3-4 Passages
Source:	Dr. T. Hamilton

Reference:	Hamilton, T., Young, R., McKoy, W., Grotzinger, K., Green, J., Chu, E., Whang-Peng, J., Rogan, A., Green, W., Ozols, R; Characterization of a Human Ovarian Carcinoma Cell line (NIH:OVCAR-3) with Androgen and Estrogen Receptors; Can. Res. 43:5379-5389, 1983
Cryopreserved:	12-21-10

3.3 OVCAR-4 cell line

Designation:	OVCAR-4
Species:	Human
Histologic type:	Adenocarcinoma
Growth medium:	RPMI 1640 + 10% FBS + 2 mM L-Glutamine
Mode of growth:	Adherent

Method of harvest:	Trypsin / EDTA - Trypsin 5-10 Minutes
Recovery phase	P+1 4-6 Days T75 P+1 2-3 Days T25
Split ratios	P+2 1:2, 5, 10 P+3 1:5, 10, 20
Assay phase split ratios/	1:5, 10, 20
Flask Inoculation densities	1:5, 10 to 1:10, 20
Approx. recovery/adaptation time & # passages:	2-3 Weeks, 3-4 Passages
Source:	Dr. T. Hamilton
Reference:	Hamilton, T., Young, R., Ozols, R.; Experimental Model Systems of Ovarian Cancer: Applications to the Design and Evaluation of New treatment Approaches; Sem. In Oncol. 11:285-298, 1984.
Cryopreserved:	10-8-10

3.4 OVCAR-5 cell line

Designation:	OVCAR-5
Species:	Human
Histologic type:	Carcinoma
Growth medium:	RPMI 1640 + 10% FBS + 2 mM L-Glutamine
Mode of growth:	Adherent
Method of harvest:	Trypsin/EDTA
Recovery phase	P+1 5 Days T75 P+1 3 Days T25
Split ratios	P+2 1:2, 5, 10 P+3 1:5, 10, 20
Assay phase split ratios/	1:10, 20, 40
Flask Inoculation densities	1:10,20 to 1:20, 40 Later
Approx. recovery/adaptation time & # passages:	2 Weeks, 3–4 Passages
Source:	Dr. T. Hamilton
Reference:	Hamilton, T., Young, R., Ozols, R.; Experimental Model Systems of Ovarian Cancer: Applications to the Design and Evaluation of New

	Treatment Approaches; Sem. In Oncol. 11:285-298, 1984.
Cryopreserved:	10-15-10

3.5 OVCAR-8 cell line

Designation:	OVCAR-8
Species:	Human
Histologic type:	Adenocarcinoma
Growth medium:	RPMI 1640 + 10% FBS + 2 mM L-Glutamine
Mode of growth:	Adherent
Method of harvest:	Trypsin / EDTA – Trypsin 5-10 Minutes
Recovery phase	P+1 3-4 Days T75, P+1 1-2 Days T25
Split ratios:	P+2 1:2, 5, 10 P+3 1:5, 10, 20
Assay phase split ratios/	1:20, 40, 80

Flask Inoculation densities:	1:40, 80
Approx. recovery/adaptation time & # passages:	2 Weeks, 3-4 Passages
Source:	Dr. T. Hamilton
Reference:	Hamilton, T., Young, R., Ozols, R.; Experimental Model Systems of Ovarian Cancer: Applications to the Design and Evaluation of New Treatment Approaches; Sem. In Oncol. 11:285-298, 1984.
Cryopreserved:	12-8-10

Appendix Four: Project Outputs

4.1 Manuscripts currently in preparation for submission:

Manuscript 1: Ovarian cancer cells that recover from treatment with a chemotherapeutic agent show decreased levels of apoptosis when re-challenged with the same agent.

Manuscript 2: Inhibition of autophagy can sensitise apoptosis incompetent cells ovarian cancer cells to chemotherapy: Caution with inhibitors is warranted for apoptosis competent cancers.

Manuscript 3: Autophagy is associated with the recovery of DNA content following paclitaxel treatment.

4.2 Poster and Oral presentations

Irish Association for Cancer Research (IACR) (2017, 2018) – poster presentations. 'Investigating a role for autophagy in ovarian cancer chemoresistance', Jennifer Quinn, Tracey R. O'Donovan, Sharon L. McKenna.

New Horizons conference (2017, 2018) – poster presentations. 'Investigating a role for autophagy in ovarian cancer chemoresistance', Jennifer Quinn, Tracey R. O'Donovan, Sharon L. McKenna.

Young cancer researchers networking (YCRN) (June 2018) – oral presentation. 'Investigating a role for autophagy in ovarian cancer chemoresistance'. Jennifer Quinn, Tracey R. O'Donovan, Sharon L. McKenna.

Breaking through conference (September 2019) – poster presentation. 'Induction of autophagy following treatment with chemotherapeutic agents, promotes recovery

and chemoresistance in ovarian cancer cells', Jennifer Quinn, Tracey R. O'Donovan, Sharon L. McKenna.

Irish Association for Cancer Research (IACR) (2020) – Oral presentation. 'Induction of autophagy following treatment with chemotherapeutic agents promotes recovery and chemoresistance in ovarian cancer cells', Jennifer Quinn, Tracey R. O'Donovan, Sharon L. McKenna. **(Awarded a best oral presentation prize).**